Crystallisation and Crystal Structure Studies of some TCNQ salts

by

Timothy James Houghton, B.Sc.

Thesis submitted to the University of Nottingham
for the degree of Doctor of Philosophy,
December 1980.

VOLUME CONTAINS CLEAR OVERLAYS

OVERLAYS HAVE BEEN SCANNED SEPERATELY AND THEN AGAIN OVER THE RELEVANT PAGE

This thesis is submitted in accordance with the regulations for the degree of Doctor of Philosophy of the University of Nottingham, and is wholly original except where due reference is made. The work was carried out between September 1977 and August 1980.

Acknowledgments

I would like to express my very sincere thanks to Dr. S.C. Wallwork and Professor D.D. Eley for the encouragement, assistance, and interest that they have shown during these last three years, and to Dr. M.R. Willis, whose interest and help has been much appreciated.

I would also like to thank Professor T.J. King and Dr. M.J. Begley for their help with the crystallography and for discussions concerning the organic reactions implied by one particular structure. I would also like to thank the academic and technical staff of the Chemistry Department and those employed in Cripps Computing Centre for use of their computing facilities and for program assistance.

Thanks go to Mrs. C. Healy for typing this work, and to my friends, especially Drs. N.J. Drew and J.K. Davies, and to Ms. F.J. Scriven, not only for proof reading this entire work, but also for her patience and understanding, I extend my very special thanks.

Finally I would like to thank my parents for their continual support and belief in me throughout my school and academic life, for without their faith and wisdom this work might never have been completed. To them I dedicate this work.

To Pam and Roy

CONTENTS

ABSTRACT

A series of salts of the radical ion $TCNQ^{\cdot-}$ were prepared by standard organic techniques or by controlled electrocrystallisation and their three-dimensional crystal structures were determined by single crystal X-ray diffractometry. The crystallisation of the two-phase system found in 1,2-bis(1-ethyl-4-pyridinio)ethene $(TCNQ)_4$ was studied using a.c. conductivity techniques. The results showed phase formation to be dependent upon both concentration and cooling rate, and no evidence was found for a third phase possessing a metallic d.c. solid state conductivity.

The structures reported in detail are:

a) 1,4-dimethylpyridinium $(TCNQ)_2$, DMPY$(TCNQ)_2$, Triclinic, $a = 7.833$, $b = 13.889$, $c = 7.171$ Å, $\alpha = 106.81$, $\beta = 112.50$, $\gamma = 95.36^{\circ}$, $Z = 1$, space group $P\bar{1}$. TCNQ moieties stacked as discrete diads with an interplanar separation of 3.21 Å within the diad. The d.c. dark conductivity was measured ($\sigma_{300} = 1.7 \times 10^{-4}$ ohm^{-1} cm^{-1}) and is consistent with the observed structure.

b) 2,3-bis(1-methyl-4-pyridinio)butane $(TCNQ)_4$, DMPB $(TCNQ)_4$, Triclinic, $a = 7.798$, $b = 14.248$, $c = 13.690$ Å, $\alpha = 109.53$, $\beta = 103.37$, $\gamma = 95.42^{\circ}$, $Z = 1$, space group $P\bar{1}$. TCNQ moieties stacked as discrete tetrads with interplanar separations of 3.13 and 3.17 Å within the tetrad. Anisotropic d.c. dark conductivity measurements were made and found to be consistent with the structure.

c) 1,2-bis(1-hydro-4-pyridinio)ethane $(TCNQ)_2$, DHPA $(TCNQ)_2$, monoclinic, $a = 29.481$, $b = 7.405$, $c = 13.470^{\circ}$, $\beta = 94.03^{\circ}$, $Z = 4$,

space group $C_{2/c}$. TCNQ moieties arranged in 4 columns of diads along c with an interplanar separation of 3.10 Å within the diad. The structure exhibits hydrogen bonding ($\overset{+}{N}$ - H--------$\overset{-}{N}$ heavy atom separation = 2.885 Å) between the cation and TCNQ moieties.

d) 1,2-bis(1-hydro-4-pyridinio)ethane $(TCNQ)_4$, DHPA $(TCNQ)_4$, monoclinic, a = 12.894, b = 3.933, c = 27.580°, β = 109.95°, Z = 1, space group $P_{2_1/c}$. TCNQ moieties in infinite stacks along b with cations in disordered positions in the channels between the stacks.

INTRODUCTION

Crystal Growth

Crystallisation of material from solution at around ambient temperature has for many years been a standard technique for the purification of compounds and their production in a suitable physical form. This form is controlled by variation of the nucleation and growth conditions such as the use of a different solvent or introduction of a seed crystal. Growth from sclution is the only method available for materials which undergo decomposition at elevated temperatures since melt growth and gaseous diffusion techniques are excluded.

Unless the crystallisation conditions are rigorously controlled, powders, highly dendritic species, and striated crystals with high concentrations of dislocations may occur. For studies which require high quality crystalline material, such as X-ray studies, solid state conductivity, photo-conduction, etc., the crystallisation process must be carefully controlled. Electrical conductivity, for example, is highly dependent upon the degree of physical fracturing present within the crystal.

Of equal importance to the crystallisation process and electrical properties of organic semiconductor materials is the degree of chemical purity obtained. The purity of the solvent, for example, is usually a major factor affecting crystal growth from solution. Rigorous treatment of all starting materials to give ultra-high purity reagents and solvents is therefore a prime requisite.

The two essential features of a solvent for crystal growth are

1) it should preferably yield crystals which show no preferred growth direction, since plate and needle crystals have dislocations (fractures) which follow this preferred growth direction causing brittleness and physical discontinuity, whereas equality of growth yields a material which may be cleaved in an appropriate manner to produce crystals of the required shape and 2) that it should provide a suitably high solubility for the solute in question and give a high, positive temperature coefficient of solubility. Three further properties are of practical interest: if the solute is denser than the solvent then crystals formed will sink and not float; low solvent volatility means that concentrations may be determined and maintained more accurately, and a low viscosity solvent enables transfer of material to be made with far greater ease.

The effect of solvent on crystal habit may take one of two forms, either producing two different morphologies of the same crystal phase as in the case of the Dewar cooled crystal growth from acetonitrile and acetone solutions of DMPP $(TCNQ)_4$ or TCNQ)[1,3], or producing two completely different crystallographic phases of the same stoichiometric material[e.g. 1,2,27,28,29]. Moreover, different cooling regimes applied to the same complex material in the same solvents can produce different phases, often distinguishable very efficiently by their differing morphologies. Sherwood et al[4] have shown the effect of the influence of varying solvent on crystal habit in nominally uni-phased systems, whilst numerous authors have discussed multiple stoichiometric and non-stoichiometric phase formation in organic TCNQ systems[e.g. 6,28,29,52,53,54].

The driving force governing crystal growth is the degree of

supersaturation, δ , defined by

$$\delta = \frac{\Delta C}{C_o}$$

where C_o is the equilibrium concentration of solute at the temperature of growth and ΔC the increment by which the true concentration exceeds this, i.e. $\Delta C = C_T - C_o$ where C_T is the concentration at the temperature T, of crystallisation. If ΔC is determined by a linear rate of lowering the temperature, as in the present author's work, the supersaturation may be controlled by matching the temperature lowering rate to the solubility curve. Some workers have used a constant temperature differential method to maintain a constant degree of supersaturation. For the temperature lowering method, Sherwood et al[4] have quoted a solubility in the range 200-1000g/1000g solvent and a ratio of solubility temperature gradient, $\frac{dS_T}{d_T}$, to solubility S_T (at temperature T) of between 0.01 and 0.03. Under these circumstances a rate of cooling of 0.5-1.0°C per day gives a supersaturation of ca. 2%[4]. For TCNQ complexes solubilities are typically of the order of 1-10g/1000g solvent, two orders of magnitude lower than those recommended by Sherwood, suggesting that crystallisation by solvent evaporation, although much more difficult to control accurately, may be more suitable. This may be especially true in view of the high volatility of the usual solvent for these complexes, acetonitrile. However, the technique which has been most commonly used in the past for the crystallisation of these complexes is that of uncontrolled temperature lowering, for example by means of a Dewar bath. Two different phases have often resulted from apparently similar

crystallisations by this method. For this reason it was considered that a controlled study of the preparative technique already in use in order to determine the precise conditions under which the different phases are formed should be made.

The use of seed crystals for the production of large perfect crystals poses special problems for the materials studied here since the surest method of mounting (that of drilling the crystal and placing a glass fibre through the hole thus formed) is proscribed by the brittle nature of the complex crystals. Similarly, as may be seen in Chapters 6, 7, the use of adhesives such as Araldite is proscribed because of the acidic nature of one of the components.

Two further factors affecting growth from solution are worthy of mention - the application of external electrical or magnetic fields, and the inclusion of solvent molecules either into the crystal lattice or as occluded solvent molecules in surface and bulk defects.

The effects of applying a pulsed or steady state high magnetic field have been studied by Gorskii and Akhromova[5] who found a steady field caused orientation of molecules in a melt causing a shift in the number of crystallisation centres (n.c.c.) at temperature T to lower temperatures (i.e. greater supercooling). The effect of an applied a.c. electrical field[5] on crystallisation from supercooled melts is again to shift the n.c.c. to lower temperatures, with the number of crystallisation centres formed under the influence of the applied field inversely proportional to T. In the field polar molecules are either parallel or perpendicular to the field provided that no strong inter-molecular bond is formed between molecules. It would be extremely

interesting to see whether such effects can be applied to the growth of TCNQ complexes from solution, perhaps dictating the stacking of TCNQ or cation molecules or even the final crystalline arrangement of moieties.

Solvent trapping is frequently as a result of too rapid growth (too high a degree of supersaturation being the prime cause). Ashwell[6] has reported that in the case of DEPE $(TCNQ)_4$ the rate of growth is controlled by the amount of water present in the solvent to the extent that at high (ca. 20% H_2O) concentrations growth is slow and DEPE $(TCNQ)_4$ is produced because the reduced solubility means that it is not possible to maintain high supersaturations whereas at low (ca. $\ll$ 1% H_2O) concentrations the material crystallised rapidly, occluding H_2O molecules within the lattice, forming a non-commensurate sub-lattice with the major crystallographic lattice. This observation is, however, open to a different interpretation : that slow growth enables an ordered cation lattice to be formed, whereas high growth rates force the cation into a situation of disorder, which in itself could provide the observed incommensurate sub-lattice, and hence account for the weak intermediate layer lines observed in oscillation photographs of this complex.

The effect of occluded solvent on the physical properties of TCNQ complexes is two-fold - one primary effect is that of structural failure under thermal cycling, whilst the other is the effect upon the electrical properties. Huttenrach and Keiner[7], investigating the production of lattice defects in pharmaceutical organics by the drying process, found that for lactose the degree of disorder, measured by X-ray densitometry, increased continuously up to approximately 50%.

Meyer[8] notes that in inorganic substances removal of occluded water causes a lesser increase in disorder than the removal of co-ordinated water molecules. In TCNQ complexes, Kemény et al[9] have shown the irreversible phase transition at 390 K observed by Murakami and Yoshimura[10] in N-methyl-quinolinium TCNQ is caused by the removal of occluded acetonitrile from the crystal lattice causing a change in the structural order, and that solvent occlusion may stabilise a phase which is thermodynamically unstable without solvent. Kemény's[9] X-ray results show a ~10% contraction between chains of TCNQ moieties and a ~2 % expansion along the chains (i.e. an increase in the TCNQ inter-molecular separations) which they attribute to the loss of acetonitrile from the lattice. The change of conductivity at the phase transition (ca. 4 orders of magnitude) is in the opposite sense to that found in Ashwell's[11] two forms of highly conducting DEPE $(TCNQ)_4$ $(H_2O)_x$ in that the higher conductivity 'metallic' phase is proposed to be hydrated DEPE $(TCNQ)_4$ $(H_2O)_x$, $x \ll 0.88$ whilst the high conductivity semi-conducting phase is proposed to be hydrated DEPE $(TCNQ)_4$ $(H_2O)_{0.88}$.

The effect of other impurities, intentional or otherwise, on the electrical properties is highly dependent upon the nature and amount of impurity present. On a gross scale, iodine in 1-20% doping quantities shows no appreciable increase in conductivity in the triphenyl phosphonium salts of TCNQ[13]; however, work on a more microscopic scale[e.g.55,56] has shown that these concentrations may well be far above the saturation point in conductivity terms. Coleman et al[14], in work on high purity N-methylphenazinium (TCNQ), found high temperature conductivity larger than previously reported and low temperature

conductivity, below the metal-insulator transition, 10x smaller than previously reported. They showed that the curvature observed in this region was due to impurities, and was consistent with NMP (TCNQ) being a magnetic Mott-Hubbard insulator below 200° K[15]. Endres et al[16] have shown that doping 5,10-dihydro-5,10-dimethylphenazinium TCNQ with 40% phenazine results in a mixed stack consisting of neutral phenazine and charged M_2P^+ in the same segregated stack. This has a d.c. dark current conductivity of $5\text{-}10\,\Omega^{-1}cm^{-1}$ at 300 K. The doped material in this case shows a d.c. conductivity approximately six orders of magnitude higher than the pure material. The effect of 'inherent' impurities, i.e. those which are a function of some chemical property of the complex itself, rather than impurities introduced via reagents, solvent, etc., may be thought of (for these complexes) mainly in terms of the TCNQ moiety. Kamaras et al[17] have observed large variations in conductivity with the method of preparation. Rapid cooling from acetonitrile, U-tube growth, and three-chamber diffusion techniques were used, producing (respectively) impurity free, variable impurity concentration, and 13% impurity. This impurity was assigned as $TCNQ^{2-}$, the di-anion, on the basis of the appearance in the u.v./visible spectra of an absorption at 500nm, which is attributed by Kommandeur[18] and these workers to the $TCNQ^{2-}$ moiety. Other workers, notably Melby[19] and Boyd[20] have attributed the species absorbing at 500nm to $(TCNQ^-)_2$, the dimer, on the basis of aqueous conductance measurements.

Whichever species is in fact present as an impurity, its effect upon the d.c. conductance of the pure material is to decrease the conductivity, showing that in this case the dominant conductivity

mechanism remains that of the TCNQ stack, rather than that of an impurity mechanism.

Recently, a number of promising techniques have been applied by various workers to the problems of crystal perfection and phase formation in TCNQ salts. Of these, three are particularly worthy of mention. Coleman[3] and other workers[50,39] pointed to the use of the three-chamber diffusive growth method, in which a central chamber initially full of pure, dry solvent only is separated by fine glass sinters from two chambers, one containing high purity solvent and cation solids, and the other containing high purity solvent and neutral TCNQ. If all materials are introduced under a high purity, dry atmosphere, and then sealed from the surroundings diffusive growth of complex occurs in the central compartment. Coleman used this apparatus to produce crystals of varying degrees of purity and defect levels, finding that both chemical impurities and physical defects have the same effects on conductivity for TTF.TCNQ i.e. the lowering of room temperature conductivity and a simultaneous raising of the temperature of the conductivity maximum, T_M, from 59K (no defect or impurity) to 130 K (numerous defects induced by repeated thermal cycling). More recently, diffusive crystallisation of this organic metal (TTF) (TCNQ) has been studied by Carlsen et al[21] in a variety of acetonitrile-related solvents (acetonitrile, butyronitrile, and two solutions of PMMA (polymethylmethacrylate) in acetonitrile) using a rotating disc method in order to determine conditions necessary for diffusive crystallisation in low gravity conditions, where gravity-induced convection will be negligible. These nearly ideal conditions of almost pure diffusion

controlled growth should significantly reduce the number of defects present in these crystals when compared to normal-gravity growth, and hence increase the magnitude of the d.c. conductivity since this is highly dependent[3] on defects disrupting the infinite stacks of moieties.

A second significantly novel and promising technique is that devised by Rosseinsky of electrocrystallisation[22,23], in which the rate of growth of the material is controlled by the rate at which the counter-ion may be produced at the electrode. This may be controlled either by constant voltage (potentiostatic) or constant current (galvanostatic) methods. Highly conducting non-stoichiometric salts of TTF with inorganic counter ions, as well as a small number of TCNQ complex salts have been prepared by these workers. Growth of the crystal occurs at the electrode surface rather than the free faces of the crystal[23a] as demonstrated by a continued growth even with the free end of the crystal out of the solution (see also Chapter 6).

A third extremely promising approach would appear to be the growth of orientated epitaxial films. Torrance et al[24,25] have produced epitaxial films of TTF (TCNQ) and NMP (TCNQ) on the cleaved (100) face of NaCl. The stoichiometry was found to be 1 : 1 in both cases by the use of their solution spectra in acetonitrile[19,26] for rapid evaporation (ca. 25nm/min) onto the substrate only. Non-stoichiometry occurred at lower evaporation rates, ca. 5nm/min. The use of preferential orientation by means of this technique (the TTF (TCNQ) complex has its stacking, and hence high conductivity axis, in the plane of the NaCl (100) substrate) for films of less than

ca. 150nm thickness is said to enable more accurate measurements of electrical properties. Seebeck, d.c. conductivity, Hall mobility and photoconduction are amongst those techniques which should be performed with greater accuracy and a greater degree of certainty with respect to crystal orientation,

Perhaps the most interesting property of organic materials of the type studied here is that of d.c. conductivity. Conductivities of these materials range from 10^{-10} to 10^{2} ohm^{-1} cm^{-1} (see Figure 1). Most of these materials are semi-conductors, and it has been shown (e.g. by Perlstein[31]) that the band conduction model may be applicable to such systems since an overlap of π-molecular orbitals can lead to band formation. Thus these materials obey the equation

$$\sigma = n_o e \mu (-\Delta E/_{2kT})$$

where σ is the conductivity, n the number of carriers of charge e and mobility μ, and ΔE the energy difference between the valence and conduction bands.

Some, however, are metallic in their electrical properties in that they possess a negative temperature dependence of conductivity (i.e. resistivity increases as temperature increases), such as some of the TCNQ salts of TTF (tetrathiofulvalene)[30] and its derivatives[31,32] and NMP (TCNQ)[34]. The possibility of an organic superconductor, in which the attractive potential required to pair the conduction electrons is provided by a polarised system of auxiliary electrons rather than by the heavy atom cores of the BCS model[35] was proposed by Little in 1964

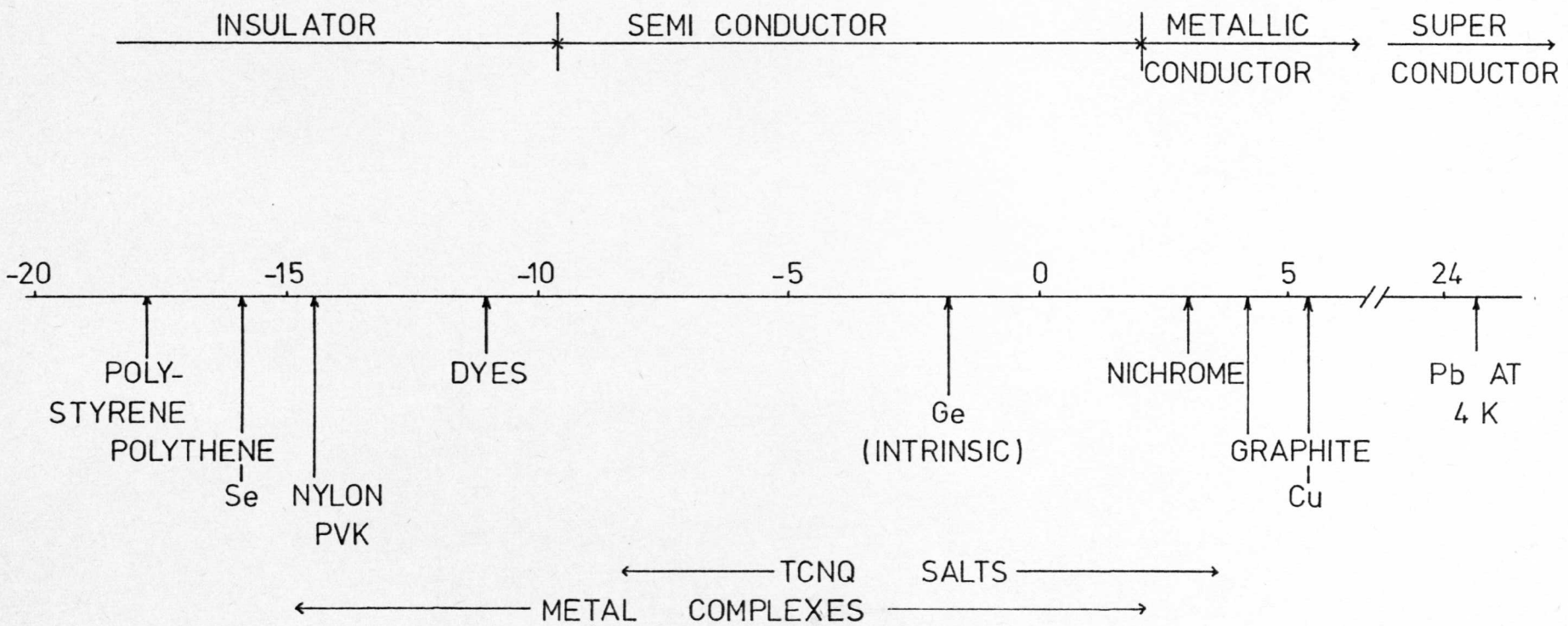

FIGURE 1

Log conductivity ($ohm^{-1}\ cm^{-1}$) ranges for various materials
(after Goodings, ENDEAVOR (1975), 34, 123)

(36,37,38). Little's model, consisting of a highly conjugated poly-ene spine with highly polarised side groups (see Figure 2) has so far eluded synthesis. In spite of this, the impetus given to research in the field by Little's proposals led to a much greater understanding of the organic conduction process, and a working definition of structural requirements for highly conducting complexes, summarised by the use of highly polarisable cations which are of suitable size and shape to enable an infinite TCNQ stack to be formed[40,41,51].

One technique which may be used to create a more regular TCNQ stack is the physical application of pressure. The effect of pressure on the conductivity of organic semiconductors has been studied as long ago as 1964 by Harada, Maruyama and Shirotani[42]. They found an increase in conductivity of ca. 10^5 in quaterylene, $C_{40}H_{20}$, and violanthrene ($C_{34}H_{16}O_2$) upon increasing pressure to 160 kbar. Further work by this group[43] showed that both tetraselenonaphthacene and iodanil undergo an increase in conductivity of 10^2 - 10^3 in changing from atmospheric pressure to 200 - 600 kbar. The same group also showed that simple salts of alkali metals with TCNQ[44] undergo an increase in conductivity up to a maximum at around 160 kbar, after which their resistivity increases with continued increasing pressure.

The discovery by Jerome, Mazaud and Ribault of super conductivity in an organic conductor[45] (albeit one containing an inorganic counter-ion, PF_6^-) at a pressure of 12 kbar must provide a stimulus to research in this field on a par with that provided by the Little model. The planar organic cation, the di-$\Delta^{2,2'}$-bi-4,5-dimethyl-1,3-diselenolium ion, forms nearly uniform stacks separated by PF_6^- moieties. At a

temperature of 0.9 K a transition to the superconducting state was observed.

Two further areas of current interest are the doping of polymeric films and the use of large, pseudo-planar rings with out-of-plane π orbitals. Kletter et al[46] have produced an organic metal derived by doping a polyacetylene film with Br_2 and subsequently with I_2, forming films of the type $[CH_{0.78}\ Br_{0.11}\ I_{0.07}]_x$ with conductivities of the order of σ_{298} = 10 ohm^{-1} cm^{-1}. Bard[47] has reported *in situ* sensitisation of inorganic n-type semi-conductors using phthalocyanine, where the use of this dye (which absorbs strongly in the visible region of the spectrum) allows utilisation of longer wavelengths to promote the steady state photocurrent. Nagami et al[48] have formed ternary cation-TCNQ-crown ether complexes, with complex salt (Crown ether)$_m$(M^+TCNQ^-)$_n$(TCNQ) conductivities three orders of magnitude greater than the simple salts (Crown ether)$_m$(M^+ $TCNQ^-$)$_n$. Hoffman, Ibers et al[49] have partially oxidised octamethyl-tetrabenzporphyrinatonickel (II) by means of elemental iodine to give Ni(OMTBP)$(I_3)_x$ (x = 0.36, 0.97) which show temperature dependent conductivities. In each case an activated conductivity occurs up to a temperature T_m above which conductivity decreases in a metallic fashion from this maximum σ_m (for the x = 0.36 complex, T_m = 300K and σ_m = 12 S cm^{-1}).

In the search for TCNQ complex salts with high conductivities possessing either semi-conducting or metallic behaviour, or perhaps even superconducting behaviour, this work has determined and studied the crystallographic structures of the so-called 'half-cation' salts (see also Chapters 2 and 3). Other structures investigated in this work are

those of electrochemically produced salts. These were studied in order to determine the effects of controlling growth conditions in this manner upon phase formation and complex stoichiometry. In view of the significance of solution growth to these materials a macroscopic study has been embarked upon in order to provide guidelines for future practical workers in the field, and to clarify the position with regard to the possibility of three-phase (low s.c. - high s.c. - metal complexes of certain bi-pyridinium salts with TCNQ. The author has also, during the course of this work, participated significantly in the solution of a number of crystallographic studies and brief structural details of these may be found in Appendix 1.

References to Introduction

1. N.J. Drew, Ph.D. Thesis, University of Nottingham (1978).
2. L.B. Coleman, Ph.D. Thesis, University of Pennsylvania (1975).
3. L.B. Coleman et al., Annals. N.Y. Acad. Sci, 313 (1978).
4. J.N. Sherwood et al., Crystal Growth, 2nd Ed. Panplin, Pergamon, London (1979).
5. F. Gorskii and A. Akhromova, Crystalline Processes Ed. Sirota, Gorskii, and Varikash, (1966).
6. G.J. Ashwell, Phy. Stat. Sol. (1978)
7. R. Hüttenrauch and I. Keiner, Int. J. Pharm. (1979), 2, 59.
8. K. Meyer, Physik-Chemische Kristall. VEB Deutscher Verlag für Grundstoffindustrie, Leipzig (1968).
9. T. Kemény Z. Pokó, G. Mihály, K. Holczer, and G. Grüner, Hung. Acad. Sci., Cent. Res. Inst. Phys, KFKI-1978-4.
10. M. Murakani and S. Yoshimura, J. Phys. Soc. Jap. (1975), 38, 488.
11. G.J. Ashwell, Phys. Stat. Sol. (1978), 86, 705.
12. G.J. Ashwell, Phys. Stat. Sol. (1978), b85 , K7.
13. D.R. Bates, Personal Communication.
14. L.B. Coleman, J.A. Cohen, A.F. Garito and A.J. Heeger, Phys. Rev.B, (1972), 7, 2122.
15. N. Mott and Z. Zinamon, Rep. Prog. Phys. (1970), 33 ; Metal-Insulator Transitions, N.F. Mott (1974).
16. H. Endres, H.J. Keller, W. Morani and D. Nothe, Acta. Cryst. (1980), B36, 1435.
17. K. Kamarás, K. Ritvay-Emandity, G. Mihály, G. Grüner and N. Rysava Hung. Acad. Sci., Cent. Res. Inst. Phys. KFKI-1977-31.

18. H.T. Jonkman and J. Kommandeur, Chem. Phys. Lett (1972), 15, 496-9.

19. L.R. Melby et al. J. Ann. Chem. Soc. (1962), 84, 3374.

20. R.H. Boyd and W.D. Phillips, J. Chem. Phys. (1965), 43, 2927.

21. L. Carlsen, I. Johansen, G. Galster and K. Bechgaard, Ber. Bins. Phys. Chem. (1980), 84, 458.

22. D.R. Rosseinsky, S.A. Mucklejohn, and P. Kathirgamanathan, J.C.S. Chem. Com. (1979), 86.

23. D.R. Rosseinsky, et. al. British Patent No. 8012883, 18.4.80.

23a. D.R. Rosseinsky, Private Communication (1979).

24. J.B. Torrance, J.F. Graczyk and E.E. Simonyi, IBM J. Res. Dev. (1978), 22, 315.

25. J.B. Torrance et al. Appl. Phys. Lett. (1974), 24, 439.

26. J.B. Torrance et al. J. Chem. Phys. (1974), 60, 5111.

27. M. Murakami and S. Yoshimura, Chem. Lett. (1977), 929.

28. M. Murakami and S. Yoshimura, Bull. Chem. Soc. Jap. (1975), 48, 157.

29. L.B. Coleman, S. Khanna, A. Garito, A. Heeger and B. Morosin, Phys. Lett. (1972), 42a, 15.

30. J. Ferraris, D. Cowan, V. Walatka and J. Perlstein, J. Am. Chem. Soc. (1973), 95, 948.

31. J. Perlestein, Angew. Chem. (1977), 16, 519 (Eng. Ed.).

32. E. Engler and V. Patel, J. Ann. Chem. Soc. (1974), 96, 7376.

33. A. Bloch, D. Cowan, K. Bechgaard, R. Pyle, R. Banks, and T. Poehler, Phys. Rev. Lett. (1975), 34, 1561.

34. J.R. Melby, Carad. J. Chem. (1965), 43, 1448.

35. J. Bardeen, L. Cooper and J. Schriefer, Phys. Rev. (1957), 106, 162 and Phys. Rev. (1957), 108, 1175.

36. W.A. Little, Phys. Rev. (A), (1964), 134, 1416.

37. W.A. Little, Sci. Am. (1965), 2.12, (2)21.

38. W.A. Little, J. Polym. Sci. (1970), 29, 17.

39. I. Begg, R. Narang, K. Roberts and J. Sherwood (1979) to be published.

40. J. Torrance, Y. Tomkiewicz, B. Silverman, Phys. Rev. (B) (1977), 15, 4738.

41. J. Torrance, B. Scott and F. Kaufman, Sol. Stat. Comm. (1975), 17, 1369.

42. Y. Harada, Y. Maruyama, I. Shirotani and H. Inokuchi, Bull. Chem. Soc. Jap. (1964), 37, 1378.

43. N. Kawai, H. Inokuchi, A. Onodera and I. Shirotani, Chem. Phys. Lett. (1974), 25, 296.

44. N. Sakai, A. Onodera, and I. Shirotani, Bull. Chem. Soc. Jap. (1975), 48, 167.

45. D. Jerome, A. Mazaud and M. Ribault, J. Physique-Letters (1980), 41 L-95.

46. H. Gibson, F. Courtney Bailey, A. Epstein, H. Rommelmann and J. Pochan, J.C.S. Chem. Comm. (1980), 426-428.

47. C. Jaeger, Fu-Ren F. Fau and A. Bard, J. Am. Chem. Soc. (1980), 102, 2592.

48. M. Morinaga, T. Nogami, Y. Kanda, T. Matsumoto, K. Matsuoka, and H. Mikana, Bull. Chem. Soc. Jap. (1980), 53, 1221.

49. T. Phillips, R. Scaringe, B. Hoffman and J. Iber, J. Am. Chem. Soc. (1979), 3435.

50. A. Lindegaard-Anderson and K. Nielson, Fifth European Crystallographic Meeting, Copenhagen, (1979).

51. T. Kamiya, S. Tsuji, K. Ogatsu and I. Shimohara, Polym. J. (1979), 11, 219.

52. G.D. Welch, Ph.D. Thesis, University of Nottingham (1976).

53. C.J. Gritchie, Acta. Cryst. (1965), 20, 892.

54. A. Rembaum, A. Herman, F. Stuart and F. Gutman, J. Phys. Chem. (1969), 73, 513.

55. E.A. Davies, Endeavor, (1971), 30, 55.

56. R. Gemmer, D. Cowan, T. Poehler, A. Block, R. Pyle and R. Banks, J. Org. Chem. (1975), 40, 3544.

CRYSTALLOGRAPHIC THEORY AND TECHNIQUES

1.1 The Diffraction of X-rays by Single Crystals

1.11 Single Crystal Photographs

The X-ray diffraction pattern of a single crystal depends primarily upon two factors: the position of each diffracted beam of X-rays is a function of the repeat distance in the periodic structure, i.e. the dimensions of the unit cell, and the intensity of such a beam is a function of the arrangement of the scattering matter within the cell, i.e. it is dependent upon the positions and atomic numbers of the atoms within the cell. The condition for a diffracted beam to be observed is given by the three Laue equations, which must be simultaneously satisfied:

$$a(\cos\alpha_o - \cos\alpha) = h\lambda \qquad (1 - a)$$

$$b(\cos\beta_o - \cos\beta) = k\lambda \qquad (1 - b)$$

$$c(\cos\gamma_o - \cos\gamma) = l\lambda \qquad (1 - c)$$

a, b, and c are the three non-coplanar periodic distances of translation (i.e. the unit cell dimensions), α_o, β_o, and γ_o are the angles between the incident beam and the corresponding unit cell axes, a, b, and c, and α, β, and γ are the corresponding angles for the diffracted beam. h, k, and l are integers.

The diffraction of X-rays can also be considered in terms of planes of atoms within the crystal so that when the path length difference between successive rays for a particular diffracted beam

is a whole multiple of the wavelength constructive interference occurs. This is known as the Bragg approach and the equation governing this phenomenon is called the Bragg equation:

$$n\lambda = 2d \sin\theta \qquad (1.2)$$

where θ is the Bragg angle, d is the perpendicular distance between successive reflective planes and n is an integer.

These two approaches to diffraction enable cell dimensions to be obtained from oscillation and Weissenberg photographs.

1.12 Collection of Intensity Data

Intensity data were collected on a Hilger and Watts four-circle computer controlled diffractometer, using Mo Kα radiation and a graphite monochromator. The diffractometer was controlled by a PDP 8I mini computer which performed all the calculations necessary in order to determine the four-circle positions for a given reflection from the cell dimensions and an orientation matrix, to determine the intensities of these reflections, and to output the acquired information in a suitable form for processing.

The diffractometer consists of a source of X-rays, a mechanical arrangement to bring any plane in a crystal into the diffracting position and a counter. In a four-circle diffractometer, three of the circles are used to bring the diffracting plane into such a position and the fourth positions the counter at twice the Bragg angle. Fig. 1.1 shows schematically the four circle arrangement. The ϕ circle is rotated in order to bring the perpendicular to the

diffracting plane into the χ plane, after which the χ circle rotates until the perpendicular to the diffracting plane is in the horizontal plane, whence the ω circle rotates so that the plane of the χ circle bisects the angle between the incident and diffracted beam so that the reflecting plane is at the Bragg angle. Then the counter (on the 2θ circle) may be rotated to receive the diffracted beam. If the counter circle rotates at twice the angular velocity of the ω circle whilst the plane passes through the diffracting position, then the scan is referred to as an $\omega/2\theta$ scan and each reflection is measured under essentially the same conditions as a zero layer Weissenberg photograph. The measurement and control of the circles is by the Moiré fringe method, giving approximately 0.01^{o} resolution.

The detector, a scintillation counter, passes the crude quantum count to a counting chain which amplifies and shapes the pulses and analyses the peaks thus produced. The integrated intensity obtained from a peak scan may be represented by:

$$P(hkl) = \frac{E.\omega}{I_o} = \lambda^3 \left(\frac{N.e^2}{mc^2}\right) |F(hkl)|^2 .L.V.P. \qquad (1.3)$$

where E = energy diffracted by crystal λ = wavelength of radiation

ω = angular velocity of rotation of specimen in X-ray beam

c = velocity of light

I_o = intensity of incident beam

V = crystal volume

m = mass of electron

P = polarisation factor

e = charge on electron

F = structure factor of plane (hkl)

N = number of unit cells per unit volume

L = Lorentz (velocity) factor

The data should be corrected for the following effects before use:

(i) Absorption of X-rays by the specimen

X-rays are absorbed by material according to the exponential law

$$\frac{I}{I_o} = e^{-\mu t} \qquad (1.4)$$

where I_o is the incident intensity, I the transmitted intensity, t the path length through the specimen, and μ the linear absorption coefficient. Since the absorption of X-rays in general increases with atomic number, and for a spherical crystal absorption will be the same for all crystal orientations, this correction is often neglected for crystals which contain only light atoms and whose external crystal dimensions are approximately equal. For these reasons none of the crystals studied in this work has had the diffracted X-ray intensities corrected for absorption.

(ii) Polarisation

Unpolarised X-ray radiation loses a quantity of energy, related to the Bragg angle, after reflection from a plane, due to polarisation

during reflection. The fraction of energy lost, ρ , is given by

$$\rho = (1 + \cos^2\theta)/2 \qquad (1.5)$$

where θ is the Bragg angle for that particular reflection.

(iii) The Lorentz factor

When a crystal rotates at a constant angular velocity, or is incremented at a constant rate, such as during a peak scan in data collection, the different reciprocal lattice points will intercept the sphere of reflection at different rates and therefore will be capable of reflecting for different periods of time. As measurements of intensity on a four-circle diffractometer are made under conditions which are equivalent to those of a zero layer Weissenberg photograph taken by the normal beam method (see earlier) then this correction takes the form

$$L = \frac{1}{\sin 2\theta} \qquad (1.6)$$

Thus, for four circle diffractometers, $L\rho$, the Lorentz and polarisation factors, may be corrected for by multiplying the measured intensities by $\frac{2 \sin 2\theta}{1 + \cos^2\theta}$ and this will give corrected intensities proportional to $|F(hkl)|^2$.

(iv) Extinction

Crystal perfection alsc affects the intensity of the diffracted

beams in two ways, known as primary and secondary extinction. In primary extinction a ray reflected off a plane within the crystal which is orientated at the Bragg angle to the X-ray beam may also be reflected from the plane above it since it too will be at the Bragg angle with respect to the reflected X-ray beam as in a perfect crystal these planes would be parallel. This second reflected ray would be 180° out of phase with the first incident ray and hence a reduction in intensity of the X-ray beam occurs as the beam passes through the crystal. This effect is decreased with the increasing mosaic nature of the crystal because of the mis-orientation of the small mosaic blocks and consequent shorter geometric order. Secondary extinction occurs when the first planes encountered by the X-ray beam reflect a large proportion of the incident radiation so that parallel planes deeper in the crystal receive less incident intensity and therefore reflect less intensity than expected. This effect is most marked with very intense reflections, and since these are usually down-weighted during structure refinement it may often be neglected.

1.2 Determination of Structure from Intensity Data

1.21 The Phase Problem

The information obtained so far consists of intensities and Miller Indices of reflecting planes in the crystal lattice. The structure factor F_{hkl} is the resultant of the N waves scattered by the N atoms in the unit cell from the diffracting plane hkl.

The contribution of each atom to the reflection is dependent upon the scattering factor for that particular atom and on its position in the cell (which determines the phase of its scattering relative to hypothetical scattering from the origin of the unit cell), so that the structure factor F_{hkl} is given by

$$F_{hkl} = \sum_{j=1}^{N} f_j \exp\left[2\pi i\,(hx_j + ky_j + lz_j)\right] \qquad (1.7)$$

where f_j is the scattering factor of the j^{th} atom and x_j, y_j, and z_j are the fractional coordinates of the j^{th} atom in the unit cell. The summation is over all the N atoms in the unit cell.

The atomic scattering factor, f_j, accounts for the finite size of the j^{th} atom's electron cloud. If all the electron density were concentrated at a point then for an atom of atomic number Z

$$f_j = Z \qquad (1.8)$$

would be true. However, electron clouds have a finite size, which is of the order of the wavelength of radiation used in X-ray crystallography, and thus interference between scattering from different parts of the atom will occur. This interference will have little effect for small values of θ, the Bragg angle, since a small angle implies a large spacing and thus the effect of the electron cloud is small with respect to the spacing. This is shown diagramatically in fig. 1.2.

Thermal motion of the electron cloud will also affect the scattering factor. If the atoms (and hence electron clouds) have

an isotropic motion, i.e. thermal motion is the same in all directions, then the Debye-Waller temperature factor of the j^{th} atom, B_j, may be applied and the scattering factor (equation 1.8) now takes the form:

$$f_j = f_j^o \exp\left(\frac{-B_j \sin^2\theta}{\lambda^2} \right) \qquad (1.9)$$

where $B_j = 8\pi^2 \overline{U_j^2}$

and $\overline{U_j^2}$ is the root mean square amplitude of the j^{th} atom from its equilibrium position in a direction normal to the reflecting plane. This amplitude will be a function of temperature and thus B_j is called the isotropic temperature factor.

In practice atoms do not usually behave isotropically and the thermal motion of an atom is best described by an ellipsoid so that the scattering factor now takes the form

$$f_j = f_j^o \exp\left[-2\pi^2 (h^2 a^{*2} U_{11} + k^2 b^{*2} U_{22} + \ldots . \right.$$

$$\left. \ldots . + 2klb^* c^* U_{23} + 2hla^* c^* U_{13}) \right] \qquad (1.10)$$

1.22 Fourier Synthesis and the electron density function

Any periodic function may be represented by a combination of waves of various amplitudes, frequencies, and phases. This process of combination is known as Fourier synthesis and in a one-dimensional case may be represented by

$$f(X) = \frac{1}{a} \sum_{h=-\infty}^{\infty} \left[A_h \cos 2\pi \frac{hX}{a} + B_h \sin 2\pi \frac{hX}{a} \right] \qquad (1.11)$$

where a is the periodic repeat distance along the X direction, and A_h and B_h are functions of the amplitude of the periodic function:

$$A_h = \int_{-a/2}^{a/2} f(X) \cos(2\pi hX/a)dX$$

and $$B_h = \int_{-a/2}^{a/2} f(X) \sin(2\pi hX/a)dX$$

If $$C_h = A_h + iB_h \quad \text{and} \quad C_{\bar{h}} = A_h - iB_h$$

then equation 1.11 can be re-written (by use of de Moivre's theorem)

$$f(X) = \frac{1}{a} \sum_{h=-\infty}^{\infty} C_h \exp(-2\pi ih.\frac{X}{a}) \qquad (1.12)$$

and $$C_h = \int f(X) \exp(2\pi ih.\frac{X}{a}).dX$$

Thus, in three dimensions,

$$f(X,Y,Z) = \frac{1}{V} \sum_{h=-\infty}^{\infty} \sum_{k=-\infty}^{\infty} \sum_{l=-\infty}^{\infty} C_{hkl} \exp(-2\pi i\left[\frac{hX}{a} + \frac{kY}{b} + \frac{lZ}{c}\right]) \qquad (1.13)$$

and $$C_{hkl} = A_{hkl} + iB_{hkl}, \quad C_{\overline{hkl}} = A_{hkl} - iB_{hkl}$$

Since it is the electron cloud of an atom which causes X-rays to be diffracted, the appropriate periodic crystallographic function for Fourier synthesis is the electron density function, $\rho(xyz)$, and the coefficients C_{hkl} of equation 1.13 are the structure factors F_{hkl} (equation 1.7). The electron density function is periodic in three dimensions by definition of the unit cell:

$$\rho(xyz) = \frac{1}{V} \sum_{h=-\infty}^{\infty} \sum_{k=-\infty}^{\infty} \sum_{l=-\infty}^{\infty} F_{hkl} \exp\left[-2\pi i(hx + ky + lz)\right] \quad (1.14)$$

where V is the volume of the unit cell and x, y, and z are fractional coordinates.

As C_{hkl} is complex so in general is F_{hkl}, i.e.

$$F_{hkl} = A_{hkl} + iB_{hkl} \quad (1.15)$$

where
$$A_{hkl} = \sum_{j=1}^{N} f_j \cos 2\pi (hx_j + ky_j + lz_j) \quad (1.15a)$$

and
$$B_{hkl} = \sum_{j=1}^{N} f_j \sin 2\pi (hx_j + ky_j + lz_j) \quad (1.15b)$$

From equations 1.15, 1.15a and 1.15b it can be shown that

$$F_{hkl} = \left|F_{hkl}\right| e^{i\alpha_{hkl}} \quad (1.16)$$

where α_{hkl} is known as the phase angle and is given by

$$\tan \alpha_{hkl} = \frac{B_{hkl}}{A_{hkl}} \quad (1.16a)$$

This also yields Friedel's Law, namely

$$\left|F_{hkl}\right| = \left|F_{\bar{h}\bar{k}\bar{l}}\right| ,$$

an important relationship in crystallography.

The term $\left|F_{hkl}\right|$ in equation 1.16 may be obtained experimentally from the measured intensities but the phase information has been lost. Thus it is not possible to calculate the electron density function $\rho(xyz)$ until some information has been obtained non-experimentally

about the phases α_{hkl}.

1.23 The Patterson function

Patterson[1,2] in 1934 suggested a function which yielded a Fourier series with zero phases and $|F_{hkl}|^2$ as the coefficients and since the intensity of a reflection from the plane hkl is:

$$I(hkl) \quad \alpha \quad |F_{hkl}|^2 \tag{1.17}$$

a series of this type is of great help in determining structure information since all the information is available from experiment for the calculation of this function.

The Patterson function, P(uvw), is the product of the electron density functions at the points (xyz) and (x+u, y+v, z+w) integrated over the volume of the unit cell:

$$P(uvw) \quad = \quad V \int_{x=0}^{1} \int_{y=0}^{1} \int_{z=0}^{1} \rho(xyz).\, \rho(x+u,\, y+v,\, z+w)\, dx\, dy\, dz \tag{1.18}$$

Substituting for electron density by equation 1.14 and applying de Moivre's theorem gives

$$P(uvw) \quad = \quad \frac{1}{V} \sum_{h} \sum_{k} \sum_{l=-\infty}^{\infty} |F_{hkl}|^2 \cos\left[2\pi(hu + kv + lw)\right] \tag{1.19}$$

which can be summed from the X-ray intensities directly. Thus P(uvw) will be at a maximum when both $\rho(xyz)$ and $\rho(x+u,\, y+v,\, z+w)$ are also maxima, a situation which will occur if there are atoms at both (xyz) and (x+u, y+v, z+w); u, v, and w define the vector between the two points. The positions of these peaks in

the Patterson function are related to the positions of the atoms in the unit cell by placing each of the N atoms in the unit cell at the origin, in parallel orientation, and mapping the vectors made with the remaining N-1 atoms. Thus the origin peak in Patterson space will be comprised of N vectors of zero length, corresponding to vectors from each atom to itself, and the remaining N(N-1) vectors will occupy the Patterson cell. The Patterson map will be centrosymmetric because $P(uvw) = P(\bar{u}\bar{v}\bar{w})$, i.e. the function (equation 1.18) is centrosymmetric.

Since the Patterson cell is the same as the crystal cell but contains of the order of N(N-1) more peaks (compared to an electron density map of the same cell) it follows that the Patterson cell must by definition be more crowded than the crystal cell. This problem is compounded by the way in which the peaks are produced (by a process known as convolution) so that the product peak of the two electron density functions has a greater width than either function on its own. This broadening of peaks in a Patterson function means that frequently overlap of Patterson peaks occurs and peak search routines may thus be unable to identify the separate peaks necessary to help determine the structure. Better resolution and thus more information may be obtained by 'sharpening'.

1.24 The Sharpened Patterson function

It can be seen from equation 1.7 and 1.9 that F_{hkl} decreases with increasing $\sin\theta$ because of the finite size of the electron cloud and its thermal motion. For a point atom at rest (where all

the electron density is concentrated at a point x y z) f_j would be constant and hence F_{hkl} would not suffer a decline due to $\sin\theta$. If F_{hkl} is modified by a function whose value increases as $(\sin\theta)/\lambda$ increases then this decrease of F_{hkl} can be compensated and will produce peaks in the modified Patterson function which are less broad than the Patterson peaks, since the convolution of two narrow width peaks will also be narrow. Thus, for example, vector patterns in the vicinity of strong peaks such as the origin may now be revealed.

The Sharpened Patterson function used in the present work is given by[3]

$$\left|F_{sharp}(hkl)\right|^2 = \left|F_{obs}(hkl)\right|^2 . M \qquad (1.20)$$

where

$$M = \frac{1}{\exp\left[-2\left(\frac{B\sin^2\theta}{\lambda}\right)\right]} \cdot \frac{1}{\left[\sum_{j=1}^{N} f_j\right]^2} \qquad (1.20b)$$

From the form of equation 1.20b it can be seen that this sharpening function comprises two parts: the inverse of the square of the correction to f_j for thermal motion (c/f equation 1.9) thus effectively bringing the atoms to rest, and the inverse of the square of the sum of all the atomic scattering factors, thus mathematically reducing the atoms to point scatterers. The effect of the sharpening function is shown in figure 1.3.

1.25 The Application of the Patterson method to TCNQ structures

The TCNQ molecule is a planar moiety and thus will produce a two-dimensional vector pattern which may often be easily recognised in the Patterson or sharpened Patterson function provided that the function is plotted in projection along a suitable cell axis. The intramolecular vector pattern due to the TCNQ moiety is shown in figure 1.4 and its significance in aiding the solution of a structure by the Patterson method can easily be seen from the following simplified case in which the example of a symmetric linear triatomic molecule is considered. For this molecule, in a general position in a centrosymmetric space group such as $P\bar{1}$, there will be two molecules per unit cell (figure 1.5a), related by the centre of symmetry.

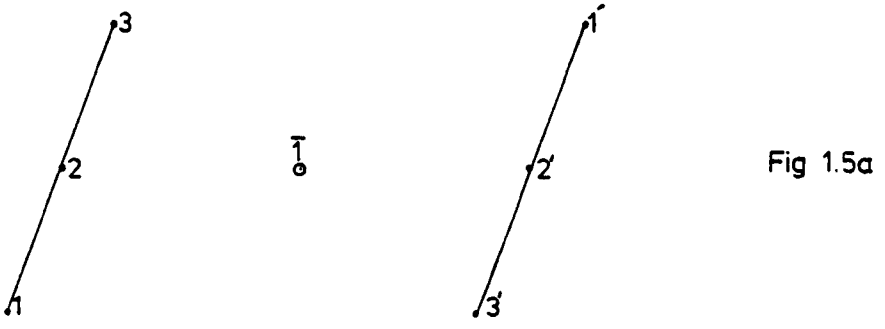

Fig 1.5a

The vectors of the Patterson cell about the origin will be obtained by translating all the vectors between the atoms within the molecules to this common origin and the orientation of these vectors in Patterson space will be the same as those in the real cell. Similarly, because the molecules in the real cell must by definition be parallel, this vector pattern will be repeated about a strong vector corresponding to the three parallel vectors between

1,3'; 2,2'; and 3,1' (see figure 1.5b).

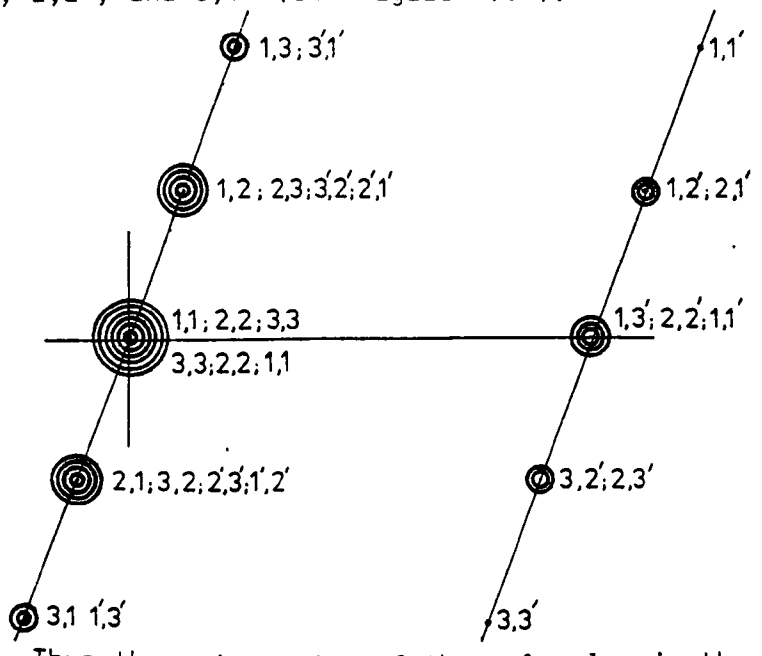

Fig 1.5b

Thus the orientation of the molecules in the real cell is the same as the linear arrays of vectors in the Patterson cell and the position of the molecular centre from the origin will be at half the centre-centre vector distance, because the molecules are related by a centre of symmetry.

From figure 1.5a it can now be seen that if the orientation of this strong vector pattern can be determined at an origin and the same orientation found about a strong non-origin peak then both the position of the molecular centre and its orientation within the cell may be determined. From this information the positions of the individual atoms within the cell for the TCNQ molecule can be calculated approximately from the interatomic vectors $\underline{a}$ and $\underline{b}$ shown in figure 1.4[4], for example the coordinates of atom C8 may be obtained with respect to the molecular centre by the vector addition $2\underline{a} + \underline{b}$.

The determination of the TCNQ molecular centre and its

orientation is shown more fully in the following example. Consider the simple case of DMPY $(TCNQ)_2$, in which there is one formula unit per cell and the space group is $P\bar{1}$ (the implications of this on the cation position will be fully discussed in Chapter 2). The strong Patterson peaks in two layers, one at $-0.06 < Z < 0.06$ and one at $0.44 < Z < 0.56$ are shown in fig. 1.6 plotted in projection down the c axis. The orientation of the TCNQ molecule can be seen in the vector pattern about the origin at (1,0,0) and confirmation of this, together with the position of the molecules within the unit cell, is obtained from the vector pattern in the same orientation about a strong peak at $x = 0.712$, $y = 0.057$, $z = 0.515$. This is the peak due to the sum of the parallel vectors between equivalent atoms in the centrosymmetrically related TCNQ moieties, and thus halving the coordinates of this peak yields the position in the real cell of the molecular centre.

The Patterson method is usually successful in solving structures where, if there is little difference in atomic weight of the constituent atoms of the cell, some or all of the moieties exhibit an easily recognisable vector pattern. If the moieties are planar and orientated in the same way within the cell then there should be strong intermolecular vectors in the Patterson, so that compounds with planar molecules which form stacks within the cell are frequently suitable for solution by Patterson methods.

However, if the molecules within the cell are non-planar, or

possess different orientations (or both) it may be difficult to interpret the Patterson function in any chemically sensible way. Under these circumstances it is sometimes possible to solve the structure by Direct Methods.

1.26 The Direct Methods Approach

In direct methods it is usual to use normalised structure factors, E_{hkl}, instead of F_{hkl} such that

$$|E_{hkl}|^2 = \frac{|F_{hkl}|^2}{\varepsilon \sum_{j=1}^{N} f_j^2} \qquad (1.21)$$

where $\sum_{j=1}^{N} f_j^2$ is the expected intensity of a reflection and ε is an integer factor to compensate for the enhanced intensities of special classes of reflections (e.g. for the space group $C_{2/c}$ $\varepsilon = 2$ for reflections in the class hkl when $h + k = 2n$, and $\varepsilon = 4$ for 0k0 when $k = 2n$ and h0l when $l = 2n$) and may be considered as the number of equivalent atoms for that reflection class.

Direct methods are based on the determination of the signs of reflections on the basis of certain statistical probabilities, notably Sayre's relationship[5] for centrosymmetric structures containing resolved atoms:

$$S(hkl).\ S(h'k'l').\ S(h-h',\ k-k',\ l-l') \approx +1 \qquad (1.22)$$

where S(hkl) indicates the sign of F_{hkl} and $\approx$ means 'probably equals'.

For planes with high E values the probability that this relationship will hold is given by[6]

$$P = \tfrac{1}{2} + \tfrac{1}{2} \tanh \left[\left(\frac{\sigma_3}{\sigma_2^{3/2}} \right) \left| E_h E_{h'} E_{h-h'} \right| \right] \qquad (1.23)$$

where h represents hkl, h' represents h'k'l' and h-h' represents h-h', k-k', l-l' and σ_n is defined by

$$\sigma_n = \sum_{i=1}^{N} n_i^n \qquad \text{where} \quad n_i = \frac{f_i}{\sum_{j=1}^{N} f_j}$$

and so n_i may be thought of as the proportion of the expected intensity of a reflection due to the i^{th} scatterer.

If a structure contains N identical atoms,

$$\sigma_3 = \sum_{i=1}^{N} n_i^3 \xrightarrow{\theta \to 0} \sum_{i=1}^{N} \frac{Z^3}{N^3 Z^3} \longrightarrow \frac{N}{N^3}$$

$$\sigma_2 = \sum_{i=1}^{N} n_i^2 \xrightarrow{\theta \to 0} \sum_{i=1}^{N} \frac{Z^2}{N^2 Z^2} \longrightarrow \frac{N}{N^2}$$

so $$\frac{\sigma_3}{\sigma_2^{3/2}} = \frac{N}{N^3} \cdot \frac{N^{-3/2}}{(N^2)^{-3/2}} = \frac{1}{N^{\frac{1}{2}}}$$

Thus, for structures where the atoms are similar,

$$P \approx \tfrac{1}{2} + \tfrac{1}{2} \tanh \left[\frac{1}{N^{1/2}} \cdot \left| E_h E_{h'} E_{h-h'} \right| \right]$$

should be a good approximation to the probability that the Sayre

relationship will be true.

In order to apply these sign relationships some signs for a number of reflections must be known. For a triclinic, monoclinic, or orthorhombic primitive centrosymmetric space group it is possible to arbitrarily assign phases to three reflections which will place the origin of the cell at one of the centres of symmetry.

The structure factor equation for a centrosymmetric crystal with an origin at 0,0,0 is (from equation 1.7)

$$F(hkl)_{0,0,0} = \sum_{j=1}^{N} f_j \cos 2\pi (hx_j + ky_j + lz_j) \qquad (1.24)$$

Moving the origin to (say) $\frac{1}{2}$, $\frac{1}{2}$, 0 translates each of the original x_j, y_j's by $-\frac{1}{2}$ along the corresponding axis, so that

$$F(hkl)_{\frac{1}{2},\frac{1}{2},0} = \sum_{j=1}^{N} f_j \cos 2\pi \left[(hx_j + ky_j + lz_j) - (h+k)/2 \right] \qquad (1.25)$$

and expanding this gives

$$F(hkl)_{\frac{1}{2},\frac{1}{2},0} = (-1)^{h+k} F(hkl)_{0,0,0} \qquad (1.26)$$

since $\sin \left[2\pi (h+k)/2 \right] = 0$. Therefore, the magnitude of F(hkl) is '<u>invariant</u> under change of origin', but its <u>sign</u> depends upon the parity of the indices, hkl. If h, k, and l are all even (eee) then the sign of F(hkl) remains the same no matter which origin is chosen, and reflections in this parity group are thus termed structure invariants. So, in order to define the origin uniquely it is

necessary to define the phases of three reflections (or less, depending upon the space group) which are not structure invariant. This may be done either by consulting tables which show the effect of a change of origin on the sign of a structure factor for different parity groups, or by chosing reflections whose Miller indices, h_i, k_i, l_i obey the determinant

$$\begin{vmatrix} m(h_1) & m(k_1) & m(l_1) \\ m(h_2) & m(k_2) & m(l_2) \\ m(h_3) & m(k_3) & m(l_3) \end{vmatrix} = \pm 1$$

where $m = I - \left[(\text{integer value of } (\left|\frac{I}{2}\right|).\ 2\right]$ and I is the integer value of the appropriate index h, k, or l. Thus m = 0 if the index is even, and m = 1 if the index is odd. m is referred to as the index modulo 2.

There is a further relation following from equation 1.22 in the special case where h = h - h', i.e. h' = 2h, 2k, 2l. Substituting and rearranging equation 1.22 gives

$$S(2h, 2k, 2l) \approx S(hkl).\ S(hkl) \qquad (1.27)$$

and the right hand side of this relation must be positive, so that (for example) S(6,4,2) = + provided that the E's for (3,2,1) and (6,4,2) are sufficiently large. This relationship is known as the $\sum_1$ relationship and it may be useful in determining some of the signs of the reflections. However, since the probability for this relationship is always less than that for equation 1.22 then this

relationship must be used with care as it can often give incorrect results.

For non-centrosymmetric structures the phases are not constrained to be 0 or π and Sayre's relationship may be written

$$\Phi_h \approx \Phi_{h'} + \Phi_{h-h'} \qquad (1.28)$$

where Φ_h is the phase of the reflection hkl. This is known as the Σ_2 relationship. Equation 1.28 applies if the known phases of two related reflections contribute to the unknown phase of a third reflection. In the case where a number of such contributors exist then the most probable value of Φ_h is given by

$$\tan \Phi_h \approx \frac{\sum_{h'} |E_{h'}, E_{h-h'}| \sin (\Phi_{h'} + \Phi_{h-h'})}{\sum_{h'} |E_{h'}, E_{h-h'}| \cos (\Phi_{h'} + \Phi_{h-h'})} \qquad (1.29)$$

This is known as the tangent formula.

One of the most frequently used programs for solving structures by direct methods is MULTAN, written by Main, Germain, and Woolfson[7]. In this, a weighted tangent formula is used to obtain a quicker convergence on a group of reflections which are linked by a large number of strong phase relations. The phases are weighted according to their reliability such that starting set phases carry unity weight, undetermined phases have zero weight, and phases estimated by the

tangent formula are weighted according to[7]

$$w_h = \tanh\left(\tfrac{1}{2}\,\alpha_h\right) \qquad (1.30)$$

where

$$\alpha_h = \left|E_h\right| \left(S_h^2 + C_h^2\right)^{\frac{1}{2}} \qquad (1.30a)$$

and the tangent formula (equation 1.29) now becomes

$$\tan \Phi_h \approx \frac{\sum_{h'} w_{h'}\, w_{h-h'} \left|E_{h'}\, E_{h-h'}\right| \sin\left(\Phi_{h'} + \Phi_{h-h'}\right)}{\sum_{h'} w_{h'}\, w_{h-h'} \left|E_{h'}\, E_{h-h'}\right| \cos\left(\Phi_{h'} + \Phi_{h-h'}\right)} = \frac{S_h}{C_h} \qquad (1.31)$$

α_h is a measure of the ability of a phase to contribute towards further phase determinations. The reliability of the estimate of α_h is defined by $K_{hh'}$, when this is determined from one pair of known phases Φ_h and $\Phi_{h-h'}$:

$$K_{hh'} = 2\,\sigma_3\,\sigma_2^{-3/2} \left|E_h\, E_{h'}\, E_{h-h'}\right|$$

and the estimated value of α_h, $\alpha_h(\text{est})$, for a reflection h, is

$$\alpha_h^2(\text{est}) = \sum_{h'} K_{hh'} + 2 \sum_{\substack{h' \\ h' \neq h''}} \sum_{h''} K_{hh'}\, K_{hh''} \frac{I_1(K_{hh'}).\ I_1(K_{hh''})}{I_o(K_{hh'}).\ I_o(K_{hh''})}$$

where I_1 and I_o are modified Bessel functions. It is necessary to estimate a value for α_h since on the first cycle of weighted tangent refinement it is necessary to know w_h, the weight of a

contributor, which itself comes from α_h (equation 1.30). This cannot be calculated initially from equation 1.30a since this requires values for the numerator and denominator of the weighted tangent formula in which the weights themselves are determined.

When a number of phases have been determined by the tangent formula the probable correctness of the resulting set of phases may be assessed in one of three ways:

a) Absolute figure of merit, ABS FOM = $$\frac{\sum_h \alpha_h - \sum \alpha_r}{\sum_h \alpha_h(\text{est}) - \sum \alpha_r}$$

where $\sum \alpha_r = \sum_h \left(\sum_{h'} K_{hh'}^2 \right)^{\frac{1}{2}}$. $\sum \alpha_r$ is the value of $\sum \alpha_h$ if the phases are random. ABS FOM should therefore be zero for random phases (since $\sum \alpha_h$ and $\sum \alpha_r$ will be equal) and unity if $\sum \alpha_h$ were equal to its expectation value (thus ABS FOM may be greater than unity in practice). As a general guide, Main et al[7] suggest that an ABS FOM of < 0.8 usually indicates an incorrect phase set, and that an ABS FOM of > 1.2 may indicate a possibly correct phase set.

b) Psi Zero, ψ_o. This is useful when more than one phase set has a high absolute figure of merit and can give a very good indication of the most probably correct phase set.

$$\psi_o = \sum_h \left| \sum_{h'} E_{h'} E_{h-h'} \right| \qquad (1.32)$$

where $\sum_h$ the outer summation is over all the small E_h's and the inner summation is over known phases. Since Sayre's equation (1.22)

can be written in terms of E's[8,9],

$$E_h = N^{\frac{1}{2}} \langle E_{h'} E_{h-h'} \rangle$$

then the inner summation of equation 1.32 may be thought of as the right hand side of the Sayre equation given above and for small $|E_h|$ the external summation should have a low value and thus ψ_o should be a minimum for a possible correct solution.

The third indication of the correctness of a phase set as given by MULTAN is called RESID and is the equivalent of the normal crystallographic residual. It is usually of much less value than a) or b) in deducing the best trial set of phases.

The version of MULTAN used in this work was MULTAN 78. Some of the equations used in this version differ from those given in this section, two of which are worthy of note: equation 1.30 becomes

$$w_h = \text{min value of } (1, 0.2\,\alpha_h)$$

and gives an approximation to the hyperbolic tangent function for computational ease, and the ψ_o (equation 1.32) figure of merit has a scaling factor to allow better comparison of ψ_o values.

1.3 Crystallographic Technique: Orientation of crystals for diffractometry

A suitable crystal was selected for each compound studied and mounted on a goniometer head by means of a fine glass fibre and a minimum amount of epoxy adhesive. Approximate cell dimensions were

obtained from oscillation and Weissenberg photographs and preliminary assignments of space group were made where possible. The goniometer head was then attached to the Φ circle of the diffractometer and the crystal centred, after which the wavelength of radiation used (Mo $K\alpha_1$, λ = 0.70926 Å was used for crystal setting and data collection) and the unit cell dimensions obtained from the single crystal photographs were input in order to calculate reciprocal cell dimensions and hence the Bragg angle Θ for any reflection. In general two reflections were selected to form an approximate orientation matrix, and a Φ scan of 180° in steps of 0.5° at low Θ was made in order to determine the Φ circle position for a particular reflection. Examination of the distribution of intensity with Φ and the zero layer Weissenberg photograph enabled one or more reflections to be identified, and these were used (after refinement of the Φ circle position and χ, ω circles in 0.02° steps) to define a more accurate orientation matrix. Identification of suitable first layer reflections confirmed the accuracy and identification of the zero layer reflections chosen and ensured that a right handed crystal system was used, according to convention.

In general, approximately 20 reflections were then selected for use in a crystal alignment routine which determines the accurate four-circle positions for a reflection by repeated scanning of the Φ, χ and ω positions, and finally new cell dimensions were obtained by a least-squares procedure. The 20 or so reflections were selected on the basis of fulfilment of the following three criteria where possible:

(i) $12^{o} < \theta < 14^{o}$

(ii) $0^{o} < \chi < -55^{o}$

(iii) Integrated intensity of the order of 10^{4}.

Once an accurate orientation matrix had been obtained, intensity data were collected within a range of theta (typically $0^{o} < \theta < 25^{o}$ for Mo radiation), measuring three standard reflections every 100 reflections in order to monitor any crystal decomposition or to detect the crystal becoming mis-set.

In the case of the data collection for DHPA $(TCNQ)_2$ (phase II) the cell dimensions and partial space group were obtained by the Niggli matrix method. The calculations were performed on the department's CAD4 system. In this method a number of four circle positions for reflections obtained by the Hilger and Watts initial reflection search routine were used to determine a primitive normal cell defined (by convention) such that $a < b < c$ and α, β and γ are all either $< 90^{o}$ or $> 90^{o}$. This cell may then be transformed by a matrix of appropriate direct cell indices until the second row of the Niggli matrix can be made to agree with one of those forms representing a genuine reduced cell, whence this cell may be transformed from the conventional cell to the cell more appropriately used for space group description.

Figure 1.1

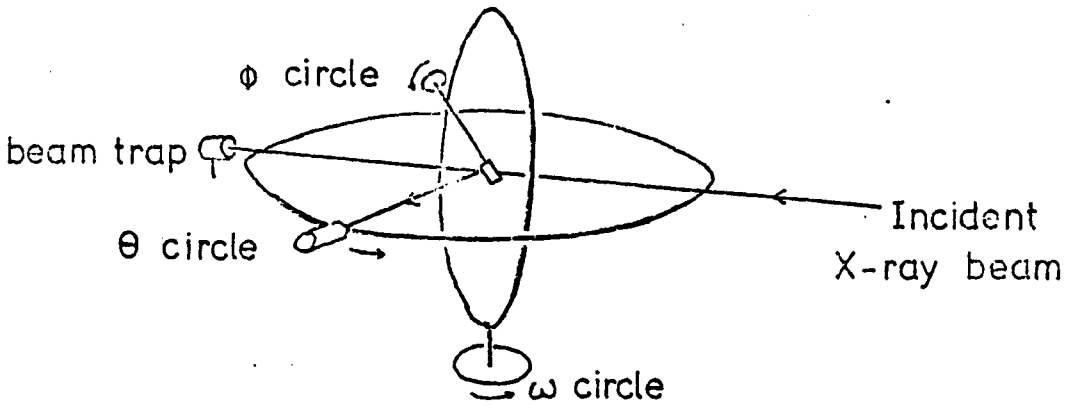

Four circle geometry

Figure 1.2

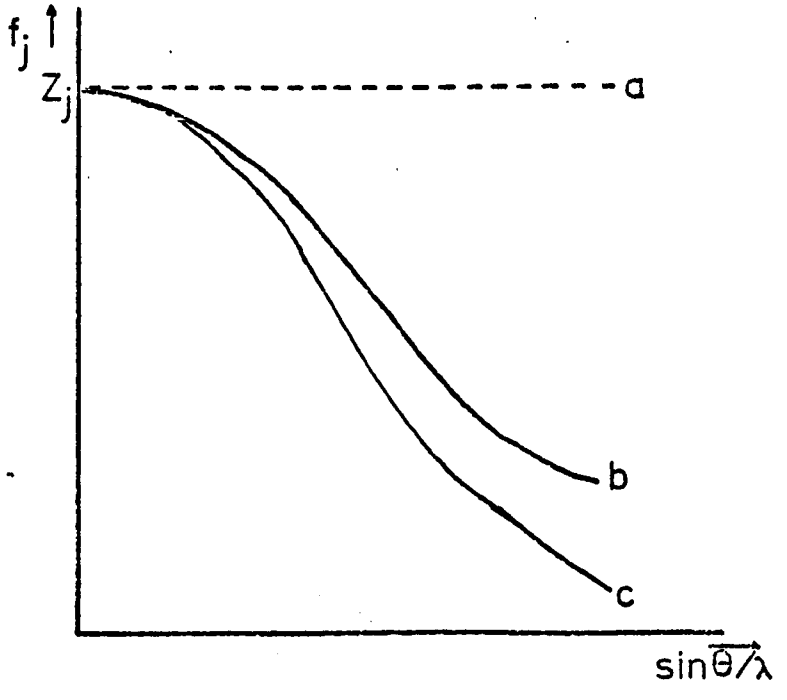

Atomic scattering factors: (a) point atom at rest, (b) stationary atom, and (c) atom corrected for thermal motion.

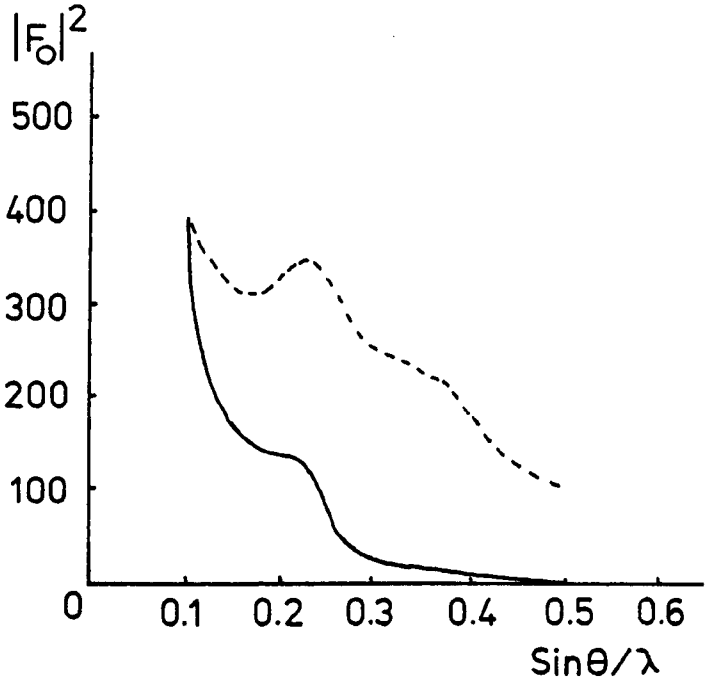

Figure 1.3

Effect of sharpening on radial decrease of local average intensity.

(Ladd & Palmer, p 226)

Figure 1.4

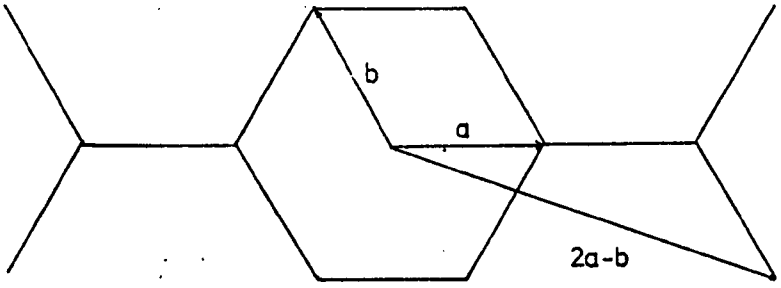

TCNQ CARBON SKELETON (showing vectors a and b)

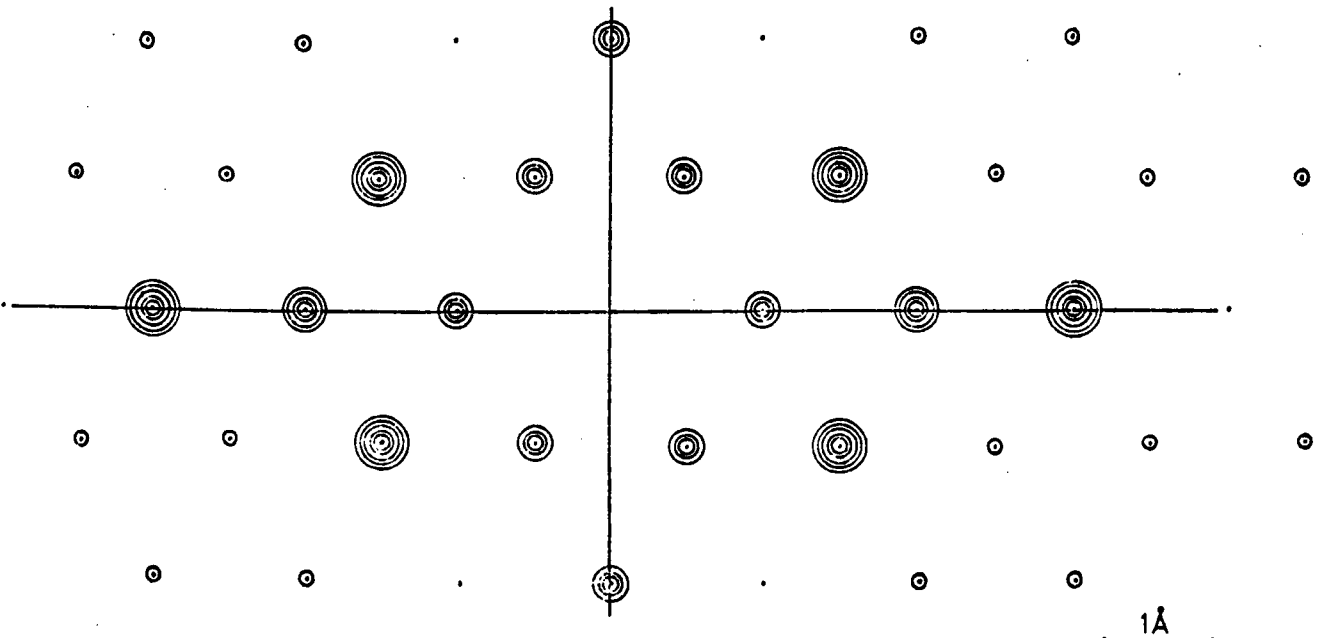

INTRAMOLECULAR TCNQ VECTORS (origin omitted)

Figure 1.6

DMPY(TCNQ)$_2$

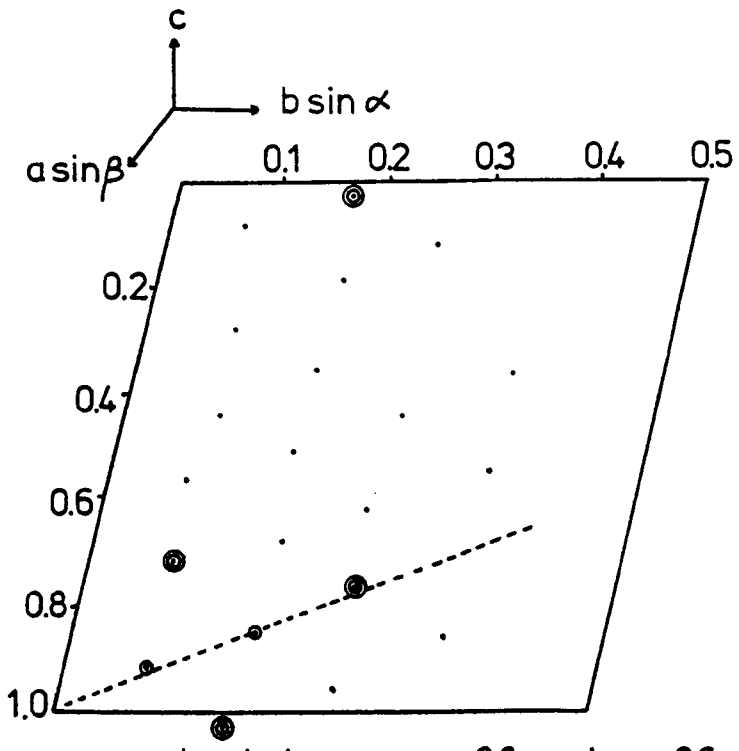

Patterson peaks between z = -.06 and z = .06

(TCNQ long axis shown -------)

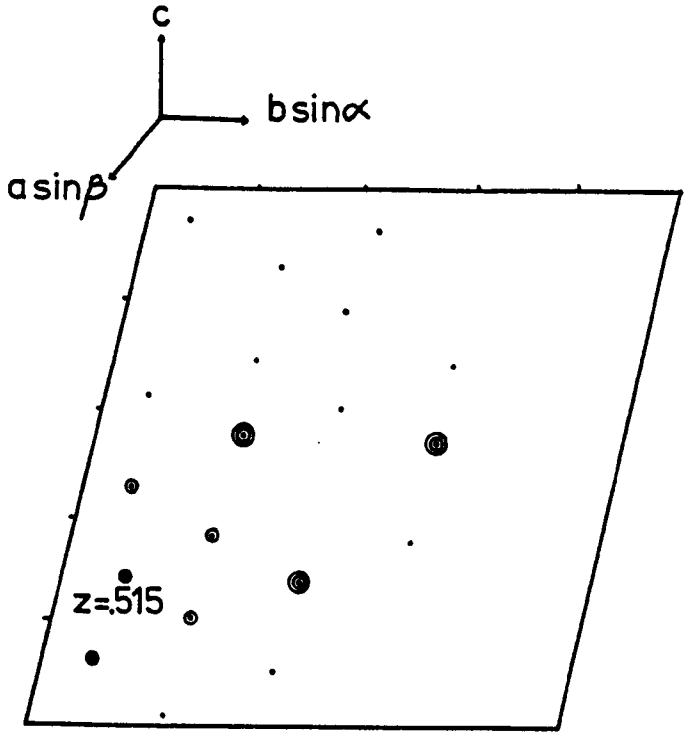

1 Å

Patterson peaks between z = .44 and z = .56

(◎ = high peak, • = centre-centre vector)

References to Chapter 1

General Bibliography

M.M. Woolfson, An Introduction to X-ray Crystallography, (Cambridge University Press, 1978).

G.H. Stout and L.H. Jensen, X-ray Crystallography.(London, Macmillan,1968)

M.F.C. Ladd and R.A. Palmer, Structure Determination by X-ray Crystallography (New York: Plennum Press, 1977).

International Tables for X-ray Crystallography, (Vol. 1, Birmingham Kynoch Press, 1971).

International Tables for X-ray Crystallography, (Vol. 3 Birmingham Kynoch Press, 1962).

P. Main, M.M. Woolfson and G. Germain, MULTAN manual (York University Printing unit, 1971).

References

1. A.L. Patterson, Phys. Rev., 46, 372, (1934).

2. A.L. Patterson, Z. Kristallogr., 90, 517, (1935).

3. J.R. Carruthers and J.S. Rollett, CRYSTALS suite of X-ray Crystal Structure Programs (Oxford University). 1972.

4. N.J. Drew, Ph.D. Thesis, University of Nottingham (1978).

5. D. Sayre, Acta Crys., 5, 60, (1952).

6. W. Cochran and M.M. Woolfson, Acta. Crys., 8, 1, (1955).

7. G. Germain, P. Main and M.M. Woolfson, Acta. Crys., A27, 368, (1971).

8. H. Hauptman and J. Karle, Solution of the Phase Problem I. The Centrosymmetric Crystal, American Crystallographic Association Monograph No. 3 (1953).

9. E.W. Hughes, Acta Crys., 6, 871, (1953).

THE CRYSTAL STRUCTURE OF 1,4-DIMETHYLPYRIDINIUM (7,7,8,8-TETRACYANOQUINODIMETHANIDE)$_2$, DMPY$^+$ (TCNQ)$_2^-$

2.1 During previous research work in this department on bipyridyl cations and their TCNQ salts it was found that one compound in particular, (1,2-bis(1-ethyl-4-pyridinio)ethylene)$^{2+}$ (TCNQ)$_4^{2-}$, DEPE (TCNQ)$_4$, yielded single crystal X-ray photographs of a highly conducting ($\sigma_{300} \approx 3\Omega^{-1}$ cm^{-1}) phase which, when the unit cell parameters were calculated from oscillation and Weissenberg photographs appeared to contain only one cation per unit cell although the lowest multiplicity consistent with the assigned space group ($P_{2_1/C}$) was two-fold. One possible interpretation of that structural contradiction was the cation might have fragmented during the synthesis of the complex into two monopyridinium cations[1]. Loss of quaternising hydrogen atoms during synthesis or re-crystallisation has already been postulated in the case of the N-hydro cations of the 1,2-bis(4-pyridinio)ethane and 1,2-bis(4-pyridinio)propane complex salts[2]. To check this possibility, a program of producing complex salts of these so-called 'half-cations' was undertaken as part of this research.

2.2 Experimental

A number of small, black, rectangular, plate-like crystals of the DMPY complex were separated from the microcrystalline powder of the product (for compound preparation see Chapter 6) and examined by means of single crystal X-ray oscillation and Weissenberg

photographs using Cu Kα radiation (λ = 1.5418 Å).
The photographs were taken on a Unicam camera.

The cell dimensions and space group were determined from these photographs and the best crystal (i.e. that which gave the least diffuse diffraction pattern) was selected for use in the intensity data collection. The data were collected on a Hilger and Watts computer-controlled four circle diffractometer at ambient temperature (19°C), using Mo Kα radiation (λ = 0.71069 Å) with a graphite monochromator. Accurate cell dimensions were obtained based on 14 selected reflections having $11^{\circ} < \theta < 13^{\circ}$ and intensity data were collected using a $\theta/2\theta$ scan for $\theta < 25^{\circ}$. As no significant variations were observed in the intensities of the three standard reflections (which were counted every 100 reflections) the data were normalised to a constant value of one single standard before data reduction. This reflection was chosen from the three standards such that it neither minimised nor maximised the effects of fluctuations in the data. Of 2362 reflections collected, 1398 were non-equivalent and considered observed in that I, the intensity of a reflection, was greater than three times its estimated standard deviation, i.e. $I > 3\sigma(I)$. The data were corrected for Lorentz and polarisation effects, but not for absorption.

Crystal Data

DMPY $(TCNQ)_2$, $(C_7H_{10}N)^+ (C_{12}H_4N_4)^-_2$, $M_r = 516.2$

Triclinic, a = 7.833(3), b = 13.889(4), c = 7.171(4)Å, $\alpha = 106.81(4)$, $\beta = 112.50(2)$, $\gamma = 95.36(3)$;

U = 671.4 Å^3, Z = 1, $D_c = 1.274$ g. cm^{-1} (Z was assigned as being equal to 1 on the basis of the cell volume and by comparison with other related structures, as insufficient material was available for the density to be measured).

Mo Kα ($\lambda = 0.71069$ Å), $\mu = 0.88$ cm^{-1}

Space group $P\bar{1}$ (No. 2), assumed.

2.3 Structure determination and refinement

Since consideration of the cell volume indicated that two TCNQ molecules were required in the unit cell, it followed from the stoichiometry of the complex that only one cation could be placed within the unit cell. This cation would have to be placed therefore on a centre of symmetry if the space group were genuinely $P\bar{1}$, and as the cation is clearly not symmetric by virtue of the quaternised nitrogen, either the space group as it stands would have to be incorrect, and ought to have been P1 (non-centrosymmetric) or there would have to be a random 180° reversal of the cation in different 'unit cells' to account for the apparent centre of symmetry. The non-centrosymmetric case is discussed more fully later.

The structure was solved by the Patterson method because of the strong and easily recognisable vector pattern of the TCNQ

molecule (see fig. 1.4, Chapter 1). Examination of the three-dimensional Patterson function revealed this typical vector pattern about the origin (shown in Fig. 2.1 related to 1,0,0) thus indicating the orientation of the TCNQ molecule, and around a strong peak at 0.704, 0.058, 0.515, which was assumed to be the common vector between the atoms of the two centrosymmetrically related TCNQ'S. In this manner, the position of the centre of the molecule was deduced at a point sited at half this vector distance from the origin.

Full matrix least-squares refinement of the positional and isotropic thermal parameters of the TCNQ molecule, followed by a difference Fourier synthesis based on ($|FO| - |FC|$), revealed the positions of the four non-hydrogen atoms of the cation within the asymmetric unit, centred about $(\frac{1}{2},\frac{1}{2},\frac{1}{2})$. Further isotropic full matrix least-squares refinement of the non-hydrogen atoms of the entire structure led to R = 0.141, at which point a difference Fourier synthesis showed the positions of possible H atoms on the TCNQ ring and the cation ring. Hydrogen atoms were then placed in calculated positions for both the cation and the TCNQ rings since the interatomic bond lengths and angles for the hydrogen peaks indicated that the positions observed in the difference Fourier synthesis for these atoms were likely to be less accurate than those obtained by calculation. Anisotropic full matrix least-squares refinement of the non-hydrogen atoms of this trial structure gave R = 0.0895 at which point a Chebyshev weighting scheme of the form:

$$W = 1.0/(A[0]T[0]'(X) + A[1]T[1]'(X) + \ldots + A[NP-1]T[NP-1]'(X))$$

with coefficients,

A[0] = 3.67 A[1] = 10.57 A[2] = 48.7 A[3] = 65.4 A[4] = 35.7, (deduced by the program so as to minimise the function $X = \sum(Fo-Fc)^4$ over all reflections) was introduced, which led to R = 0.0898. Attempts to determine the positions of the methyl hydrogens were unsuccessful, with a difference Fourier synthesis indicating scattering matter in the vicinity of the methyl C atom but no preferred orientation. Examination of the ratios of each calculated parameter shift to the estimated standard deviation of that parameter indicated that the structure had converged as far as appeared to be possible under the circumstances (max. shift/e.s.d. = 0.19, more typical shift/e.s.d. = 0.05). At this stage in the solution of the structure it was decided to investigate whether or not there was any evidence for a non-disordered cation in a non-centrosymmetric space group, so a new trial structure was attempted based on the space group P1.

After fixing the x, y, and z coordinates of a carbon atom within one of the TCNQ rings in order to define the origin, the solution of the structure, on the basis of a cation whose scattering matter for all the ring atoms was described in terms of atomic scattering factors for carbon, proceded routinely until apparent convergence occurred at R = 0.0674, with a maximum value of the ratio shift/e.s.d. of 0.68 (and more typically around 0.2).

At this stage in the refinement it was apparent that the geometry of the molecules within the unit cell was somewhat distorted,

with the TCNQ moieties in particular showing a degree of asymmetry, as is shown in figures 2.2 and 2.3. Although the angles in the cation (see figure 2.4) indicated a possible preferred position for the nitrogen atom at 0.572, 0.461, 0.653, by comparison with the geometries of other salts containing methyl pyridinium groups[7,10,11], this was not borne out by the bond lengths and the geometry again was rather distorted.

Numerous attempts were made to distinguish the N^+ hetero-atom by assigning atomic scattering factors for N to the 1 and 4 positions of the ring in turn; however, subsequent refinements of the thermal, positional, and occupancy parameters for each of the possible configurations showed no significant differences ($R = 0.0688$ and $R = 0.0698$ for N in the 1 and 4 positions respectively and thermal parameters for each configuration almost identical). Refinement based on a homonuclear ring of C atoms gave $R = 0.0657$ and inspection of the atomic scattering factors calculated from 6/7 of neutral nitrogen scattering[3], as an approximation to the scattering of N^+, showed there to be little difference between these figures and the atomic scattering factors for carbon.

A Hamilton weighted R - test[3] on the two trial structures based on 1398 reflections showed the P1 trial to be a significantly more reliable structure. It was not, however, possible to analyse the structures in the manner of Rothskin, Richardson and Bell[4], which is possibly more applicable than the Hamilton R test ratio for problems in which two or more structural models are expressed in terms of the same sets of parameters.

In spite of the evidence of the Hamilton R test ratio, it was considered that the evidence for one preferred cation orientation in the space group P1 was weak, and in view of the large deviations from symmetrical geometry of the TCNQ molecules in this space group it was finally decided that the most likely structure was that in which the cation was subject to a random 180° reversal, giving the space group $P\bar{1}$. Accordingly, the structural discussion is based on this sclution. The thermal motion of the atoms was analysed in terms of rigid body motion[5] and librational ccrrections were applied on the basis of this analysis. Least-squares planes were also calculated for the non-hydrogen atoms of the TCNQ moiety and the half-cation of the asymmetric unit.

2.4 Description and Discussion of the Structure

Figures 2.5, 2.6 and 2.7 show projections of the structure down the a, b and c axes respectively of the unit cell, and Table 2.4 shows details of the short intermolecular contacts. The TCNQ molecules may be considered to form stacks in two ways, either as a stack of dimers along c, or as a stack of dimers along the $[1\ 0\ \bar{1}]$ diagonal axis. In the first case the stack may be defined by the molecules A", A, and A'; the second case is defined by the molecules A", A, and A'''. The separation of the planes (see Table 2.3 for details of molecular planes) of the A' - A molecular pair is 3.14 Å when the least squares plane of the whole molecule is considered, and those of A" - A and A''' - A are 3.21 Å and

3.15 Å respectively. When the ring planes of the molecules are considered these separations become A' - A = 3.23 Å, A" - A = 3.11 Å, and A''' - A = 3.22 Å. The changes in the mean plane positions, according to how much of the molecule is considered, arise mainly from a bowing of the TCNQ moieties away from that moiety (A") with which it forms a good overlap (see Figure 2.8) and the shortest intermolecular contacts. Because of the close similarity of the interplanar spacings and intermolecular contacts of various symmetry related molecules it is not possible to say with any degree of certainty whether or not there is a preferred stacking axis. The molecular overlaps of A' - A and A''' - A are almost identical, with the displacement of the adjacent dimer involving A''' being very slightly greater than the displacement of the adjacent dimer involving A', and the inter-diad contacts are not significantly shorter for A' or A''' so that no evidence for a preferred stack is found from this information.

The cation must be disordered by virtue of the space group symmetry (see Section 2.3) and lies in the channel at the centre of the cell between the TCNQ molecules and on average is centro-symmetrically disposed about the centre of symmetry at $(\frac{1}{2},\frac{1}{2},\frac{1}{2})$. There are no short nearest neighbour contacts (< 3.8 Å) between cations; however, a number of TCNQ - cation contacts lie within 3.6 Å, the shortest being 3.274 Å (N(2) - C(31^{vi})) and 3.298 Å (N(2) - C(27^{v})), both of which are contacts to terminal nitrogen atoms of the cyano groups. These values are just greater

than the sum of the van der Waals radii[17] of the atoms. The shortest intra-diad contacts are 3.200 Å (C(3) - C(5^{i})) and 3.222 Å (C(1) - C(10')), indicating some slight degree of interaction, whilst the shortest inter-diad contacts, at 3.349 Å (C(9) - N(3")) and 3.355 Å (C(6) - C(3^{vii})) are only slightly longer, and still indicate some degree of interaction.

The molecular geometry of the TCNQ and cation moieties is shown in Figures 2.9 and 2.10. The bond angles and distances for the TCNQ moiety are intermediate between those of $TCNQ^{o}$[6] and the mean values obtained for $TCNQ^{-}$[7], and all chemically equivalent bonds are equal to within 1σ. The charge on the molecule was determined by the method of Chasseau and Flandrois[8] and found to be -0.49e, insignificantly different from the -0.5e expected from the centrosymmetric space group and the number of TCNQ moieties in the unit cell. The disordered cation appears to have a geometry consistent with the superposition of two cations of normal dimensions with opposite orientations. The length of the bond parallel to the long molecular axis (1.365(9) Å) and the mean length of the bonds joining this bond to the carbon and nitrogen to which the ring substituents are attached (mean = 1.35(2) Å)* are in close agreement with the equivalent bonds in 1-methyl-pyridinium iodide[9] where the bond parallel to the molecular axis has a mean of 1.35(3) Å, a C-C distance of 1.42(3) Å, and a C-N distance of 1.34(2) Å,

* Deviations for the mean values are calculated from the formula

$$\sigma_{n-1} = \frac{1}{n-1} \cdot \Sigma (\bar{x} - x_i)$$

as well as the corresponding bond lengths 1.34(2) Å, 1.40(3) Å and 1.35(1) Å in 1,2-bis (1-methyl-4-pyridinio)ethane $TCNQ_4$ [10], and means of 1.375(21) Å, 1.391(14) Å, and 1.346(4) Å in the halide salts of the 1,1'-dimethyl-44'-bipyridylium ions[11]. The exocyclic bond (1.509(8) Å) is in good agreement with that of C-N^+ = 1.495(6) Å in 1,1'-dimethyl-4,4'-bipyridylium $TCNQ_3$ [7] but appears to be slightly longer than the values 1.409(15) Å, 1.466(9) Å, and 1.450(15) Å observed for the equivalent bond in the substituted bipyridyl salts[11]. The equivalent bond in the 1,2-bis-(1-methyl-4-pyridinio)ethane $TCNQ_4$ complex is 1.48(1) Å [10], whilst the distances found for the same bond in the inorganic complexes such as the 1,1'-dimethyl-4,4'bipyridylium salt with $CoCl_4^{2-}$ [12] and the 4-methyl-pyridine bis thio- acetate of Nickel[13] are 1.48 Å and 1.50(2) Å respectively. The exocyclic bond is also similar to the substituent bond length of 1.51(3) Å seen in the 4-methyl-pyridine platinum complex with ethylene, $C_8H_{11}Cl_2NPt$ [14]. As is expected from the disorder, the length of the exocyclic bond in the present structure is intermediate between the lengths of typical C-N and C-C exocyclic bonds [e.g. 16]. Unfortunately, the anisotropic thermal parameters of C(25) and C(31) do not show any particular major axis of thermal motion, whereas a greater apparent thermal motion along the molecular axis might be expected as a feature of the disordered nature of the cation.

The bowing of the TCNQ molecule referred to above is thought to be genuine, and has been observed in the DMPB $(TCNQ)_4$ complex

investigated by the author (see Chapter 3) as well as the 1,3-(1-pyridinio) propane $TCNQ_4$ structure[15], the substituted morpholinium series of salts $MEM(TCNQ)_2$, $DEM(TCNQ)_2$, and $DMM(TCNQ)_2$[18,19,20], and other TCNQ complex salts[e.g. 7,10], and appears to relieve repulsions between the slightly negatively charged[21] and highly electronegative terminal cyano groups of TCNQ moieties within the dimer. As well as being bowed, the TCNQ moieties are also distorted by a twist of the $C(CN)_2$ groups with respect to the ring plane of the molecule. This can be seen in the deviations from the least squares plane of the molecule (see Table 2.3), and the C(7) - C(9) and C(10) - C(12) groups form dihedral angles of 3.9° and 2.8° respectively with the plane of the ring. The TCNQ molecule makes an angle of 4.4° with the (001) plane, whilst the cation plane, based upon the entire cation including centrosymmetrically related bonding atoms, forms a dihedral angle of 51.1° with the plane of the TCNQ ring. The long molecular axis of the cation, defined by the atoms C(31) - C(25) - C(25') - C(31'), is inclined at 46.5° to the (001) plane and at 22.0° to both the (010) and (100) planes.

The structure therefore consists of a disordered cation sited apparently centrosymmetrically about $(\frac{1}{2},\frac{1}{2},\frac{1}{2})$ and surrounded by diadic groups of TCNQ moieties which are themselves sited above and almost exactly half-way between two similar diads. The powder compaction electrical conductivity (see Figure 2.11) for this compound ($\sigma_{300} = 1.7 \times 10^{-4} \Omega^{-1}\ cm^{-1}$) is fairly typical for an organic semiconductor, and is consistent with the absence of a continuous stack

of TCNQ moieties. These conductivities are in line with those measured by other workers, e.g. Przybylski et al[45] who obtained a compaction value of $\sigma_{300} = 3.54 \times 10^{-4}$ ohm^{-1} cm^{-1}, and Ahmed and Shields[46], who found $\sigma_{290} = 4.2 \times 10^{-4}$ ohm^{-1} cm^{-1}. Anisotropic measurements, should suitable crystals be obtained, would be expected to show similar conductivities along $[100]$ and $[00\bar{1}]$ because of the disinclination of the structure to form discreet stacks, and a lower conductivity along $[010]$, across the cation planes. Figure 2.12 shows the relations between the crystallographic axes and crystal morphology.

Figure 2.1

DMPY(TCNQ)$_2$

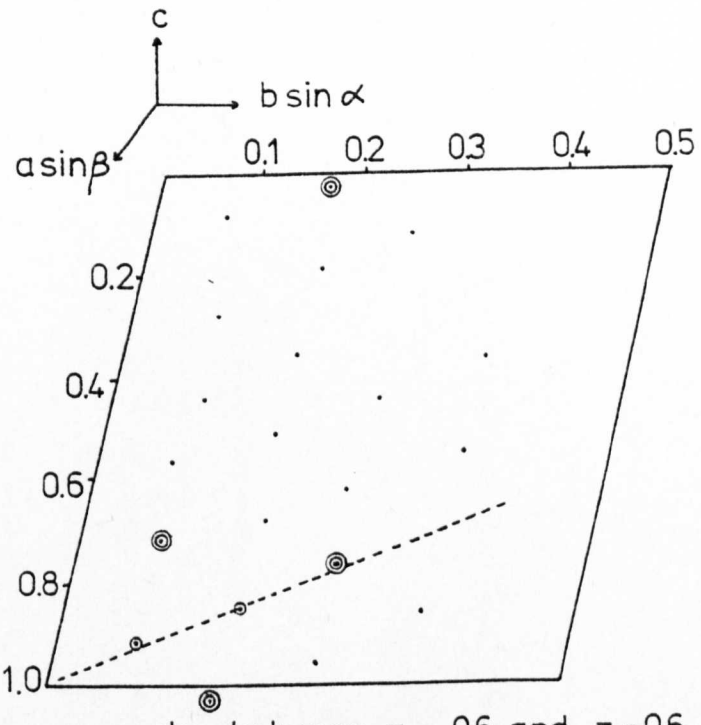

Patterson peaks between z = -.06 and z = .06

(TCNQ long axis shown -------)

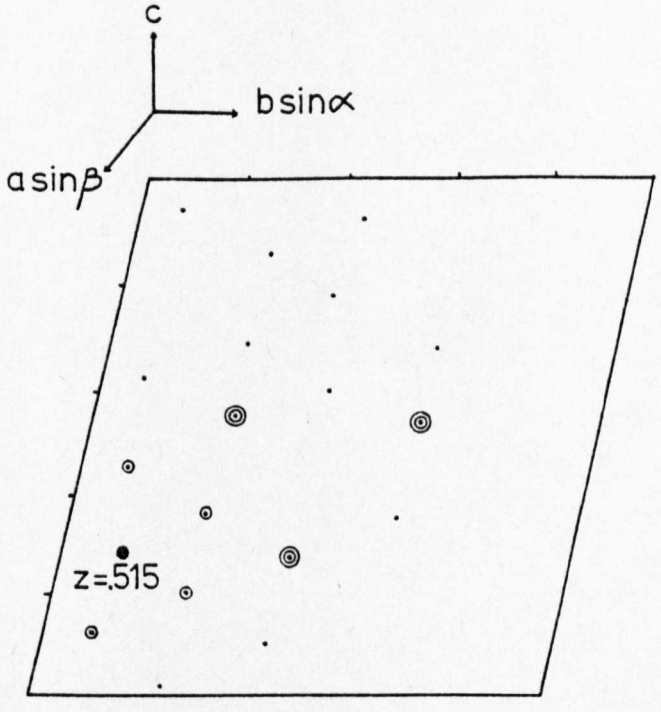

1 Å

Patterson peaks between z = .44 and z = .56

(◎ = high peak, • = centre-centre vector)

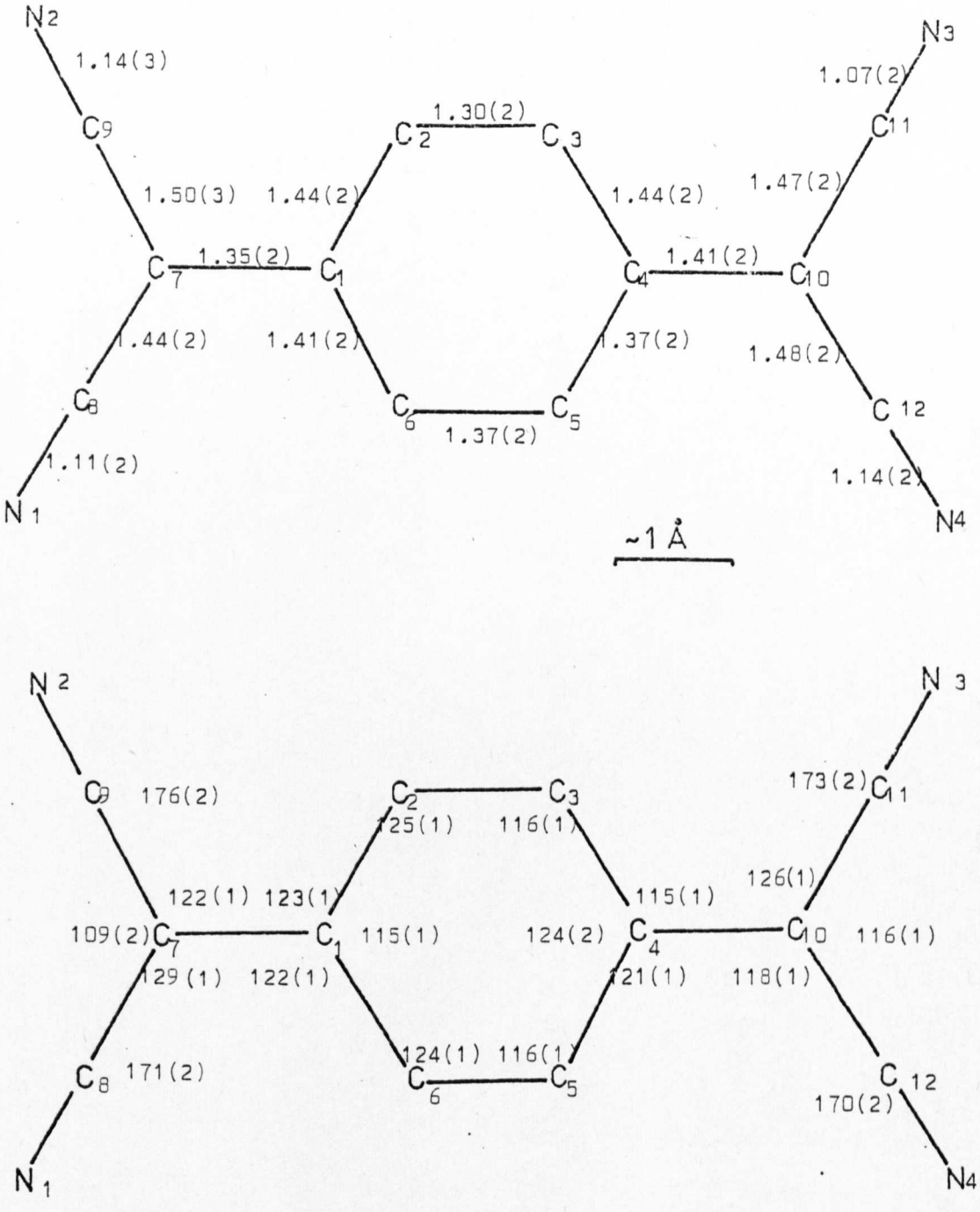

Figure 2.2 DMPY $(TCNQ)_2$ - P1 trial.

Bond lengths and angles for TCNQ(A)

(not corrected for libration).

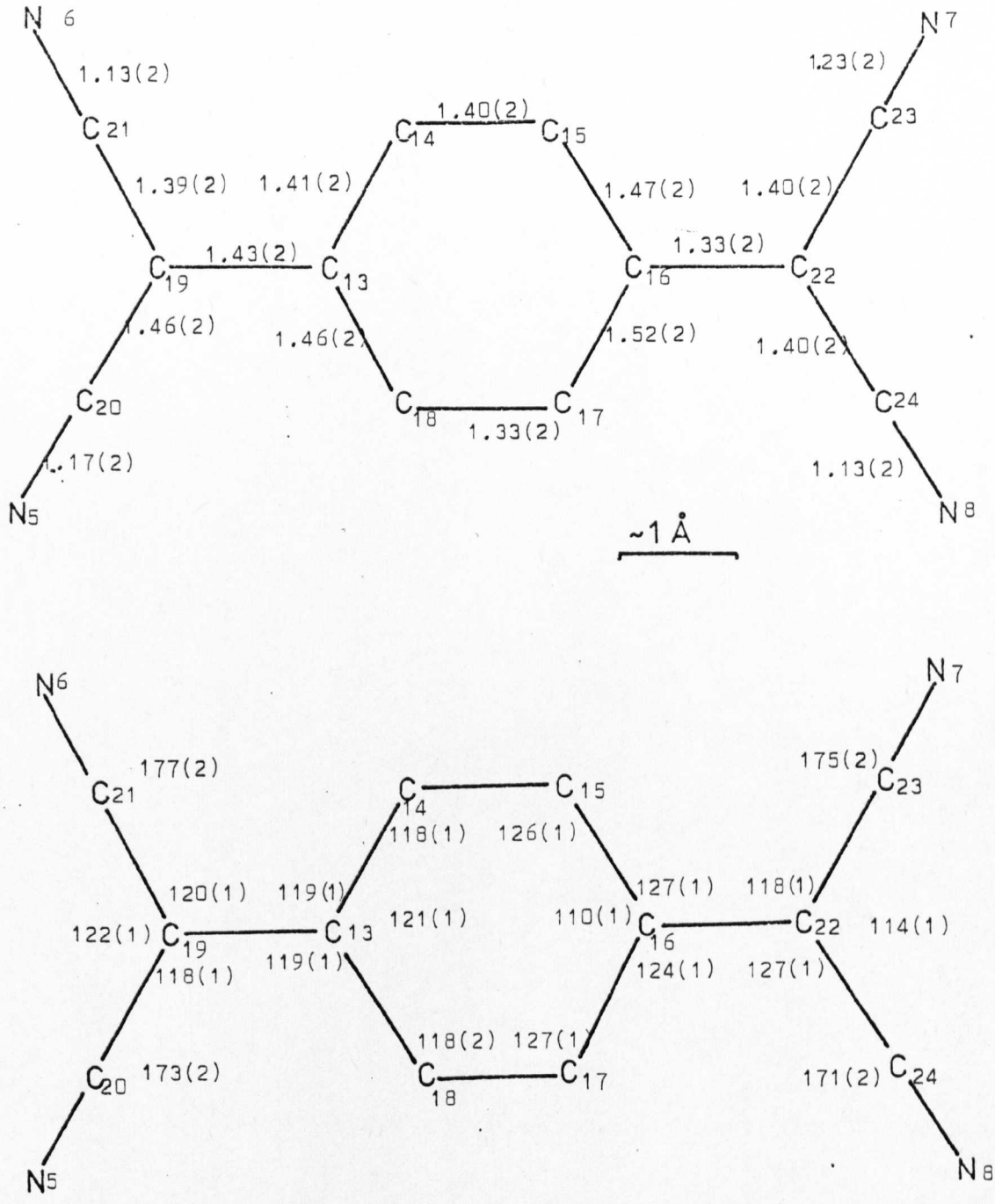

Figure 2.3 DMPY $(TCNQ)_2$ - P1 trial.

Bond lengths and angles for TCNQ (B)

(not corrected for libration).

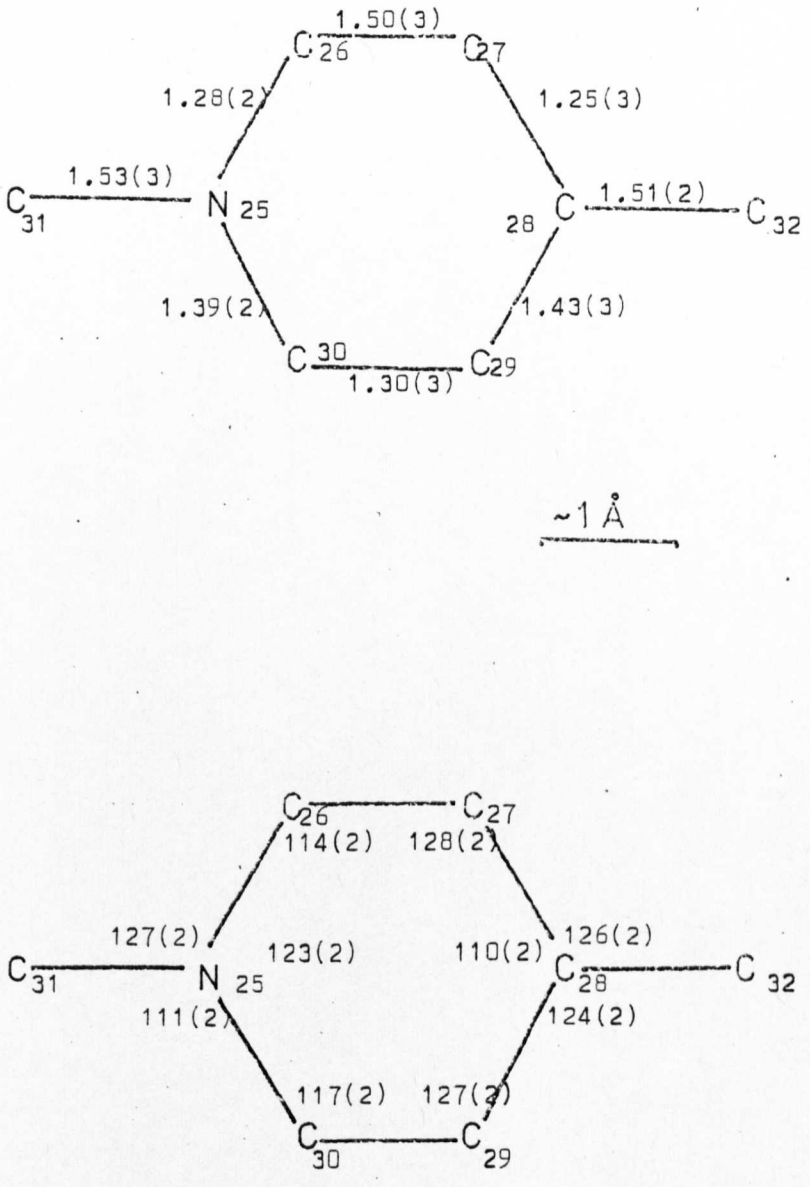

Figure 2.4 DMPY $(TCNQ)_2$ - P1 trial

Bond lengths and angles for cation

(uncorrected for libration).

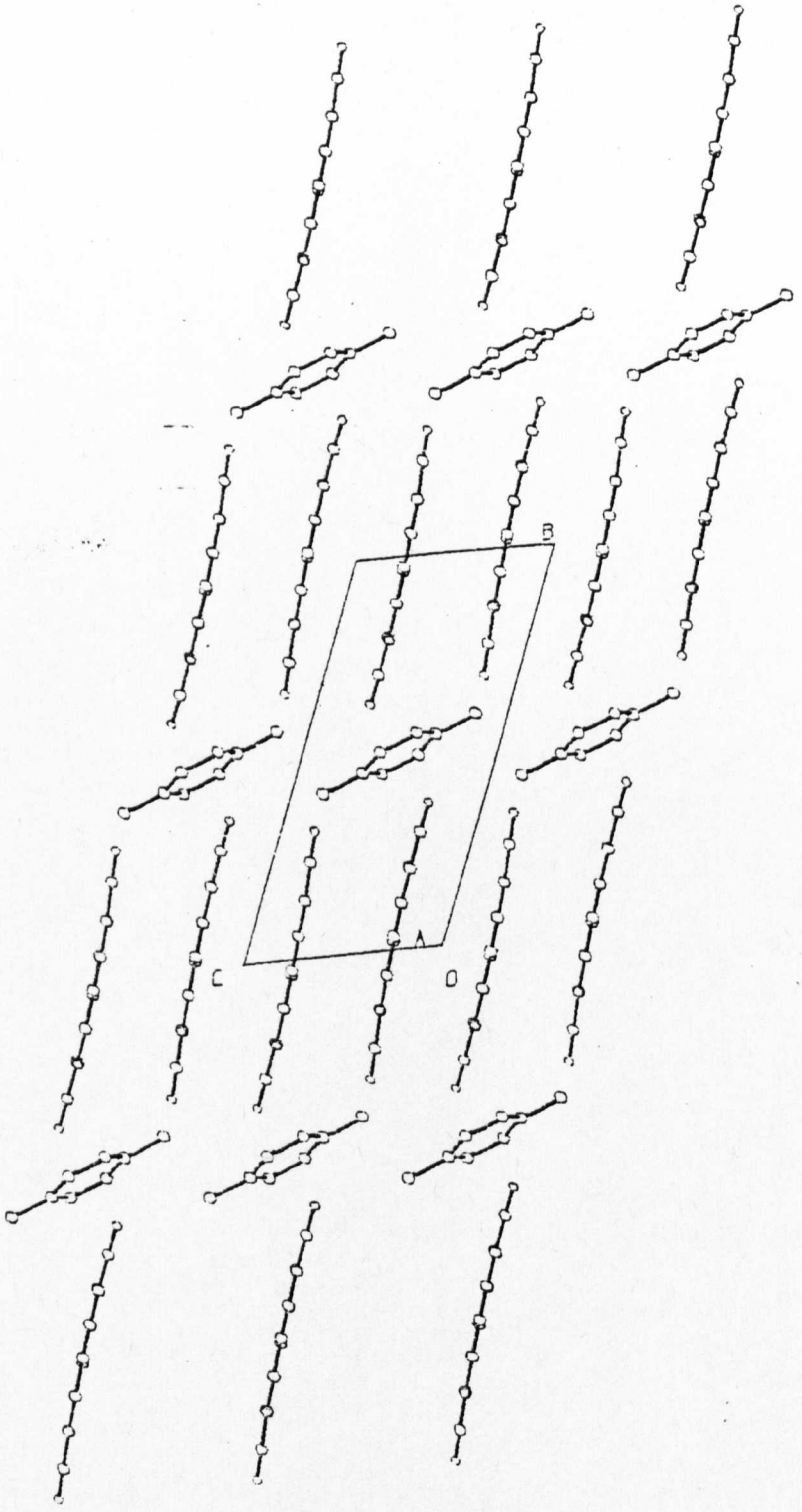

DMPY(TCNQ)$_2$ - view along a axis

Figure 2.5

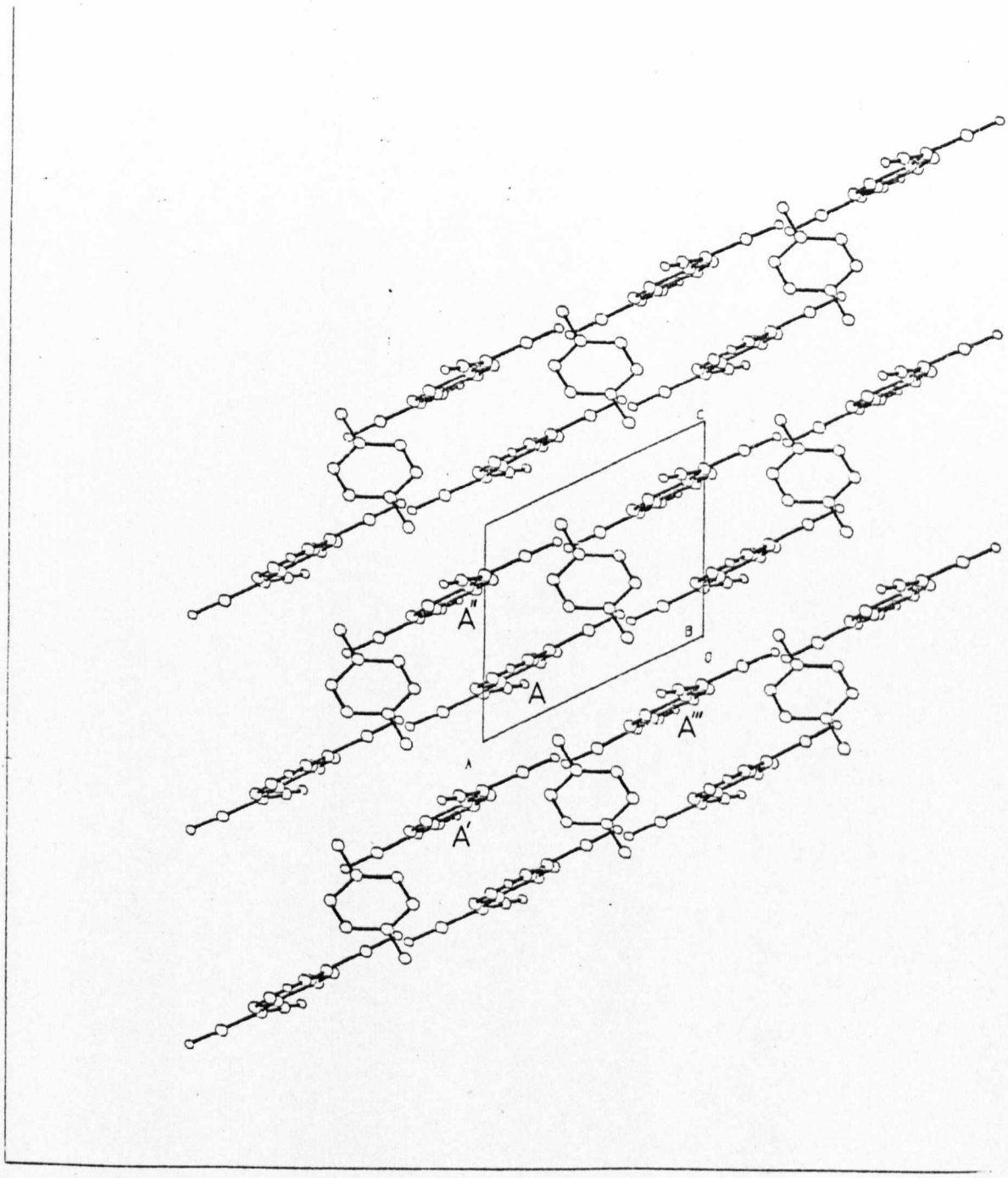

DMPY(TCNQ)$_2$- view along b axis

Figure 2.6

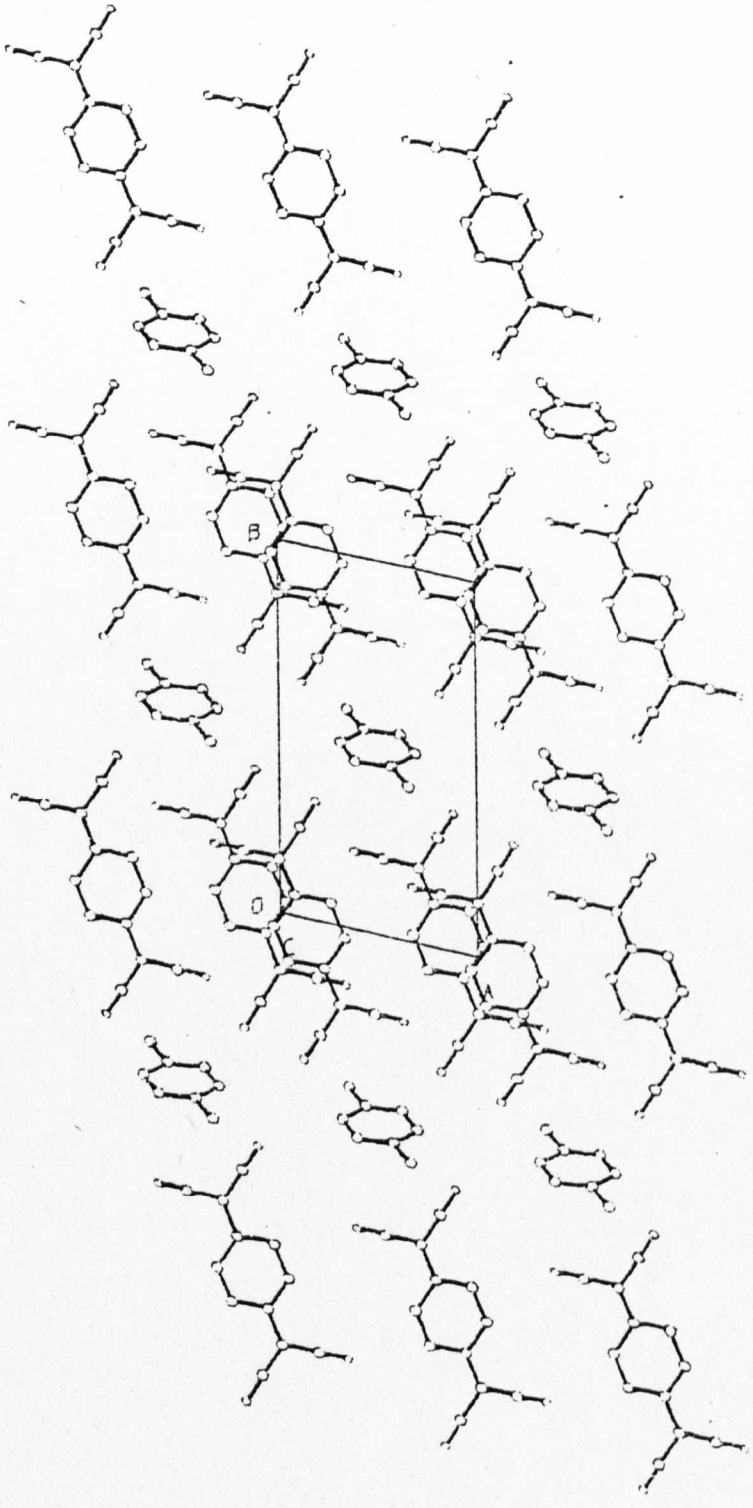

DMPY$(TCNQ)_2$ - view along c axis

FIGURE 2.7

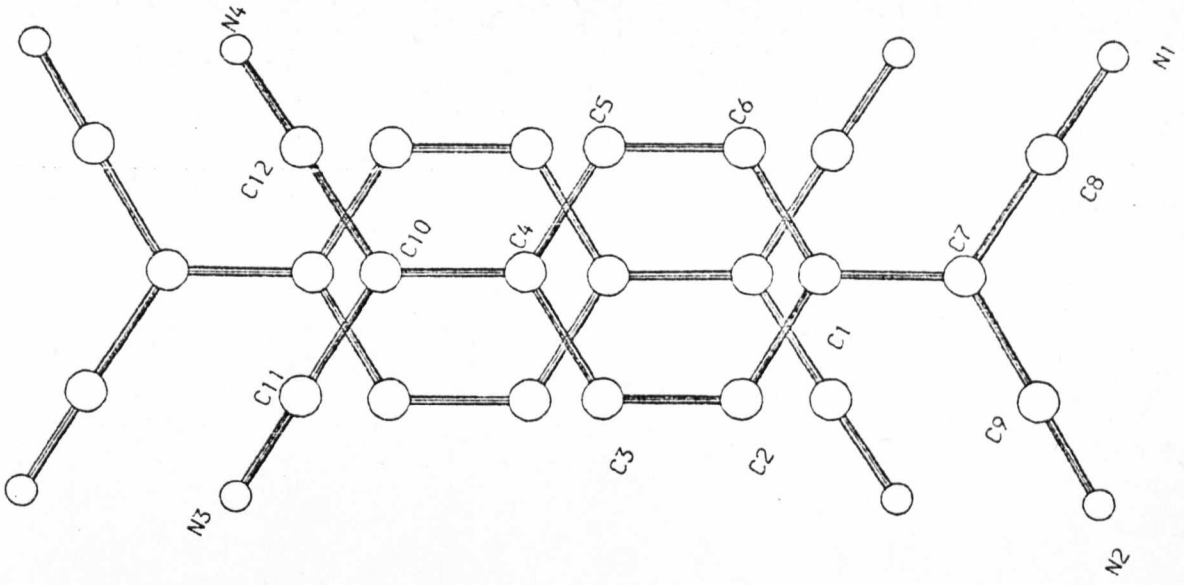

A'' on A

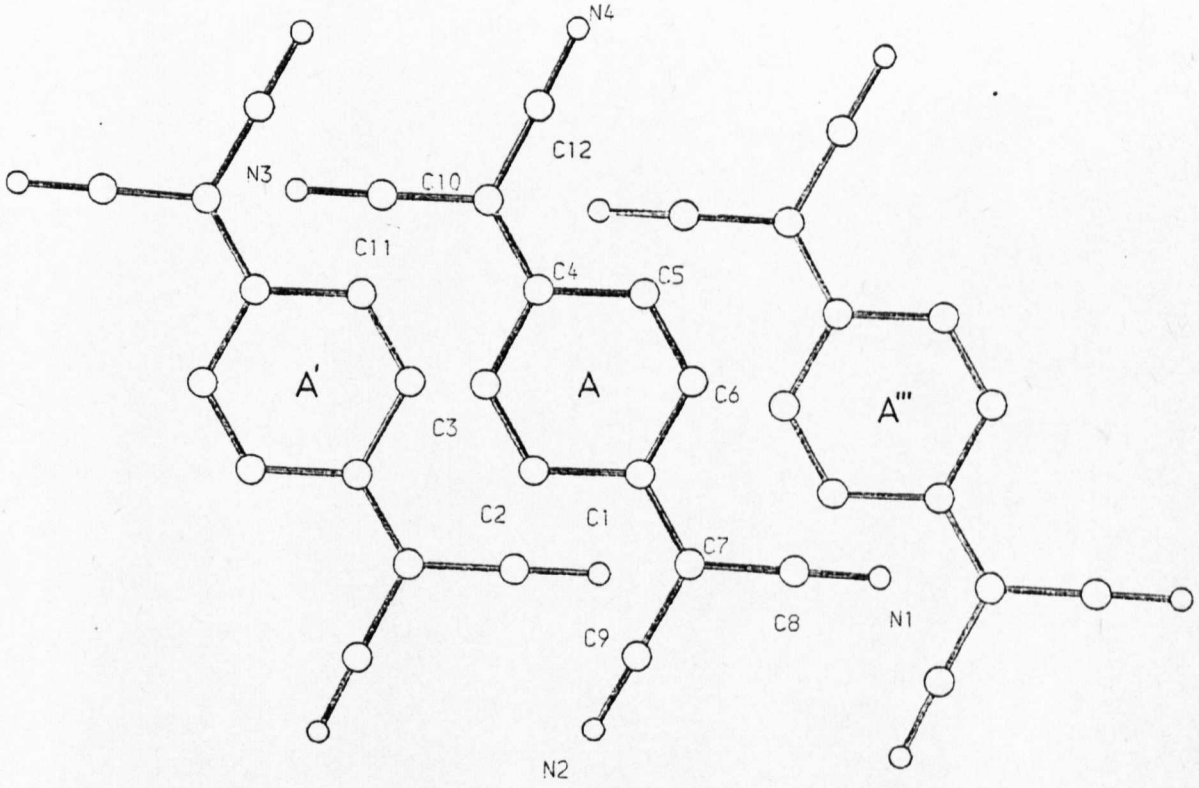

Figure 2.8 Molecular overlaps

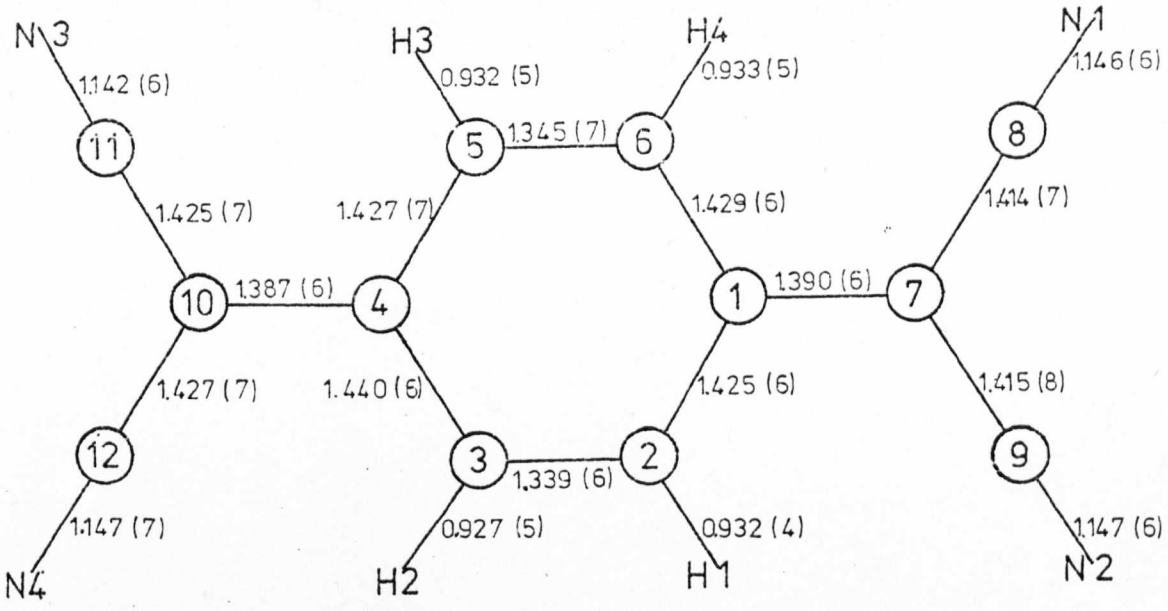

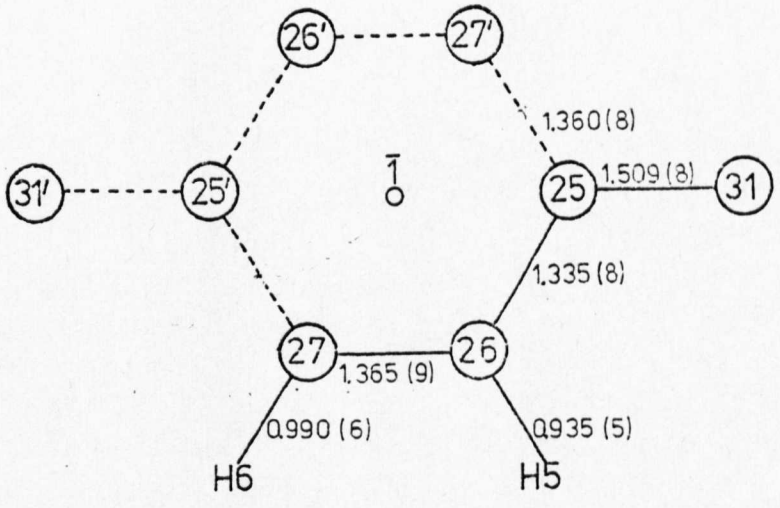

DMPY(TCNQ)$_2$ - BOND LENGTHS IN Å

(not corrected for libration)

FIGURE 2.9

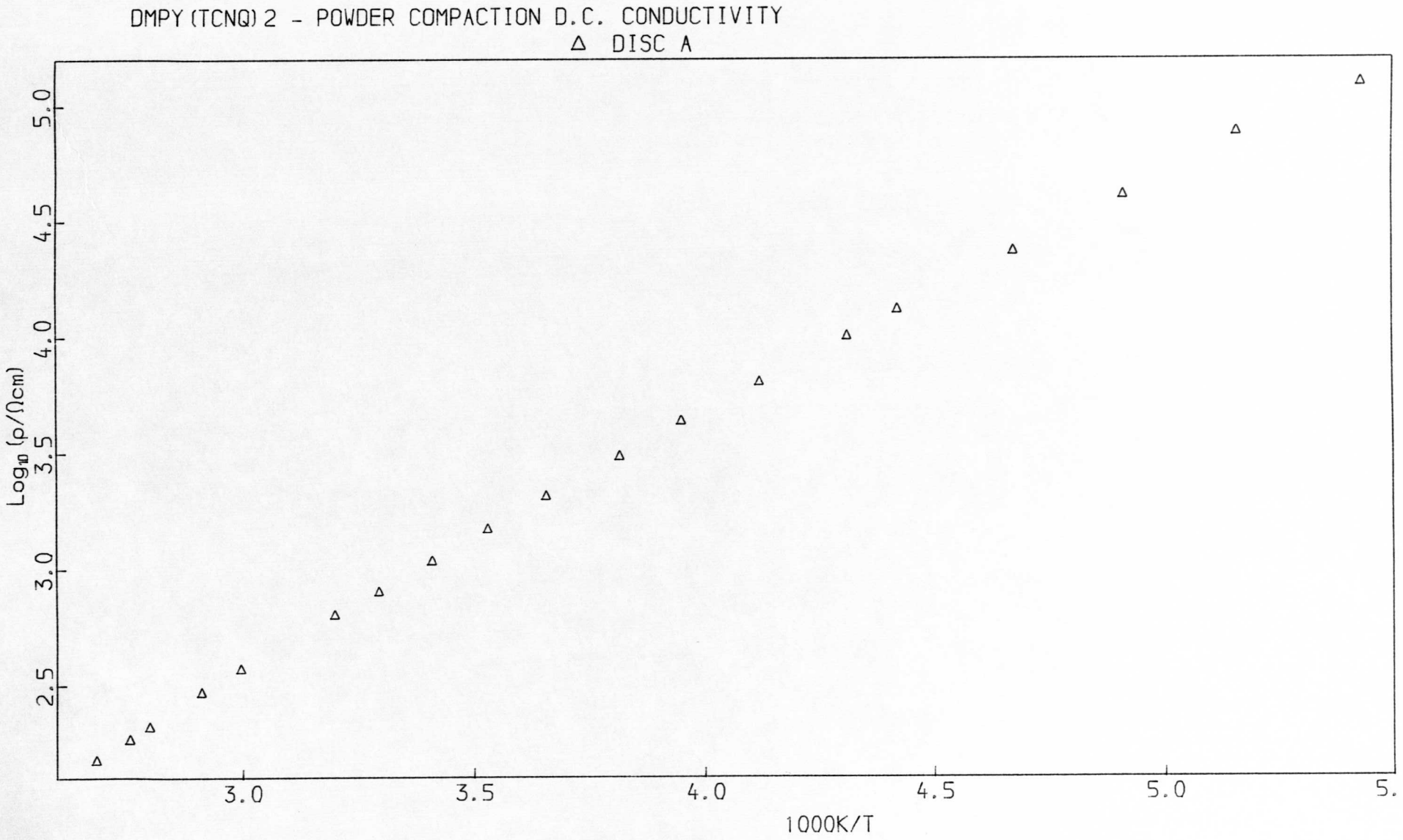
DMPY(TCNQ)2 - POWDER COMPACTION D.C. CONDUCTIVITY
Δ DISC A
Log10 (ρ/Ωcm)
5.0
4.5
4.0
3.5
3.0
2.5
3.0
3.5
4.0
4.5
5.0
5.
1000K/T

FIGURE 2.11

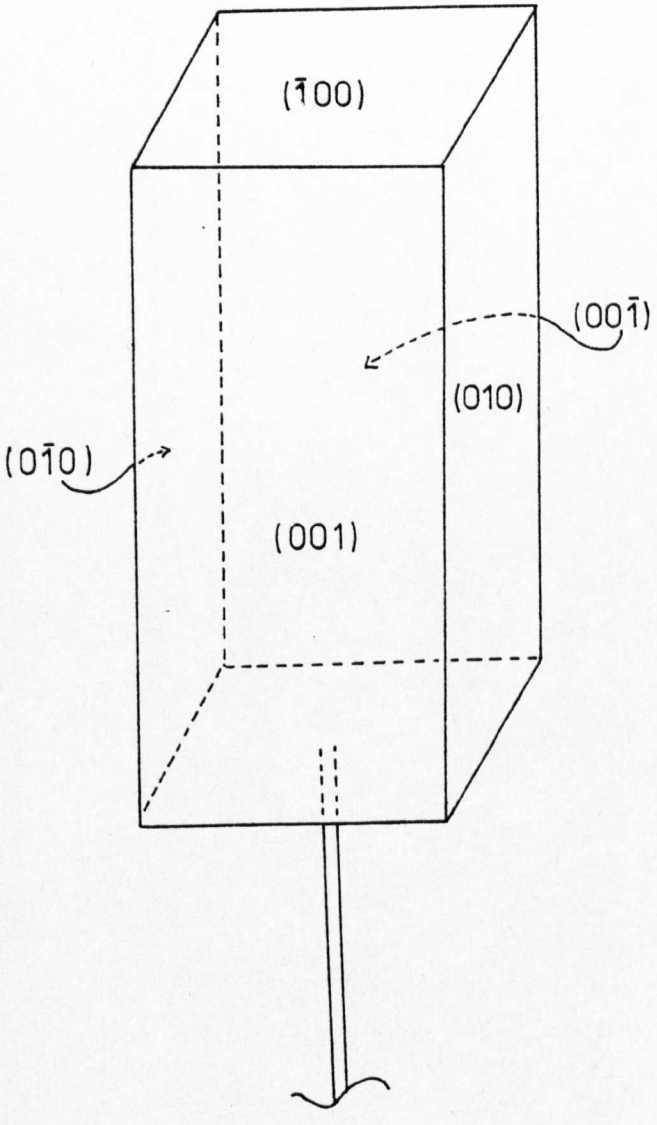

FIGURE 2.12

DMPY $(TCNQ)_2$ crystallographic and crystal faces.

TABLE 2.1 BOND LENGTHS FOR DMPY $(TCNQ)_2$

(ESTIMATED STANDARD DEVIATIONS IN PARENTHESES, $\times 10^3$)

1,4-dimethyl pyridinium cation	Uncorrected	Librationally corrected
C(25) - C(26)	1.335(8)	1.342
C(26) - C(27)	1.365(9)	1.372
C(27) - C(25')	1.360(8)	-
C(31) - C(25)	1.509(8)	1.516
7,7,8,8-tetracyanoquinodimethanide		
C(1) - C(2)	1.425(6)	1.431
C(1) - C(6)	1.429(6)	1.436
C(2) - C(3)	1.339(6)	1.340
C(3) - C(4)	1.440(6)	1.447
C(4) - C(5)	1.427(7)	1.443
C(5) - C(6)	1.345(7)	1.346
C(1) - C(7)	1.390(6)	1.392
C(7) - C(8)	1.414(7)	1.421
C(7) - C(9)	1.415(8)	1.422
C(8) - N(1)	1.146(6)	1.151
C(9) - N(2)	1.147(6)	1.153
C(10) - C(4)	1.387(6)	1.388
C(10) - C(11)	1.425(7)	1.432
C(10) - C(12)	1.427(7)	1.434
C(11) - N(3)	1.142(6)	1.148
C(12) - N(4)	1.147(7)	1.152

TABLE 2.2 $DMPY(TCNQ)_2$

Bond angles in degrees (estimated standard deviations in parentheses, $\times 10^2$)

1,4-dimethylpyridinium cation	Uncorrected	Librationally corrected
C(26) - C(25) - C(31)	122.5(6)	122.4
C(26) - C(25) - C(27')	118.4(5)	-
C(31) - C(25) - C(27')	119.2(7)	-
C(25) - C(26) - C(27)	121.4(8)	121.4
C(26) - C(27) - C(25').	120.2(6)	-
TCNQ molecule		
C(6) - C(1) - C(2)	117.4(4)	117.6
C(6) - C(1) - C(7)	121.6(4)	121.5
C(2) - C(1) - C(7)	121.0(4)	120.8
C(1) - C(2) - C(3)	121.4(5)	121.2
C(2) - C(3) - C(4)	121.6(5)	121.5
C(3) - C(4) - C(5)	116.7(5)	117.0
C(3) - C(4) - C(10)	121.2(4)	121.1
C(5) - C(4) - C(10)	122.1(4)	121.9
C(4) - C(5) - C(6)	121.6(5)	121.4
C(5) - C(6) - C(1)	121.4(5)	121.3
C(1) - C(7) - C(8)	122.8(5)	122.6
C(1) - C(7) - C(9)	121.3(4)	121.2

(Cont./..)

Table 2.2 continued.

TCNQ molecule

C(8) - C(7) - C(9)	115.9(5)	116.1
C(7) - C(8) - N(1)	179.6(6)	179.6
C(7) - C(9) - N(2)	179.4(7)	179.4
C(4) - C(10) - C(11)	122.3(4)	122.1
C(4) - C(10) - C(12)	122.1(5)	122.0
C(11) - C(10) - C(12)	115.6(5)	115.8
C(10) - C(11) - N(3)	179.1(6)	179.1
C(10) - C(12) - N(4)	178.3(7)	178.3

Table 2.3

Details of molecular planes (*denotes atoms not defining the plane).

1) TCNQ molecule

Equation of plane (all atoms):

$$-0.00963x + 0.97026y - 6.34350z + 1.578 = 0$$

Equation of plane (ring atoms):

$$-0.01012x - 1.04934y + 6.36165z - 1.605 = 0$$

x, y, and z are in crystal fractions.

Distances of atoms from planes:

Atom	Molecule (Å)	Ring (Å)
C1	-0.041	-0.006
C2	-0.051	0.000
C3	-0.051	0.006
C4	-0.030	-0.006
C5	-0.033	0.000
C6	-0.044	0.006
C7	-0.010	-0.043 *
C8	-0.029	-0.020 *
C9	0.070	-0.131 *
C10	-0.009	-0.022 *

Cont./..

Table 2.3 continued.

Atom	Molecule (Å)	Ring (Å)
C11	-0.025	-0.010 *
C12	0.074	-0.096 *
N1	-0.048	-
N2	0.146	-
N3	-0.050	-
N4	0.132	-

2) Equation of cation: (including C31)

$-2.2420x + 0.68994y + 3.43073z - 5.443 = 0$

Equation of plane (excluding C31):

$-2.24874x + 9.66935y + 3.44412z - 5.437 = 0$

Distances of atoms from the plane:

Atom	Molecule (Å)	Ring (Å)
C25	-0.001	0.000
C26	-0.001	0.000
C27	0.001	0.000
C31	0.001	0.005 *

TABLE 2.4 Short intermolecular contacts

Intra-diad (A - A") 3.4 Å

Atoms	Å
C(1) - C(10^{i})	3.222
C(1) - C(11^{i})	3.373
C(2) - C(10^{i})	3.380
C(2) - C(12^{i})	3.343
C(3) - C(4^{i})	3.356
C(3) - C(5^{i})	3.200
C(4) - C(5^{i})	3.372
C(6) - C(10^{i})	3.378
C(6) - C(11^{i})	3.251

Inter-diad (A-A', A-A"' , etc) 3.6 Å

C(1) - N(3^{ii})	3.542
C(2) - C(11^{ii})	3.488
C(3) - C(3^{ii})	3.402
C(7) - C(3^{ii})	3.431
C(9) - N(3^{ii})	3.349
C(2) - N(1^{v})	3.364
C(3) - N(1^{v})	3.398
C(4) - N(1^{x})	3.479
C(5) - N(1^{x})	3.472
C(6) - N(3^{vii})	3.355

Cont./..

Table 2.4 continued

C(6) - C(6^{x})	3.474
C(10) - N(1^{x})	3.527
C(12) - N(1^{x})	3.515

TCNQ - cation 3.6 Å

C(9) - C(27^{iii})	3.561
N(1) - C(25^{iv})	3.449
N(1) - C(26^{iv})	3.333
N(2) - C(26^{v})	3.561
N(2) - C(27^{v})	3.298
N(2) - C(31^{vi})	3.274
N(2) - C(27^{iii})	3.426
N(4) - C(31^{viii})	3.505
N(4) - C(26^{ix})	3.588

Symmetry operations

i	2-x	-y	1-z	vi	x	y	-z
ii	2-x	-y	-z	vii	x-1	y	z
iii	1-x	1-y	1-z	viii	x	y-1	z-1
iv	x	y	z	ix	1-x	y	1-z
v	1+x	y	z	x	1-x	-y	-z

ATOM	X/A	Y/B	Z/C	U(ISO)
C(1)	0.7773(6)	0.1191(4)	0.2722(7)	
C(2)	0.9593(7)	0.1198(4)	0.2736(7)	
C(3)	1.0310(7)	0.0354(4)	0.2607(8)	
C(4)	0.9262(7)	-0.0603(4)	0.2429(7)	
C(5)	0.7444(7)	-0.0602(4)	0.2436(8)	
C(6)	0.6738(7)	0.0250(4)	0.2584(8)	
C(7)	0.7027(7)	0.2064(4)	0.2803(8)	
C(8)	0.5241(8)	0.2097(4)	0.2846(8)	
C(9)	0.8013(8)	0.2975(4)	0.2820(9)	
C(10)	0.9999(7)	-0.1478(4)	0.2261(7)	
C(11)	1.1826(8)	-0.1479(4)	0.2282(8)	
C(12)	0.8950(8)	-0.2446(4)	0.1983(9)	
H(1)	0.3794(7)	0.2118(4)	0.2881(8)	
H(2)	0.8802(8)	0.3710(4)	0.2811(9)	
H(3)	1.3295(7)	-0.1487(4)	0.2319(8)	
H(4)	0.8147(8)	-0.3232(4)	0.177(1)	
C(25)	0.5706(9)	0.4598(4)	0.6605(9)	
C(26)	0.384(1)	0.4523(5)	0.560(1)	
C(27)	0.3118(9)	0.4922(5)	0.401(1)	
C(31)	0.654(1)	0.4167(6)	0.838(1)	
H(1)	1.0310	0.1802	0.2834	0.0600
H(2)	1.1507	0.0384	0.2631	0.0600
H(3)	0.6725	-0.1204	0.2336	0.0600
H(4)	0.5546	0.0225	0.2589	0.0600
H(5)	0.3016	0.4189	0.5992	0.0600
H(6)	0.1860	0.5030	0.3170	0.0600

ATOM	U(11)	U(22)	U(33)	U(23)	U(13)	U(12)
C(1)	0.039(3)	0.048(3)	0.038(3)	0.013(2)	0.015(2)	0.007(2)
C(2)	0.046(3)	0.042(3)	0.046(3)	0.022(2)	0.022(3)	0.008(2)
C(3)	0.041(3)	0.053(3)	0.046(3)	0.021(2)	0.023(2)	0.009(2)
C(4)	0.045(3)	0.045(3)	0.040(3)	0.017(2)	0.018(2)	0.007(2)
C(5)	0.039(3)	0.048(3)	0.043(3)	0.012(2)	0.017(2)	0.001(2)
C(6)	0.038(3)	0.049(3)	0.047(3)	0.016(2)	0.018(2)	0.005(2)
C(7)	0.037(3)	0.050(3)	0.051(3)	0.016(2)	0.020(2)	0.008(2)
C(8)	0.046(3)	0.052(3)	0.052(3)	0.014(3)	0.016(3)	0.007(3)
C(9)	0.052(3)	0.053(3)	0.069(4)	0.018(3)	0.028(3)	0.016(3)
C(10)	0.049(3)	0.042(3)	0.042(3)	0.014(2)	0.021(2)	0.006(2)
C(11)	0.066(4)	0.045(3)	0.047(3)	0.016(3)	0.032(3)	0.018(3)
C(12)	0.069(4)	0.049(3)	0.065(4)	0.019(3)	0.034(3)	0.012(3)
N(1)	0.050(3)	0.073(4)	0.089(4)	0.019(3)	0.030(3)	0.012(3)
N(2)	0.078(4)	0.062(3)	0.119(5)	0.039(3)	0.044(3)	0.013(3)
N(3)	0.072(4)	0.070(3)	0.090(4)	0.036(3)	0.052(3)	0.028(3)
N(4)	0.100(4)	0.054(3)	0.115(5)	0.028(3)	0.055(4)	0.001(3)
C(25)	0.075(4)	0.036(3)	0.061(3)	0.014(2)	0.032(3)	0.007(3)
C(26)	0.082(5)	0.064(4)	0.096(5)	0.026(4)	0.056(4)	0.001(3)
C(27)	0.062(4)	0.066(4)	0.091(5)	0.017(4)	0.029(4)	0.023(3)
C(31)	0.149(8)	0.092(5)	0.096(6)	0.054(5)	0.033(5)	0.031(5)

H	/FO/	/FC/	PHI
** K= 0 L= 0 **			
1	93	121	0
2	161	156	180
3	197	192	0
5	22	17	0
6	46	43	0
** K= 1 L= 0 **			
-7	87	92	180
-6	43	41	0
-5	27	19	180
-4	191	174	0
-3	266	273	0
-2	104	93	0
-1	143	148	0
0	261	327	0
1	590	590	0
2	47	41	0
3	39	36	0
4	147	144	0
7	45	38	0
** K= 2 L= 0 **			
-7	53	48	180
-4	37	39	0
-3	359	372	0
-2	86	94	0
-1	192	221	180
0	100	83	0
1	42	70	0
2	24	28	180
3	50	60	0
5	25	24	180
6	20	8	180
7	57	54	0
8	26	18	180
** K= 3 L= 0 **			
-6	55	54	180
-5	56	61	0
-3	303	323	180
-2	49	57	180
-1	142	167	0
0	336	336	180
1	378	365	0
2	51	50	180
3	54	50	180
4	57	47	180
5	72	78	180
7	30	20	180
** K= 4 L= 0 **			
-7	32	37	0
-6	53	61	180
-3	25	28	0
-2	118	119	0
-1	68	85	180
1	422	413	180
2	53	50	180
3	57	59	0
4	69	66	180
5	139	134	180
6	34	32	0
7	27	12	180
** K= 5 L= 0 **			
-7	22	5	0
-6	63	74	0
-5	58	63	180
-3	179	186	0
-2	317	302	0
-1	80	83	0
0	20	18	0
1	391	390	180
2	47	36	180
4	121	123	180
5	92	92	180
** K= 6 L= 0 **			
-6	220	224	0
-5	115	117	0
-4	21	11	180
-3	61	53	0
-2	26	10	0
-1	127	124	0
0	112	108	0
1	85	83	180
2	127	119	180
3	19	0	180
4	44	40	0
5	44	41	180
6	26	18	180
** K= 7 L= 0 **			
-7	22	15	180
-6	133	130	0
-5	168	168	0
-4	48	47	0
-3	22	37	0
-2	78	70	0
-1	118	116	0
1	21	15	180
2	90	84	180
5	44	45	0
** K= 8 L= 0 **			
-5	84	90	0
-3	40	51	0
-2	72	79	0
-1	29	29	180
0	19	12	180
1	178	186	0
5	73	74	180
6	30	39	0
** K= 9 L= 0 **			
-8	25	16	0
-5	55	59	0
-3	35	35	180
-2	37	38	0
-1	148	147	180
0	39	34	0
1	30	34	180
4	33	26	180
5	27	8	0
** K= 10 L= 0 **			
-7	34	34	180
-5	38	44	180
-4	32	34	180
-3	33	31	0
-2	26	10	180
-1	105	105	180
0	72	68	180
1	34	33	180
2	71	77	180
3	39	48	180
4	56	48	0
5	24	5	0
-3	31	9	180
2	20	9	180
5	32	34	0
** K=-13 L= 1 **			
-2	30	28	180
1	27	5	0
3	62	65	0
** K=-12 L= 1 **			
-1	90	95	0
0	182	189	0
1	27	7	180
3	47	56	0
6	28	8	0
** K=-11 L= 1 **			
-3	24	28	0
-1	54	57	0
0	227	231	0
1	74	77	0
2	65	64	180
3	52	51	0
4	54	53	0
5	54	59	180
6	36	35	0
** K=-10 L= 1 **			
-4	62	60	0
-3	93	97	0
-2	45	46	0
-1	95	91	180
0	67	67	0
2	59	58	0
5	33	34	0
7	40	43	0
** K= -9 L= 1 **			
-2	50	45	180
-1	50	44	0
0	67	64	180
1	126	135	0
2	42	35	180
3	21	16	0
4	27	19	0
5	31	36	180
7	38	32	0
** K= -8 L= 1 **			
-6	34	39	180
-5	31	39	0
-4	52	52	180
-3	106	106	180
-2	37	33	0
-1	60	67	0
0	107	107	180
1	49	48	180
2	75	74	0
3	32	32	0
5	23	16	0
** K= -7 L= 1 **			
-5	51	50	180
-4	47	42	0
-3	121	118	0
-2	45	44	0
-1	61	54	0
1	161	160	180
2	56	54	180
3	72	72	0
4	93	88	180
5	69	73	180
6	107	112	0
** K= -6 L= 1 **			
-6	81	77	0
-5	64	62	0
-4	28	36	180
-3	66	58	0
-2	179	169	0
-1	95	91	180
0	278	267	0
1	209	208	180
2	27	14	0
3	35	30	0
4	79	81	180
5	51	45	180
6	65	58	0
7	32	42	0
** K= -5 L= 1 **			

H	/FO/	/FC/	PHI
-6	257	251	0
-5	56	61	0
-3	127	123	0
-1	85	79	0
0	53	51	0
1	238	216	180
2	125	119	180
3	139	136	0
4	78	81	0
5	35	28	0
6	22	11	180
7	32	36	0
** K= -4 L= 1 **			
-8	30	11	0
-6	51	62	0
-5	163	156	0
-4	42	39	180
-3	70	66	0
-2	229	228	0
0	91	93	180
1	330	320	0
2	72	69	180
3	56	51	180
** K= -3 L= 1 **			
-5	79	84	0
-4	24	30	0
-3	46	38	180
-1	84	94	180
0	90	71	180
1	517	540	0
2	64	56	0
4	72	69	180
5	83	84	180
8	24	19	180
** K= -2 L= 1 **			
-6	57	52	180
-5	74	72	0
-3	25	10	0
-2	354	345	0
-1	144	126	180
0	121	160	180
1	255	252	180
2	153	145	180
3	20	5	0
4	140	134	0
7	54	55	180
** K= -1 L= 1 **			
-6	37	29	0
-5	124	117	180
-4	65	63	180
-3	90	89	0
-2	137	114	0
-1	509	528	180
0	207	252	0
2	32	36	180
4	66	67	0
5	76	76	0
6	29	32	180
7	28	7	180
** K= 0 L= 1 **			
-8	42	43	0
-6	49	51	0
-5	121	110	180
-4	23	6	180
-3	19	8	0
-2	506	464	180
-1	160	189	180
0	196	224	180
1	427	475	0
2	311	310	0
3	114	108	180
4	47	37	0
5	82	74	0
6	26	27	180
** K= 1 L= 1 **			
-7	41	43	0
-6	26	22	0
-5	80	80	180
-4	201	201	180
-3	116	115	0
-2	306	281	0
-1	114	95	180
0	101	100	0
1	176	174	0
2	259	251	180
3	27	16	0
5	49	50	0
-8	27	9	0
-7	38	33	180
-7	46	52	0
-6	21	27	180
-4	45	41	180
-3	65	64	180
-2	27	33	0
-1	356	347	0
0	203	194	180
1	131	133	0
2	82	75	180
3	59	55	180
4	22	12	0
5	54	51	180
6	30	28	0
** K= 3 L= 1 **			
-8	27	18	0
-5	167	166	0
-4	31	29	0
-3	100	103	0
-2	37	44	180
-1	876	899	180
0	380	372	0
1	29	29	0
2	100	103	180
3	56	52	0
5	77	78	180
** K= 4 L= 1 **			
-8	46	58	0
-7	41	46	180
-5	64	53	180
-3	54	63	180
-2	64	63	0
-1	158	139	0
0	148	139	180
1	25	31	180
2	51	54	180
3	96	98	180
4	34	29	0
5	81	83	180
6	105	100	180
** K= 5 L= 1 **			
-8	27	9	0
-7	38	33	180
-4	123	117	180
-3	73	72	180
-2	140	137	0
-1	64	63	0
2	86	83	180
3	35	37	180
5	55	62	180
6	133	136	180
** K= 6 L= 1 **			
-7	44	55	180
-6	106	110	180
-5	76	75	0
-4	193	188	0
-3	95	98	180
-2	34	41	180
-1	248	246	0
0	241	229	180
1	53	55	0
2	82	79	180
3	81	80	180
6	43	39	180
** K= 7 L= 1 **			
-6	103	99	180
-5	55	48	0
-4	24	32	0
-3	29	41	180
-1	74	80	0
0	91	91	0
1	46	40	180
2	51	50	180
3	26	23	180
** K= 8 L= 1 **			
-8	34	22	0
-5	25	15	180
-3	51	53	180
-2	25	24	180
0	71	69	0
1	57	60	180
2	34	36	0
3	57	59	0
4	26	6	0
** K= 9 L= 1 **			
-7	58	56	180
-6	31	25	0
-5	26	12	0
-2	31	27	180
-1	59	61	180
1	24	25	0
3	56	55	180
** K= 10 L= 1 **			
-3	29	36	180
0	87	86	180
2	28	18	180
4	61	60	180
** K= 11 L= 1 **			
-4	40	40	180
-1	36	31	180
0	215	222	180
1	46	42	180
** K= 12 L= 1 **			
-6	30	29	180
-3	74	79	180
-1	28	14	180
0	63	64	180
1	82	80	180
2	26	10	0
** K= 13 L= 1 **			
-5	30	12	180
-4	27	20	180
-3	34	31	180
-1	29	26	0
** K= 14 L= 1 **			
-3	28	3	0
-2	32	30	0
-1	28	12	0
** K=-16 L= 2 **			
-1	49	50	180
3	27	21	0
** K=-15 L= 2 **			
1	78	77	0
** K=-13 L= 2 **			
-2	49	51	0
-1	26	16	0
3	32	33	0
4	48	47	0
** K=-12 L= 2 **			
-5	26	6	180
-2	46	41	180
-1	47	48	180
0	139	137	0
1	77	70	0
2	38	42	0
4	68	69	0
** K=-11 L= 2 **			
-3	27	26	0
-1	29	21	180
0	116	117	0
1	102	113	0
3	33	26	0
5	78	74	0
** K=-10 L= 2 **			
-6	25	22	180
-5	47	34	180
-4	28	39	180
-3	71	76	0
-2	69	73	0
-1	82	82	0
1	144	140	0
2	33	24	180
3	34	24	180
4	36	39	0
5	24	14	180
** K= -9 L= 2 **			
-6	33	33	180
-5	72	59	0
-1	89	94	180
0	24	33	0
1	68	70	0
4	43	41	180

H	/FO/	/FC/	PHI
5	30	21	180
7	24	9	180
** K= -8	L=	2 **	
-5	52	44	0
-4	37	28	0
-2	23	11	0
-1	119	123	180
0	49	54	180
1	32	41	0
2	124	121	180
3	55	53	180
4	49	47	0
5	121	126	180
6	25	16	180
** K= -7	L=	2 **	
-5	33	28	180
-4	46	52	180
-3	33	36	180
-2	211	194	0
-1	35	37	0
1	207	196	180
2	25	22	0
3	32	30	180
4	78	79	180
5	99	101	180
6	138	132	180
** K= -6	L=	2 **	
-7	33	52	180
-6	60	62	0
-4	32	38	0
-3	37	35	0
-2	39	31	0
-1	209	200	0
0	167	161	180
1	33	20	0
2	155	133	180
3	75	72	180
4	39	47	0
5	70	76	180
6	130	132	180
** K= -5	L=	2 **	
-6	37	46	180

H	/FO/	/FC/	PHI
-5	186	187	0
-4	157	159	0
-3	106	109	180
-2	133	117	0
-1	471	458	0
0	24	23	0
1	145	123	180
2	170	167	180
3	118	123	180
5	66	70	0
7	29	19	180
** K= -4	L=	2 **	
-8	47	34	0
-6	25	17	0
-5	74	74	0
-4	48	46	0
-3	51	53	0
-2	42	39	180
-1	181	190	0
0	120	102	0
1	86	77	0
2	52	44	180
3	81	82	0
4	21	7	0
5	27	43	180
6	37	42	0
7	27	10	180
** K= -3	L=	2 **	
-8	32	19	0
-6	45	45	180
-5	126	127	0
-4	81	75	0
-3	50	56	180
-2	100	97	0
-1	327	329	180
0	126	149	0
1	44	47	180
2	37	80	0
3	45	43	0
5	30	21	180
6	36	38	0
** K= -2	L=	2 **	
-8	35	16	0
-7	120	115	180

H	/FO/	/FC/	PHI
-6	71	69	0
-5	34	35	180
-4	97	96	180
-3	50	41	0
-2	84	78	180
-1	140	147	180
0	75	60	0
2	147	141	180
3	185	205	180
4	63	65	180
7	58	51	0
** K= -1	L=	2 **	
-8	24	18	0
-6	63	53	180
-4	104	102	180
-3	203	193	180
-2	98	92	0
-1	355	353	180
0	903	912	180
2	39	34	0
3	176	171	180
4	74	71	180
7	34	41	0
** K= 0	L=	2 **	
-9	23	9	180
-8	23	9	0
-7	37	38	0
-6	26	41	180
-5	22	16	180
-4	63	46	180
-3	141	128	180
-2	26	25	0
-1	240	261	180
0	1132	1172	180
1	200	208	180
2	48	47	0
3	23	25	180
4	54	61	180
6	26	23	180
** K= 1	L=	2 **	
-8	29	7	180
-7	119	126	0
-6	50	47	180
-5	30	25	0

H	/FO/	/FC/	PHI
-4	171	155	180
-3	453	448	180
-2	84	79	180
-1	215	231	0
0	162	178	180
1	215	218	180
3	70	66	180
4	33	35	180
6	25	20	0
** K= 2	L=	2 **	
-9	23	8	180
-6	78	83	0
-5	25	22	180
-4	53	55	180
-3	93	93	180
-2	34	33	0
-1	93	95	180
0	178	186	0
1	129	134	180
5	28	34	0
** K= 3	L=	2 **	
-8	27	9	180
-7	24	24	180
-6	66	66	0
-5	76	83	180
-4	98	96	0
-3	259	263	0
-2	104	100	180
-1	95	91	0
1	51	53	180
2	82	79	0
3	32	25	180
4	50	52	0
5	64	64	0
** K= 4	L=	2 **	
-6	39	43	0
-5	52	49	0
-4	75	78	180
-3	121	125	180
-2	61	53	180
-1	118	112	180
0	106	106	0
1	276	279	0
4	48	54	0

H	/FO/	/FC/	PHI
5	87	95	0
** K= 5	L=	2 **	
-8	28	7	180
-6	124	131	180
-5	21	16	180
-4	27	24	0
-3	124	126	180
-2	293	274	180
-1	71	74	0
0	111	104	180
1	155	153	0
2	90	87	0
3	24	18	180
4	31	38	0
5	57	53	0
** K= 6	L=	2 **	
-6	260	254	180
-5	118	120	180
-4	32	36	180
-2	75	83	0
-1	233	233	180
1	48	53	0
2	44	44	0
4	31	27	180
** K= 7	L=	2 **	
-6	70	71	180
-5	177	177	180
-3	34	35	180
-2	139	131	180
-1	42	37	0
0	25	22	180
1	70	68	180
2	62	54	0
5	27	2	180
** K= 8	L=	2 **	
-8	35	37	180
-5	56	54	180
-4	31	22	180
-3	23	18	180
1	60	63	180
2	33	17	180
4	27	26	0

H	/FO/	/FC/	PHI
** K= 9	L=	2 **	
-5	49	43	180
-4	30	32	0
-2	41	43	180
-1	135	139	0
2	29	23	0
4	28	14	180
** K= 10	L=	2 **	
-7	35	23	0
-5	63	66	0
-1	81	83	0
0	75	73	0
3	25	19	0
** K= 11	L=	2 **	
-6	25	9	0
-5	49	50	0
-4	61	66	0
-3	22	16	0
-2	27	27	0
-1	85	84	0
0	83	81	0
1	46	43	180
2	35	22	180
** K= 12	L=	2 **	
-5	31	29	0
-4	44	47	0
-1	21	6	180
0	47	41	0
** K= 13	L=	2 **	
-5	31	20	180
-4	38	34	0
** K=-16	L=	3 **	
-1	86	84	0
** K=-15	L=	3 **	
-1	44	30	180
1	38	40	0
3	28	20	0

H	/FO/	/FC/	PHI
** K=-14	L=	3 **	
1	25	8	0
3	35	25	180
** K=-13	L=	3 **	
-4	48	44	180
-2	49	50	0
-1	83	91	180
2	37	31	180
3	42	50	180
** K=-12	L=	3 **	
-3	29	3	180
-2	39	39	180
-1	79	78	180
0	245	248	180
2	39	40	0
3	55	49	180
5	25	23	0
** K=-11	L=	3 **	
-4	48	56	180
-3	45	60	180
-1	29	30	180
0	157	156	180
1	60	62	180
5	22	9	0
** K=-10	L=	3 **	
-6	30	34	0
-4	66	59	180
-3	99	108	180
-1	95	96	0
0	23	31	180
1	52	45	180
4	23	21	180
** K= -9	L=	3 **	
-7	35	33	0
-5	25	12	0
-4	36	43	0
-3	70	61	0
-1	66	68	180
0	69	62	0
1	68	69	180
3	37	31	180
4	23	18	0
** K= -8	L=	3 **	
-6	27	36	0
-3	28	33	0
-1	75	79	180
0	111	115	0
1	43	47	0
2	40	31	180
5	36	31	0
6	28	23	180
** K= -7	L=	3 **	
-4	50	55	180
-3	102	107	180
-2	127	114	180
-1	36	40	0
0	120	110	180
1	168	170	0
2	44	38	0
3	55	53	180
4	97	95	0
6	64	69	180
** K= -6	L=	3 **	
-8	25	1	0
-6	204	202	180
-5	39	47	180
-4	35	45	0
-3	99	88	180
-2	68	60	180
-1	55	51	180
0	74	76	180
1	100	94	0
4	33	33	180
6	28	15	180
** K= -5	L=	3 **	
-6	207	214	180
-5	134	134	180
-3	72	79	180
-2	122	109	180
-1	40	33	0
0	79	73	180
1	115	111	0
2	65	56	0
3	101	101	180
5	25	29	180
** K= -4	L=	3 **	
-7	41	47	0
-6	70	70	180
-5	132	131	180
-4	27	24	0
-3	90	90	180
-2	77	81	180
-1	62	59	180
0	143	129	0
1	340	331	180
2	32	35	0
3	70	80	0
** K= -3	L=	3 **	
-7	39	44	180
-6	58	66	0
-5	116	127	180
-4	42	39	180
-3	120	110	0
-2	125	119	180
-1	118	115	0
0	44	36	180
1	60	71	180
4	35	41	0
5	33	22	0
6	32	16	180
** K= -2	L=	3 **	
-8	36	25	180
-4	75	76	0
-3	140	136	180
-2	205	196	180
-1	167	161	0
0	129	123	0
1	78	86	0
2	77	77	0
4	90	98	180
5	24	0	180
** K= -1	L=	3 **	
-9	22	3	180
-8	31	22	180
-7	37	33	180
-6	22	16	0
-5	120	117	0
-3	65	63	0
-2	61	61	0
-1	244	250	0
0	89	88	180
1	64	60	180
2	56	63	180
3	30	44	0
4	31	23	180
5	56	49	180
** K= 0	L=	3 **	
-8	29	50	180
-6	100	104	180
-5	116	108	0
-4	142	129	0
-3	82	82	180
-2	193	194	0
-1	107	114	0
0	56	58	0
1	227	230	180
2	41	33	180
3	36	32	0
5	44	41	180
6	36	19	0
** K= 1	L=	3 **	
-7	93	96	180
-6	42	40	0
-5	77	64	0
-4	95	87	0
-2	201	196	180
-1	119	122	180
0	84	87	0
1	45	46	180
2	60	59	0
4	23	13	180
** K= 2	L=	3 **	
-8	41	35	180
-5	74	78	180
-4	53	53	0
-3	33	34	180
-1	115	124	0
0	47	58	180
1	57	55	180
2	54	54	0
** K= 3	L=	3 **	
-8	37	25	180
-7	24	8	0
-5	96	99	180
-4	79	72	180
-2	80	83	0
-1	231	234	0
0	82	78	180
3	30	22	0
5	59	57	0
** K= 4	L=	3 **	
-8	60	59	180
-7	71	62	0
-5	61	61	0
-4	79	79	0
-3	35	27	0
-2	139	134	180
0	24	17	0
1	23	7	0
2	59	60	0
5	45	43	0
** K= 5	L=	3 **	
-7	30	32	0
-6	60	64	0
-3	42	45	0
-2	24	23	0
-1	147	140	180
0	64	62	0
2	36	40	0
3	41	44	0
4	27	16	180
** K= 6	L=	3 **	
-8	31	12	0
-6	118	113	0
-5	101	96	180
-4	104	104	180
-3	90	91	0
-2	48	45	180
-1	58	52	180
0	45	45	0
2	57	67	0
3	38	26	0
** K= 7	L=	3 **	
-7	24	29	180
-6	53	51	0
-4	30	18	180
-2	61	59	0
-1	80	82	180
0	46	41	180
1	53	49	0
** K= 8	L=	3 **	
-7	27	4	0
-3	57	55	0
-2	38	40	180
-1	63	60	0
0	45	46	180
** K= 9	L=	3 **	
-7	66	61	0
-3	23	24	180
-2	52	58	0
** K= 10	L=	3 **	
-7	33	20	0
-6	27	27	0
-5	39	33	180
-3	43	37	0
-2	53	49	180
-1	38	44	0
0	97	96	0
** K= 11	L=	3 **	
-3	29	19	0
0	113	115	0
1	52	43	0
** K= 12	L=	3 **	
-4	27	18	0
-3	52	58	0
** K= 13	L=	3 **	

H	/FO/	/FC/	PHI
-3	31	11	0
** K=-15	L=	4	**
1	53	53	180
** K=-14	L=	4	**
-3	30	32	180
0	34	31	0
3	27	16	180
** K=-13	L=	4	**
-2	58	62	180
-1	38	33	0
0	42	36	180
3	32	22	180
** K=-12	L=	4	**
-2	81	87	0
0	115	113	180
1	71	67	180
4	33	39	180
** K=-11	L=	4	**
-2	70	71	180
-1	38	38	0
0	59	61	180
1	109	110	180
4	29	25	180
5	41	33	180
** K=-10	L=	4	**
-6	27	16	0
-5	33	29	0
-3	72	79	180
-1	70	73	180
0	31	24	0
1	68	68	180
** K= -9	L=	4	**
-7	27	22	180
-6	35	33	0
-5	90	91	180
-3	50	51	0
-1	126	130	0
0	29	26	180
1	50	49	180
2	37	41	0
5	37	41	0
** K= -8	L=	4	**
-7	26	15	0
-2	23	26	180
-1	29	33	0
0	26	34	0
1	46	44	0
2	40	34	0
4	30	15	0
5	76	75	0
** K= -7	L=	4	**
-8	44	32	180
-5	32	28	0
-4	45	35	0
-2	147	140	180
-1	31	23	180
1	56	60	0
2	23	23	0
3	40	41	0
5	76	74	0
** K= -6	L=	4	**
-6	27	33	180
-5	100	103	180
-4	92	87	180
-3	48	36	0
-2	47	44	180
-1	190	181	180
0	61	54	0
1	28	17	0
2	115	104	0
** K= -5	L=	4	**
-6	24	17	0
-5	136	137	180
-4	90	97	180
-2	35	31	180
-1	271	274	180
1	37	26	0
2	57	52	0
3	65	63	0
** K= -4	L=	4	**
-8	42	41	180
-7	37	39	180
-5	78	76	180
-4	67	66	180
-3	21	20	0
-1	51	47	0
0	115	113	180
3	58	62	180
4	26	23	0
5	25	16	0
** K= -3	L=	4	**
-7	45	53	0
-6	26	26	180
-5	56	59	180
-4	21	2	180
-2	43	41	0
-1	69	70	0
1	23	15	0
2	40	33	180
3	62	67	0
** K= -2	L=	4	**
-7	60	64	0
-6	18	0	180
-5	24	25	0
-4	56	57	0
-3	63	62	0
-2	47	48	180
-1	162	164	0
0	61	52	0
1	34	36	0
2	81	76	0
3	59	66	0
4	61	61	0
5	26	11	180
** K= -1	L=	4	**
-6	32	26	0
-4	96	93	0
-3	54	55	0
-1	132	133	0
0	527	524	0
2	38	43	180
3	81	86	0
4	42	33	0
** K= 0	L=	4	**
-7	98	106	180
-6	73	74	0
-4	27	22	0
-3	201	192	0
-1	80	85	0
0	324	317	0
1	123	130	0
4	45	47	0
** K= 1	L=	4	**
-9	31	27	0
-8	28	16	180
-7	59	63	180
-6	31	26	180
-4	160	156	0
-3	171	181	0
-1	108	113	180
0	35	39	0
1	82	84	0
2	26	3	0
3	27	34	0
** K= 2	L=	4	**
-8	33	34	0
-7	47	49	180
-6	52	50	180
-5	52	53	0
-4	69	69	180
-2	23	4	0
-1	37	25	0
0	80	80	180
1	58	64	0
** K= 3	L=	4	**
-7	63	60	0
-6	72	75	180
-3	96	97	180
-2	40	35	0
1	56	62	180
** K= 4	L=	4	**
-5	27	7	180
-4	24	16	0
-3	107	105	0
-2	98	95	0
1	105	107	180
2	28	27	180
3	24	5	0
4	35	28	180
** K= 5	L=	4	**
-7	41	41	0
-6	155	151	0
-5	35	27	0
-3	52	45	0
-2	76	68	0
-1	49	49	0
0	32	28	0
1	77	81	180
2	26	33	180
3	28	4	0
** K= 6	L=	4	**
-7	23	5	180
-6	173	172	0
-5	134	133	0
-2	30	33	0
-1	65	64	0
0	21	6	180
2	36	40	180
3	23	14	0
** K= 7	L=	4	**
-8	27	4	0
-5	100	100	0
-3	30	36	0
-2	30	8	0
-1	21	15	0
1	34	31	0
** K= 8	L=	4	**
-5	49	46	0
-3	24	18	180
-2	29	35	0
-1	48	40	180
** K= 9	L=	4	**
-2	22	21	180
-1	69	65	180
1	29	31	180
** K= 10	L=	4	**
-5	44	43	180
-4	25	18	180
-1	80	75	180
0	49	50	180
** K= 11	L=	4	**
-5	40	40	180
-4	47	57	180
-3	25	7	0
-1	35	23	180
** K=-13	L=	5	**
-1	63	64	0
0	72	71	0
1	22	11	0
3	41	41	0
** K=-12	L=	5	**
-3	40	42	0
-1	87	82	0
0	165	168	0
2	33	13	180
** K=-11	L=	5	**
-4	48	71	0
-3	46	41	0
-2	25	28	0
-1	40	35	180
0	93	92	0
1	57	56	0
4	24	12	0
** K=-10	L=	5	**
-4	24	14	0
-3	81	89	0
-2	29	33	180
-1	37	20	180
1	37	28	0

H	/FO/	/FC/	PHI
** K= -9	L= 5 **		
-6	45	42	180
-4	47	40	180
-3	87	92	180
-2	70	65	0
-1	32	28	0
0	62	62	180
1	33	35	0
2	23	3	180
** K= -8	L= 5 **		
-3	60	60	0
-2	27	27	180
-1	48	49	0
1	72	73	180
4	30	22	180
** K= -7	L= 5 **		
-7	24	31	0
-6	30	38	0
-5	30	25	0
-4	49	49	0
-3	37	31	0
-2	127	122	0
-1	29	26	180
0	38	41	0
1	70	67	180
2	34	27	180
** K= -6	L= 5 **		
-7	31	22	0
-6	206	219	0
-5	49	55	0
-4	41	40	180
-3	86	88	0
-1	30	42	0
0	36	35	0
1	69	69	180
3	38	32	0
** K= -5	L= 5 **		
-6	141	147	0
-5	131	130	0
-3	30	32	0
-2	87	89	0

H	/FO/	/FC/	PHI
-1	23	14	180
1	29	37	0
2	25	25	180
** K= -4	L= 5 **		
-7	25	35	180
-5	106	112	0
-3	22	23	0
-1	21	21	0
0	29	18	180
1	105	107	0
** K= -3	L= 5 **		
-8	26	14	0
-5	68	65	0
-4	28	12	180
-2	64	65	0
-1	56	61	180
0	26	25	180
** K= -2	L= 5 **		
-6	24	12	180
-5	36	49	180
-4	25	5	180
-3	31	24	0
-2	67	62	0
-1	136	130	180
0	22	18	180
2	44	34	180
4	33	33	0
** K= -1	L= 5 **		
-9	25	16	0
-8	37	36	0
-6	33	30	0
-5	82	77	180
-4	62	56	180
-2	89	90	180
-1	65	72	180
1	61	59	0
2	36	39	0
3	44	43	180
** K= 0	L= 5 **		
-9	30	20	0

H	/FO/	/FC/	PHI
-7	44	48	0
-5	83	80	180
-4	58	60	180
-1	53	51	180
1	88	97	0
2	30	20	180
** K= 1	L= 5 **		
-8	23	25	0
-4	68	73	180
-3	38	41	0
-2	37	35	0
-1	52	56	0
0	56	48	180
** K= 2	L= 5 **		
-7	25	21	0
-5	52	54	0
-4	25	31	0
-3	23	30	180
-1	88	97	180
0	52	53	0
2	35	28	180
3	26	5	0
** K= 3	L= 5 **		
-8	59	53	0
-7	41	44	180
-5	29	39	0
-3	20	3	0
-2	35	29	180
-1	57	51	180
** K= 4	L= 5 **		
-8	27	14	0
-6	37	33	180
-5	65	64	180
-4	26	13	180
-2	58	53	0
-1	23	3	0
2	43	37	180
** K= 5	L= 5 **		
-7	45	50	180
-6	62	65	180

H	/FO/	/FC/	PHI
-5	42	44	0
-3	25	31	180
-2	25	2	180
-1	62	66	0
0	36	35	180
2	34	34	180
** K= 6	L= 5 **		
-7	28	1	0
-6	65	68	180
-5	28	31	0
-4	57	56	0
-3	35	35	180
1	28	7	180
** K= 7	L= 5 **		
-7	22	10	0
-6	27	24	180
-2	21	5	180
** K= 8	L= 5 **		
-3	21	11	180
** K= 9	L= 5 **		
-3	27	11	180
** K=-14	L= 6 **		
-3	36	28	0
-2	32	22	0
0	33	16	180
** K=-13	L= 6 **		
0	43	46	0
** K=-12	L= 6 **		
-4	29	20	180
-2	27	14	180
0	62	65	0
1	69	68	0
** K=-11	L= 6 **		
-3	55	48	0

H	/FO/	/FC/	PHI
1	65	57	0
** K=-10	L= 6 **		
-5	23	16	0
1	41	38	0
** K= -9	L= 6 **		
-5	51	52	0
-2	33	25	180
-1	48	50	180
** K= -8	L= 6 **		
-7	34	3	0
-6	31	20	180
-4	27	25	0
-3	32	26	180
-2	67	63	0
-1	34	21	180
0	32	18	180
2	26	18	180
** K= -7	L= 6 **		
-7	32	29	180
-5	20	8	0
-3	44	38	0
-2	42	44	0
-1	38	43	0
1	36	30	180
2	27	36	180
3	29	18	180
** K= -6	L= 6 **		
-5	89	91	0
-4	86	87	0
-3	68	68	180
-2	56	62	0
-1	113	114	0
0	35	30	180
2	50	49	180
** K= -5	L= 6 **		
-6	29	9	180
-5	88	91	0
-4	33	31	0

H	/FO/	/FC/	PHI
-3	37	34	0
-1	87	89	0
0	30	32	0
1	24	6	180
** K= -4	L= 6 **		
-6	29	21	180
-5	34	40	0
-4	59	63	0
-3	46	51	180
-2	25	16	0
0	37	31	0
1	22	15	0
** K= -3	L= 6 **		
-7	51	57	180
-6	30	23	0
-4	26	24	180
-1	47	43	180
2	24	9	180
3	31	27	180
** K= -2	L= 6 **		
-7	44	39	180
-6	30	15	180
-4	24	28	180
-3	34	45	180
-2	24	22	0
-1	80	84	180
0	112	113	180
1	30	16	180
3	45	43	180
** K= -1	L= 6 **		
-7	26	12	0
-6	37	30	180
-4	43	46	180
-3	39	42	180
-1	71	70	180
0	207	207	180
1	29	24	180
** K= 0	L= 6 **		
-7	71	70	0
-6	29	26	180

H	/FO/	/FC/	PHI
-5	20	7	0
-4	59	64	180
-3	93	97	180
0	105	105	180
1	65	72	180
** K=	1	L=	6 **
-7	49	52	0
-5	29	22	180
-4	34	32	180
-3	66	73	180
-1	26	28	0
1	31	32	180
** K=	2	L=	6 **
-6	42	40	0
-4	30	23	0
-3	27	25	0
-1	27	3	0
0	37	31	0
1	28	14	180
** K=	3	L=	6 **
1	53	53	0
** K=	4	L=	6 **
-6	43	43	180
-4	32	29	180
-3	35	31	180
-2	57	63	180
1	46	42	0
** K=	5	L=	6 **
-6	121	108	180
-5	51	60	180
-3	29	20	180
** K=	6	L=	6 **
-6	86	85	180
-5	72	74	180
-4	27	10	180
-2	35	23	180
** K=	7	L=	6 **

H	/FO/	/FC/	PHI
-5	64	66	180
** K=-12		L=	7 **
-3	37	35	180
-1	52	39	180
0	89	83	180
** K=-11		L=	7 **
-4	50	49	180
-3	38	40	180
0	46	52	180
** K=-10		L=	7 **
-3	24	18	180
0	23	17	0
1	35	28	180
** K= -9		L=	7 **
-4	37	30	0
-2	23	12	180
** K= -8		L=	7 **
1	37	32	0
** K= -7		L=	7 **
-6	88	84	180
-5	32	29	180
-3	49	49	180
-2	45	43	180
0	22	17	180
** K= -6		L=	7 **
-6	138	140	180
-5	51	53	180
-4	22	8	180
-2	37	41	180
** K= -5		L=	7 **
-7	31	22	0
-6	84	79	180
-5	101	106	180
-2	33	22	180

H	/FO/	/FC/	PHI
1	25	26	180
** K= -4		L=	7 **
-5	47	52	180
1	33	27	180
** K= -3		L=	7 **
-5	28	23	180
-3	34	36	180
-1	49	52	0
** K= -2		L=	7 **
-5	52	53	0
-4	20	9	180
-3	29	21	0
-1	63	58	0
** K= -1		L=	7 **
-6	26	19	180
-5	35	39	0
-4	62	63	0
-2	30	25	0
-1	38	42	0
1	41	40	180
** K= 0		L=	7 **
-7	36	38	180
-5	37	33	0
-4	31	28	0
-1	23	6	0
0	24	25	0
** K= 1		L=	7 **
-7	31	20	180
-5	26	23	180
-4	29	25	0
** K= 2		L=	7 **
-5	34	30	180
-4	34	15	180
-2	25	14	0
** K= 4		L=	7 **

H	/FO/	/FC/	PHI
-6	38	38	0
** K= -8		L=	8 **
-5	28	14	0
-2	30	29	180
** K= -7		L=	8 **
-2	28	35	180
** K= -6		L=	8 **
-5	63	61	180
-1	48	50	180
** K= -5		L=	8 **
-5	30	43	180
-1	40	31	180
** K= -4		L=	8 **
-5	31	23	180
** K= -2		L=	8 **
-4	35	34	0
** K= -1		L=	8 **
-6	32	11	0
-5	26	13	0
-4	27	19	0
-3	41	39	0
** K= 0		L=	8 **
-4	42	48	0
-3	33	34	0

The Crystal Structure of 2,3-bis-(1-methyl-4-pyridinio)butane (7,7,8,8-tetracyanoquinodimethanide)$_4$, DMPB^{2+} (TCNQ)$_4^{2-}$

3.1 Experimental

This compound, prepared in the usual manner from the mono-cation diiodide, 1-methyl-4-ethylpyridinium iodide, formed black, well facetted, irregular octagonal crystals when a solution of complex in dry acetonitrile was allowed to cool in a 5l closed Dewar vessel from an initial temperature of 70°C to a final temperature of 23°C over a period of 40 hours. A typical crystal, with the major crystallographic faces assigned, is shown in plate 3.1. A number of crystals were examined by means of oscillation and Weissenberg photographs using Cu Kα radiation (λ = 1.5418 Å) and a suitable crystal selected for diffractometry.

The crystal was transferred to the Hilger and Watts computer-controlled four-circle diffractometer where, after centering, an approximate orientation matrix was obtained as before, by comparison of angular relationships between regions of high diffracted X-ray intensity observed during a 180° ϕ scan at low theta, and the angular relationships between the assigned diffracted intensities observed on the Weissenberg photographs. An accurate orientation matrix was then obtained based on 23 strong reflections with $10^\circ < \theta < 13^\circ$. Graphite monochromated Mo Kα radiation (λ = 0.71069 Å) was used and intensity data were collected at ambient temperature (19°C) using a $\theta/2\theta$ scan for $\theta \leqslant 25^\circ$. No significant variations were observed in the intensities of three standard reflections measured

every 100 reflections and so the data were normalised to a constant value of a single reflection before data reduction. The data were corrected for Lorentz and polarisation factors, but no correction was made for absorption of X-rays by the crystal. Out of 4583 reflections collected, 2892 were considered observed such that $I > 3\sigma(I)$. Five of the reflections collected had intensities greater than 250,000 units and these were re-collected at reduced X-ray intensity in order to compensate for counter tube saturation. The re-scaled intensities for these reflections were input before data reduction.

Crystal Data

DMPB $(TCNQ)_4$ $(C_{16}H_{22}N_2)^{2+}$ $(C_{12}H_4N_4)_4^{2-}$, Mr = 1058.3.

Triclinic, a = 7.798, b = 14.249, c = 13.690 Å, α = 109.53 β = 103.37, γ = 95.42°.

U = 1388 Å^3, Z = 1, Dc = 1.266 g cm^{-1}, D_m = 1.272(4) g cm^{-1}

Mo Kα (λ = 0.71069 Å), μ = 0.87 cm^{-1}

Space group $P\bar{1}$ (N°. 2), assumed.

3.2 Structure Determination and Refinement

The structure was solved on the basis of the Patterson and Sharpened Patterson functions. A plot of the three-dimensional sharpened Patterson vector map along the c axis showed the typical vector pattern of intramolecular TCNQ vectors about the origin at

(1,0,0) (see figure 3.1) and examination of the strong vectors in the Patterson map showed a possible partial trial structure based on TCNQ molecules with molecular centres derived from attributing the vector at 0.781, 0.058, 0.757 to the A-A' intermolecular vector and that at 0.110, 0.030, 0.646 to the B-B' vector (A and B being the two crystallographically independent TCNQ moieties within the asymmetric unit). However, this trial structure was found to be unsuccessful, and closer examination of the molecular centres chosen showed that this choice did not produce satisfactory agreement of found and calculated vectors A-B and A-B'.

The vector map was therefore examined again, and the vector at 0.781, 0.058, 0.757 was seen to be more correctly assigned as the B-A' vector, with that at 0.945, 0.044, 0.256 being assigned as the A-A' vector. This yielded satisfactory assignments of the B-B' and A-B vectors at 0.629, 0.071, 0.258 and 0.843, 0.011, 0.500 respectively, and accordingly a trial structure based on molecular centres derived from these intermolecular vectors was attempted. Two cycles of isotropic full matrix least-squares refinement gave R = 0.42, and a subsequent difference Fourier synthesis based on $|FO-FC|$ yielded the entire non-hydrogen skeleton of the cation apart from the methyl carbon of the butane linkage. Further isotropic refinement based on this fuller trial structure, followed by another difference Fourier synthesis, revealed the position of the remaining non-hydrogen atom. A difference Fourier synthesis based on structure factors calculated for the entire non-hydrogen atom structure yielded possible positions for the hydrogen atoms of the

TCNQ molecules, and indicated some electron density in approximately sp^2 positions with respect to the cation ring. Hydrogen atoms were placed in their calculated positions on the basis of sp^2 hybridisation of the ring carbon atoms in view of the less than entirely satisfactory positions obtained from the difference Fourier synthesis. Subsequent structure factor calculations included these atoms but their positional and thermal parameters were not refined in any least-squares procedure. After placement of the methyl hydrogen atoms in positions calculated from an sp^3 arrangement with one C-H bond in the plane of the cation ring, anisotropic refinement of the structure eventually led to R = 0.0972. Examination of the structure at this stage showed the C-C distance in the butyl methyl - C_2 bond to be slightly less than expected for a C-C single bond, whilst the angle formed by the bond between the two substituted methylene groups of the butane link and the bond from the substituted pyridinium ring to the butane link was considerably greater than expected. It was also found to be impossible to place the hydrogen atom present at the linking C atom with any degree of success.

In view of the difficulties encountered in obtaining a satisfactory geometry about the butane link, and the difficulty experienced in obtaining acceptable positions for hydrogen atoms in the earlier difference Fourier synthesis, combined with the inability of the structure to refine to a more usually acceptable R value, an examination of the original intensity data was undertaken which revealed a possibly significant variation of R with indices directly

related to the axis of rotation of the crystal.

As a result of this analysis, and for the structural reasons discussed earlier, it was decided to obtain intensity data for another crystal of the compound, a measure which would also give confirmation or otherwise of the 'dimeric' nature of the cation present in the complex salt.

A further crystal was therefore selected and mounted, and oscillation, zero, and first layer Weissenberg photographs were taken on a Unicam camera using Cu radiation (λ = 1.5418 Å). Initial cell dimensions obtained from these single crystal photographs were, within experimental error, the same as those obtained previously. The crystal was then transferred to the Nonius Enraf CAD4 four-circle computer-controlled diffractometer, and an accurate orientation matrix obtained based on 22 reflections with $19^{\circ} < \Theta < 30^{\circ}$. The final cell obtained was found to be similarly identical to the cell derived for the previous crystal, with all the unit cell parameters except that of the a cell dimension being well within 0.1% of the previous cell parameters (the a cell dimension differed by 0.2%).

Intensity data were collected at ambient temperature, ca. 19°C, using Cu Kα radiation (λ = 1.5418 Å) and a nickel filter. Examination of the peak profile for a few selected peaks showed the most appropriate scan mode to be a pure omega scan (which may be one reason for the poor quality of the data obtained previously which had used a $\Theta/2\Theta$ scan) and intensity data were collected in this manner for $1^{\circ} < \Theta \leq 66^{\circ}$. One reflection was measured as a

standard every 200 reflections throughout the data collection, and, as no significant variation was observed in the intensity or position of this reflection, the data were not normalised to a constant value for this standard before data reduction. Two reflections were considered sufficiently intense to warrant re-determination at reduced X-ray intensity; however, as the re-scaled intensities for these reflections did not significantly differ from the uncorrected intensities, no correction for loss of counter efficiency was applied before data reduction.

Of 4867 reflections collected, 3236 were considered observed such that $I > 3\sigma(I)$. The data were corrected for Lorentz and polarisation factors, but no correction was made for absorption.

Crystal Data

DMPB $(TCNQ)_4$ $(C_{16}H_{22}N_2)^{2+}$ $(C_{12}H_4N_4)_4^{2-}$, Mr = 1058.3

Triclinic, a = 7.798(18), b = 14.249 (8), c = 13.690(10) Å

α = 109.53(2), β = 103.37(5), γ = 95.4(1)

U = 1388 Å^3, Z = 1, D_c = 1.266 g.cm^{-1}, D_m = 1.272(4) g.cm^{-1}

Cu Kα (λ = 1.5418 Å) μ = 6.52 cm^{-1}

Space group $P\bar{1}$ (No. 2), assumed .

Structure determination

In view of the uncertainty in the earlier structure it was decided to re-determine the entire structure on the basis of the new Patterson function. Accordingly, the strong vectors in the

three dimensional Patterson map were examined and a single weight vector at 0.947, 0.041, 0.255 was found which could be interpreted as an A-A' vector, and a single weight vector at 0.622, 0.074, 0.256 was assigned as the B-B' vector. Vectors corresponding to A-B' and A-B were found to be double weight, as expected, and in close agreement with the calculated positions. The molecular centres and orientation were found to be in very close agreement with those obtained previously and so the refined atomic parameters for all the non-hydrogen atoms of the previous structure were input as a trial structure. This was found to be a substantially correct trial structure as evidenced by a respectable R value after only two cycles of anisotropic refinement (R = 0.0878) and the appearance in a difference Fourier synthesis based on $|FO - FC|$ of all the ring hydrogen atoms on both the TCNQ moieties and the cation, all forming very acceptable bond lengths and angles with respect to the ring atoms. This also confirms the greater accuracy of the intensity data collected from the second crystal. Ring hydrogen atoms were originally placed in their observed, as opposed to calculated, positions in view of the well defined nature of these positions. The scattering due to these ring hydrogens was included in structure factor calculations, but none of the positional or thermal parameters of any hydrogen atoms were included in the least-squares block diagonal refinement. Further refinement and searches for the remaining hydrogen atoms showed there to be electron density about the methyl carbons but in a disordered manner, indicating no preferred conformation of the methyl groups, and electron density at the

tri-substituted sp^3 link. However, it was not possible to place a hydrogen atom on this centre with any degree of reliance, and the structure refined to R = 0.067 with these seven hydrogen atoms missing. The structural implications of this are discussed in the next section.

A Chebyshev weighting scheme (see Chapter 1) was introduced with coefficients (determined by the program so as to minimise the function $X = \sum (FO - FC)^4$):

A[0] = 1455.9 A[1] = 1288.6 A[2] = -419.6 A[3] = -291.2 A[4] = 38.0

The structure finally converged to R = 0.0661 with a maximum value of the ratio shift/e.s.d. of -0.33 in the positional parameters of the terminal butyl carbon atom and more typically ~ 0.06 for every other parameter. The positional and anisotropic thermal parameters of the non-hydrogen atoms were subjected to a rigid-body thermal motion analysis in which the two entire TCNQ moieties and the whole of the cation present in the asymmetric unit were considered as independent rigid bodies. Bond lengths and angles were librationally corrected as a result of this analysis. The structure was also analysed by a least-squares best planes procedure and details of the molecular geometries are given later.

3.3 Description and Discussion of the Structure

Figures 3.4a, 3.4b and 3.4c show projections of the structure down the a,b and c axes respectively of the unit cell. The molecular arrangement of the TCNQ moieties may be considered as a non-stacking series of tetrads, since, as in DMPY $(TCNQ)_2$ (see Chapter 2), the TCNQ 'stack' may be considered in two possible ways. If stacking is considered along the c axis then the molecules defining the stack are B", B, A, A', B'; however, the alternative possibility of molecules stacking along $[1\ 0\ 1]$, defined by A''', B''', B, A, etc. must also be considered. The molecular overlaps of the moieties are shown in figure 3.5. Within the tetrad only the overlap of moieties A, B and B', A' are of the exocyclic bond-ring type asscciated with high conductivity in an infinite stack, however, the overlap of A-A' is of the displaced molecule variety and may be considered to provide sufficient overlap of the pi system required for reasonably high conductivities (ca. $> 10^{-2}\Omega^{-1}\ cm^{-1}$). Between tetrads, however, nearest molecules are significantly displaced, again in the almost symmetric manner observed in DMPY $(TCNQ)_2$, as is shown in the projection of B''' and B'' onto B. The separations of the planes (see table 3.3 for details of molecular planes) of the A-B molecular pair is 3.13Å when the least squares plane of the whole molecule is considered, whilst that of A-A' is 3.37Å. The separation of the planes of the adjacent ends of the tetramers, given by the B''' - B and B'' - B separations, are 3.10Å and 3.04Å respectively. When the least squares planes of the ring atoms only

are considered, these separations become A-B = 3.13Å, A-A' = 3.32Å, B'''-B = 3.19Å and B''-B = 3.18Å. These differences in the mean plane positions depending upon whether the whole molecule or a particular fragment is considered are due, in the main, to the bowing of the TCNQ moieties B and A so as to relieve the repulsions created by the short intermolecule contacts between A and B. The similar separations of the planes of B'''-B and B''-B, and the almost identical dispositions of the two related moieties projected onto B, make it impossible to define a preferred stacking axis on the basis of this information alone. Inter-tetrad contacts (see table 3.4 for details of close intermolecular contacts) are slightly shorter from B''' to B, with the closest contact being 3.399Å, compared with a shortest contact of 3.446Å for the B'' to B separation. It is therefore concluded that there is no significant overlap between any of the tetrads and therefore no approximation to a continuously overlapping stack.

The cation is centrosymmetrically sited about $(\frac{1}{2}, \frac{1}{2}, 0)$ and sits in the channel between TCNQ tetrads. There are no cation-cation ccntacts less than 3.8Å as might be expected from the packing of the cation within the cell. The shortest contacts from the TCNQ moieties to the cation are from TCNQ(A) to the cation ring, with the closest contact being 3.212Å (N(1) - $C(25^{vi})$), whereas the closest TCNQ (B) to cation ccntact is 3.295Å (N(8) - $C(30^{iv})$). These distances are slightly greater than the sum of the van der Waals radii for the heavy atoms involved (3.2Å), but less

than the sum of the van der Waals radii for nitrogen and hydrogen, plus a C-H covalent bond (= 3.5Å) [17], and may indicate a degree of charge interaction between the slightly negatively charged CN groups[21] and the delocalised positive charge on the cation ring.

The molecular geometries of the TCNQ and cation moieties are shown in figures 3.2a, 3.2b and 3.3. The bond lengths and angles of TCNQ (A) and TCNQ (B) show the expected mmm symmetry (if the bowing of the molecule is neglected), and the bond lengths of TCNQ (A) are in excellent agreement with the mean values for the $TCNQ^{\frac{1}{2}-}$ moiety given by Ashwell *et al*[22]. The TCNQ (B) moiety does not show quite such good agreement; indeed, the exocyclic carbon-carbon bonds exhibit some $TCNQ^{o}$ character in terms of their bond lengths, however the heavy atom bonds in the two TCNQ moieties are equal to within 2σ. The charge on the TCNQ (A) moiety, calculated by the method of Flandrois and Chasseau[8] on the basis of the means of the chemically equivalent bonds, is determined as -0.445e, close to the -0.5e expected for $TCNQ^{\frac{1}{2}-}$. The charge on TCNQ (B), calculated in the same manner, yields a result of -0.275e, which is different from that expected solely on the grounds of maintainance of charge neutrality. If this value for the charge on TCNQ (B) is significantly different from the expected -0.5e it could be explained in two possible ways; either in terms of a back donation of charge from the nitrogen of the donor molecule, or by the presence of some mono-cationic species within the crystal. However, it is possible that $\sim$ -0.3e is not significantly different from -0.5e in view of the fact that the indications from the individual bond lengths of all the heavy atom

bonds give possible values of charge ranging from -0.11e to -0.70e.

The cation ring shows mm symmetry to within 1σ of the bond lengths, and is in particularly close agreement with the ring structure of the cation in 1,1'-dimethyl-4,4'-bipyridylium $(TCNQ)_4$ [7] and the pyridinium ring in the 1,1'-dibenzyl-4,4'-bipyridylium $(TCNQ)_4$ complex[23]. The $N-CH_3$ bond length of 1.496(4)Å in the present structure compares well with 1.495(6)Å in DMPB $(TCNQ)_3$ [7] and 1.48(1)Å in DMPA $(TCNQ)_4$ [10]. It is longer than the equivalent bond in the 1-methyl substituted bipyridyl salts[11] which are 1.409(15), 1.466(9) and 1.450(15)Å for the dichloride, dibromide, and diiodide respectively, and slightly longer than the $N-CH_3$ bond (1.46Å) in 1-methyl-pyridinium iodide[9] and 1.46(2)Å in DPP $(TCNQ_4)$ [15]. The C(27)-C(31) bond length of 1.512Å in the present structure is similar to 1.508Å in DEPE $(TCNQ)_4$ - phase II[22], 1.505(6)Å in DEPA $(TCNQ)_5$[24], 1.49(1)Å in DMPA $(TCNQ)_4$[10], and 1.51(2)Å in the organo-metallic compound dichlorobis-(4-ethylpyridine) copper(II)[25].

The C(31)-C(31') separation is 1.487(7)Å, somewhat shorter than the equivalent bond in DEPA $(TCNQ)_5$ [24] (of length 1.529(8)Å) and the 1.52(2)Å bond length across the centre of symmetry in the complex salt DPP $(TCNQ)_4$ [10]. The C(31)-C(32) bond, at 1.422(5)Å, appears to be intermediate between a single carbon-carbon bond and a carbon-carbon double bond. There would appear to be two possible ways by which the geometry of the 2,3-butane link could be explained, either by a disordered butane linked cation whereby the R,R-enantiomer would be present in some of the unit cells, and the

S,S-enantiomer present in others, or as a structure in which the disorder was provided by having an alternative cation, based on a trans-buta-1,3-diene linkage, present in some unit cells. Since the reactant monomer (1-methyl-4-ethyl pyridinium iodide) was shown by n.m.r. not to have undergone any dimerisation during previous recrystallisation (which occurred over a period of some three months, see also Chapter 6.) it was assumed that the dimerisation must have occurred during either the initial reaction with $TCNQ^{o}$ or during subsequent recrystallisation of the complex. As $TCNQ^{\cdot-}$, the radical ion, is an excellent hydrogen abstractor[29], it is possible to envisage a situation in which an α-hydrogen of the 4-ethyl substituent is abstracted, leaving a radical cation:

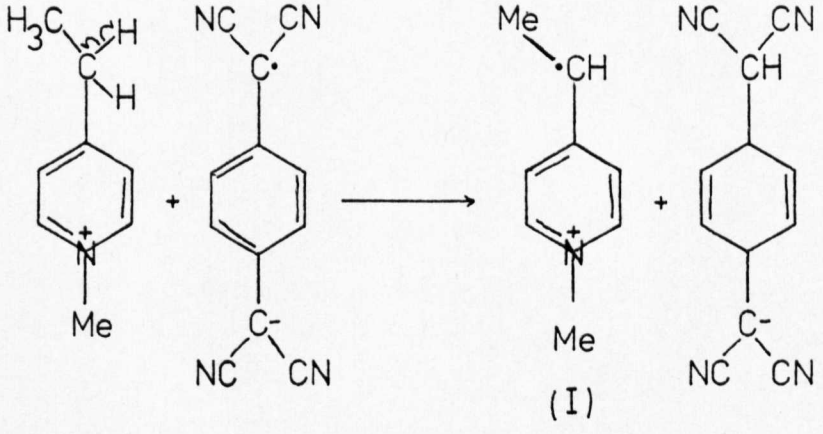

3.1

Two moieties of (I) could then join to form the required butane linked dimer:

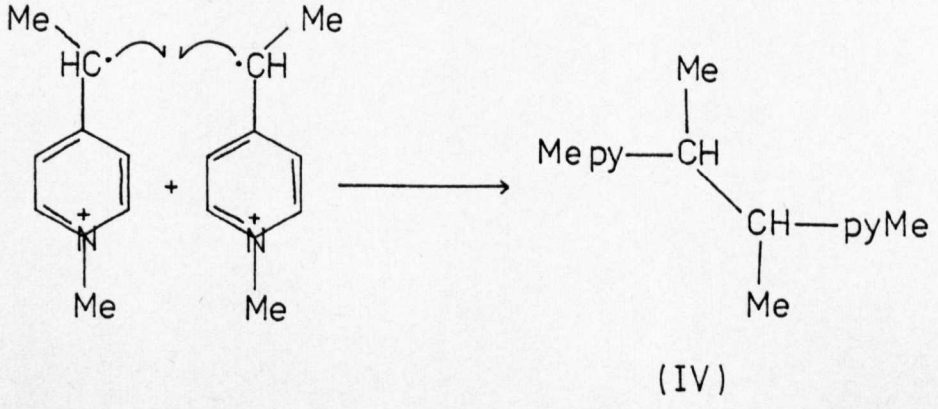

3.2

(IV)

Alternatively, if the $TCNQ^-$ radical ion were to abstract two adjacent hydrogen atoms from the ethyl substituent, it may be possible to form the vinyl substituted pyridinium ion,

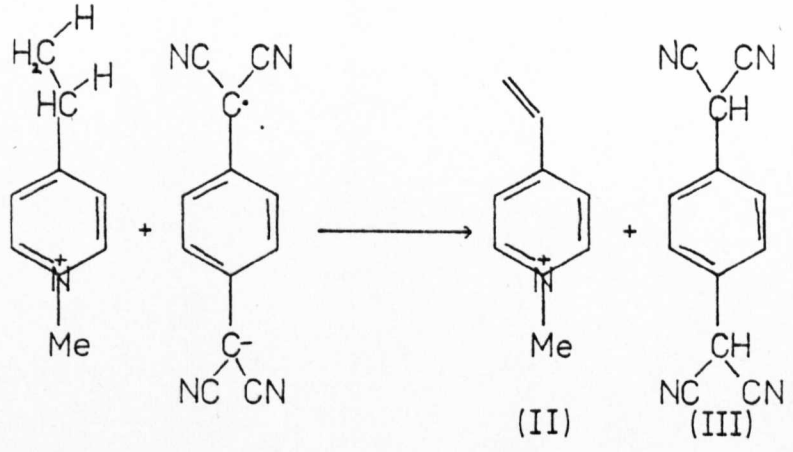

3.3

Reaction between two molecules of (II), together with the recovery of the abstracted hydrogens from (III), could lead to the butane linked dimeric species (IV).

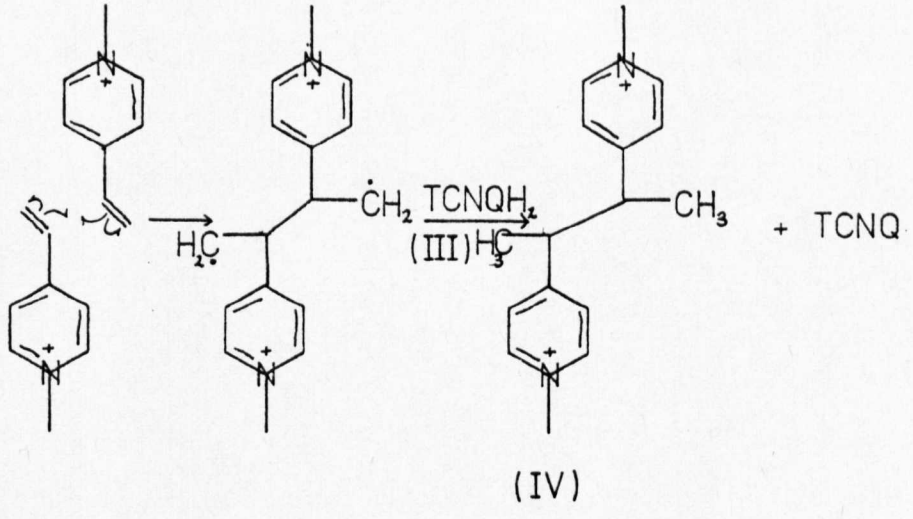

(IV)

3.4

Abstraction of the α-hydrogen of the vinyl substituent of (II) to give a radical cation, by analogy to the formation of (I) from

the ethyl-substituted moiety, followed by dimerisation by radical bond formation could also occur, giving the buta-1,3-diene species (V):

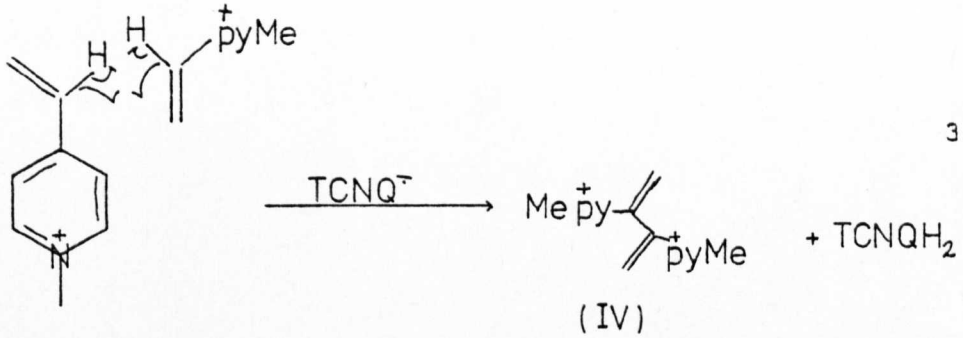

3.5

(IV)

It is of course possible that the butane linked dimer (IV) should undergo hydrogen abstraction to form the buta-1,3-diene species in a manner directly analogous to reaction 3.3 since if the monomer may undergo abstraction then so may the dimeric species.

Within this scheme it is possible to conceive of a situation in which there are up to three possible types of unit cells present, two containing butane-linked cation species (in R,R- and S,S- enantiomeric forms) and one containing a trans-buta-1,3-diene linked cation species. In view of the distortion of the geometry of the cation at the linkage to a geometry which appears to be an intermediate between sp^2 and sp^3 hybridisation of C(31) and C(32) it seems unlikely that the disorder may be explained solely in terms of R,R- and S,S- enantiomeric forms of the butane linked species. The most likely explanation would therefore seem to be a crystal in which some 'unit cells' contained the R,R- enantiomer of the 2,3-butane linked cation and some contained the

trans vinyl dimer, the cation species with the buta-1,3-diene link (V). This type of scheme could provide rationalisation of two features of the present structure: the difficulty experienced in determining hydrogen positions on C(31) and C(32), since this would now be a disordered situation to which some sp^3 and some sp^2 centres were contributing, and the short C(31)-C(32) bond. The observed bond length of 1.422(5)Å could then be viewed in terms of an intermediate between 1.37(2)Å in the dichlorobis-(4-vinyl-pyridinium) cobalt(II) complex[26] and the terminal C-C single bonds of length 1.51(2) and 1.48Å in the two compounds dichlorobis-(4-ethylpyridine)M(II) where M is copper and cobalt. The solid-state polymerisation of vinyl groups in inorganic complexes of transition metals with substituted pyridines has been discussed by Laing and Horsfield[27] and Admiral and Gaffner[26] who conclude that non-bonding contacts of less than 4Å, correct orientation of reacting groups, and high thermal motion are necessary conditions for facile polymerisation. Thus, the possibility of a solid state reaction after crystallisation cannot be entirely ruled out.

The marked bowing of TCNQ (B) is a reflection of the greater molecular separation of the B moieties due to their displaced overlap, thus allowing these moieties to distort to relieve repulsions between the cyano groups. Examination of the distances of atoms from the least squares planes of the two TCNQ moieties showed that the $C(CN)_2$ groups in each TCNQ are twisted with respect to the ring planes of the moieties, with those of TCNQ (B) being more twisted

than those of TCNQ (A). The dihedral angles between the planes of C(7)-C(8)-C(9)-N(1)-N(2) and C(10)-C(11)-C(12)-N(3)-N(4) and the ring plane of TCNQ (A) are 1.7° and 1.3° respectively whilst those of the planes of C(19)-C(20)-C(21)-N(5)-N(6) and C(22)-C(23)-C(24)-N(7)-N(8) with the ring plane of TCNQ (B) are 3.5° and 6.4° respectively. The dihedral angle between the ring planes of the two crystallographically independent TCNQ moieties is 1.6°, whilst the dihedral angles between the cation ring plane and TCNQ (A) and TCNQ (B) are 60.8° and 60.3° respectively.

The structure therefore consists of a non-overlapping series of tetrads with the cation moiety sitting in channels between the tetrads. The single crystal d.c. conductivity measurements for this compound are illustrated in figure 3.6 and show the lowest conductivity axis to be along [0 1 0] as expected since this corresponds to conduction across the cation planes. The [1 0 0] and [0 0 1] axes have a similar conductivity, which may be interpreted as being indicative of the non-infinite stack nature of the structure and the similarity of the sideways contacts between TCNQ moieties and the contacts between displaced tetrads.

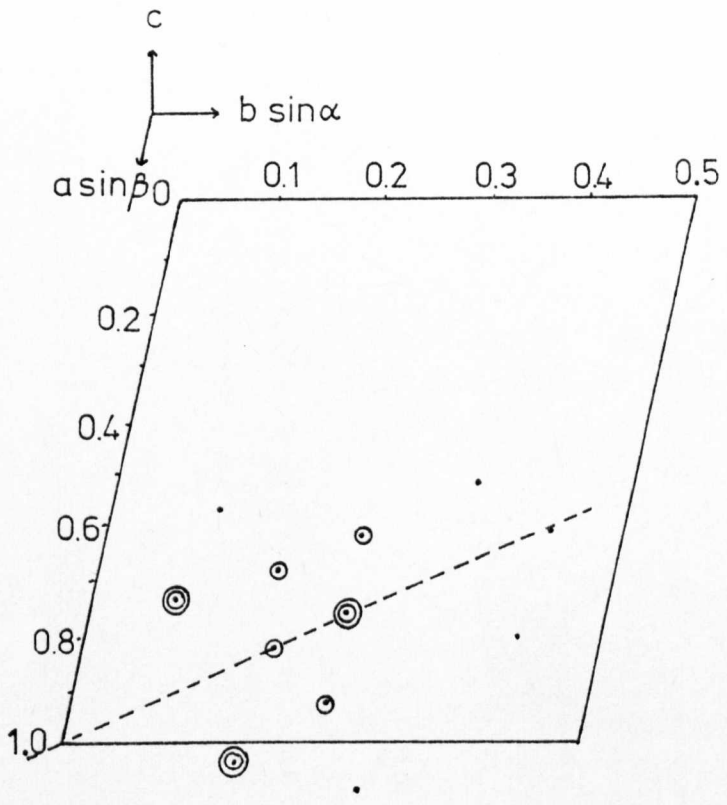

FIGURE 3.1

DMPB $(TCNQ)_4$ Sharpened Patterson showing strong vectors about the origin at 1,0,0 (TCNQ long axis shown------)

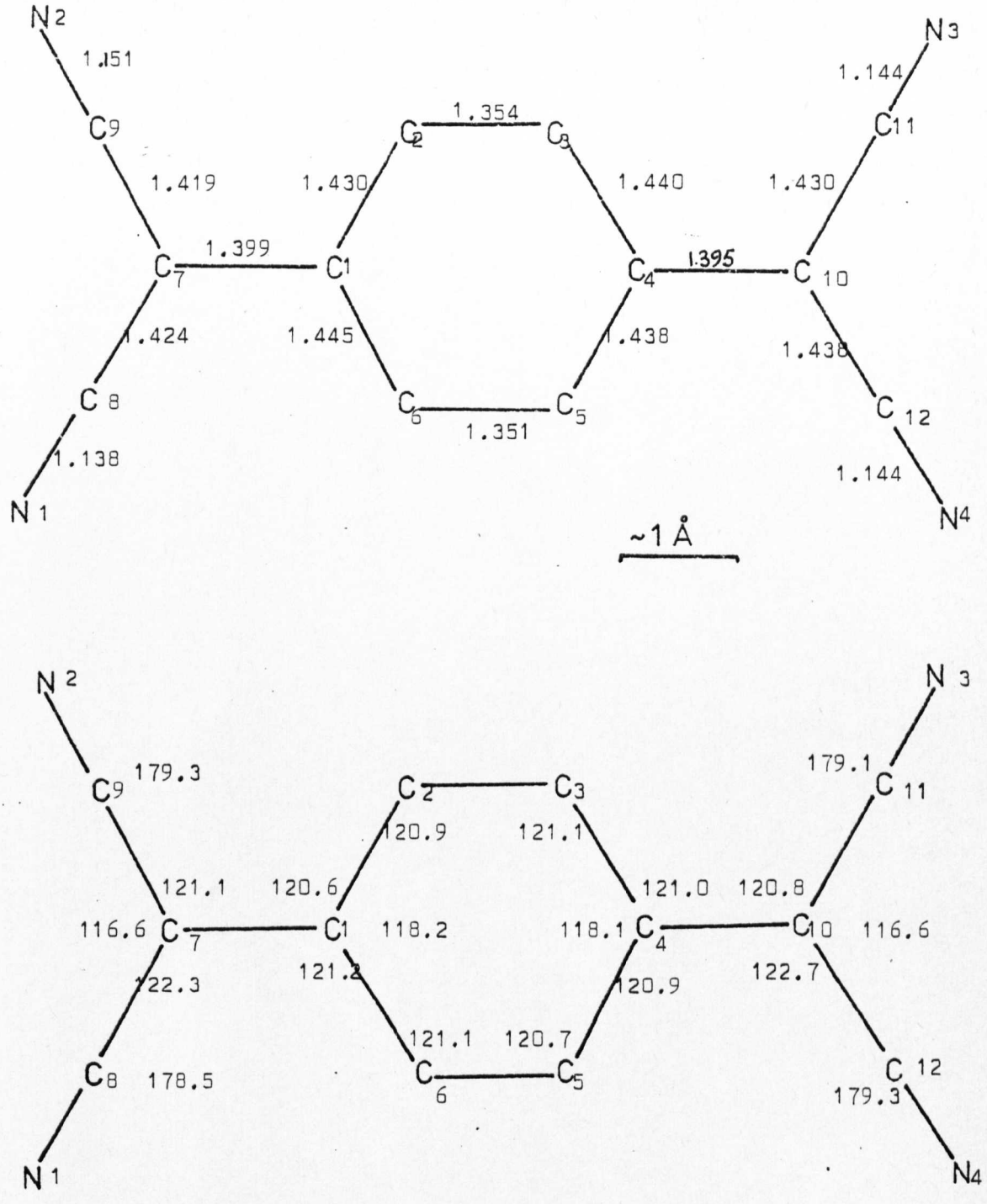

Figure 3.2a DMPB $(TCNQ)_4$ - Librationally corrected bond lengths (Å) and angles (degrees).

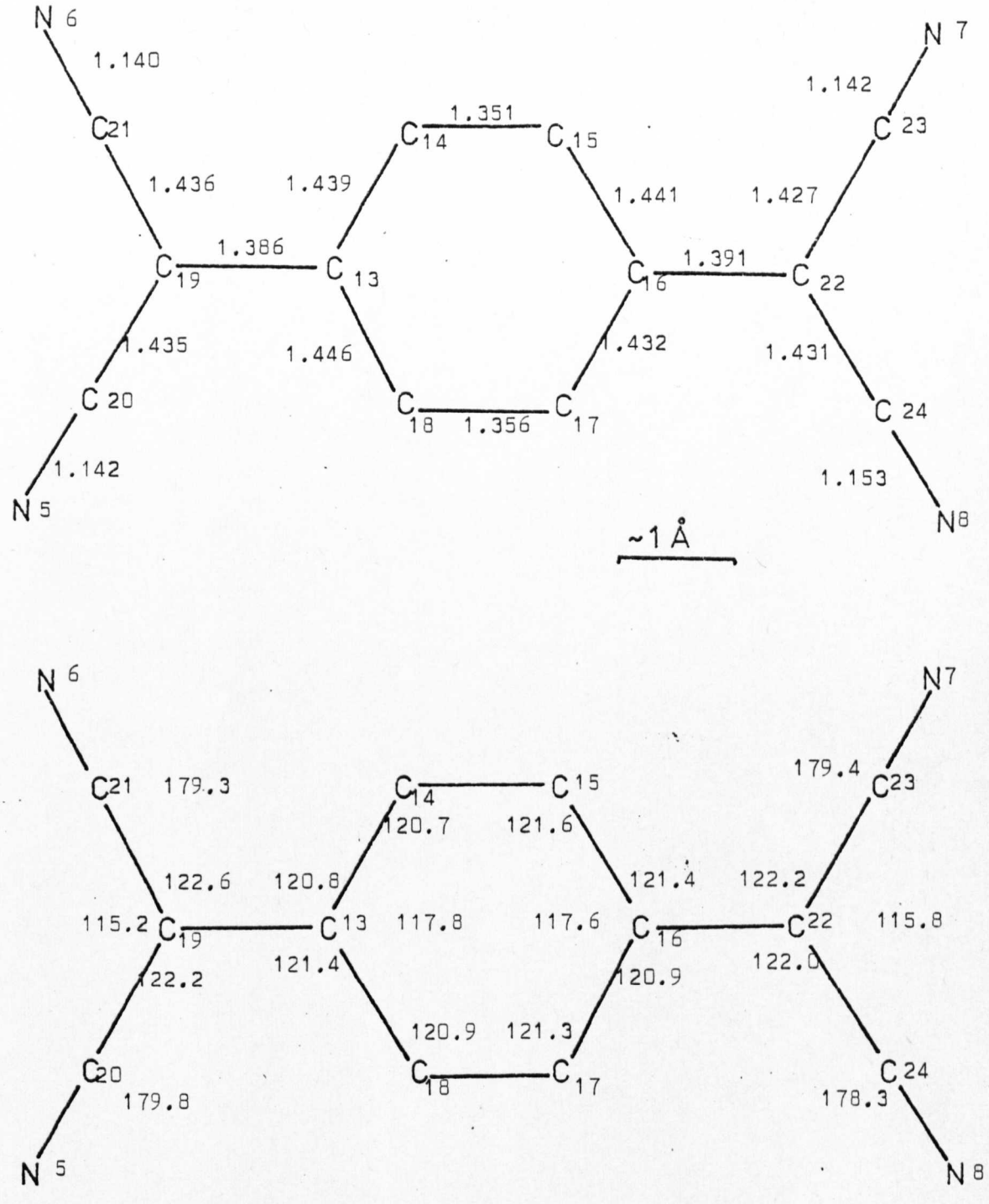

Figure 3.2b DMPB $(TCNQ)_4$ - Librationally corrected bond lengths (Å) and angles (degrees)

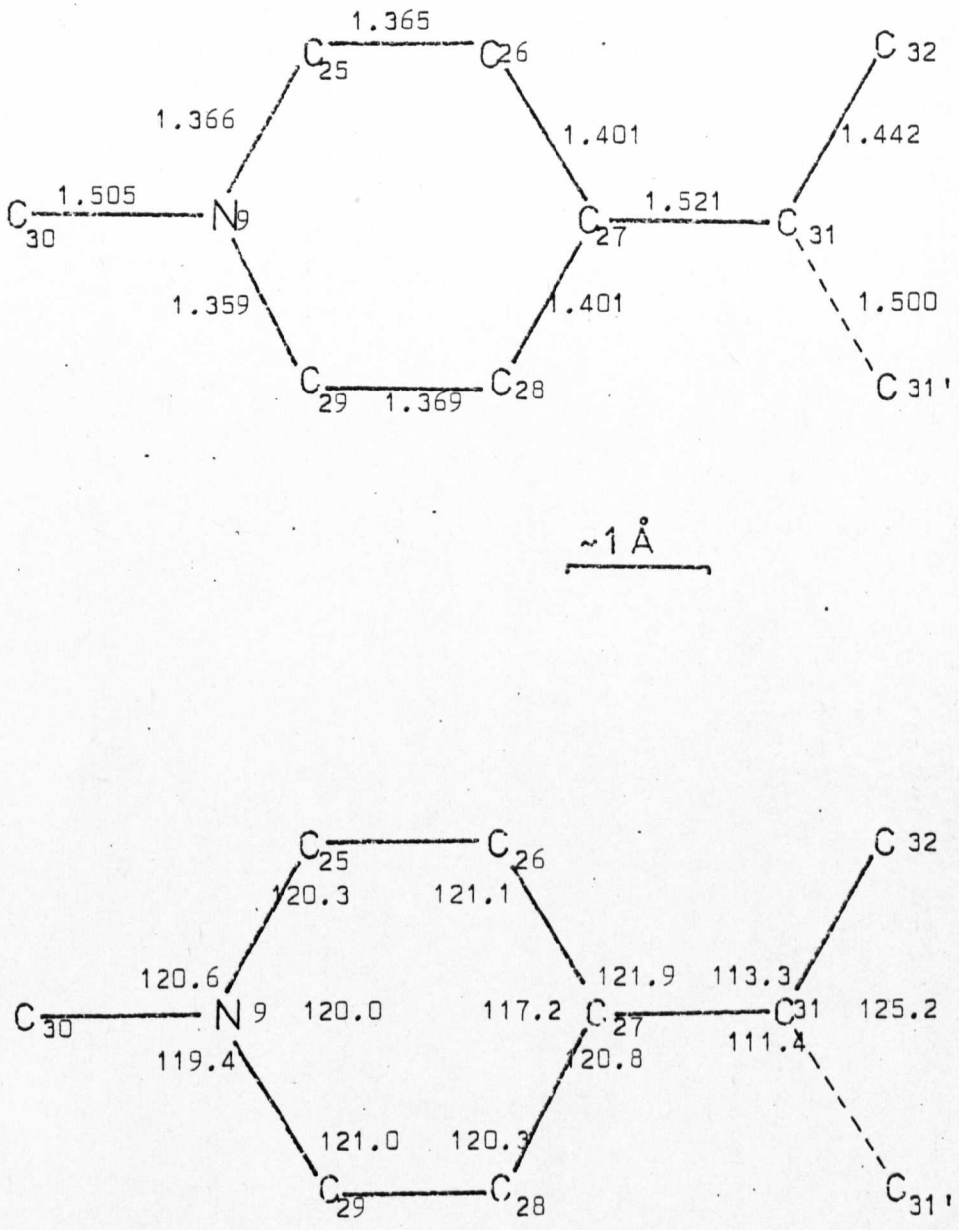

Figure 3.3 DMPB $(TCNQ)_4$ - Librationally corrected bond distances (Å) and angles (degrees)

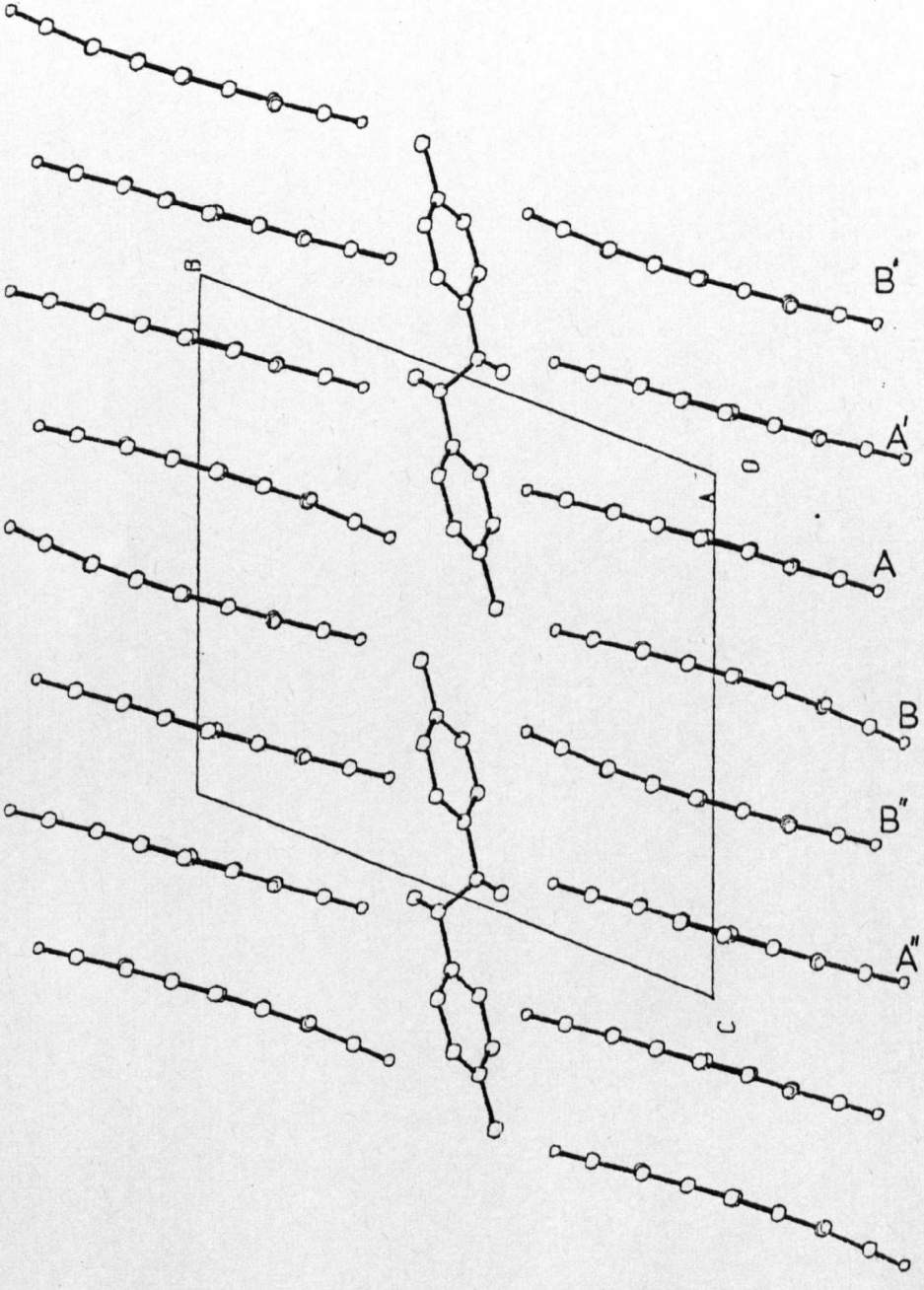

FIGURE 3.4a

Projection along a

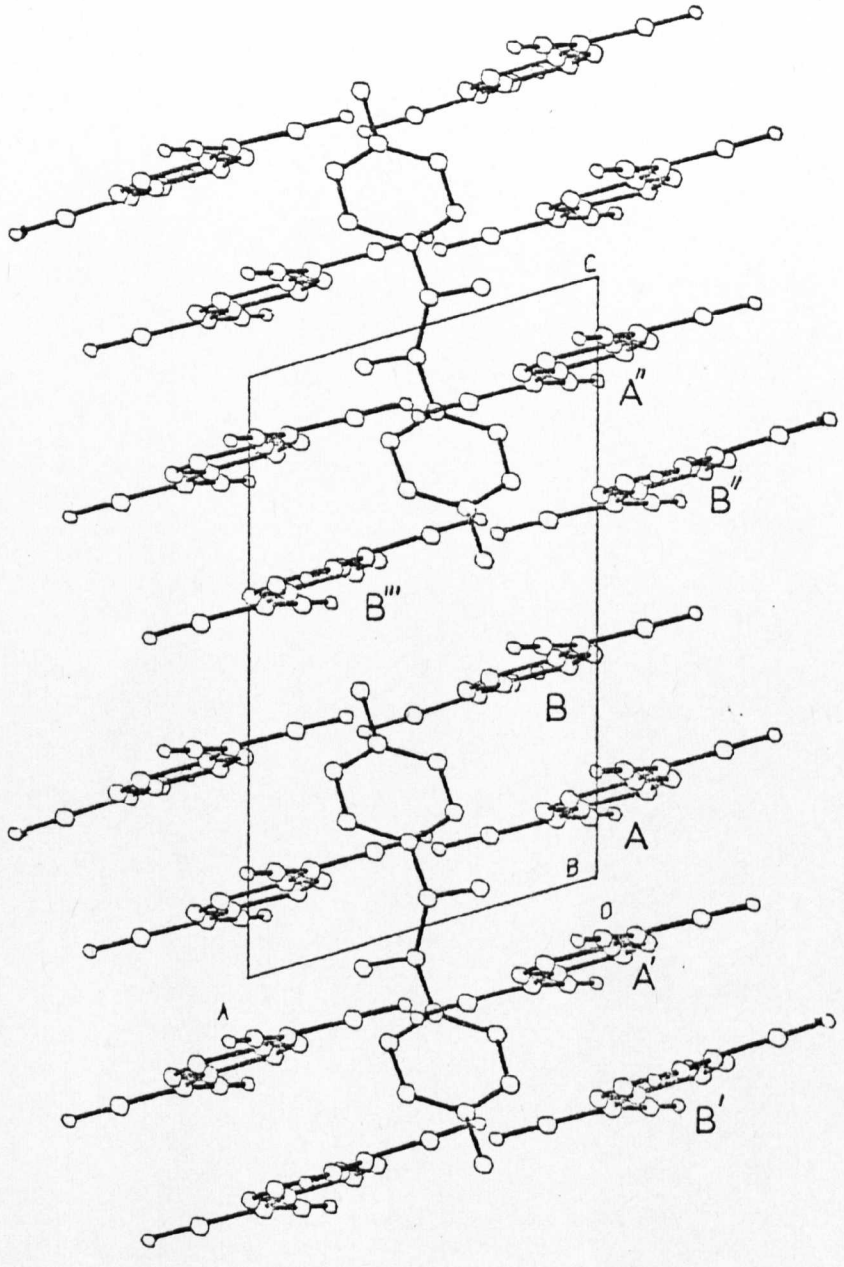

FIGURE 3.4b

Projection along b

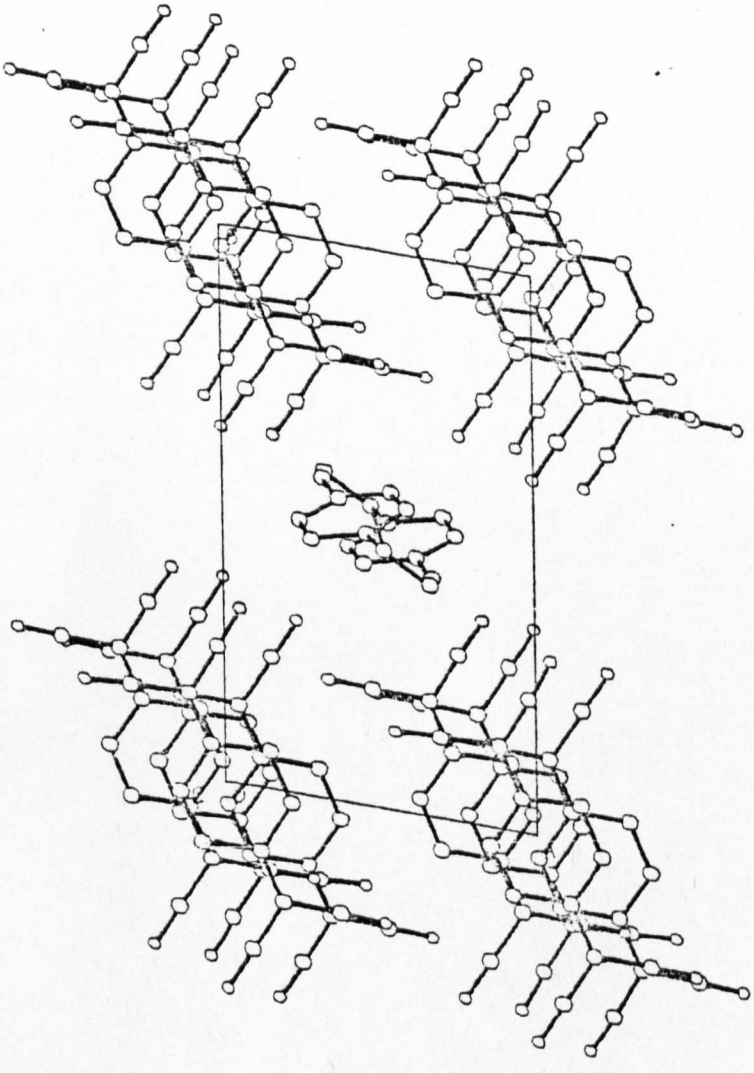

FIGURE 3.4c

Projection along c

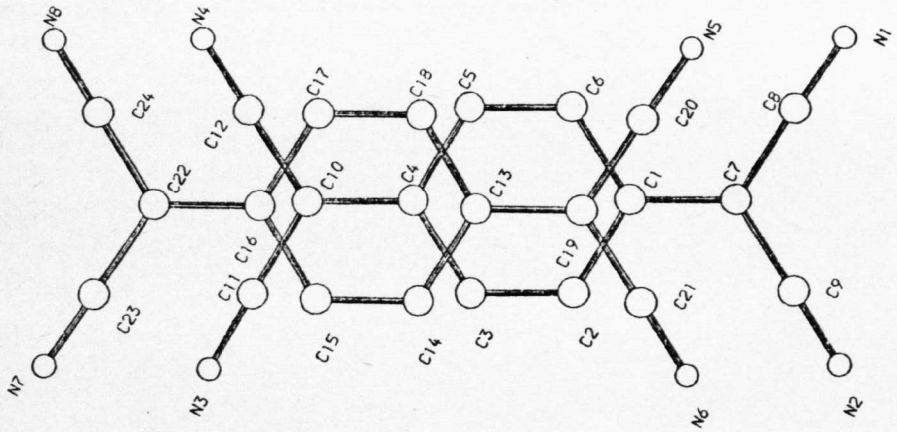

A on B

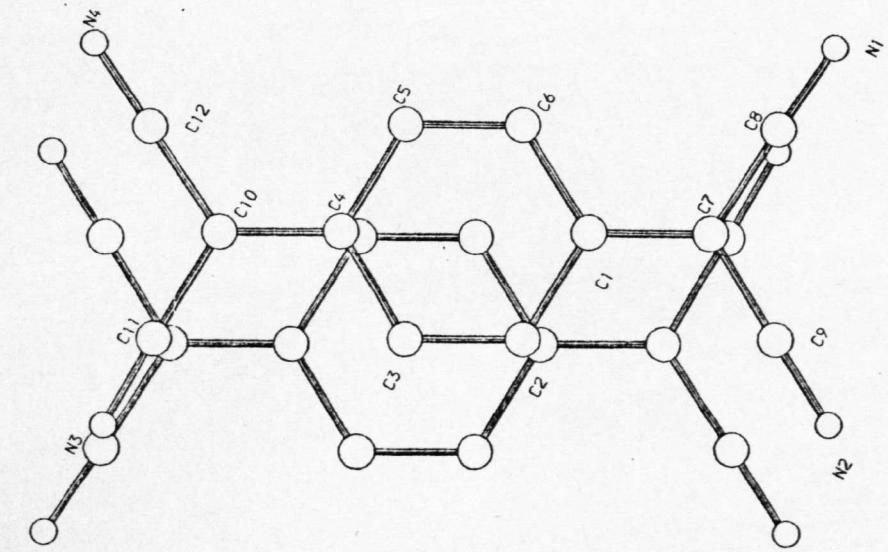

A on A'

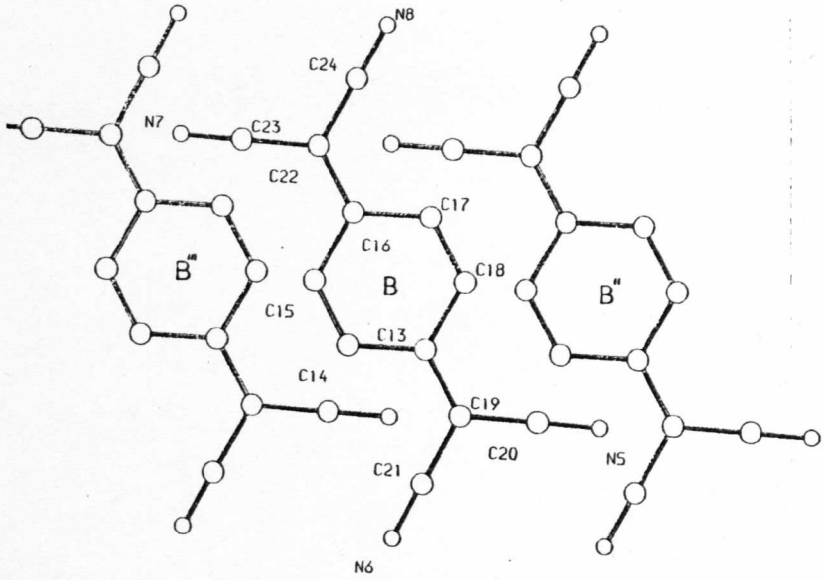

FIGURE 3.5

Molecular overlaps

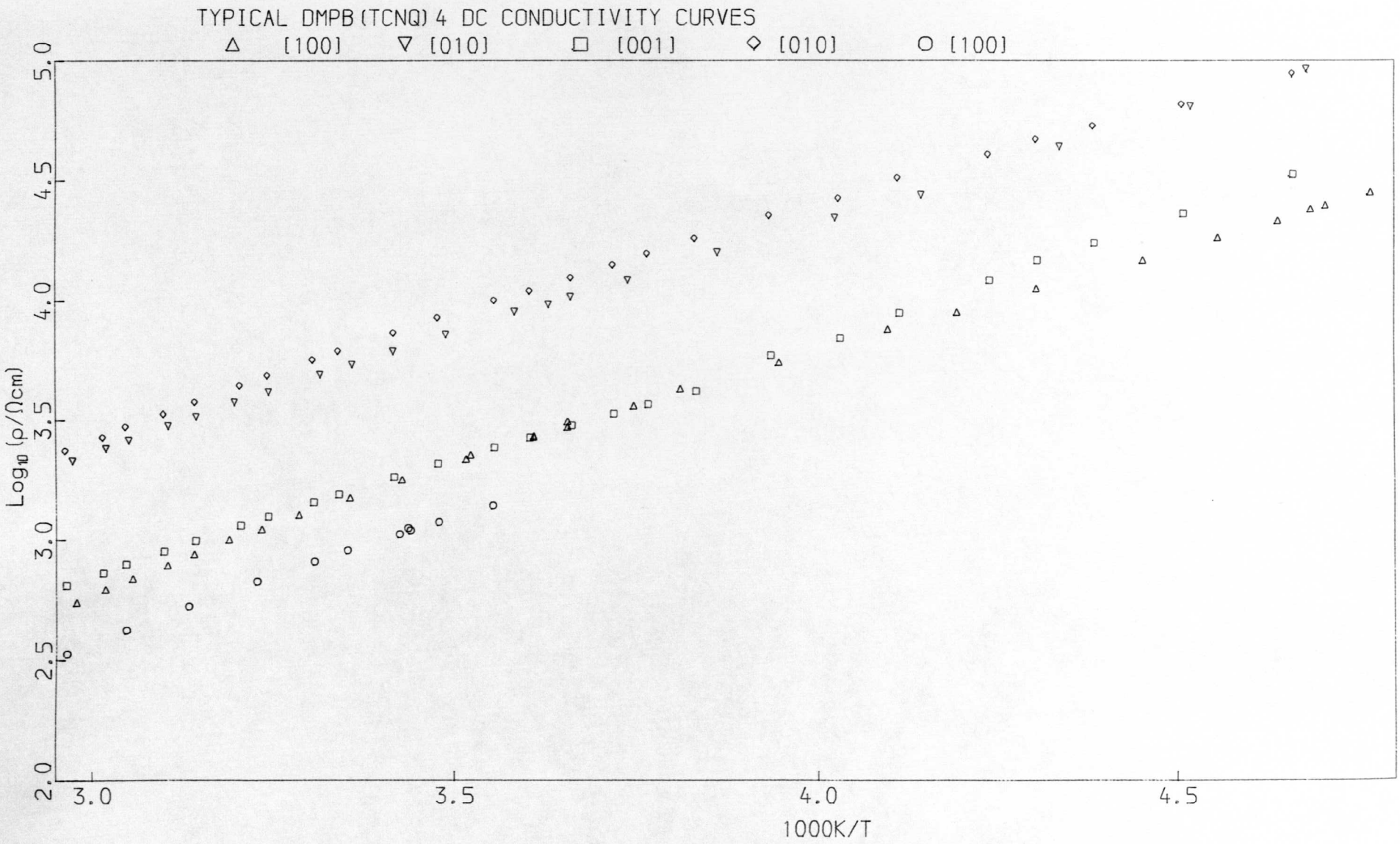
TYPICAL DMPB(TCNQ)4 DC CONDUCTIVITY CURVES
△ [100] ▽ [010] □ [001] ◇ [010] ○ [100]
Log10 (ρ/Ωcm)
2.0
2.5
3.0
3.5
4.0
4.5
5.0
3.0
3.5
4.0
4.5
1000K/T

FIGURE 3.6

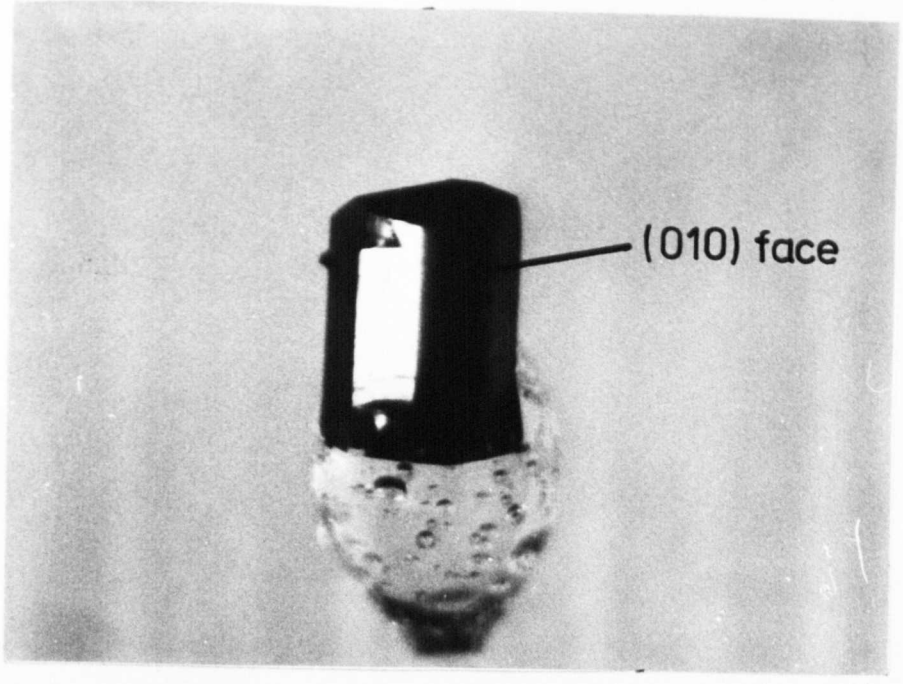

x 50

DMPB(TCNQ)$_4$ - showing 010 face
(rotation about a)
and (001) , (00$\bar{1}$) faces.

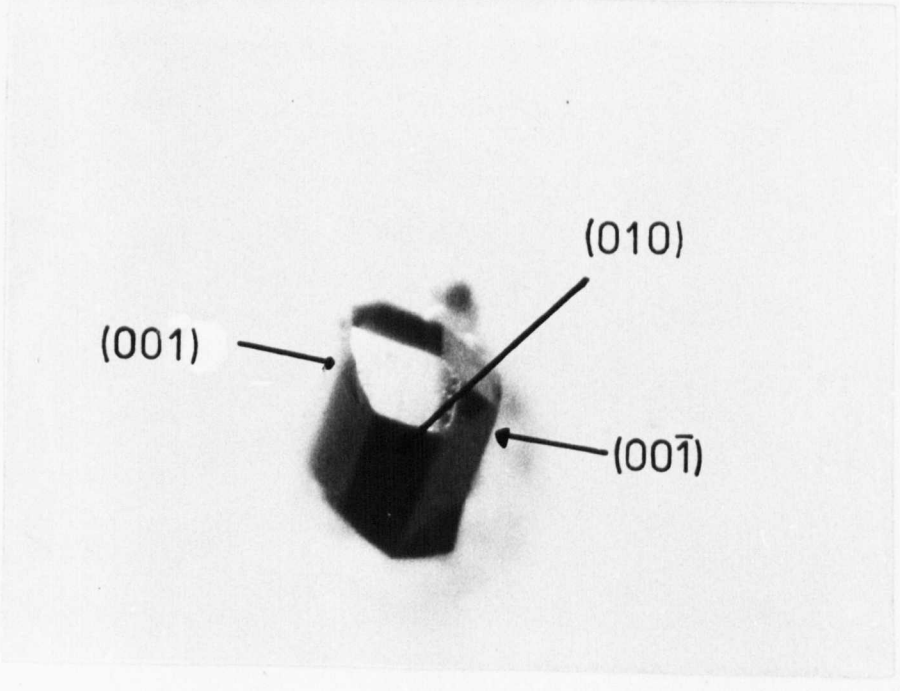

x 50

PLATE 3.1

TABLE 3.1

Bond lengths and standard deviations (in parentheses) in Å for $(DMPB)(TCNQ)_4$

Bond	Uncorrected	Corrected for Libration
C(1) - C(2)	1.423(4)	1.430
C(1) - C(6)	1.437(4)	1.445
C(1) - C(7)	1.397(4)	1.399
C(2) - C(3)	1.352(4)	1.354
C(3) - C(4)	1.433(4)	1.440
C(4) - C(5)	1.431(4)	1.438
C(4) - C(10)	1.393(4)	1.395
C(5) - C(6)	1.349(4)	1.351
C(7) - C(8)	1.417(4)	1.424
C(7) - C(9)	1.412(4)	1.419
C(8) - N(1)	1.132(4)	1.138
C(9) - N(2)	1.145(4)	1.151
C(10) - C(11)	1.423(4)	1.430
C(10) - C(12)	1.431(4)	1.438
C(11) - N(3)	1.139(4)	1.144
C(12) - N(4)	1.139(4)	1.144
C(13) - C(14)	1.433(4)	1.439
C(13) - C(18)	1.440(4)	1.446
C(13) - C(19)	1.384(4)	1.386

Cont./..

Table 3.1 continued

Bond	Uncorrected	Corrected for Libration
C(14) - C(15)	1.349(4)	1.351
C(15) - C(16)	1.435(4)	1.441
C(16) - C(17)	1.427(4)	1.432
C(16) - C(22)	1.388(4)	1.391
C(17) - C(18)	1.354(4)	1.356
C(19) - C(20)	1.430(4)	1.435
C(19) - C(21)	1.430(4)	1.436
C(20) - N(5)	1.138(4)	1.142
C(21) - N(6)	1.135(4)	1.140
C(22) - C(23)	1.421(4)	1.427
C(22) - C(24)	1.425(4)	1.431
C(23) - N(7)	1.138(4)	1.142
C(24) - N(8)	1.148(4)	1.153
N(9) - C(25)	1.349(4)	1.366
N(9) - C(29)	1.343(4)	1.359
N(9) - C(30)	1.496(4)	1.505
C(25) - C(26)	1.357(5)	1.365
C(26) - C(27)	1.385(5)	1.401
C(27) - C(28)	1.383(5)	1.401
C(27) - C(31)	1.512(5)	1.521
C(28) - C(29)	1.361(5)	1.369
C(31) - C(31')	1.487(7)	1.500
C(31) - C(32)	1.422(5)	1.442

TABLE 3.2

Bond angles for DMPB$(TCNQ)_4$ (estimated standard deviations $\times 10^2$ in parentheses)

Bond	Uncorrected	Corrected for Libration
C(2)-C(1)-C(6)	117.9(3)	118.2
C(2)-C(1)-C(7)	120.8(3)	120.6
C(6)-C(1)-C(7)	121.3(3)	121.2
C(1)-C(2)-C(3)	121.0(3)	120.9
C(2)-C(3)-C(4)	121.2(3)	121.1
C(3)-C(4)-C(5)	117.9(3)	118.1
C(3)-C(4)-C(10)	121.1(3)	121.0
C(5)-C(4)-C(10)	121.0(3)	120.9
C(4)-C(5)-C(6)	120.8(3)	120.7
C(5)-C(6)-C(1)	121.2(3)	121.1
C(1)-C(7)-C(8)	122.4(3)	122.3
C(1)-C(7)-C(9)	121.2(3)	121.1
C(8)-C(7)-C(9)	116.4(3)	116.6
C(7)-C(8)-N(1)	178.5(4)	178.5
C(7)-C(9)-N(2)	179.8(4)	179.8
C(4)-C(10)-C(11)	120.9(3)	120.8
C(4)-C(10)-C(12)	122.8(3)	122.7
C(11)-C(10)-C(12)	116.4(3)	116.6
C(10)-C(11)-N(3)	179.1(3)	179.1
C(10)-C(12)-N(4)	179.3(4)	179.3

Cont./..

Table 3.2 continued

Bond	Uncorrected	Corrected for Libration
C(14)-C(13)-C(18)	117.6(3)	117.8
C(14)-C(13)-C(19)	120.9(3)	120.8
C(18)-C(13)-C(19)	121.5(3)	121.4
C(13)-C(14)-C(15)	120.8(3)	120.7
C(14)-C(15)-C(16)	121.7(3)	121.6
C(15)-C(16)-C(17)	117.5(3)	117.6
C(15)-C(16)-C(22)	121.5(3)	121.4
C(17)-C(16)-C(22)	121.0(3)	120.9
C(16)-C(17)-C(18)	121.4(3)	121.3
C(13)-C(18)-C(17)	121.0(3)	120.9
C(13)-C(19)-C(20)	122.3(3)	122.2
C(13)-C(19)-C(21)	122.7(3)	122.6
C(20)-C(19)-C(21)	115.0(3)	115.2
C(19)-C(20)-N(5)	179.7(4)	179.8
C(19)-C(21)-N(6)	179.3(4)	179.3
C(16)-C(22)-C(23)	122.3(3)	122.2
C(16)-C(22)-C(24)	122.1(3)	122.0
C(23)-C(22)-C(24)	115.6(3)	115.8
C(22)-C(23)-N(7)	179.4(4)	179.4
C(22)-C(24)-N(8)	178.3(4)	178.3

Cont./..

Table 3.2 continued

Bond	Uncorrected	Corrected for Libration
C(25)-N(9)-C(29)	119.6(3)	120.0
C(25)-N(9)-C(30)	120.7(3)	120.6
C(29)-N(9)-C(30)	119.7(3)	119.4
N(9)-C(25)-C(26)	120.4(3)	120.3
C(25)-C(26)-C(27)	121.4(3)	121.1
C(26)-C(27)-C(28)	116.8(3)	117.2
C(26)-C(27)-C(31)	122.2(3)	121.9
C(28)-C(27)-C(31)	121.0(3)	120.8
C(27)-C(28)-C(29)	120.5(3)	120.3
N(9)-C(29)-C(28)	121.3(3)	121.0
C(27)-C(31)-C(31')	112.0(3)	111.4
C(27)-C(31)-C(32)	113.1(4)	113.3
C(31')-C(31)-C(32)	125.0(5)	125.2

Table 3.3

Details of molecular planes (* denotes atoms not defining the plane).

1) TCNQ molecule A

Equation of plane (all atoms defining the plane):

$-0.16084x - 1.48915y + 12.90097z - 1.686 = 0$

Equation of plane defined by ring atoms:

$-0.14809x - 1.49438y + 12.89696z - 1.661 = 0$

x, y, and z are in crystal fractions.

Distances from planes:

Atom	Whole molecule	Ring
C1	-0.014	0.008
C2	-0.032	-0.007
C3	-0.025	0.001
C4	-0.022	0.004
C5	-0.025	-0.002
C6	-0.026	-0.004
C7	-0.007	0.014 *
C8	0.007	0.025 *
C9	0.016	0.038 *
C10	-0.002	0.025 *

Cont./..

Table 3.3 continued

Atom	Whole molecule	Ring
C11	0.005	0.034 *
C12	0.012	0.038 *
N1	0.022	0.039 *
N2	0.032	0.055 *
N3	0.024	0.055 *
N4	0.033	0.059 *

Distances from planes - molecule B

2) TCNQ molecule B

Equation of the plane defined by all atoms:

$$0.06043x - 1.05867y + 12.68872z - 4.822 = 0$$

Equation of plane defined by ring atoms:

$$-0.00329x - 1.22029y + 12.76248z - 4.785 = 0$$

Distances from planes:

Atom	Whole molecule/Å	Ring/Å
C13	-0.039	0.009
C14	-0.035	0.002
C15	-0.055	-0.010
C16	-0.060	0.007

Cont/..

Table 3.3 continued

Atom	Whole molecule/Å	Ring/Å
C17	-0.074	0.004
C18	-0.081	-0.012
C19	-0.001	0.038 *
C20	-0.048	0.003 *
C21	0.112	0.131 *
C22	-0.018	0.057 *
C23	-0.057	0.007 *
C24	0.101	0.197 *
N5	-0.084	-0.025 *
N6	0.192	0.194 *
N7	-0.083	-0.028 *
N8	0.229	0.342 *

3) Cation molecule

Equation of plane defined by N(9) to C(31):

$$-3.31005x + 10.61658y + 4.86399z - 4.38230 = 0$$

Equation of plane defined by ring atoms only:

$$-3.31542x + 10.66518y + 4.79068z - 4.39931 = 0$$

Cont./..

Table 3.3 continued

Atom	Whole molecule	Ring
N9	0.015	-0.007
C25	0.023	0.005
C26	0.013	0.004
C27	-0.005	-0.011
C28	0.020	0.009
C29	0.018	-0.000
C30	-0.048	-0.079 *
C31	-0.036	-0.033 *
C32	1.033 *	1.039 *

TABLE 3.4 Short Intermolecular Distances for DMPB $(TCNQ)_4$

Intra - Stack

A-B Contacts 3.4 Å

Atoms	Å
C(1) - C(19')	3.228(4)
C(1) - C(20')	3.325(4)
C(2) - C(19')	3.356(4)
C(2) - C(21')	3.340(4)
C(3) - C(13')	3.342(4)
C(3) - C(14')	3.197(4)
C(4) - C(13')	3.252(4)
C(4) - C(14')	3.386(4)
C(4) - C(18')	3.364(4)
C(5) - C(18')	3.241(4)
C(6) - C(20')	3.293(4)
C(10) - C(15')	3.355(4)
C(10) - C(16')	3.214(4)
C(10) - C(17')	3.378(4)
C(11) - C(15')	3.192(4)
C(11) - C(16')	3.351(6)
C(12) - C(16')	3.383(4)
C(12) - C(17')	3.326(4)

Cont./..

Table 3.4 continued

Atoms	Å
A - A' contacts 3.5 Å	
C(2) - C(4")	3.326(4)
C(7) - C(11")	3.377(4)
C(8) - N(3")	3.412(4)
C(11) - C(7")	3.377(5)
N(3) - C(8")	3.412(5)
Inter-stack	
B - B" contacts 3.6 Å	
C(16) - N(5"')	3.521(4)
C(17) - C(20"')	3.446(4)
C(17) - N(5"')	3.562(4)
C(18) - C(18"')	3.398(6)
C(22) - N(5"')	3.432(5)
C(24) - N(5"')	3.303(5)
B - B"' contacts 3.6 Å	
C(13) - $N(7^{iv})$	3.506(4)
C(14) - $C(23^{iv})$	3.425(4)
C(14) - $N(7^{iv})$	3.547(5)
C(15) - $C(15^{iv})$	3.399(6)
C(19) - $N(7^{iv})$	3.451(5)
C(21) - $N(7^{iv})$	3.386(5)

Cont./..

Table 3.4 continued

Other Inter-Stack contacts	3.4 Å
C(2) - C(7^{v})	3.333(4)
C(3) - N(1^{v})	3.372(4)
C(5) - N(3^{vi})	3.269(4)
C(6) - N(3^{vi})	3.270(4)
N(3) - C(5^{v})	3.269(4)
N(3) - C(6^{v})	3.270(4)
C(17) - N(7^{vi})	3.368(4)

Cation - TCNQ (A)	3.5 Å
N(1) - C(25^{vi})	3.212(5)
N(2) - C(25^{i})	3.363(5)
N(2) - C(26^{i})	3.294(5)
N(2) - C(28^{vi})	3.497(5)
N(2) - C(29^{vi})	3.317(5)
N(3) - C(32^{vii})	3.493(7)

Cation - TCNQ (B)	3.5 Å
N(7) - C(28^{viii})	3.484(5)
N(8) - C(29^{ix})	3.303(5)
N(8) - C(30^{iv})	3.295(5)

Cont./..

Table 3.4 continued

Symmetry Operations:

i	x	y	z	iv	1-x	-y	1-z
ii	-x	-y	-z	v	1+x	y	z
iii	-x	-y	1-z	vi	x-1	y	z
vii	x	y-1	z	viii	-x	-1-y	-z
ix	x-1	y-1	z				

ATOM	X/A	Y/B	Z/C	U(ISO)
C(1)	-0.1101(5)	0.1129(3)	0.1415(3)	
C(2)	0.0742(5)	0.1141(3)	0.1425(3)	
C(3)	-0.1470(5)	0.0308(3)	0.1339(3)	
C(4)	0.0427(5)	-0.0631(3)	0.1224(3)	
C(5)	-0.1424(5)	-0.0648(3)	0.1196(3)	
C(6)	-0.2150(5)	0.0185(3)	0.1282(3)	
C(7)	-0.1843(5)	0.1990(3)	0.1509(3)	
C(8)	-0.3621(6)	0.2007(3)	0.1497(4)	
C(9)	-0.0803(6)	0.2924(3)	0.1648(4)	
C(10)	0.1101(5)	-0.1481(3)	0.1152(3)	
C(11)	0.3030(6)	-0.1460(3)	0.1180(3)	
C(12)	0.0196(5)	-0.2429(3)	0.1039(3)	
N(1)	-0.5118(5)	0.2041(3)	0.1500(4)	
N(2)	0.0034(6)	0.3674(3)	0.1764(4)	
N(3)	0.4507(5)	-0.1426(3)	0.1214(4)	
N(4)	-0.0505(5)	-0.3179(3)	0.0962(4)	
C(13)	0.1183(5)	0.0552(3)	0.3812(3)	
C(14)	0.3016(5)	0.0540(3)	0.3804(3)	
C(15)	0.3711(5)	-0.0304(3)	0.3714(3)	
C(16)	0.2665(5)	-0.1225(3)	0.3638(3)	
C(17)	0.0830(5)	-0.1214(3)	0.3638(3)	
C(18)	0.0114(5)	-0.0375(3)	0.3707(3)	
C(19)	0.0472(5)	0.1420(3)	0.3912(3)	
C(20)	-0.1363(6)	0.1446(3)	0.3888(3)	
C(21)	0.1529(6)	0.2369(3)	0.4076(4)	
C(22)	0.3403(5)	-0.2079(3)	0.3598(3)	
C(23)	0.5207(6)	-0.2122(3)	0.3557(4)	
C(24)	0.2424(6)	-0.2966(3)	0.3622(4)	
N(5)	-0.2824(6)	0.1475(3)	0.3871(3)	
N(6)	0.2354(6)	0.3122(3)	0.4199(4)	
N(7)	0.6638(5)	-0.2163(3)	0.3523(4)	
N(8)	0.1659(6)	-0.3669(3)	0.3668(4)	
N(9)	0.6253(5)	0.4591(3)	0.3275(3)	
C(25)	0.4533(6)	0.4349(4)	0.2652(4)	
C(26)	0.4070(6)	0.4602(4)	0.1763(4)	
C(27)	0.5342(6)	0.5116(3)	0.1470(4)	
C(28)	0.7086(6)	0.5376(3)	0.2137(4)	
C(29)	0.7508(6)	0.5104(3)	0.3017(4)	
C(30)	0.6773(8)	0.4264(4)	0.4217(4)	
C(31)	0.4875(7)	0.5396(4)	0.0476(4)	
C(32)	0.347(1)	0.5966(6)	0.0469(5)	
H(1)	0.1549	0.1019	0.1504	0.0500
H(2)	0.2847	0.0340	0.1355	0.0500
H(3)	-0.2235	-0.1334	0.1100	0.0500
H(4)	-0.3530	0.0148	0.1251	0.0500
H(5)	0.3836	0.1207	0.3864	0.0500
H(6)	0.5070	-0.0297	0.3694	0.0500
H(7)	0.0022	-0.1881	0.3585	0.0500
H(8)	-0.1264	-0.0398	0.3685	0.0500
H(9)	0.3530	0.3959	0.2865	0.0500
H(10)	0.2712	0.4399	0.1276	0.0500
H(11)	0.8195	0.5787	0.1950	0.0500
H(12)	0.8865	0.5293	0.3510	0.0500

ATOM	U(11)	U(22)	U(33)	U(23)	U(13)	U(12)
C(1)	0.044(2)	0.054(2)	0.053(2)	0.025(2)	0.010(2)	0.004(2)
C(2)	0.042(2)	0.051(2)	0.055(2)	0.025(2)	0.012(2)	0.002(2)
C(3)	0.041(2)	0.051(2)	0.053(2)	0.024(2)	0.013(2)	0.002(2)
C(4)	0.043(2)	0.051(2)	0.048(2)	0.021(2)	0.010(2)	0.003(2)
C(5)	0.043(2)	0.052(2)	0.060(3)	0.025(2)	0.013(2)	0.000(2)
C(6)	0.040(2)	0.054(2)	0.061(3)	0.025(2)	0.011(2)	0.001(2)
C(7)	0.042(2)	0.054(2)	0.067(3)	0.027(2)	0.014(2)	0.007(2)
C(8)	0.056(3)	0.055(3)	0.087(3)	0.031(2)	0.018(2)	0.010(2)
C(9)	0.051(3)	0.055(3)	0.086(3)	0.031(2)	0.017(2)	0.012(2)
C(10)	0.043(2)	0.048(2)	0.057(2)	0.022(2)	0.015(2)	0.003(2)
C(11)	0.057(3)	0.047(2)	0.064(3)	0.024(2)	0.021(2)	0.007(2)
C(12)	0.049(2)	0.054(3)	0.067(3)	0.024(2)	0.015(2)	0.007(2)
N(1)	0.054(3)	0.082(3)	0.140(4)	0.047(3)	0.033(3)	0.016(2)
N(2)	0.069(3)	0.065(3)	0.150(4)	0.047(3)	0.031(3)	0.009(2)
N(3)	0.056(2)	0.079(3)	0.111(3)	0.043(3)	0.036(2)	0.012(2)
N(4)	0.072(3)	0.058(2)	0.117(4)	0.035(2)	0.029(3)	-0.002(2)
C(13)	0.049(2)	0.051(2)	0.047(2)	0.021(2)	0.011(2)	0.004(2)
C(14)	0.046(2)	0.052(2)	0.054(3)	0.022(2)	0.008(2)	-0.002(2)
C(15)	0.042(2)	0.054(2)	0.051(2)	0.022(2)	0.007(2)	0.002(2)
C(16)	0.043(2)	0.053(2)	0.047(2)	0.021(2)	0.010(2)	0.004(2)
C(17)	0.043(2)	0.053(2)	0.053(2)	0.026(2)	0.014(2)	0.002(2)
C(18)	0.045(2)	0.056(2)	0.053(2)	0.026(2)	0.015(2)	0.006(2)
C(19)	0.054(2)	0.052(2)	0.052(2)	0.021(2)	0.014(2)	0.006(2)
C(20)	0.068(3)	0.054(3)	0.059(3)	0.026(2)	0.023(2)	0.014(2)
C(21)	0.066(3)	0.057(3)	0.070(3)	0.027(2)	0.016(2)	0.010(2)
C(22)	0.049(2)	0.050(2)	0.057(3)	0.021(2)	0.010(2)	0.004(2)
C(23)	0.059(3)	0.053(3)	0.063(3)	0.023(2)	0.011(2)	0.009(2)
C(24)	0.057(3)	0.057(3)	0.067(3)	0.027(2)	0.011(2)	0.009(2)
N(5)	0.068(3)	0.089(3)	0.092(3)	0.040(3)	0.034(2)	0.023(2)
N(6)	0.093(3)	0.060(3)	0.111(4)	0.036(3)	0.021(3)	-0.005(2)
N(7)	0.056(3)	0.082(3)	0.100(3)	0.032(2)	0.019(2)	0.016(2)
N(8)	0.076(3)	0.070(3)	0.112(4)	0.047(3)	0.015(3)	0.001(2)
N(9)	0.069(3)	0.054(2)	0.075(3)	0.031(2)	0.016(2)	0.006(2)
C(25)	0.060(3)	0.070(3)	0.095(4)	0.037(3)	0.021(3)	-0.002(2)
C(26)	0.059(3)	0.071(3)	0.084(3)	0.035(3)	0.009(3)	0.004(2)
C(27)	0.065(3)	0.051(3)	0.071(3)	0.027(2)	0.018(2)	0.019(2)
C(28)	0.060(3)	0.067(3)	0.084(3)	0.040(3)	0.020(3)	0.009(2)
C(29)	0.057(3)	0.065(3)	0.078(3)	0.031(3)	0.013(2)	0.002(2)
C(30)	0.108(4)	0.089(4)	0.075(3)	0.054(3)	0.014(3)	0.012(3)
C(31)	0.103(4)	0.082(4)	0.073(3)	0.043(3)	0.028(3)	0.053(3)
C(32)	0.220(8)	0.162(6)	0.113(5)	0.081(5)	0.075(5)	0.151(6)

H	/FO/	/FC/	PHI
** K= 0 L= 0 **			
1	200	257	0
2	53	67	0
3	79	68	0
5	181	163	180
6	72	67	0
8	33	42	0
** K= 1 L= 0 **			
-8	22	18	0
-7	47	37	0
-6	29	29	0
-5	69	68	180
-4	251	225	180
-3	39	35	180
-2	42	13	0
-1	350	341	0
0	469	583	0
2	65	68	180
3	72	58	180
4	103	108	180
5	150	154	180
6	26	32	0
7	20	22	180
8	21	15	0
** K= 2 L= 0 **			
-7	95	94	0
-5	104	97	180
-4	77	85	180
-3	21	10	0
-2	17	18	0
-1	527	575	180
0	290	263	0
1	94	85	0
2	113	104	180
3	27	21	0
4	24	24	180
5	125	134	0
6	68	84	180
7	31	39	0
8	20	17	0
** K= 3 L= 0 **			
-8	32	33	0
-5	243	246	0
-4	24	12	180
-3	80	67	0
-2	50	34	0
-1	541	594	0
0	692	727	180
1	772	763	0
2	147	151	180
3	26	27	0
4	50	45	0
5	155	161	0
** K= 4 L= 0 **			
-8	58	57	0
-7	65	62	180
-6	45	47	0
-5	79	77	180
-4	140	135	0
-3	80	71	180
-2	40	42	0
-1	72	102	180
0	42	16	0
1	725	714	180
2	121	104	180
5	267	270	0
6	124	124	0
7	23	24	180
8	16	16	0
** K= 5 L= 0 **			
-8	34	31	0
-7	46	45	180
-6	58	56	180
-5	27	26	0
-4	212	212	180
-3	37	36	0
-2	142	144	0
-1	118	120	0
0	13	9	180
1	783	752	180
2	123	121	180
3	34	27	0
4	51	54	0
5	176	193	0
6	438	440	0
** K= 6 L= 0 **			
-7	72	64	180
-6	269	268	180
-5	28	25	180
-4	154	153	0
-3	56	56	180
-2	53	43	0
-1	81	92	0
0	233	212	0
1	157	154	180
2	190	176	180
3	75	70	180
4	26	25	0
5	74	72	0
6	131	142	0
7	34	28	0
** K= 7 L= 0 **			
-6	285	278	180
-4	32	36	0
-3	26	30	0
-1	152	145	0
0	22	30	0
1	60	63	180
2	183	180	180
3	27	21	0
4	23	22	180
5	91	90	180
6	18	20	180
** K= 8 L= 0 **			
-8	18	22	0
-7	38	37	0
-5	64	61	180
-4	27	11	180
-3	21	15	180
-2	86	98	0
-1	37	36	180
0	33	41	180
1	268	274	0
2	26	18	180
3	32	26	180
4	36	34	0
5	61	58	0
6	58	52	180
** K= 9 L= 0 **			
-7	66	55	180
-6	54	45	0
-5	47	46	180
-3	18	22	180
-2	23	22	0
-1	159	163	180
0	85	82	0
1	49	46	180
2	35	33	0
3	32	27	0
4	32	29	180
6	33	34	180
** K= 10 L= 0 **			
-7	89	82	180
-2	16	12	0
-1	119	127	180
0	101	94	180
1	19	24	180
2	101	95	180
3	67	77	180
4	47	50	0
** K= 11 L= 0 **			
-7	15	15	0
-6	45	50	180
-5	111	115	0
-3	28	32	180
-1	128	134	180
0	181	184	180
2	32	21	0
4	27	29	180
5	15	18	0
** K= 12 L= 0 **			
-7	36	33	0
-6	36	33	180
-5	45	46	0
-4	29	36	0
-2	31	36	180
-1	50	53	180
0	221	220	180
1	78	76	0
3	32	40	180
** K= 13 L= 0 **			
-1	52	52	0
1	43	43	180
2	25	30	180
** K= 14 L= 0 **			
-5	60	56	180
-4	18	20	0
-1	28	30	180
0	41	40	0
** K= 15 L= 0 **			
-4	35	33	180
-2	17	17	180
-1	75	73	180
1	18	17	0
** K=-16 L= 1 **			
2	30	28	0
3	28	20	0
** K=-15 L= 1 **			
1	46	48	0
3	23	21	180
4	18	22	180
** K=-14 L= 1 **			
-1	20	15	180
** K=-13 L= 1 **			
-4	43	49	180
-3	50	43	180
1	24	16	180
2	31	31	180
3	72	76	0
4	64	72	0
** K=-12 L= 1 **			
-1	60	72	180
0	152	149	0
1	87	90	0
2	27	26	0
3	47	51	0
4	54	65	0
5	38	35	0
** K=-11 L= 1 **			
-4	87	97	180
-3	55	56	180
0	85	84	0
1	178	181	0
2	24	24	0
3	20	15	0
4	63	71	0
5	37	39	0
** K=-10 L= 1 **			
-5	47	45	180
-4	98	100	180
-3	199	218	180
-2	92	85	180
0	56	51	0
1	122	130	0
5	21	21	0
7	16	15	0
** K= -9 L= 1 **			
-6	27	33	180
-5	87	92	0
-3	42	31	0
-2	43	41	0
-1	43	42	0
0	83	75	180
1	217	224	0
2	44	51	180
4	22	25	0
5	63	69	180
8	29	24	0
** K= -8 L= 1 **			
-7	24	20	0
-6	27	33	0
-5	58	66	180
-4	148	146	0
-3	132	145	0
-2	36	35	180
0	57	49	0
1	83	77	180
2	142	148	180
3	90	87	180
5	77	75	180
6	27	28	180

H	/FO/	/FC/	PHI
** K= -7	L= 1 **		
-7	17	8	180
-6	23	30	180
-5	65	80	0
-4	147	147	180
-3	174	181	180
-2	124	173	180
-1	66	76	180
0	19	32	0
1	232	245	180
2	135	115	180
4	61	60	180
5	123	122	180
6	42	46	0
** K= -6	L= 1 **		
-5	97	115	180
-4	132	134	0
-3	182	163	180
-2	216	200	180
-1	46	48	180
0	34	24	0
1	204	189	180
2	75	54	180
3	193	180	180
4	71	69	0
5	29	32	180
7	54	59	0
** K= -5	L= 1 **		
-7	29	28	0
-6	112	116	180
-5	32	39	0
-4	15	20	0
-3	153	164	180
-2	107	90	180
-1	246	227	180
0	26	18	0
1	280	272	180
2	679	649	180
3	267	276	180
4	129	129	180
5	43	46	0
6	20	12	180
** K= -4	L= 1 **		
-7	23	18	180
-6	25	31	180
-5	176	189	180
-4	110	113	0
-3	171	183	180
-2	231	258	180
-1	90	108	180
0	163	139	180
1	393	390	0
2	149	152	180
3	27	34	0
4	114	102	0
5	50	59	180
7	51	47	0
8	56	59	180
** K= -3	L= 1 **		
-6	38	36	180
-5	33	37	180
-4	65	73	180
-3	121	123	0
-2	106	103	180
-1	304	319	0
0	79	51	0
1	111	115	0
2	219	224	0
3	603	576	0
4	68	59	180
5	32	31	0
** K= -2	L= 1 **		
-7	42	46	0
-6	37	26	0
-5	103	105	180
-4	36	39	0
-3	14	23	180
-2	457	450	180
-1	54	51	0
0	34	42	0
1	57	60	0
2	433	417	180
3	883	844	180
4	72	81	180
5	30	19	180
6	16	18	180
7	61	76	180
8	27	30	180
** K= 2	L= 1 **		
-8	50	48	0
-6	32	30	180
-5	34	41	0
-4	189	186	0
-3	330	321	0
-2	272	270	180
-1	107	104	0
0	78	69	180
1	251	247	0
2	20	24	0
3	26	33	180
4	216	218	0
5	138	150	0
6	68	58	0
** K= 3	L= 1 **		
-8	35	35	0
-7	23	17	180
-5	174	173	180
-4	101	90	180
-3	166	176	180
-2	148	143	180
-1	942	931	0
0	197	210	180
1	146	129	180
2	41	37	180
3	127	129	0
4	100	89	0
5	123	134	0
6	23	24	180
8	47	50	180
** K= 4	L= 1 **		
-9	27	22	180
-8	64	59	0
-5	34	23	0
-3	60	48	180
-2	259	256	0
-1	237	250	180
0	126	127	0
1	260	245	0
2	24	17	0
3	130	136	180
4	121	125	0
5	248	248	0
** K= 5	L= 1 **		
-8	21	26	0
-6	14	19	180
-4	168	163	0
-3	99	106	0
-2	16	11	0
-1	546	569	180
0	237	254	0
1	127	141	180
2	24	22	0
3	118	125	180
4	38	34	0
5	51	55	0
7	24	33	0
8	16	9	180
** K= 6	L= 1 **		
-8	21	23	180
-7	42	39	180
-5	99	98	180
-4	268	266	180
-3	84	81	0
-2	206	200	0
-1	305	303	180
0	76	66	0
1	46	43	0
2	104	90	0
4	75	80	180
5	98	98	0
6	36	47	0
7	14	19	180
** K= 7	L= 1 **		
-5	92	100	180
-4	87	87	180
-3	122	127	0
-2	101	104	180
-1	96	97	0
0	55	47	180
2	132	133	0
3	66	70	180
4	28	30	0
5	75	73	180
6	24	22	0
** K= 8	L= 1 **		
-8	70	71	0
-7	18	16	0
-6	18	20	0
-3	112	110	0
-2	128	134	0
-1	65	68	180
0	25	25	180
1	109	112	180
2	22	21	180
3	31	33	0
5	101	90	0
6	38	33	180
** K= 9	L= 1 **		
-7	40	31	180
-6	24	24	180
-5	27	24	180
-4	23	26	0
-3	42	44	180
-2	16	17	0
0	44	42	0
1	24	20	180
3	22	11	180
4	78	80	0
** K= 10	L= 1 **		
-7	66	63	180
-6	25	23	0
-3	49	49	0
-2	22	18	0
-1	49	50	180
0	27	22	0
1	61	75	0
2	73	70	0
3	110	103	0
4	88	92	180
** K= 11	L= 1 **		
-7	24	22	0
-4	62	63	0
-3	43	50	0
-2	50	52	180
-1	102	107	180
0	65	63	0
1	43	37	180
2	49	50	180
4	40	40	0
** K= 12	L= 1 **		

H	/FO/	/FC/	PHI
-7	38	31	0
-4	24	31	0
-3	87	98	0
-2	50	45	180
-1	18	19	0
0	49	39	180
2	18	14	180
3	34	25	0
4	23	18	180

** K= 13 L= 1 **

H	/FO/	/FC/	PHI
-5	21	20	0
-3	84	89	0
-2	72	66	0
2	56	53	0
3	32	31	0

** K= 14 L= 1 **

H	/FO/	/FC/	PHI
-2	38	34	180
-1	18	13	180
0	29	25	180

** K= 15 L= 1 **

H	/FO/	/FC/	PHI
-3	16	17	180
-2	21	21	180
-1	63	65	180
0	38	40	0

** K=-16 L= 2 **

H	/FO/	/FC/	PHI
0	18	18	180

** K=-15 L= 2 **

H	/FO/	/FC/	PHI
1	21	24	180
2	22	19	0
4	48	42	0

** K=-14 L= 2 **

H	/FO/	/FC/	PHI
-2	36	28	180
0	28	30	180
4	40	37	180

** K=-13 L= 2 **

H	/FO/	/FC/	PHI
-2	62	70	180
-1	86	97	0
0	26	21	0
2	35	37	0
3	92	98	180
4	33	41	180

** K=-12 L= 2 **

H	/FO/	/FC/	PHI
-2	44	46	0
-1	219	213	0
0	407	409	0
1	49	51	0
2	32	32	180
3	47	47	0
4	119	131	180
5	30	37	180
7	41	40	0

** K=-11 L= 2 **

H	/FO/	/FC/	PHI
-5	24	24	180
-1	55	64	0
0	371	373	0
1	106	114	0
3	72	77	180
5	110	105	180

** K=-10 L= 2 **

H	/FO/	/FC/	PHI
-6	39	26	180
-5	46	43	180
-4	41	47	180
-2	16	5	0
-1	224	222	180
0	71	68	0
1	93	92	0
3	50	54	0
4	61	63	180
5	21	24	0
7	37	34	180

** K= -9 L= 2 **

H	/FO/	/FC/	PHI
-6	33	39	180
-5	70	73	0
-4	29	32	0
-3	32	29	0
-2	88	89	180
-1	221	221	0
0	154	141	180
1	189	197	0
3	29	28	180
4	42	52	0
5	69	61	0
8	18	22	0

** K= -8 L= 2 **

H	/FO/	/FC/	PHI
-5	60	56	0
-4	28	17	0
-3	38	33	180
-2	76	72	0
-1	97	113	0
0	196	218	180
1	117	110	180
2	29	36	0
3	34	38	180
4	40	44	180
5	213	216	0

** K= -7 L= 2 **

H	/FO/	/FC/	PHI
-6	46	52	180
-5	30	21	180
-4	42	41	180
-3	62	56	0
-2	76	60	180
-1	104	93	0
0	54	54	0
1	301	307	180
2	50	45	180
3	24	30	0
4	146	141	0
5	333	322	0
6	302	301	0
7	18	17	180

** K= -6 L= 2 **

H	/FO/	/FC/	PHI
-7	77	78	180
-6	33	39	0
-4	17	16	0
-2	245	240	0
-1	308	309	180
0	547	534	0
1	348	344	180
2	29	19	180
3	49	46	180
4	64	68	0
5	165	167	0
6	312	307	0
7	34	41	0

** K= -5 L= 2 **

H	/FO/	/FC/	PHI
-6	185	192	180
-5	138	151	0
-4	71	80	0
-3	73	71	0
-2	56	63	180
-1	28	20	0
0	68	51	0
1	367	372	180
2	185	178	180
3	46	44	0
4	113	117	180
5	185	176	180
6	63	59	0

** K= -4 L= 2 **

H	/FO/	/FC/	PHI
-8	56	56	0
-6	54	53	0
-4	22	22	0
-2	281	273	0
-1	145	146	180
0	198	181	180
1	714	667	0
2	101	91	180
3	31	22	180
4	46	39	0
5	96	87	0
6	120	113	180
7	64	61	0

** K= -3 L= 2 **

H	/FO/	/FC/	PHI
-8	41	41	0
-7	56	50	0
-6	92	88	180
-5	108	108	0
-4	33	28	0
-3	23	16	180
-2	71	79	180
-1	57	32	0
0	198	163	180
1	725	731	0
2	40	23	0
3	28	35	180
4	42	44	0
5	148	155	0
6	104	105	180
7	21	23	180

** K= -2 L= 2 **

H	/FO/	/FC/	PHI
-8	35	26	0
-7	220	219	180
-6	145	150	0
-5	68	64	180
-4	18	18	180
-3	53	47	0
-2	424	418	0
-1	207	249	180
0	125	209	180
1	403	388	180
2	168	143	180
3	66	66	0
4	47	46	180
5	39	39	180
6	72	80	180
7	90	102	180
8	21	18	180

** K= -1 L= 2 **

H	/FO/	/FC/	PHI
-8	35	31	0
-6	134	129	180
-5	145	139	0
-4	59	55	180
-2	96	77	0
-1	618	654	180
0	272	380	0
1	142	87	0
2	60	66	180
3	19	7	180
4	55	50	0
5	53	54	180
6	91	96	0
7	134	151	180

** K= 0 L= 2 **

H	/FO/	/FC/	PHI
-8	20	27	0
-7	45	50	0
-6	83	86	180
-4	13	14	0
-3	58	56	0
-2	585	546	180
-1	315	309	180
0	329	393	180
1	488	535	0
2	366	362	0
3	102	104	180
4	20	23	180
5	41	34	180
6	92	86	0
7	32	26	180
8	27	30	180

** K= 1 L= 2 **

H	/FO/	/FC/	PHI
-7	207	228	0
-6	128	124	180
-5	136	125	0
-4	21	14	180
-3	81	81	0
-2	402	373	0
-1	73	47	180
0	56	71	0
1	396	370	0
2	355	355	180
3	70	77	0
4	68	74	0
5	35	38	180
6	20	4	180
7	71	66	0

** K= 2 L= 2 **

H	/FO/	/FC/	PHI
-7	71	71	0
-6	147	161	0
-5	51	58	180
-4	15	2	180
-3	76	73	180
-2	33	47	0
-1	519	502	0
0	167	167	180
2	31	37	0
3	99	95	180
7	82	79	0
8	33	33	180

** K= 3 L= 2 **

H	/FO/	/FC/	PHI
-7	34	32	180
-6	122	119	0
-5	227	235	180
-4	43	48	180
-3	47	39	0

H	/FO/	/FC/	PHI
-2	109	119	180
0	591	557	0
1	61	76	0
2	203	199	180
3	57	52	0
4	33	33	180
5	46	44	180
6	36	43	180

** K= 4 L= 2 **

H	/FO/	/FC/	PHI
-7	45	39	180
-6	74	70	0
-5	109	101	0
-4	54	58	0
-3	50	48	180
-2	215	214	0
-1	139	135	0
0	124	116	180
1	22	12	0
2	49	47	0
3	63	60	180
4	27	25	180
5	71	80	180
6	59	65	0

** K= 5 L= 2 **

H	/FO/	/FC/	PHI
-8	19	17	180
-7	25	22	180
-6	112	114	180
-4	45	45	0
-3	34	32	0
-2	126	125	0
-1	183	180	0
0	74	68	180
1	162	154	0
2	146	141	180
4	74	74	180
5	67	65	180
6	51	44	0
7	39	45	0

** K= 6 L= 2 **

H	/FO/	/FC/	PHI
-7	31	30	180
-6	426	426	180
-5	175	175	180
-4	140	144	180
-3	89	92	180
-2	45	45	0
-1	321	326	0
0	419	419	180
1	121	132	0
2	25	29	180
3	20	11	180
4	36	32	0
6	18	8	180

** K= 7 L= 2 **

H	/FO/	/FC/	PHI
-6	119	121	180
-5	349	355	180
-3	91	89	0
-2	37	41	180
-1	193	199	0
0	110	120	0
1	68	71	180
2	16	17	180
4	33	37	0
5	23	28	0

** K= 8 L= 2 **

H	/FO/	/FC/	PHI
-8	16	23	180
-5	58	58	180
-4	44	39	180
-3	16	13	180
-2	17	22	0
-1	20	22	180
0	131	131	0
1	159	159	180
3	18	13	0
4	68	74	180
5	80	72	180
6	27	31	0

** K= 9 L= 2 **

H	/FO/	/FC/	PHI
-8	23	22	180
-7	23	20	0
-6	18	16	0
-5	105	99	180
-4	32	29	0
-2	40	40	180
-1	117	120	180
0	59	52	0
2	73	62	0
3	54	47	180
4	30	30	0

** K= 10 L= 2 **

H	/FO/	/FC/	PHI
-7	41	40	0
-6	17	16	180
-5	75	66	0
-1	71	74	180
0	126	126	180
1	84	79	0
2	34	23	180
3	51	44	0
4	17	14	0
5	31	30	0

** K= 11 L= 2 **

H	/FO/	/FC/	PHI
-7	19	19	180
-5	55	57	0
-4	65	70	0
-3	93	96	180
0	365	353	180
1	117	108	180
2	25	20	0
3	56	45	180

** K= 12 L= 2 **

H	/FO/	/FC/	PHI
-5	16	20	0
-4	62	72	0
-3	21	22	0
0	172	170	180
1	139	131	180
3	56	50	0

** K= 13 L= 2 **

H	/FO/	/FC/	PHI
-4	39	39	0
0	24	24	0
1	23	36	180
2	56	56	0

** K= 14 L= 2 **

H	/FO/	/FC/	PHI
-1	25	22	0
1	14	10	180

** K= 15 L= 2 **

H	/FO/	/FC/	PHI
-2	15	13	0

** K=-16 L= 3 **

H	/FO/	/FC/	PHI
0	20	26	180
2	45	37	180
3	18	11	180

** K=-15 L= 3 **

H	/FO/	/FC/	PHI
1	79	85	0
2	84	79	0

** K=-14 L= 3 **

H	/FO/	/FC/	PHI
-3	24	30	180
-2	52	42	180
-1	17	16	0
2	62	63	180
3	17	21	180

** K=-13 L= 3 **

H	/FO/	/FC/	PHI
-7	57	46	180
-2	50	59	180
-1	18	14	180
0	42	42	0
1	56	58	180
3	164	162	180
4	18	19	180
6	30	28	0

** K=-12 L= 3 **

H	/FO/	/FC/	PHI
-2	60	66	0
0	30	31	180
1	94	100	0
2	27	24	0
3	23	31	180
4	53	60	180
6	22	24	180

** K=-11 L= 3 **

H	/FO/	/FC/	PHI
-5	23	23	0
-3	62	65	180
-1	31	27	180
0	61	63	180
1	30	32	0
2	97	104	0
3	132	141	180
4	19	23	180
6	13	18	0

** K=-10 L= 3 **

H	/FO/	/FC/	PHI
-6	34	31	0
-5	47	49	0
-4	44	42	0
-3	101	101	180
-2	72	72	180
-1	25	27	180
0	49	45	180
1	80	79	0
2	109	115	180
3	67	68	0
4	38	40	180
5	21	20	0
7	80	82	0

** K= -9 L= 3 **

H	/FO/	/FC/	PHI
-7	23	18	180
-6	44	37	0
-5	104	104	180
-4	61	58	180
-3	46	31	0
-2	23	28	0
-1	59	60	0
0	14	8	180
1	38	38	180
3	68	59	180
4	16	14	0
6	17	11	0

** K= -8 L= 3 **

H	/FO/	/FC/	PHI
-8	67	62	0
-5	150	154	180
-4	94	77	180
-3	105	100	180
-2	217	218	0
-1	217	234	180
0	22	27	0
1	67	55	0
2	50	53	0
3	75	65	180
4	184	177	0
5	90	81	0
7	30	40	0

** K= -6 L= 3 **

H	/FO/	/FC/	PHI
-6	147	146	180
-5	96	103	180
-4	85	95	180
-3	84	77	180
-2	53	57	0
-1	132	139	180
0	155	148	180
1	204	205	0
2	58	54	180
3	179	168	180
4	83	82	0
5	44	40	0

** K= -5 L= 3 **

H	/FO/	/FC/	PHI
-8	18	11	180
-7	24	17	0
-6	32	26	180
-5	325	335	180
-4	264	276	180
-3	261	266	0
-2	196	186	180
-1	238	200	180
0	90	69	0
1	134	130	0
2	80	77	0
3	216	217	180
4	119	121	180
5	24	19	180
7	21	19	0
8	63	69	180

** K= -4 L= 3 **

H	/FO/	/FC/	PHI
-8	67	62	0
-5	150	154	180
-4	94	77	180
-3	105	100	180
-2	217	218	0
-1	217	234	180

H	/FO/	/FC/	PHI
0	11	29	0
1	373	364	180
2	19	14	180
3	152	157	0
4	59	45	0
8	16	13	180

** K= -3 L= 3 **

H	/FO/	/FC/	PHI
-8	27	26	0
-6	33	43	0
-5	203	213	180
-4	143	140	180
-3	63	73	0
-2	184	179	180
-1	266	266	0
0	62	75	180
1	470	468	180
2	33	17	0
4	52	54	0
5	76	75	0
6	22	22	180
8	24	32	180

** K= -2 L= 3 **

H	/FO/	/FC/	PHI
-8	43	36	0
-7	81	80	180
-5	49	48	0
-4	190	198	0
-3	45	48	180
-2	387	365	0
-1	51	33	180
0	223	224	0
1	385	383	0
2	213	199	0
4	243	232	180

** K= -1 L= 3 **

H	/FO/	/FC/	PHI
-8	31	26	0
-7	43	50	0
-6	30	24	180
-5	74	64	0
-4	190	178	0
-3	375	349	0
-2	206	186	180
-1	105	72	0
0	289	289	180
1	56	42	180
2	61	59	180
3	21	14	180
4	75	73	180
5	89	88	180
7	21	25	0
8	19	24	180

** K= 0 L= 3 **

H	/FO/	/FC/	PHI
-8	70	79	0
-5	35	35	0
-4	144	110	0
-3	269	258	0
-2	279	277	180
-1	110	132	0
0	60	44	180
1	666	662	180
2	375	364	180
3	200	180	0
4	95	83	180
5	73	66	180

** K= 1 L= 3 **

H	/FO/	/FC/	PHI
-9	17	21	0
-8	31	22	180
-7	115	125	0
-5	25	27	0
-4	281	284	0
-3	889	869	0
-2	365	354	0
-1	100	108	180
0	67	68	0
1	67	57	180
2	391	366	0
3	54	40	180
5	29	24	180
7	28	31	180

** K= 2 L= 3 **

H	/FO/	/FC/	PHI
-8	51	56	0
-5	25	26	180
-4	111	115	0
-3	230	234	0
-2	136	126	180
-1	149	151	0
0	72	65	180
1	211	206	180
2	141	137	0
3	66	54	0
4	34	20	180
5	51	48	0

** K= 3 L= 3 **

H	/FO/	/FC/	PHI
-5	30	37	0
-4	158	155	180
-3	504	505	180
-2	172	168	0
-1	455	465	180
0	62	56	0
1	82	83	180
2	124	118	0
3	70	68	180
4	18	10	0
5	63	72	0
6	41	42	0
7	19	24	0

** K= 4 L= 3 **

H	/FO/	/FC/	PHI
-8	71	64	0
-7	50	38	180
-5	15	17	0
-4	87	89	0
-3	213	205	0
-2	77	68	0
-1	210	215	0
0	32	38	0
1	159	156	0
2	133	126	0
3	150	161	0
4	73	69	180
5	48	43	0
6	25	32	0

** K= 5 L= 3 **

H	/FO/	/FC/	PHI
-6	24	28	0
-5	61	63	180
-4	34	37	0
-3	164	169	0
-2	583	585	0
-1	107	118	180
0	37	34	0
1	86	83	0
2	126	126	0
3	71	66	0
4	59	59	180
6	39	29	0

** K= 6 L= 3 **

H	/FO/	/FC/	PHI
-7	26	21	180
-6	21	8	180
-5	107	112	0
-4	21	24	180
-3	109	111	0
-2	159	189	180
-1	343	351	0
0	41	36	180
1	24	23	0
2	151	138	0
3	151	152	0
4	22	18	0

** K= 7 L= 3 **

H	/FO/	/FC/	PHI
-7	18	15	180
-6	30	33	0
-5	99	102	0
-4	71	73	0
-3	53	54	180
-2	280	286	0
0	22	24	180
1	46	47	0
2	89	83	0
3	38	31	0
4	28	23	180

** K= 8 L= 3 **

H	/FO/	/FC/	PHI
-7	20	20	0
-6	41	38	180
-5	89	88	0
-4	40	33	180
-3	122	130	0
-2	70	69	180
-1	46	46	0
0	17	21	180
2	64	54	180
3	101	97	180
4	34	34	180

** K= 9 L= 3 **

H	/FO/	/FC/	PHI
-4	26	21	0
-3	74	72	180
-2	102	108	0
-1	170	174	180
0	25	20	0
2	38	30	0
3	85	88	0

** K= 10 L= 3 **

H	/FO/	/FC/	PHI
-6	28	24	180
-5	20	22	180
-4	38	36	180
-3	47	49	0
-2	71	75	180
-1	83	86	180
0	52	49	180
2	40	42	0
3	103	99	0
4	101	100	0

** K= 11 L= 3 **

H	/FO/	/FC/	PHI
-5	50	49	180
-4	51	53	180
-3	57	56	180
-1	121	122	180
0	61	56	180
1	24	20	0

** K= 12 L= 3 **

H	/FO/	/FC/	PHI
-4	61	70	180
-3	37	40	180
-2	20	17	180
-1	23	25	180
0	42	45	180
1	50	55	0
2	18	13	180

** K= 13 L= 3 **

H	/FO/	/FC/	PHI
-4	43	43	180
-3	47	53	180
-2	25	26	0
0	20	17	180

** K= 14 L= 3 **

H	/FO/	/FC/	PHI
-1	20	20	180

** K=-16 L= 4 **

H	/FO/	/FC/	PHI
-1	60	63	180
1	30	37	0
2	20	20	180

** K=-15 L= 4 **

H	/FO/	/FC/	PHI
-3	29	24	180
0	18	21	180
1	75	76	0
4	30	31	0

** K=-14 L= 4 **

H	/FO/	/FC/	PHI
-3	50	44	0
-1	25	27	0
0	62	62	180
4	32	35	180
5	58	57	0

** K=-13 L= 4 **

H	/FO/	/FC/	PHI
-2	71	64	0
0	72	69	0
1	27	22	180
5	56	54	180
6	41	42	0

** K=-12 L= 4 **

H	/FO/	/FC/	PHI
-2	93	83	180
-1	47	49	180
0	253	255	0
1	95	98	0
2	27	28	0
4	45	53	180
5	27	33	180

** K=-11 L= 4 **

H	/FO/	/FC/	PHI
-3	55	61	0
-2	57	61	0
0	163	165	0
1	105	111	0
3	40	39	0
4	24	30	0
5	136	137	180
6	72	72	0

** K=-10 L= 4 **

H	/FO/	/FC/	PHI
-6	80	77	0
-3	72	82	0
-2	74	78	0
-1	119	122	0
0	23	25	180
1	151	151	0
3	41	38	180
4	23	31	180
5	86	91	0
6	53	48	180
7	71	71	0

** K= -9 L= 4 **

H	/FO/	/FC/	PHI
-7	36	41	0
-6	46	38	0
-5	51	52	180
-4	19	12	180
-3	61	68	180
-2	53	59	180
-1	185	195	180
0	36	40	0
1	86	83	0
2	85	85	180
3	61	59	0
5	19	11	0

** K= -8 L= 4 **

H	/FO/	/FC/	PHI
-7	34	33	180
-6	56	65	0
-4	18	18	0
-3	23	18	0
-2	77	68	0
-1	149	143	180
0	42	43	180
1	25	29	0
2	22	17	180
3	24	24	180
5	93	90	0
6	54	46	0
7	17	18	180

** K= -7 L= 4 **

H	/FO/	/FC/	PHI
-5	40	43	0
-4	18	14	180
-3	49	47	0
-2	345	330	0
-1	34	41	0
0	12	8	180
1	212	203	180
2	29	23	180
3	24	27	0
4	121	122	180
6	270	279	0
7	30	29	0

** K= -6 L= 4 **

H	/FO/	/FC/	PHI
-7	51	45	180
-6	391	388	180
-5	122	127	180
-4	38	43	180
-3	35	34	0
-2	76	66	0
-1	446	426	0
0	319	302	180
1	95	83	0
2	92	75	180
4	15	16	0
6	128	131	0
7	41	40	0

** K= -5 L= 4 **

H	/FO/	/FC/	PHI
-7	21	26	180
-6	368	362	180
-5	253	256	180
-4	45	42	180
-2	237	209	0
-1	921	892	0
0	61	60	0
1	171	157	180
2	16	19	180
3	115	113	0
4	83	85	0
5	51	52	0
6	19	32	180
7	48	51	0
8	32	32	180

** K= -4 L= 4 **

H	/FO/	/FC/	PHI
-8	16	14	180
-7	76	84	0
-6	116	129	180
-5	218	216	180
-4	24	18	0
-2	27	40	0
-1	112	111	0
0	233	194	0
1	71	67	180
2	120	108	180
3	86	84	180
4	74	68	180
5	76	80	180
6	20	25	0
8	28	30	180

** K= -3 L= 4 **

H	/FO/	/FC/	PHI
-8	15	9	180
-7	80	82	180
-6	103	109	0
-5	205	209	180
-4	61	52	180
-3	20	15	180
-2	125	109	0
-1	535	535	180
0	239	287	0
1	116	135	180
2	89	77	0
3	50	52	180
4	47	45	180
5	55	62	180
6	22	29	180
8	16	27	180

** K= -2 L= 4 **

H	/FO/	/FC/	PHI
-8	34	29	180
-7	56	54	0
-6	27	29	180
-4	137	132	0
-3	21	15	0
-2	100	105	0
-1	407	385	180
0	129	83	0
1	45	73	0
2	38	33	180
3	115	113	0
4	214	205	0
6	40	47	0
7	79	90	180

** K= -1 L= 4 **

H	/FO/	/FC/	PHI
-7	61	58	180
-6	47	48	0
-5	193	176	0
-4	30	30	180
-3	28	12	180
-1	774	759	180
1	70	60	180
2	23	23	180
3	69	66	180
4	70	65	0
5	115	108	0
6	75	77	180

** K= 0 L= 4 **

H	/FO/	/FC/	PHI
-8	18	16	180
-6	53	54	180
-5	25	21	0
-4	135	132	180
-3	114	108	0
-2	167	161	0
-1	26	26	180
0	30	32	180
1	309	421	180
2	429	456	180
3	22	13	0
4	44	37	0
5	101	92	0

** K= 1 L= 4 **

H	/FO/	/FC/	PHI
-7	156	163	180
-6	52	54	0
-5	113	110	0
-4	60	55	0
-3	32	21	180
-2	61	56	0
-1	293	318	0
0	239	246	180
1	399	375	180
2	85	68	0
4	53	55	0
5	53	58	0
6	19	25	180

** K= 2 L= 4 **

H	/FO/	/FC/	PHI
-8	31	38	180
-6	63	59	180
-5	50	55	180
-4	105	114	0
-3	83	97	180
-2	99	94	180
-1	29	33	180
0	218	220	0
1	221	221	180
4	32	31	180
5	94	102	180
6	46	50	0
7	27	31	180

** K= 3 L= 4 **

H	/FO/	/FC/	PHI
-9	19	12	0
-8	41	35	180
-5	96	105	180
-4	86	81	180
-3	93	106	0
-2	13	14	180
-1	132	132	180
0	159	151	0
1	123	124	180
2	179	177	0
3	30	28	180
5	143	141	180
6	30	45	180

** K= 4 L= 4 **

H	/FO/	/FC/	PHI
-8	64	65	180
-7	94	93	0
-6	46	48	180
-5	34	38	0
-4	21	11	0
-2	84	71	180
0	66	55	0
1	547	542	0
2	30	32	180
4	26	24	180
5	176	189	180
6	187	185	180

** K= 5 L= 4 **

H	/FO/	/FC/	PHI
-7	39	36	0
-6	166	171	0
-4	63	67	0
-3	85	91	180
-2	105	106	180
-1	36	30	180
0	36	30	180
1	197	186	0
2	181	180	0
4	28	25	180
5	121	124	180
6	205	221	180

** K= 6 L= 4 **

H	/FO/	/FC/	PHI
-8	21	22	0
-7	66	66	0
-6	286	283	0
-5	22	26	0
-4	120	117	180
-3	124	125	0
-2	16	8	180
-1	157	164	180
0	79	83	180
1	152	147	0
2	52	50	0
3	24	24	0
4	18	10	0
5	29	26	0
6	44	45	180

** K= 7 L= 4 **

H	/FO/	/FC/	PHI
-7	42	39	180
-6	142	139	0
-5	16	17	0
-4	52	48	0
-3	123	131	180
-1	35	35	180
0	28	25	0
1	136	132	180
2	108	100	0
5	17	14	0

** K= 8 L= 4 **

H	/FO/	/FC/	PHI
-8	16	18	180
-6	35	36	180
-5	74	67	0
-4	85	74	180
-3	119	119	0
-2	94	98	180
-1	53	55	0
0	42	40	180
1	31	34	180
2	39	31	180
3	20	18	0
5	22	24	180

H	/FO/	/FC/	PHI
** K= 0	L= 4	**	
-7	80	74	0
-6	43	39	180
-5	22	15	0
-4	58	55	0
-3	86	93	180
-2	51	51	0
-1	107	108	0
2	33	26	0
** K= 10	L= 4	**	
-7	44	44	0
-6	27	26	0
-5	53	57	180
-4	72	65	180
-3	80	87	0
-2	54	52	180
-1	115	120	0
0	96	92	0
1	34	28	0
2	25	27	0
** K= 11	L= 4	**	
-6	23	28	0
-5	79	71	180
-4	20	18	0
-3	42	43	180
-2	68	62	0
-1	85	87	0
0	169	165	0
1	39	40	180
2	38	39	0
** K= 12	L= 4	**	
-6	22	21	0
-5	29	25	180
-4	44	46	180
-3	38	39	0
-2	25	25	180
0	83	77	0
1	23	14	180
2	18	16	0
** K= 13	L= 4	**	
-1	35	33	180

H	/FO/	/FC/	PHI
** K= 14	L= 4	**	
-2	16	19	0
** K=-16	L= 5	**	
0	34	36	180
1	38	38	0
2	30	30	180
** K=-15	L= 5	**	
-3	27	19	180
0	19	26	0
1	102	107	180
2	26	25	0
** K=-14	L= 5	**	
-4	18	17	180
-3	52	44	0
-1	17	15	0
1	56	57	0
2	21	20	180
3	27	33	180
4	39	43	180
** K=-13	L= 5	**	
-5	22	23	0
-4	84	87	0
0	58	52	180
3	73	81	180
4	40	48	180
** K=-12	L= 5	**	
-5	25	30	0
-3	20	21	0
-1	29	25	0
0	216	214	180
1	180	181	180
4	84	94	180
5	28	24	180
6	20	22	0
** K=-11	L= 5	**	
-5	27	17	0
-4	144	160	0

H	/FO/	/FC/	PHI
-3	129	141	0
-2	33	36	0
-1	18	21	0
0	84	88	180
1	105	110	180
2	62	56	180
5	37	34	180
6	29	30	180
** K=-10	L= 5	**	
-4	93	94	0
-3	159	188	0
-1	37	37	180
0	52	54	0
1	266	260	180
2	114	109	0
4	41	43	180
5	17	20	0
7	32	36	180
** K= -9	L= 5	**	
-7	14	13	180
-5	64	63	180
-4	119	112	180
-3	153	158	180
-1	33	36	180
0	20	11	180
1	18	21	180
2	46	41	180
3	46	39	0
4	36	42	0
5	45	39	0
** K= -8	L= 5	**	
-4	16	12	180
-3	18	11	180
-2	106	91	0
-1	40	42	0
0	32	32	0
1	47	51	0
2	295	285	0
4	24	26	180
5	98	95	0
6	17	7	0
** K= -7	L= 5	**	

H	/FO/	/FC/	PHI
-4	93	89	0
-3	198	190	0
-2	224	212	0
-1	25	27	0
0	70	73	180
1	328	306	0
2	89	114	180
3	95	92	0
4	36	38	0
5	28	29	0
6	68	75	180
7	27	31	180
** K= -6	L= 5	**	
-8	24	17	0
-7	19	14	180
-6	97	94	0
-5	24	24	0
-4	132	125	180
-3	192	186	0
-2	123	110	0
-1	145	128	0
1	79	80	0
2	402	356	0
3	152	140	0
4	19	18	180
5	32	30	0
7	39	33	180
** K= -5	L= 5	**	
-8	30	22	180
-6	113	114	0
-5	111	115	0
-3	116	136	0
-2	123	150	0
-1	115	130	0
0	31	17	0
1	174	158	0
2	314	312	0
3	177	174	0
4	19	15	0
6	20	21	0
** K= -4	L= 5	**	
-6	41	36	0
-5	130	132	0
-4	82	61	180

H	/FO/	/FC/	PHI
-3	175	165	0
-2	114	110	0
-1	52	62	180
1	361	341	180
2	64	78	180
3	228	222	180
4	23	20	180
** K= -3	L= 5	**	
-6	25	21	180
-5	122	117	0
-4	96	87	0
-3	218	207	180
-2	220	231	0
-1	85	84	180
0	52	53	180
1	37	31	0
2	28	24	180
3	27	22	0
4	24	23	0
7	19	21	0
** K= -2	L= 5	**	
-9	26	28	0
-8	26	22	180
-4	131	128	180
-3	246	240	0
-2	257	240	0
-1	309	287	180
0	18	23	180
1	41	34	0
2	326	318	0
3	457	438	0
4	154	147	0
5	32	31	180
6	26	27	0
7	57	63	0
** K= -1	L= 5	**	
-8	25	22	0
-7	56	52	180
-5	141	139	180
-4	24	31	0
-3	125	126	180
-2	19	8	180
-1	274	288	180
0	61	81	0

H	/FO/	/FC/	PHI
1	41	26	180
2	144	153	180
3	287	277	0
4	122	111	0
5	34	34	0
7	24	30	0
** K= 0	L= 5	**	
-9	23	26	180
-8	47	48	180
-7	41	37	0
-6	33	39	0
-5	112	112	180
-4	190	176	180
-3	109	108	0
-2	289	287	180
-1	61	49	180
0	248	206	0
1	82	63	0
2	80	64	180
3	63	59	0
4	111	116	0
5	18	7	0
** K= 1	L= 5	**	
-9	50	53	180
-8	52	44	0
-7	44	44	180
-5	85	77	180
-4	172	177	180
-3	121	116	180
-2	234	228	0
-1	20	21	180
0	86	81	180
1	145	145	0
2	69	63	0
3	125	126	0
4	29	31	0
5	31	36	0
6	30	35	180
** K= 2	L= 5	**	
-8	73	73	180
-7	65	65	0
-6	22	24	180
-5	95	101	0
-4	67	75	180

H	/FO/	/FC/	PHI
-3	79	71	0
-1	26	25	180
0	89	89	180
1	108	108	0
2	29	5	0
3	31	27	180
4	18	16	180
5	64	76	180

** K= 3 L= 5 **

H	/FO/	/FC/	PHI
-7	31	34	180
-5	105	108	0
-4	123	121	0
-3	68	77	0
-2	99	112	180
-1	201	196	180
0	111	103	0
1	26	24	180
2	33	34	180
3	36	30	0
4	99	107	180
5	103	94	180

** K= 4 L= 5 **

H	/FO/	/FC/	PHI
-9	31	30	0
-8	115	107	180
-7	57	51	0
-6	28	32	180
-5	68	63	180
-4	139	140	180
-3	114	108	180
-2	54	54	0
0	103	100	180
1	153	151	180
2	23	13	0
4	92	94	180
5	145	161	180

** K= 5 L= 5 **

H	/FO/	/FC/	PHI
-8	24	26	0
-6	57	58	0
-3	109	109	180
-2	93	50	180
-1	35	28	0
0	73	65	0
1	142	138	180
2	62	57	180
3	24	14	0
4	63	51	180
5	67	67	180
6	25	29	180

** K= 6 L= 5 **

H	/FO/	/FC/	PHI
-7	34	32	0
-5	148	151	0
-4	144	137	0
-3	107	103	180
-2	43	41	0
-1	32	34	0
0	45	41	180
1	32	25	0
2	84	81	180
4	34	30	0
5	23	30	180

** K= 7 L= 5 **

H	/FO/	/FC/	PHI
-7	32	28	180
-4	59	58	0
-3	60	59	180
-2	79	77	180
0	62	54	0
2	25	31	180

** K= 8 L= 5 **

H	/FO/	/FC/	PHI
-8	50	50	180
-4	39	36	180
-3	53	57	180
0	32	29	180
1	89	80	0
4	27	30	180

** K= 9 L= 5 **

H	/FO/	/FC/	PHI
-7	43	39	0
-4	21	22	0
-2	48	50	180
-1	27	23	0
1	68	60	180
2	27	29	180
3	35	33	180

** K= 10 L= 5 **

H	/FO/	/FC/	PHI
-4	43	42	180
-3	41	38	180
-2	42	41	0
-1	60	64	0
0	48	47	180
2	27	24	180
3	28	32	180

** K= 11 L= 5 **

H	/FO/	/FC/	PHI
-4	17	27	180
-3	31	34	180
-2	21	18	0
-1	32	33	0
1	39	30	0
2	32	27	0

** K= 12 L= 5 **

H	/FO/	/FC/	PHI
-4	23	27	180
-3	72	76	180

** K= 13 L= 5 **

H	/FO/	/FC/	PHI
-3	29	30	180
-2	17	16	180

** K=-16 L= 6 **

H	/FO/	/FC/	PHI
-2	26	22	0
-1	109	111	0

** K=-15 L= 6 **

H	/FO/	/FC/	PHI
-1	76	76	180
0	50	53	0
2	17	13	180
3	34	33	180
4	16	16	180

** K=-14 L= 6 **

H	/FO/	/FC/	PHI
-2	61	63	0
-1	27	21	0
0	19	17	180
1	24	19	0
3	57	60	0
4	29	35	0
5	22	23	180

** K=-13 L= 6 **

H	/FO/	/FC/	PHI
-5	17	22	0
-4	18	18	180
-2	31	34	0
-1	226	225	180
0	120	122	180
3	27	31	0
4	73	85	0
5	30	35	0

** K=-12 L= 6 **

H	/FO/	/FC/	PHI
-5	27	29	0
-2	76	70	180
-1	166	164	180
0	473	480	180
1	52	52	180
4	91	94	0
5	23	28	0
6	23	26	0

** K=-11 L= 6 **

H	/FO/	/FC/	PHI
-5	24	23	0
-3	17	19	0
-2	42	44	0
-1	57	54	0
0	224	226	180
1	87	92	180
3	28	25	0
5	104	103	0
6	31	32	180

** K=-10 L= 6 **

H	/FO/	/FC/	PHI
-5	23	28	0
-3	77	73	180
-1	109	113	0
1	142	136	180
3	41	41	180
4	43	37	0
5	89	88	180
6	33	32	0

** K= -9 L= 6 **

H	/FO/	/FC/	PHI
-7	20	20	180
-6	34	32	0
-5	99	99	180
-3	49	42	0
-2	19	21	180
-1	200	207	180
0	132	133	0
1	33	35	180
3	58	58	0
4	72	68	180
5	29	21	180
6	26	21	180

** K= -8 L= 6 **

H	/FO/	/FC/	PHI
-7	15	13	0
-5	23	20	180
-3	20	12	180
-2	27	29	0
-1	117	115	180
0	198	203	0
1	88	75	0
3	25	30	180
4	50	49	0
5	305	304	180
6	51	52	180

** K= -7 L= 6 **

H	/FO/	/FC/	PHI
-8	61	51	180
-7	16	6	0
-6	40	43	0
-5	26	23	0
-3	53	54	180
-2	116	117	180
-1	103	106	0
0	302	290	180
1	338	320	0
2	43	31	0
4	192	198	180
5	161	163	180
6	248	267	180

** K= -6 L= 6 **

H	/FO/	/FC/	PHI
-7	72	74	0
-6	87	77	0
-5	44	43	180
-4	28	19	180
-3	32	29	180
-2	65	37	180
-1	19	13	180
0	58	79	180
1	155	149	0
2	54	53	0
4	117	119	0
5	81	88	180
6	141	141	180

** K= -5 L= 6 **

H	/FO/	/FC/	PHI
-6	91	95	0
-5	79	74	180
-4	38	42	180
-3	56	54	180
-2	124	133	180
-1	170	165	0
0	203	172	180
1	147	125	0
2	40	36	0
3	40	39	180
5	135	143	0
7	20	22	180

** K= -4 L= 6 **

H	/FO/	/FC/	PHI
-8	78	71	180
-7	80	78	180
-6	22	21	0
-4	48	38	180
-2	57	40	180
-1	133	129	180
0	337	302	0
1	593	544	180
2	75	69	0
3	46	50	0
4	37	35	180
5	117	124	180
6	80	79	0

** K= -3 L= 6 **

H	/FO/	/FC/	PHI
-8	22	22	180
-7	108	103	0
-6	52	53	180
-5	32	27	180
-4	23	25	0
-3	19	17	0
-2	105	107	180
-1	219	223	0
0	198	178	180
1	41	14	0
5	29	29	180
6	70	70	0
7	23	30	0

H	/FO/	/FC/	PHI
** K= -2	L= 6 **		
-8	25	15	180
-7	123	116	0
-6	19	24	180
-4	49	45	180
-3	49	42	180
-2	252	251	180
-1	174	166	0
0	251	250	0
1	33	20	180
2	45	38	0
3	57	58	180
5	36	41	0
7	74	87	0
** K= -1	L= 6 **		
-8	47	49	180
-6	83	83	0
-5	108	100	180
-4	91	87	0
-3	16	13	180
-2	201	208	0
-1	375	376	0
0	124	127	180
1	41	28	180
2	43	53	180
3	22	24	0
6	33	26	180
7	54	60	0
** K= 0	L= 6 **		
-7	130	149	180
-6	124	129	0
-5	19	23	180
-4	87	82	180
-2	102	109	0
-1	116	117	0
0	200	191	0
1	330	317	180
2	53	32	0
3	22	16	0
4	28	22	180
5	32	31	0
6	46	53	180
** K= 1	L= 6 **		
-7	126	137	180
-5	103	98	180
-4	80	74	0
-3	116	107	180
-2	195	215	180
-1	235	240	180
0	81	83	0
1	42	34	180
2	23	10	0
6	24	21	0
** K= 2	L= 6 **		
-7	43	44	180
-6	119	123	180
-5	179	186	0
-4	27	23	180
-3	86	81	0
-2	39	52	0
-1	236	238	0
0	124	129	180
1	16	12	180
2	86	85	0
5	33	32	0
** K= 3	L= 6 **		
-9	16	18	180
-7	50	47	0
-6	70	68	180
-4	37	42	0
-3	18	8	180
-2	79	67	0
-1	333	352	0
0	131	123	180
4	19	17	0
5	36	43	0
** K= 4	L= 6 **		
-6	41	39	180
-4	87	97	180
-3	37	34	180
-2	169	166	180
-1	49	52	180
0	45	10	0
1	68	59	180
2	49	47	0
4	44	45	0
5	65	67	0
6	40	42	180
** K= 5	L= 6 **		
-7	42	37	0
-6	223	221	0
-4	84	86	0
-3	25	19	0
-2	59	61	180
-1	157	153	180
0	124	122	0
1	63	62	180
2	21	25	0
3	23	20	0
5	29	34	0
** K= 6	L= 6 **		
-8	18	17	180
-6	226	224	0
-5	240	234	0
-1	127	125	180
0	86	88	0
1	52	57	180
2	28	31	0
4	22	28	180
5	20	16	180
** K= 7	L= 6 **		
-6	54	55	0
-5	132	136	0
-4	18	17	0
-3	22	19	180
-1	81	79	180
0	73	69	180
1	97	97	0
** K= 8	L= 6 **		
-7	17	12	180
-5	67	62	0
-4	18	22	0
-1	47	42	0
0	48	48	180
1	23	15	0
4	33	35	0
** K= 9	L= 6 **		
-7	32	28	180
-4	38	38	180
-2	26	20	0
-1	40	41	0
2	24	22	180
-4	19	14	180
-3	25	25	0
-2	39	43	0
0	80	83	180
1	26	26	0
3	77	79	0
4	37	39	0
** K=-12	L= 7 **		
-5	35	38	180
-4	27	21	0
-2	74	74	180
-1	30	33	0
0	122	126	0
1	120	119	180
2	62	60	180
3	66	73	0
4	37	38	0
** K=-11	L= 7 **		
-6	32	31	180
-5	18	12	180
-4	72	73	180
-3	79	77	0
-2	51	60	0
-1	16	11	180
0	23	26	0
2	24	20	180
3	66	57	0
** K=-10	L= 7 **		
-6	42	33	180
-5	29	31	180
-3	51	64	0
0	21	23	0
1	25	30	180
2	57	61	0
3	42	42	180
4	53	46	0
** K= -9	L= 7 **		
-7	18	18	0
-6	22	23	180
-5	147	152	0
-4	34	29	0
-1	49	53	180
2	16	6	0
3	131	132	0
4	85	81	180
** K= -8	L= 7 **		
-6	23	24	180
-5	40	46	180
-3	35	34	180
-2	51	44	0
-1	44	42	180
0	78	84	180
2	72	77	0
3	33	36	180
4	27	32	0
5	85	84	180
** K= -7	L= 7 **		
-6	61	61	0
-4	86	88	180
-2	108	99	0
-1	27	30	0
0	96	93	0
1	177	163	180
3	155	155	0
4	187	187	180
7	24	27	180
** K= -6	L= 7 **		
-6	144	136	0
-5	223	221	0
-4	191	192	0
-3	95	100	180
-2	61	61	0
-1	55	45	0
0	29	28	0
1	65	55	180
4	111	122	0
5	63	67	180
** K= -5	L= 7 **		
-7	30	37	180

H	/FO/	/FC/	PHI
-5	242	239	0
-4	147	148	0
-3	64	59	180
-2	31	38	180
-1	184	184	0
0	77	84	180
1	42	47	180
2	45	38	180
3	173	171	0
4	88	93	180
5	33	34	0
6	18	20	180

** K= -4 L= 7 **

H	/FO/	/FC/	PHI
-8	56	51	180
-6	34	36	180
-5	129	129	0
-4	123	113	0
-3	18	20	180
-2	40	41	0
-1	65	60	180
0	91	95	0
1	356	347	0
3	169	169	180
4	58	69	0
5	42	42	180

** K= -3 L= 7 **

H	/FO/	/FC/	PHI
-8	17	17	180
-7	40	36	0
-5	91	89	0
-3	17	17	0
-2	133	128	180
-1	59	50	0
0	128	134	180
2	56	51	180
3	81	83	0
4	55	63	180

** K= -2 L= 7 **

H	/FO/	/FC/	PHI
-8	39	33	180
-6	74	71	180
-4	126	134	180
-3	110	106	180
-2	14	1	180
-1	124	113	180
0	40	42	0
1	182	184	180
2	53	46	180
3	42	46	180
4	150	155	0

** K= -1 L= 7 **

H	/FO/	/FC/	PHI
-8	55	52	180
-5	26	25	180
-4	141	142	180
-3	120	120	180
-2	67	78	0
-1	105	102	0
0	108	115	0
1	251	241	0
2	84	81	0
3	28	20	180
4	32	24	0
5	46	50	0

** K= 0 L= 7 **

H	/FO/	/FC/	PHI
-7	40	42	180
-6	32	29	180
-5	19	21	180
-4	117	101	180
-3	342	349	180
-1	114	117	180
0	55	44	0
1	226	210	0
2	42	44	0
3	61	65	180
5	37	30	0
6	15	9	180

** K= 1 L= 7 **

H	/FO/	/FC/	PHI
-8	28	27	180
-7	48	48	180
-4	207	210	180
-3	343	346	180
-2	63	70	180
-1	49	53	0
0	82	78	180
1	33	25	0
2	119	119	180
4	22	20	0
5	22	17	180

** K= 2 L= 7 **

H	/FO/	/FC/	PHI
-4	79	74	0
-3	26	24	0
-2	43	48	0
-1	47	45	0
0	54	51	0
1	61	65	0
2	52	50	180
6	19	18	180

** K= 3 L= 7 **

H	/FO/	/FC/	PHI
-8	44	41	180
-7	22	10	0
-6	42	45	0
-5	45	50	180
-4	35	40	0
-3	134	135	0
-2	73	78	180
-1	43	44	0
0	26	22	180
1	22	20	180
2	47	40	180
3	29	33	180
4	43	45	0
5	56	56	180

** K= 4 L= 7 **

H	/FO/	/FC/	PHI
-7	19	20	0
-6	23	21	180
-5	50	54	0
-4	65	67	180
-3	153	141	180
-2	156	148	180
0	33	33	180
1	67	69	180
2	87	89	180
3	37	34	180
4	23	16	0

** K= 5 L= 7 **

H	/FO/	/FC/	PHI
-8	27	24	180
-7	18	13	0
-6	20	4	180
-5	36	34	180
-3	82	87	180
-2	142	133	180
-1	36	34	180
2	82	89	180
3	71	75	180
4	23	27	0
5	23	25	180

** K= 6 L= 7 **

H	/FO/	/FC/	PHI
-8	20	20	0
-6	60	55	180
-5	76	80	180
-4	30	26	180
-2	47	47	180
-1	101	98	180
0	29	24	0
2	30	33	180
3	52	49	180

** K= 7 L= 7 **

H	/FO/	/FC/	PHI
-7	16	9	0
-5	94	93	180
-3	42	40	180
-2	42	36	180
4	28	31	0

** K= 8 L= 7 **

H	/FO/	/FC/	PHI
-5	31	34	180
0	27	27	0

** K= 9 L= 7 **

H	/FO/	/FC/	PHI
-4	37	40	0
-2	17	14	0
-1	54	54	0
0	45	36	0

** K= 11 L= 7 **

H	/FO/	/FC/	PHI
-5	40	41	0
-4	35	40	0
-3	24	26	0
-1	56	54	0

** K=-16 L= 8 **

H	/FO/	/FC/	PHI
-6	41	31	180

** K=-15 L= 8 **

H	/FO/	/FC/	PHI
-2	25	29	180
-1	28	31	0
1	39	42	180
2	15	8	0

** K=-14 L= 8 **

H	/FO/	/FC/	PHI
-3	51	52	180
-1	75	74	180
0	66	66	0
2	18	16	180
4	29	33	0

** K=-13 L= 8 **

H	/FO/	/FC/	PHI
-2	61	67	180
-1	106	107	0
0	168	163	180
4	20	21	0
5	19	25	0

** K=-12 L= 8 **

H	/FO/	/FC/	PHI
-2	127	124	0
-1	79	79	180
0	121	123	180
1	95	86	180
2	21	13	0
3	28	30	180
5	67	73	0

** K=-11 L= 8 **

H	/FO/	/FC/	PHI
-6	43	41	180
-5	19	14	0
-3	94	104	180
-2	170	171	180
-1	81	83	0
0	122	118	180
1	81	85	180
2	28	18	180

** K=-10 L= 8 **

H	/FO/	/FC/	PHI
-5	25	19	0
-4	26	23	0
-3	28	25	180
-2	54	57	0
-1	121	127	180
0	62	62	0
1	87	84	180
2	45	44	0

** K= -9 L= 8 **

H	/FO/	/FC/	PHI
-7	30	21	0
-6	85	85	180
-5	46	52	0
-3	75	75	0
-1	254	257	0
0	72	75	180
1	39	32	180
5	38	33	180

** K= -8 L= 8 **

H	/FO/	/FC/	PHI
-6	19	19	180
-5	46	51	180
-4	30	30	180
-3	61	57	180
-2	106	94	180
0	50	52	0
1	50	37	0
2	40	32	0
3	22	25	180
4	21	16	0
6	86	91	180

** K= -7 L= 8 **

H	/FO/	/FC/	PHI
-7	57	49	0
-6	95	88	0
-5	57	64	0
-4	36	35	0
-3	45	41	180
-2	234	234	180
-1	57	55	180
0	58	62	0
1	43	42	0
2	21	14	0
3	27	30	0
4	75	73	0
6	122	142	180

H	/FO/	/FC/	PHI
** K= -6	L= 8 **		
-8	24	20	0
-7	40	41	0
-6	403	389	0
-5	111	111	0
-3	31	64	180
-1	413	416	180
0	37	31	0
2	45	40	0
3	82	89	180
4	67	68	180
5	24	25	0
6	28	21	180
** K= -5	L= 8 **		
-6	214	215	0
-5	206	208	0
-3	19	19	180
-2	99	107	180
-1	387	380	180
1	80	78	0
2	20	11	180
** K= -4	L= 8 **		
-8	24	24	0
-7	37	38	180
-6	31	37	0
-5	146	151	0
-4	37	21	0
-3	19	21	0
-2	28	5	180
-1	170	134	0
0	180	178	180
1	15	21	0
2	103	94	0
3	40	45	0
4	47	47	0
5	42	50	0
** K= -3	L= 8 **		
-8	23	20	0
-6	46	49	180
-5	104	103	0
-4	37	38	180
-3	19	20	180
-1	138	146	0
0	40	53	180
1	27	27	0
2	124	122	180
4	19	22	180
5	23	18	0
6	19	22	180
** K= -2	L= 8 **		
-8	25	21	0
-5	67	63	180
-4	15	9	180
-2	63	67	180
-1	362	357	0
0	231	247	0
1	28	17	0
2	95	101	0
3	85	88	180
4	106	112	180
5	25	24	180
** K= -1	L= 8 **		
-8	42	41	0
-5	81	80	180
-4	62	65	180
-3	15	26	0
-2	74	79	0
-1	273	272	0
0	967	985	0
1	109	106	0
2	63	71	180
3	77	87	0
4	39	43	180
5	57	57	180
** K= 0	L= 8 **		
-8	20	22	0
-7	71	75	0
-6	32	30	0
-5	101	98	180
-4	45	43	180
-2	32	29	180
-1	135	140	0
0	509	477	0
1	186	176	0
2	24	26	0
3	45	49	180
5	50	49	180
6	17	24	0
** K= 1	L= 8 **		
-7	73	77	0
-4	60	60	180
-3	93	99	0
-1	187	184	180
0	68	72	0
1	151	144	0
2	45	43	180
3	20	23	0
** K= 2	L= 8 **		
-8	20	19	0
-6	34	35	0
-5	19	23	0
-3	46	41	180
-2	44	54	0
-1	71	65	0
0	131	128	180
1	64	71	0
4	27	26	0
5	58	53	0
** K= 3	L= 8 **		
-8	38	40	0
-7	52	49	180
-6	25	29	0
-5	51	52	0
-3	23	33	180
-1	21	18	0
0	16	12	180
1	103	110	180
2	46	40	180
5	95	106	0
** K= 4	L= 8 **		
-8	41	35	0
-7	54	48	180
-6	33	33	180
-5	39	36	180
-3	28	37	0
-2	80	77	0
0	39	38	180
1	161	153	180
2	43	43	180
4	21	13	0
** K= 5	L= 8 **		
-7	58	55	180
-6	178	178	180
-2	38	37	0
-1	61	62	0
0	23	18	0
1	110	106	180
2	51	51	180
** K= 6	L= 8 **		
-7	18	22	180
-6	149	145	180
-5	23	26	180
-3	17	12	180
-1	66	65	0
2	53	50	180
3	19	18	0
** K= 7	L= 8 **		
-7	34	33	0
-6	53	53	180
-2	22	16	0
1	33	32	0
** K= 8	L= 8 **		
-7	20	15	180
-6	39	38	0
-5	45	45	180
-1	40	43	180
** K= 9	L= 8 **		
-5	27	26	0
-1	64	68	180
0	30	21	180
** K= 10	L= 8 **		
-5	32	36	0
-4	16	14	0
-1	80	82	180
0	30	79	180
** K= 11	L= 8 **		
-2	18	13	180
** K=-16	L= 9 **		
-1	20	15	0
1	27	28	0
** K=-15	L= 9 **		
-3	14	13	180
1	42	48	0
2	18	19	180
** K=-14	L= 9 **		
-4	38	39	180
-3	34	30	180
0	28	30	180
1	47	49	180
2	33	35	0
3	26	32	0
4	23	28	0
** K=-13	L= 9 **		
-5	35	38	180
-4	33	36	180
0	151	144	0
1	85	83	0
2	44	43	180
3	52	54	0
4	50	60	0
** K=-12	L= 9 **		
-4	41	54	180
-3	98	98	180
-2	23	21	0
-1	20	16	180
0	156	154	0
1	123	119	0
2	79	85	0
3	27	29	180
4	31	32	0
5	16	18	0
** K=-11	L= 9 **		
-5	57	51	180
-4	144	143	180
-3	76	85	180
-2	81	77	180
0	17	21	0
1	161	160	0
2	55	61	180
3	38	41	0
** K=-10	L= 9 **		
-5	50	46	0
-3	123	127	180
-2	95	95	0
-1	21	25	0
0	34	40	180
1	95	90	0
2	23	27	0
3	42	49	180
** K= -9	L= 9 **		
-4	90	79	0
-3	167	171	0
-2	148	153	180
-1	32	29	0
2	95	100	180
5	43	46	180
** K= -8	L= 9 **		
-4	31	25	180
-3	157	156	180
-2	25	30	0
-1	70	71	180
0	18	14	180
1	124	113	180
2	64	67	180
5	34	31	180
6	26	36	0
** K= -7	L= 9 **		
-7	24	16	0
-6	25	21	180
-5	27	29	180
-4	40	44	180
-3	43	23	180
-2	238	244	180
-1	34	33	0
1	115	107	180
2	82	87	180

H	/FO/	/FC/	PHI
3	104	93	180
6	32	42	0
** K= -6 L= 9 **			
-7	26	24	180
-6	126	127	180
-5	36	35	180
-4	72	75	0
-3	162	174	180
-1	117	122	180
1	90	78	180
2	239	232	180
3	33	32	180
4	33	29	180
** K= -5 L= 9 **			
-6	38	37	180
-5	132	137	180
-3	35	32	180
-2	125	130	180
-1	36	45	0
0	27	30	180
1	47	40	0
2	33	22	180
3	93	91	180
4	57	58	0
** K= -4 L= 9 **			
-7	21	22	180
-5	104	110	180
-3	55	47	180
-2	40	37	180
0	71	72	0
1	76	73	0
2	25	19	0
3	120	126	0
4	48	54	180
** K= -3 L= 9 **			
-5	55	54	180
-4	16	9	0
-2	70	68	180
-1	54	57	0
1	19	17	180
2	25	17	180
3	190	200	180
** K= -2 L= 9 **			
-8	18	22	0
-5	59	57	0
-4	20	22	0
-3	41	26	180
-2	104	106	180
-1	202	201	0
1	36	33	180
2	130	124	180
3	99	99	180
4	116	114	180
** K= -1 L= 9 **			
-7	17	19	0
-6	23	25	180
-5	88	92	0
-4	58	55	0
-2	135	128	0
-1	30	31	180
0	123	120	180
1	37	36	0
2	87	86	0
3	149	153	180
4	39	46	180
** K= 0 L= 9 **			
-5	73	72	0
-4	119	124	0
-3	50	49	0
-2	61	59	180
-1	120	125	0
0	89	86	180
1	88	90	180
4	62	64	180
** K= 1 L= 9 **			
-4	87	89	0
-3	21	15	180
-2	20	17	0
-1	58	55	180
0	95	90	0
1	69	71	180
3	57	65	180
4	18	17	0
** K= 2 L= 9 **			
-8	17	19	0
-5	79	76	180
-4	43	43	180
-2	54	54	180
-1	86	86	0
4	35	34	0
5	30	35	0
** K= 3 L= 9 **			
-8	38	37	0
-4	18	4	0
-2	77	84	0
1	48	48	0
4	49	59	0
** K= 4 L= 9 **			
-8	31	27	0
-7	25	27	180
-5	48	49	0
-4	45	42	0
-3	73	70	0
-2	27	33	180
-1	29	32	0
1	85	81	0
2	22	16	0
4	48	44	0
** K= 5 L= 9 **			
-6	33	36	180
-5	54	56	180
-3	37	32	0
-2	27	27	0
-1	55	56	180
1	36	35	0
2	47	48	0
** K= 6 L= 9 **			
-6	27	27	0
-5	61	63	180
-4	73	68	180
-3	58	57	0
1	17	13	180
2	28	32	0
** K= 7 L= 9 **			
-7	17	16	0
-6	16	10	180
-5	19	18	0
-3	25	24	0
1	37	36	180
** K= 8 L= 9 **			
-3	24	24	0
** K= 9 L= 9 **			
-1	24	32	180
0	16	18	0
** K= 10 L= 9 **			
-2	22	19	180
** K=-15 L= 10 **			
0	24	22	180
** K=-14 L= 10 **			
-2	71	68	180
-1	84	87	0
0	43	44	0
3	39	45	180
** K=-13 L= 10 **			
-2	54	50	0
-1	146	152	0
0	197	197	0
1	48	49	0
3	23	22	180
4	58	71	180
** K=-12 L= 10 **			
-5	25	23	180
-1	132	127	0
0	283	289	0
4	45	51	180
** K=-11 L= 10 **			
-5	26	21	180
-1	126	124	180
0	113	106	0
1	108	115	0
2	23	24	180
4	20	18	180
5	21	18	180
** K=-10 L= 10 **			
-6	28	25	180
-3	39	44	0
-2	54	55	180
-1	42	41	0
0	32	22	180
1	26	10	0
2	23	24	0
4	26	24	0
5	19	21	0
** K= -9 L= 10 **			
-5	47	46	0
-4	48	47	180
-3	41	41	180
-2	86	83	0
-1	63	62	0
0	108	116	180
1	27	35	0
2	17	24	180
5	95	107	0
** K= -8 L= 10 **			
-6	41	43	180
-4	48	54	0
-3	29	24	0
-2	46	44	180
-1	58	60	0
1	128	127	180
4	58	65	0
5	135	154	0
** K= -7 L= 10 **			
-7	51	55	180
-6	41	34	180
-4	28	33	180
-3	57	60	0
-2	107	107	0
-1	46	48	180
0	45	53	0
1	110	103	180
2	38	38	180
4	22	18	0
5	96	112	0
** K= -6 L= 10 **			
-7	21	13	180
-6	96	102	180
-5	30	26	0
-4	37	42	0
-2	24	26	0
-1	21	9	0
0	77	71	0
1	97	84	180
4	30	38	180
** K= -5 L= 10 **			
-8	37	39	0
-5	45	44	0
-3	50	51	0
-2	66	67	0
-1	23	20	180
0	35	29	180
1	83	79	0
** K= -4 L= 10 **			
-8	32	37	0
-7	33	33	0
-6	20	22	180
-4	46	47	0
-3	23	30	180
1	117	112	0
2	79	78	180
4	32	28	0
5	36	41	0
** K= -3 L= 10 **			
-7	108	101	180
-6	54	55	0
-4	23	24	180
-3	28	31	0
-2	83	91	0
-1	88	97	180
0	22	15	180
2	54	52	0
3	17	12	180

H	/FO/	/FC/	PHI
** K= -2	L= 10 **		
-7	48	50	180
-6	27	27	180
-5	26	27	0
-4	22	24	0
-1	160	157	180
0	45	53	180
1	48	47	0
2	60	56	180
3	56	55	0
** K= -1	L= 10 **		
-8	74	81	0
-7	23	25	0
-6	50	55	180
-5	39	37	0
-3	17	11	180
-2	77	80	180
-1	126	130	180
0	21	10	180
2	60	54	0
3	44	44	180
4	25	22	0
** K= 0	L= 10 **		
-7	102	106	0
-6	54	52	180
-5	42	45	0
-3	48	50	0
-2	19	31	0
0	80	84	180
1	159	158	0
2	78	79	180
3	25	25	0
** K= 1	L= 10 **		
-7	71	65	0
-6	40	45	0
-5	37	40	180
-2	73	67	0
-1	37	34	0
1	49	53	180
2	58	59	0
3	27	24	180
** K= 2	L= 10 **		
-6	44	44	0
-5	36	29	180
-4	28	28	180
-2	78	73	180
-1	115	117	180
0	49	46	0
1	52	51	0
2	77	80	180
3	19	19	0
** K= 3	L= 10 **		
-7	22	17	180
-6	52	50	0
-4	45	46	0
-1	78	79	180
0	50	47	0
1	21	20	180
2	30	34	0
3	23	26	180
** K= 4	L= 10 **		
-7	22	18	180
-6	49	53	180
-5	18	14	0
-4	24	27	180
-3	44	47	0
-2	54	53	0
-1	39	37	0
0	25	27	180
1	56	57	0
2	45	44	180
** K= 5	L= 10 **		
-7	23	26	180
-6	131	128	180
-5	83	78	180
-3	43	45	180
-2	39	40	0
-1	67	64	0
0	31	33	180
1	17	14	0
** K= 6	L= 10 **		
-6	91	94	180
-5	97	99	180
-3	29	27	0
-2	19	21	180
-1	52	52	0
** K= 7	L= 10 **		
-5	66	69	180
0	23	26	0
1	26	26	180
** K= 8	L= 10 **		
-5	18	19	180
-2	21	20	180
** K=-15	L= 11 **		
-2	22	19	180
** K=-14	L= 11 **		
-3	49	46	180
-1	18	20	0
1	30	30	180
2	33	31	180
** K=-13	L= 11 **		
-4	23	22	180
0	25	16	180
1	40	40	0
3	54	61	180
** K=-12	L= 11 **		
-4	39	38	0
-1	21	22	180
0	74	78	180
1	42	43	0
2	35	33	0
3	42	41	180
4	19	20	180
** K=-11	L= 11 **		
-5	39	34	0
-4	19	16	0
-3	72	71	180
-1	28	28	0
0	22	25	180
1	27	29	180
4	18	18	180
** K=-10	L= 11 **		
-6	29	25	0
-5	53	54	180
-4	34	27	180
-3	18	10	0
-2	32	29	180
2	30	30	180
3	30	39	180
4	20	21	0
** K= -9	L= 11 **		
-5	55	52	180
-3	35	32	180
-2	35	32	0
0	23	22	0
1	34	33	180
3	25	21	180
** K= -8	L= 11 **		
-5	34	33	0
-4	24	29	180
-3	36	39	0
-2	74	68	180
1	77	75	0
2	40	41	180
3	24	28	180
4	40	40	0
5	23	20	0
** K= -7	L= 11 **		
-6	33	34	180
-5	53	60	180
-4	37	33	0
-3	76	79	180
0	50	55	180
1	63	56	0
2	29	31	0
3	28	29	180
5	20	18	0
** K= -6	L= 11 **		
-7	18	19	0
-6	70	70	180
-5	135	135	180
-4	161	162	180
-3	154	160	0
-2	74	73	180
-1	49	55	180
0	33	39	0
1	34	38	0
3	52	47	180
5	19	22	0
** K= -5	L= 11 **		
-5	125	135	180
-4	38	38	180
-3	76	82	180
-2	66	62	0
-1	32	30	180
0	23	23	180
1	68	73	180
** K= -4	L= 11 **		
-5	63	63	180
-4	94	99	180
-3	108	116	0
-2	50	47	180
1	97	94	180
2	29	24	0
** K= -3	L= 11 **		
-8	34	35	0
-7	35	33	180
-4	61	64	0
-3	39	41	180
-2	78	82	0
0	39	36	0
1	47	51	0
** K= -2	L= 11 **		
-8	13	9	0
-7	21	19	0
-5	32	29	0
-4	52	51	0
-3	90	91	0
-2	61	63	180
0	50	53	180
2	27	22	0
3	20	12	180
4	43	50	180
** K= -1	L= 11 **		
-8	42	44	0
-6	19	20	0
-4	90	97	0
-3	66	71	0
-1	33	26	180
0	29	33	180
1	149	144	180
2	35	37	180
3	45	45	0
4	15	16	180
** K= 0	L= 11 **		
-7	35	35	0
-4	89	93	0
-3	168	172	0
-2	18	13	0
-1	31	35	0
1	50	52	180
2	19	15	0
** K= 1	L= 11 **		
-4	45	48	0
-3	98	95	0
-2	27	24	180
-1	28	35	180
0	61	53	0
1	38	34	180
2	25	22	0
** K= 2	L= 11 **		
-6	23	24	180
-4	49	51	180
-3	33	28	180
-2	21	21	0
0	59	55	180
1	30	26	0
2	17	16	0
** K= 3	L= 11 **		
-5	17	14	180
-2	25	23	0
0	48	43	0

H	/FO/	/FC/	PHI
2	31	31	0
** K= 4 L= 11 **			
-4	22	16	0
-3	58	53	0
-2	86	81	0
1	51	46	0
2	42	43	0
** K= 5 L= 11 **			
-6	33	36	0
-5	31	33	0
-4	17	15	0
-3	24	23	0
-2	41	43	0
-1	25	22	0
0	23	22	0
1	20	12	180
** K= 6 L= 11 **			
-5	65	68	0
-2	32	31	0
-1	27	26	0
0	23	21	180
** K= 7 L= 11 **			
-5	34	39	0
** K=-14 L= 12 **			
-2	26	26	0
** K=-13 L= 12 **			
0	79	81	0
** K=-12 L= 12 **			
-4	18	16	0
-3	29	35	0
-2	22	12	0
0	82	84	0
1	55	56	0
** K=-11 L= 12 **			

H	/FO/	/FC/	PHI
-3	82	77	0
-2	44	42	0
0	26	24	0
1	46	44	0
** K=-10 L= 12 **			
-5	37	39	180
-4	21	21	180
-3	30	28	180
-1	22	21	180
1	44	42	0
2	19	15	180
4	13	10	0
** K= -9 L= 12 **			
-6	33	36	0
-3	17	12	180
-2	27	20	180
-1	76	81	180
0	34	39	0
1	21	21	180
** K= -8 L= 12 **			
-3	43	40	0
-2	126	122	0
0	40	54	180
2	21	20	180
** K= -7 L= 12 **			
-7	37	38	180
-6	152	154	180
-5	66	70	180
-2	89	93	0
-1	106	106	0
1	34	37	180
** K= -6 L= 12 **			
-7	42	43	180
-6	202	204	180
-5	63	66	180
-4	46	46	180
-2	67	72	0
-1	193	203	0
0	43	58	180
3	36	34	0

H	/FO/	/FC/	PHI
** K= -5 L= 12 **			
-7	22	20	0
-6	100	106	180
-5	145	149	180
-4	61	59	0
-3	19	19	180
-2	16	15	0
-1	82	77	0
0	49	59	0
1	39	45	180
2	24	25	180
** K= -4 L= 12 **			
-5	33	35	180
-4	61	61	180
-3	37	32	0
-2	17	13	180
-1	27	26	180
0	30	27	0
3	18	23	180
4	22	21	180
** K= -3 L= 12 **			
-6	25	27	0
-5	58	58	180
-4	76	75	0
-3	34	30	180
-2	19	13	0
-1	129	125	180
3	26	31	0
4	33	37	0
** K= -2 L= 12 **			
-5	80	83	0
-4	42	44	180
-3	26	25	0
-2	18	22	180
-1	139	147	180
0	249	265	180
1	44	38	180
** K= -1 L= 12 **			
-7	23	26	180
-4	81	79	0
-3	42	39	180

H	/FO/	/FC/	PHI
-1	141	139	180
0	202	200	180
1	46	47	180
3	16	15	180
** K= 0 L= 12 **			
-7	55	54	180
-5	57	60	0
-4	19	18	180
-3	20	19	180
-1	24	17	0
0	148	145	180
1	97	94	180
2	36	29	0
** K= 1 L= 12 **			
-7	32	36	180
-5	31	31	180
-4	41	45	0
-3	31	36	180
-1	27	30	0
1	27	28	180
** K= 2 L= 12 **			
-6	25	30	180
-3	27	28	0
0	46	39	0
1	18	11	180
2	35	32	0
** K= 3 L= 12 **			
-5	18	19	180
1	81	81	0
** K= 4 L= 12 **			
-6	60	61	0
-5	25	22	0
-3	24	21	180
-2	36	36	180
0	20	15	0
1	41	38	0
** K= 5 L= 12 **			
-2	17	22	180

H	/FO/	/FC/	PHI
-1	37	37	180
** K= 6 L= 12 **			
-1	19	21	180
** K=-13 L= 13 **			
-3	21	24	0
-1	20	12	180
0	112	112	180
1	51	56	180
** K=-12 L= 13 **			
-4	50	57	0
-3	63	62	0
-2	25	27	0
-1	21	15	0
0	77	79	180
1	107	107	180
** K=-11 L= 13 **			
-4	80	77	0
-3	67	68	0
1	73	79	180
** K=-10 L= 13 **			
-5	15	12	180
-4	33	33	180
-1	19	23	180
1	21	18	180
2	19	22	0
** K= -9 L= 13 **			
-5	17	20	180
-4	33	33	180
-2	27	26	0
1	28	26	0
2	28	30	0
3	18	17	0
** K= -8 L= 13 **			
-4	40	32	0
-3	31	29	0
-2	51	53	0

H	/FO/	/FC/	PHI
-1	18	17	0
1	62	59	0
2	46	36	0
** K= -7 L= 13 **			
-6	54	56	0
-3	77	74	0
-2	68	73	0
1	56	52	0
2	80	88	0
3	35	34	0
** K= -6 L= 13 **			
-6	85	89	0
-5	53	60	0
-3	19	27	0
-2	36	31	0
-1	23	29	0
2	70	68	0
3	30	30	0
** K= -5 L= 13 **			
-6	36	36	0
-5	90	96	0
-4	28	19	180
-3	47	41	0
-2	40	49	0
-1	31	34	180
1	23	21	180
** K= -4 L= 13 **			
-6	23	23	180
-5	56	58	0
-4	36	36	0
-3	15	1	0
-1	31	34	0
0	45	41	180
3	27	28	0
** K= -3 L= 13 **			
-4	27	26	180
-3	39	34	0
-2	30	38	0
-1	91	91	180
0	20	18	0

H	/FO/	/FC/	PHI
1	18	20	0
2	37	35	0
3	52	61	0
** K= -2	L= 13	**	
-5	34	34	180
0	21	19	0
2	18	19	0
3	59	65	0
** K= -1	L= 13	**	
-6	35	24	0
-5	61	62	180
-4	71	72	180
-1	39	41	180
0	78	82	0
** K= 0	L= 13	**	
-6	19	24	180
-4	53	60	180
-3	23	23	180
1	51	51	0
** K= 1	L= 13	**	
-6	16	17	0
0	33	24	180
1	30	30	0
** K= 2	L= 13	**	
-5	41	38	0
** K= 3	L= 13	**	
-5	18	24	180
-3	24	23	180
** K= 4	L= 13	**	
-4	18	15	180
-3	19	16	180
** K=-12	L= 14	**	
-1	35	33	180
0	112	117	180

H	/FO/	/FC/	PHI
** K=-11	L= 14	**	
-3	20	18	180
-2	21	19	0
-1	41	37	0
0	47	52	180
1	25	21	180
** K=-10	L= 14	**	
0	38	39	0
1	26	22	180
** K= -9	L= 14	**	
-5	33	35	180
-2	20	18	180
-1	36	34	180
0	24	28	0
1	30	28	0
** K= -8	L= 14	**	
-4	24	21	180
-3	18	24	180
-2	18	18	180
1	44	46	0
** K= -7	L= 14	**	
-3	29	28	180
-2	37	42	180
0	29	25	180
1	51	50	0
** K= -6	L= 14	**	
-6	29	27	0
-4	16	9	0
-2	33	37	180
** K= -5	L= 14	**	
-6	17	23	0
-4	19	16	180
1	26	27	180
** K= -4	L= 14	**	
-5	21	22	180

H	/FO/	/FC/	PHI
-4	15	5	0
-2	33	32	180
1	29	23	180
2	16	11	0
** K= -3	L= 14	**	
-6	17	12	180
-5	15	11	0
-4	22	22	180
-3	16	15	180
-1	60	67	0
** K= -2	L= 14	**	
-6	22	24	0
-5	42	41	180
-4	24	18	0
-1	79	82	0
0	22	25	0
** K= -1	L= 14	**	
-4	22	21	180
-2	18	15	0
-1	36	36	0
1	36	37	180
** K= 0	L= 14	**	
-5	23	23	180
-4	21	20	0
-3	20	17	180
-2	29	35	180
0	27	27	0
1	24	25	180
** K= 1	L= 14	**	
-5	32	34	0
** K= 2	L= 14	**	
-2	22	19	0
-1	32	32	0
** K= -9	L= 15	**	
-3	18	19	180

H	/FO/	/FC/	PHI
** K= -8	L= 15	**	
1	32	37	180
** K= -7	L= 15	**	
-4	24	25	0
-2	22	26	0
1	22	23	180
** K= -6	L= 15	**	
-5	92	102	0
-4	47	47	0
-1	15	16	0
** K= -5	L= 15	**	
-5	47	57	0
-4	51	50	0
-3	20	20	180
1	36	38	0
** K= -3	L= 15	**	
-3	16	15	180
** K= -2	L= 15	**	
-4	39	42	180
-3	26	32	180
0	23	23	0
** K= -1	L= 15	**	
-4	40	48	180
-3	48	48	180
-2	22	22	180
** K= 0	L= 15	**	
-4	40	43	180
-3	53	59	180
-2	14	15	0
** K= -8	L= 16	**	
-2	56	57	180
** K= -7	L= 16	**	

H	/FO/	/FC/	PHI
-2	49	53	180
-1	61	69	180
** K= -6	L= 16	**	
-2	22	24	180
-1	60	64	180
** K= -5	L= 16	**	
-1	25	25	180

H	/FO/	/FC/	PHI

The Crystal Structure of 1,2-bis-(1-hydro-4-pyridine)ethane (7,7,8,8-tetracyanoquinodimethanide)$_2$, $DHPA^{2+}(TCNQ)_2^{2-}$

4.1 Experimental

This compound, which was grown by electrocrystallisation from dry acetonitrile solution under nitrogen (see also Chapter 6), formed regular hexagonal crystals on a pseudo-spherical electrode. One of the few suitable crystals formed was removed and mounted upon a glass fibre by means of a minimum of rapid setting epoxy adhesive and, after mounting on a goniometer head and subsequent alignment of the crystal, an oscillation photograph was taken using Cu Kα (λ = 1.5418 Å) radiation and a Unicam camera. Inspection of the developed photograph showed that the crystal was not mounted about a true crystallographic axis, but possibly about a diagonal axis. The crystal was therefore transferred to the Hilger and Watts four circle diffractometer, and after realignment an automatic reflection search was instigated for reflections whose Bragg angle, θ , lay within the range $2^\circ < \theta < 7^\circ$.

Since at this stage the unit cell was still unknown, although inspection of the peak intensities observed during the automated reflection search showed that the crystal was possibly monoclinic, four-circle setting information for 17 strong reflections with $5^\circ < \theta < 7.1^\circ$ was transferred to the departments Enraf Nonius CAD4 diffractometer system. Inspection of the Niggli matrices suggested that the cell was a centred monoclinic cell, and appropriate matrix

transformations showed that the cell was in fact C face centred. From this information, and from examination of the systematic absences, the space group was determined as $C_{2/c}$.

An accurate orientation matrix was then obtained based on 23 reflections of strong intensity having $11^{\circ} < \theta < 13^{\circ}$ and intensity data were collected on the Hilger and Watts instrument, at ambient temperature (19° C) using Mo Kα radiation (λ = 0.71026 Å) and a graphite monochromator. The data were collected using an $\omega/2\theta$ scan for $\theta \leq 25^{\circ}$. Three standard reflections were measured at 100 reflections intervals throughout the data collection and since no significant variation was observed in the intensities of these reflections the data were normalised to a constant value for one single standard before data reduction.

Out of 2843 reflections collected, 1918 were regarded as observed in that the intensity of a reflection, I, was greater than three times its estimated deviation, i.e. $I > 3\sigma(I)$. The data were corrected for Lorentz and polarisation effects, but not for absorption.

Crystal Data

DHPA $(TCNQ)_2$ $(C_{12}H_{14}N_2)^{2+}$ $(C_{12}H_4N_4)_2^{2-}$ M_r = 594.2

Monoclinic, a = 29.481 Å, b = 7.405 Å, c = 13.470 Å, β = 94.03°

U = 2933.3 Å^3, Z = 4, D_c = 1.346 g.cm^{-1}.

MoKα (λ = 0.71069 Å) μ = 0.92 cm^{-1}

Space group $C_{2/c}$ (number 15)

4.2 Structure Determination and Refinement

Initially attempts were made to solve the structure on the basis of the Patterson function and the Sharpened Patterson function since at the outset of the structure investigation there was no reason to suppose that the structure would not contain stacks of overlapping TCNQ moieties. Another factor which should have aided the solution of the structure by Patterson techniques was the higher symmetry of the space group, so that examination of the Harker peaks should have simplified the process of assigning the positions of the molecular species within the cell. However, all attempts to solve the structure in this manner were unsuccessful and the structure was eventually solved by direct methods, using MULTAN 78[50]. This yielded the position of the entire TCNQ molecule, together with the expected half-cation of the asymmetric unit. The TCNQ atomic positions were refined by a least-squares full-matrix method using the CRYSTALS suite of crystallographic programs[51] and a difference Fourier synthesis based on $|Fo - Fc|$ revealed the half cation in the same position within the unit cell as that determined by MULTAN 78. Further least-squares full-matrix refinement of these non-hydrogen atoms, followed by another difference Fourier synthesis, revealed the positions of all the hydrogen atoms with acceptable bond lengths and angles, and so the hydrogen atoms, (with the exception of the hydrogen atom attached to the quaternised nitrogen centre) were input in their calculated positions on the basis of sp^2 hybridisation of the heterocyclic ring and sp^3 hybridisation of the carbon atoms present in the ethane link of the cation.

The hydrogen atom connected to the quaternised nitrogen atom was input in the position determined by the difference Fourier synthesis because, as this atom is involved in hydrogen bonding with a TCNQ nitrogen atom (see next section), the bond lengths and angles were expected to be somewhat distorted with respect to the calculated geometry. The hydrogen atoms were included in the structure factor calculations but their thermal and positional parameters were not included in the refinement at this stage.

The structure refined isotropically to R = 0.070, and four further cycles of anisotropic least-squares refinement reduced this to R = 0.0505. At this stage a weighting scheme based on a Chebyshev series with coefficients

$A[0] = 159.9 \quad A[1] = 255.6 \quad A[2] = 145.7 \quad A[3] = 67.2 \quad A[4] = 19.7$

was introduced, their values being selected by the program on the basis of minimising the function $X = \sum (Fo - Fc)^4$ over all reflections. Four further cycles of weighted anisotropic refinement gave R = 0.0453, and refinement of the positional and isotropic thermal parameters of the quaternising hydrogen atom gave R = 0.0451, with a maximum value of the ratio of the shift of a parameter to the estimated standard deviation of that parameter for any parameter (with the exception of the quaternising hydrogen) of 0.02. The value of this ratio for the quaternising hydrogen was a maximum of -0.51 for the final cycle of refinement.

A final difference Fourier synthesis did not show the presence of any unaccounted for scattering matter, and the structure was therefore assumed to be fully refined and solved.

The anisotropic thermal parameters of the non-hydrogen atoms were analysed in terms of a rigid body motion and the bond lengths and angles of the structure were librationally corrected on the basis of the results of this analysis. Least-squares planes were also calculated for the TCNQ moiety and the half-cation present in the asymmetric unit.

4.3 Description and Discussion of the Structure

Figures 4.3a, b, and c show the structure of DHPA $(TCNQ)_2$ projected along the a,b, and c axes of the unit cell respectively. The TCNQ moieties are arranged as diads stacked along c in four columns centred about ($x = \frac{1}{4}$, $y = \frac{1}{4}$), ($x = \frac{1}{4}$, $y = \frac{3}{4}$), ($x = \frac{3}{4}$, $y = \frac{1}{4}$), and ($x = \frac{3}{4}$, $y = \frac{3}{4}$). The moieties of the diadic groups, shown in Figure 4.3b as A and A', are related by the centre of symmetry at ($\frac{1}{4}$, $\frac{1}{4}$, $\frac{1}{2}$), and show overlap of the exocyclic bond-to-ring type (see Figure 4.4), whilst the inter-diad overlap (A-A'' and A'-A''') is non-existent. Pairs of diads A-A' and A''-A''' are related by the screw axis parallel to b acting at $x = \frac{1}{4}$, $z = \frac{1}{4}$, and since therefore the planes of A and A'' (and hence A' and A''') are not parallel the separation between diads can only be quoted in terms of nearest intermolecular contacts between non-parallel molecules (see Table 4.3).

The separation of the planes of the diad A-A', calculated by determining the perpendicular distance of the centre of molecule A' (centred at $1\frac{1}{2}-x$, $\frac{1}{2}-y$, $1-z$) from the plane of molecule A, sited at x, y, z, is 3.10Å compared with 3.15Å in another simple salt, that of $Ph_4P(TCNQ)_2$[37]. The stacking of the TCNQ moieties is similar to that observed in this tetraphenylphosphonium $(TCNQ)_2$ salt[37] except that the segregation of the pairs of diadic species is greater in the present structure. The cation is sited in sheets at $x = 0$ and $\frac{1}{2}$ between the TCNQ colums and the two cation halves are related by the two-fold axis acting at a quarter along c. The geometry of the cation is shown in a stereo view (see Figure 4.5) and it can be

seen that the moiety exists as the gauche conformer with respect to the pyridinium rings. The explanation for this unusual geometry, as opposed to the anti conformation normally observed, would appear to be found in the interactions between the cation and TCNQ moieties. The quaternising hydrogen atom (H(9)), sited upon N(5), is only 2.052Å from a terminal nitrogen atom, symmetry related to N(1), of one of the cyano groups of the TCNQ moiety. The molecular geometry of this interaction is shown in Figure 4.6 and the N-.-N distance of 2.885(4)Å would appear to indicate a fairly strong N-H...N bond when compared with the average heavy atom N^+-H...N distance of 2.92Å and N-H...N of 3.17Å [30]. The H...N separation of 2.052Å is less than the average H...N contact distance of 2.2Å given by Hamilton and Ibers based on neutron diffraction studies[38] but is slightly longer than the 1.989Å H...N separation of N^+-H..N observed in HEM $(TCNQ)_2$ by van Bodegom[39] (H atom in calculated position), and the N...N separation (2.885Å) is just less than the shortest N..N contact of 2.920Å in morpholinium (TCNQ) [40]. The shortest hydrogen-bonded heavy atom contacts in the simple salts NMP (TCNQ)-phase I[33] (which is in fact $(NHPH)^+$ $(TCNQ)^-$) and quinolinium TCNQ [34] are 2.735Å and 3.13Å respectively and the value observed in the present work lies within this range. The perpendicular distance of the hydrogen bonded $N(1^{vii})$ of the TCNQ from the plane of the cation is 0.43Å, whilst the hydrogen atom involved in the bonding, H(9), shows no significant deviation from the plane of the cation.

There are no other close contacts to the hydrogen atom involved in hydrogen bonding which are less than the sum of the van der Waals

radii. The shortest heavy atom contacts between the cation and the TCNQ moiety are 3.16Å (N(3)-C(17^{ix})) and 3.246Å (N(4)-N(5^{xi})), both of which are within the covalent bond distance of 1Å for a C-H bond plus the sum (2.7Å) of the van der Waals radii[17] of hydrogen and nitrogen and indicate a degree of charge interaction between the slightly negatively charged cyano groups and the cation ring. The shortest TCNQ- TCNQ intra-diad contacts are 3.105Å(C(2)-C(6^{ii})) and 3.143Å(C(1)-C(1^{ii})), significantly shorter than the nearest inter-diad contact, between columns of TCNQ diads whose centres are at the same x coordinate but are separated by $y/_2$, which is 3.371Å (C(2)-N(2^{iv})). Thus the contact distances also indicate the discrete diadic nature of the TCNQ columnar structure.

The molecular geometry of the TCNQ and cation moieties is shown in Figures 4.1 and 4.2. The librationally uncorrected bond distances of the TCNQ moiety are in close agreement with the mean values obtained by Ashwell *et al*[7] for the $TCNQ^-$ ion and in view of the small differences between librationally corrected and uncorrected bond lengths and angles (as expected from the almost isotropic nature of the anisotropic temperature factors, see table 4.5) the present geometry corresponds well with the $TCNQ^-$ ion. The charge on the TCNQ moiety, calculated from the mean of the chemically equivalent bonds by the method of Chasseau and Flandrois[8], was found to be -0.89e. This value may be within experimental error of the -1.0e expected for $TCNQ^-$, or may support the suggestion by Drew[2] that in the case where the hydrogen is directly linked to a nitrogen atom, such as in the complexes of the 1-hydro-substituted cations, the hydrogen

may be displaced and removed by $TCNQ^-$ in solution. If, in the present case, some of the unit cells of the crystal possessed only a formally singly charged cation species, the average overall charge on the TCNQ moieties within the crystal would not be a full -1e charge. A third possibility is that the effective charge on the TCNQ moiety has been decreased by back donation of positive charge from the cation species, a possibility which cannot be ruled out in view of the short contact distance between the two species.

The cation geometry shows the expected increased bond angle and decreased bond lengths about the N atom when compared with the distances and internal angle at the 4- position of the pyridinium ring. The N-C bonds, at 1.332Å and 1.329Å, are slightly shorter than the equivalent bonds in DMPB $(TCNQ)_4$ (see Chapter 3), (which are 1.366 and 1.359Å), as might be expected since the N-H bond will be more polarised than the $N-CH_3$ bond due to the lack of positive inductive effect from the substituent. The C-C bond lengths C(14)-C(15) and C(16)-C(15), which are 1.393 and 1.385Å respectively (mean 1.389Å), are similar to the equivalent bonds in other cations of TCNQ salts (e.g.[10,15]) and particularly close to those observed in the ethane-bridged 1,2-bis(1-ethyl-4-pyridinio)ethane $(TCNQ)_4$[24], which range from 1.393(7) to 1.382(6)Å, mean 1.388Å, as might be expected from the close similarity of the cation species. The exocyclic bond C(15)-C(18), with a bond length of 1.500Å, is similar to the mean value of the equivalent bonds in DEPA$(TCNQ)_4$[24] of 1.495(6)Å but is somewhat less than that found by Ashwell *et al*[35] in the benzyl substituted analogue DBPA $(TCNQ)_5$, which is 1.551Å. However, the

authors state that the bond adjacent to the one in question in their structure has a "clearly erroneous" bond length of 1.10(2)Å and ascribe this to incomplete resolution of one of the participating carbon atoms. It may not be unreasonable to assume that, by the same argument, the bond adjacent to this might be slightly lengthened and should in reality be a little shorter.

There is a very slight bowing of the TCNQ moiety as evidenced by the positive deviations of the non-quinonoid atoms from the least squares plane of the molecule. However, a greater deviation from planarity is that due to the twisting of the $C(CN)_2$ groups with respect to the plane of the ring atoms. The combined effect of these two distortions is that the ring plane of the TCNQ moiety forms dihedral angles of 5.0° and 9.1° with the planes defined by the $C(CN)_2$ groups C(7) to N(2) and C(10) to N(4). The ring plane of the TCNQ also makes an angle of 7.8° with the plane of the cation. The long axis of the TCNQ moiety, defined by the atoms C(7)-C(1)-C(4)-C(10), is inclined at 20.1° to the (0 1 0) plane, 24.2° to the (0 0 1) plane, and 60.6° to the (1 0 0) plane, and the TCNQ and cation ring planes form dihedral angles of 35.4° and 33.4° respectively with the (0 0 1) plane.

The structure may therefore be described in terms of pairs of columns of doubly charged(dipositive) cations sited in a c- face centred arrangement thereby forming layers of cations parallel to (1 0 0) at $x = 0$ and $x = \frac{1}{2}$, with the TCNQ diads stacked in columns along c at $x = \frac{1}{4}$ and $\frac{3}{4}$ and $y = \frac{1}{4}$ and $\frac{3}{4}$.

The d.c. dark conductivities for four selected crystals are shown in Figures 4.7 - 4.10 as a function of temperature. The relationship between crystallographic and crystal planes is shown in Figure 4.11. Two features are apparent from the conductivity graphs : firstly, the phase change occurring reversibly between 328 K and 300 K, and secondly the anisotropy of the system. The reversibility of the phase change is demonstrated in Figure 4.12. It is unlikely that any cracking/annealing process could yield such close correlation between the two regimes during thermal cycling, and it is therefore assumed that the phase change is genuine. Phase transitions of this nature have been observed in these type of complexes before, some being irreversible and caused by solvent molecule - TCNQ chain interactions[41,43]. The mixed salt, $[(C_6H_5)_3PCH_3]^+_{1-x}$ $[(C_6H_5)A_3CH_3]_x^+$ $(TCNQ^-)_2$ $(0 \leqslant x \leqslant 1)$[42] shows a phase transition at 315.7 K at 1 atmosphere, and recently the 1,4-bis-(1,1,1,-triphenylphosphonium)-butane $(TCNQ)_4$ complex salt has been found to undergo a reversible phase transition at ca. 307 K[44].

Attempts by the author to determine the crystal structure of the high temperature phase using the recently acquired variable temperature attachment for the CAD-4 diffractometer were unfortunately thwarted by teething problems mainly associated with gas flow regulation. Thus, not only was the crystal specimen used in the room temperature determination destroyed, but so were all the remaining single crystal samples of this material. It is to be hoped that future workers may repeat the preparation and investigate the structural changes occurring in this compound.

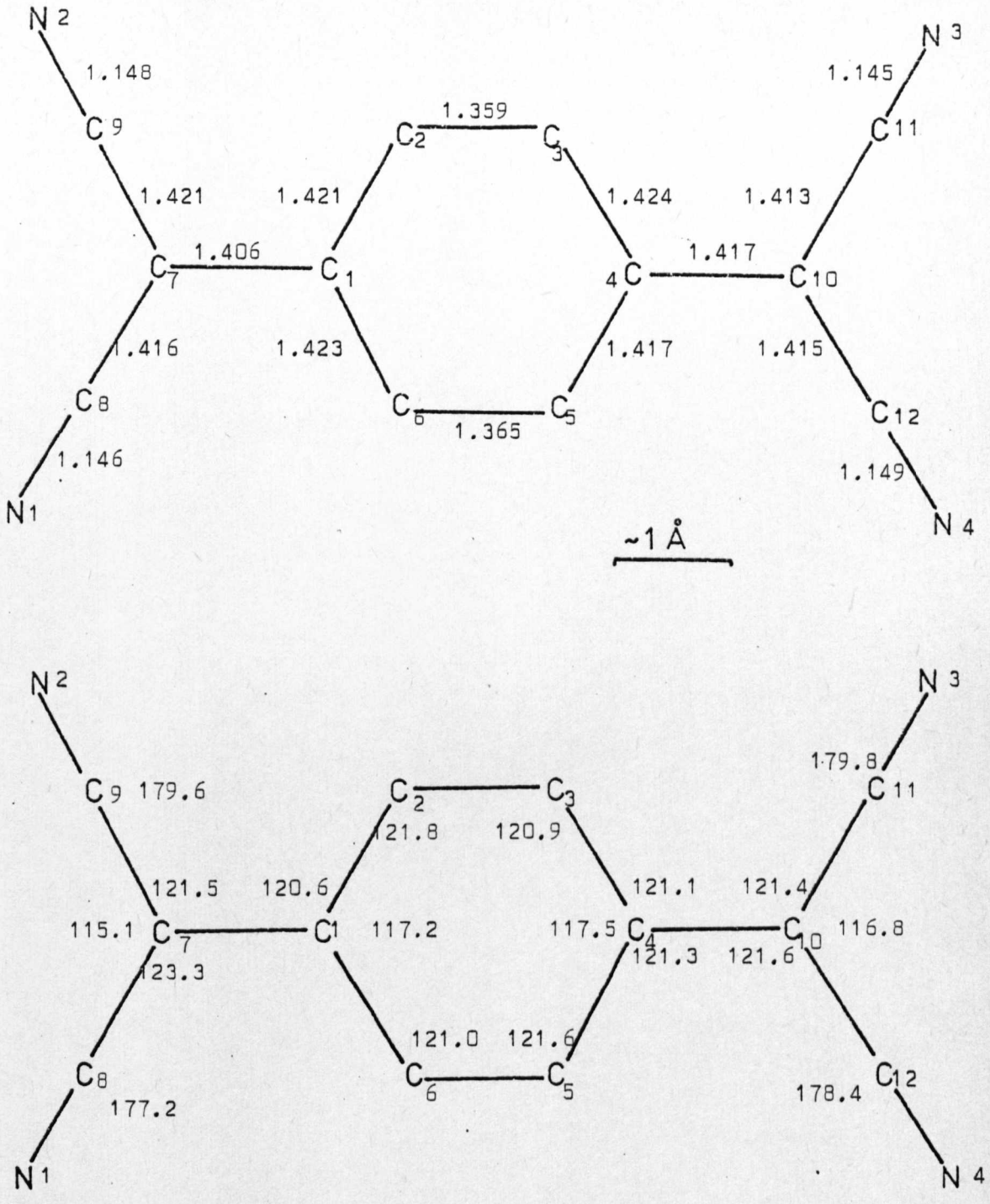

Figure 4.1 DHPA $(TCNQ)_4$ Librationally Corrected Bond Distances (Å) and Angles (Degrees)

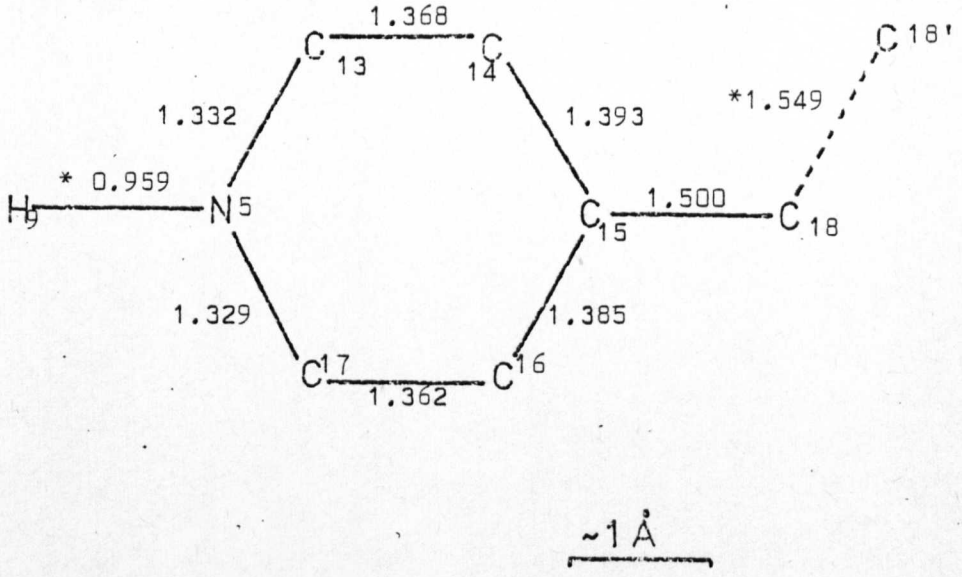

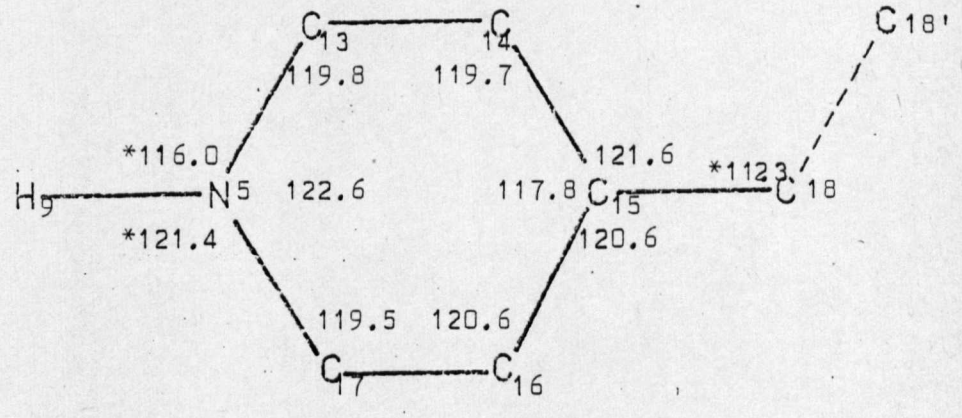

Figure 4.2 DHPA $(TCNQ)_4$ Librationally Corrected

Bond Distances (Angstroms) and Angles (Degrees)

* Not Corrected For Libration

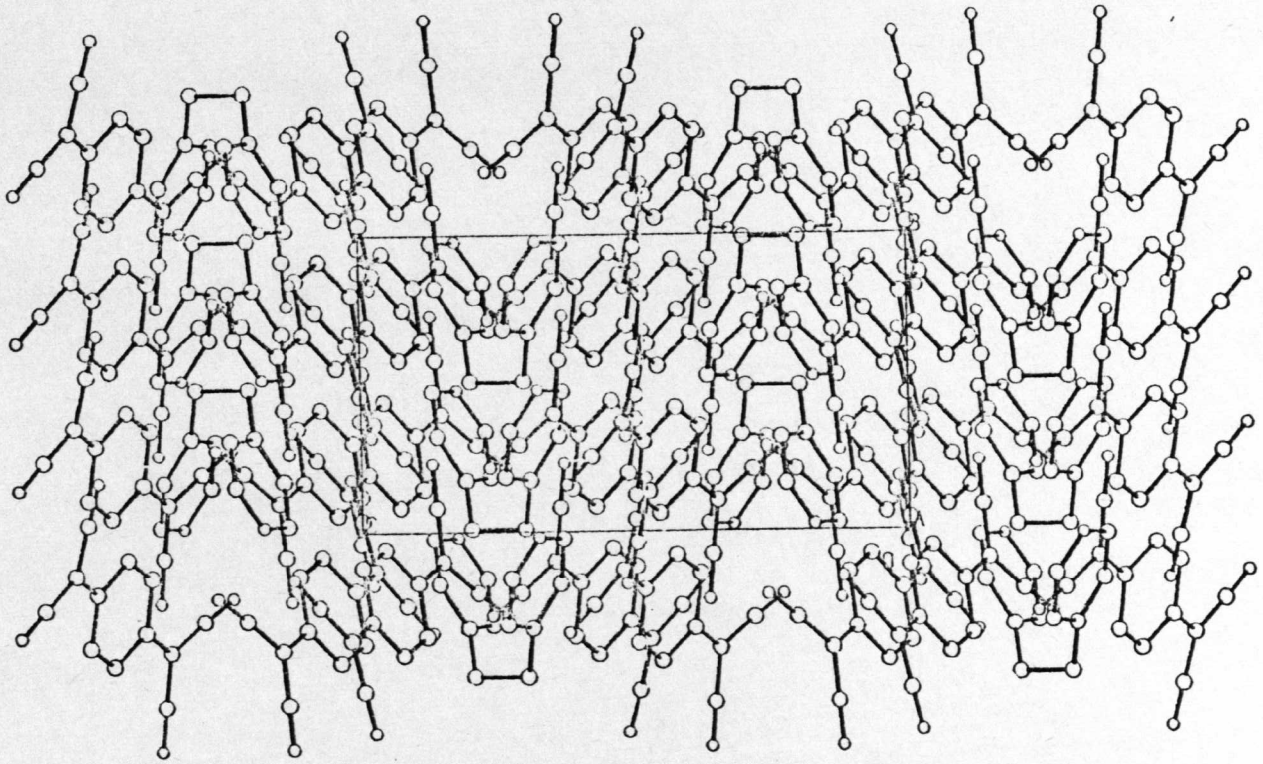

FIGURE 4.3a

DHPA(TCNQ)2 STEREO VIEW OF CELL DOWN B AXIS

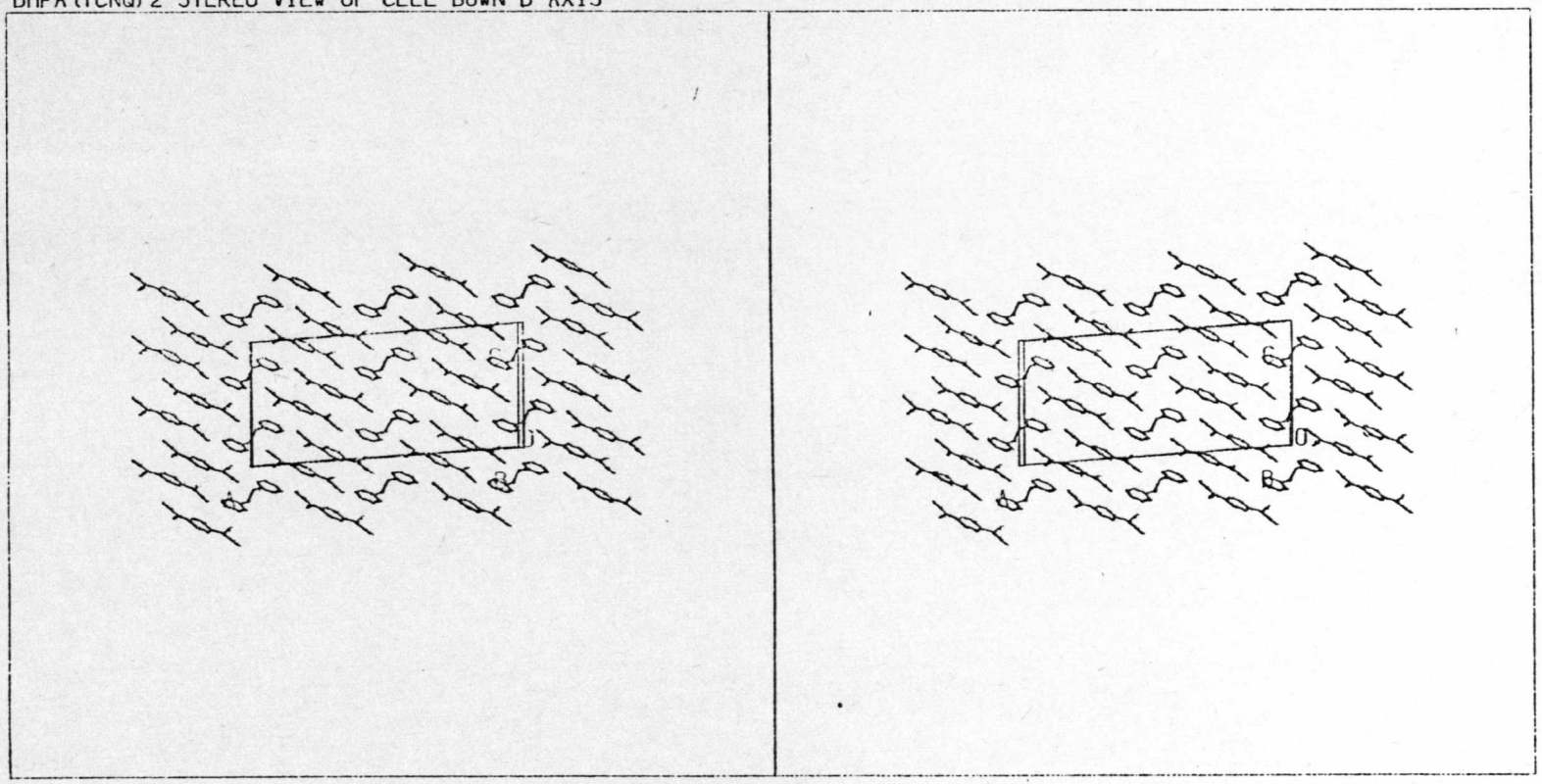

FIGURE 4.3b

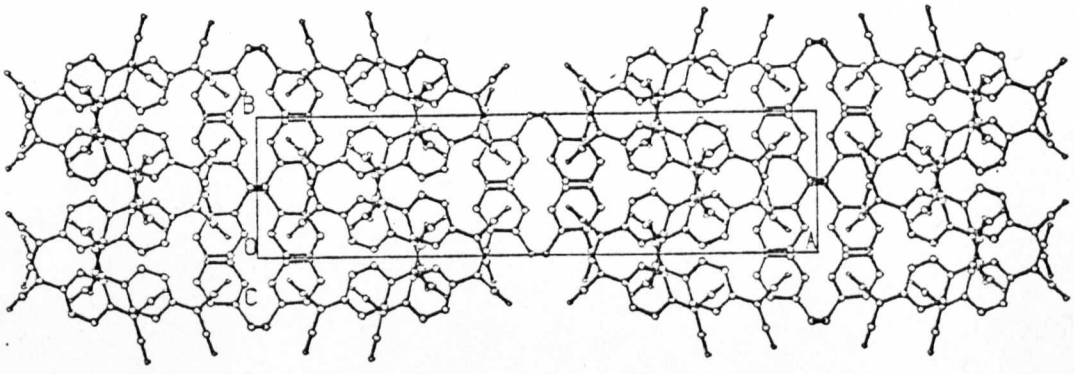

FIGURE 4.3c

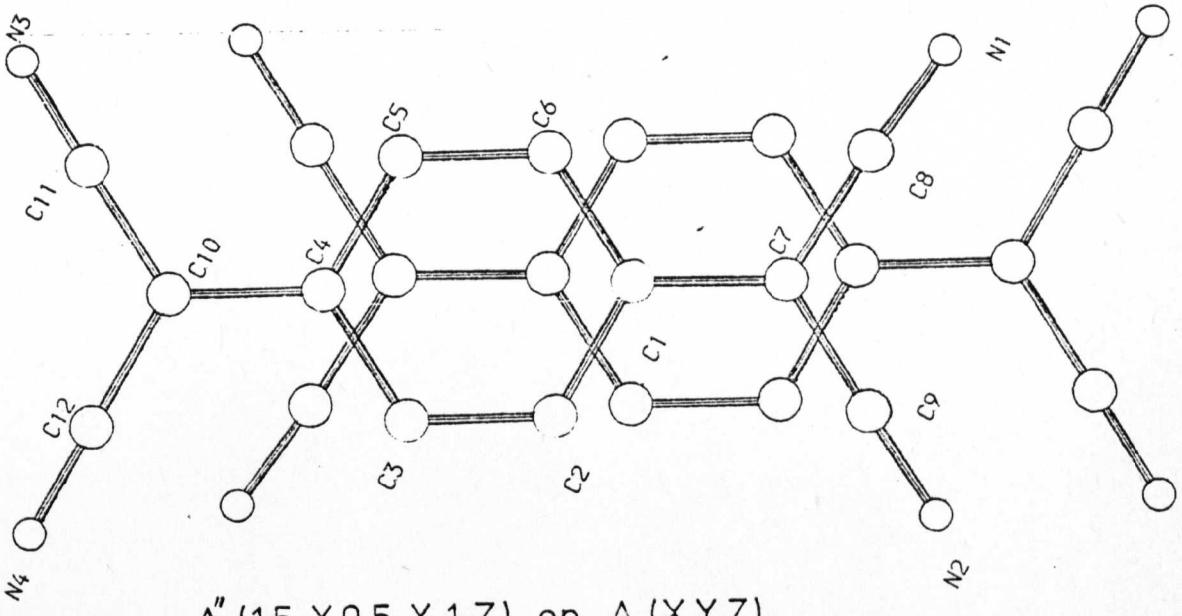

A" (1.5-X,0.5-Y,1-Z) on A (X,Y,Z)

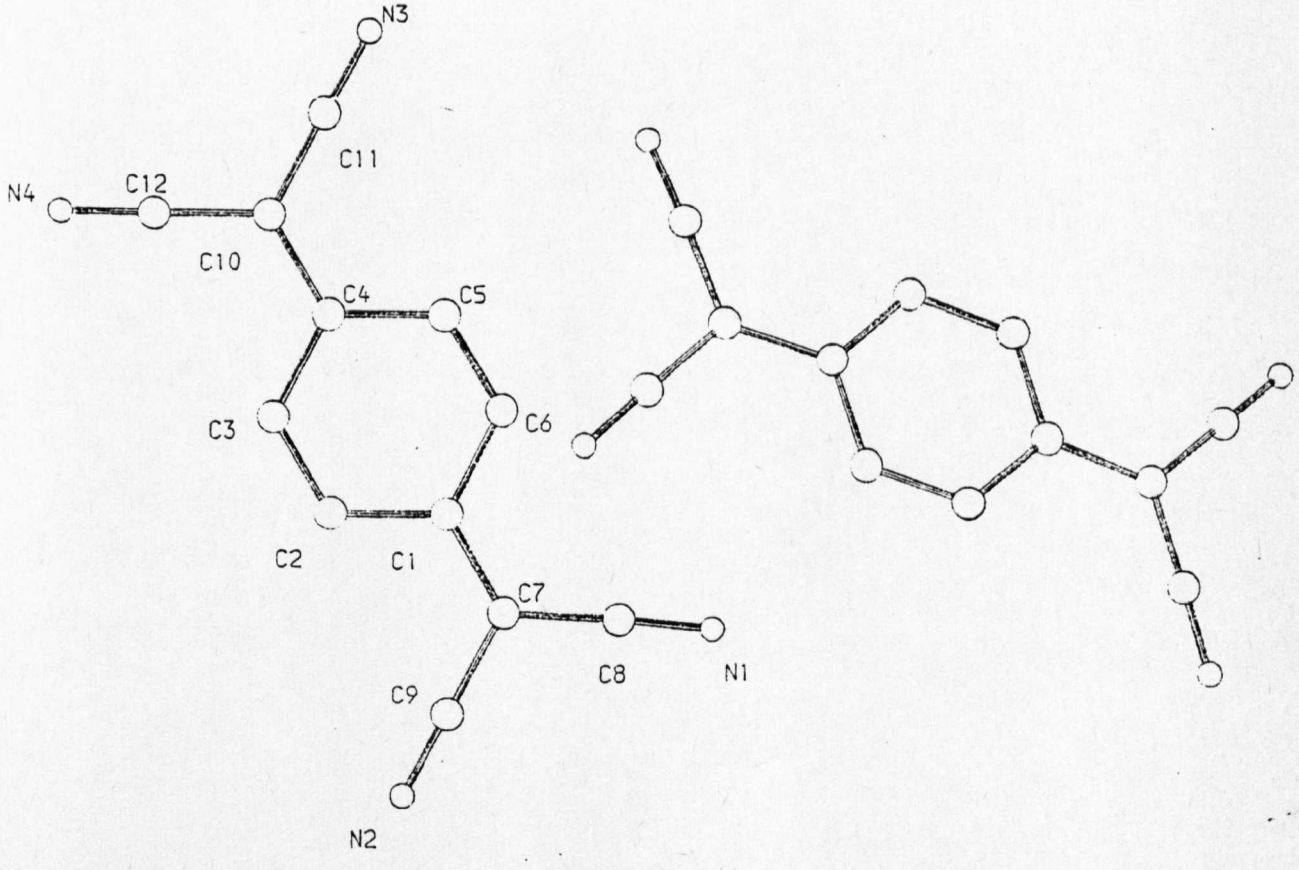

A' (1.5-X, 0.5+Y, 0.5-Z) on A (X,Y,Z)

FIGURE 4.4

STEREO VIEW OF DHPA(TCNQ)2 CATION

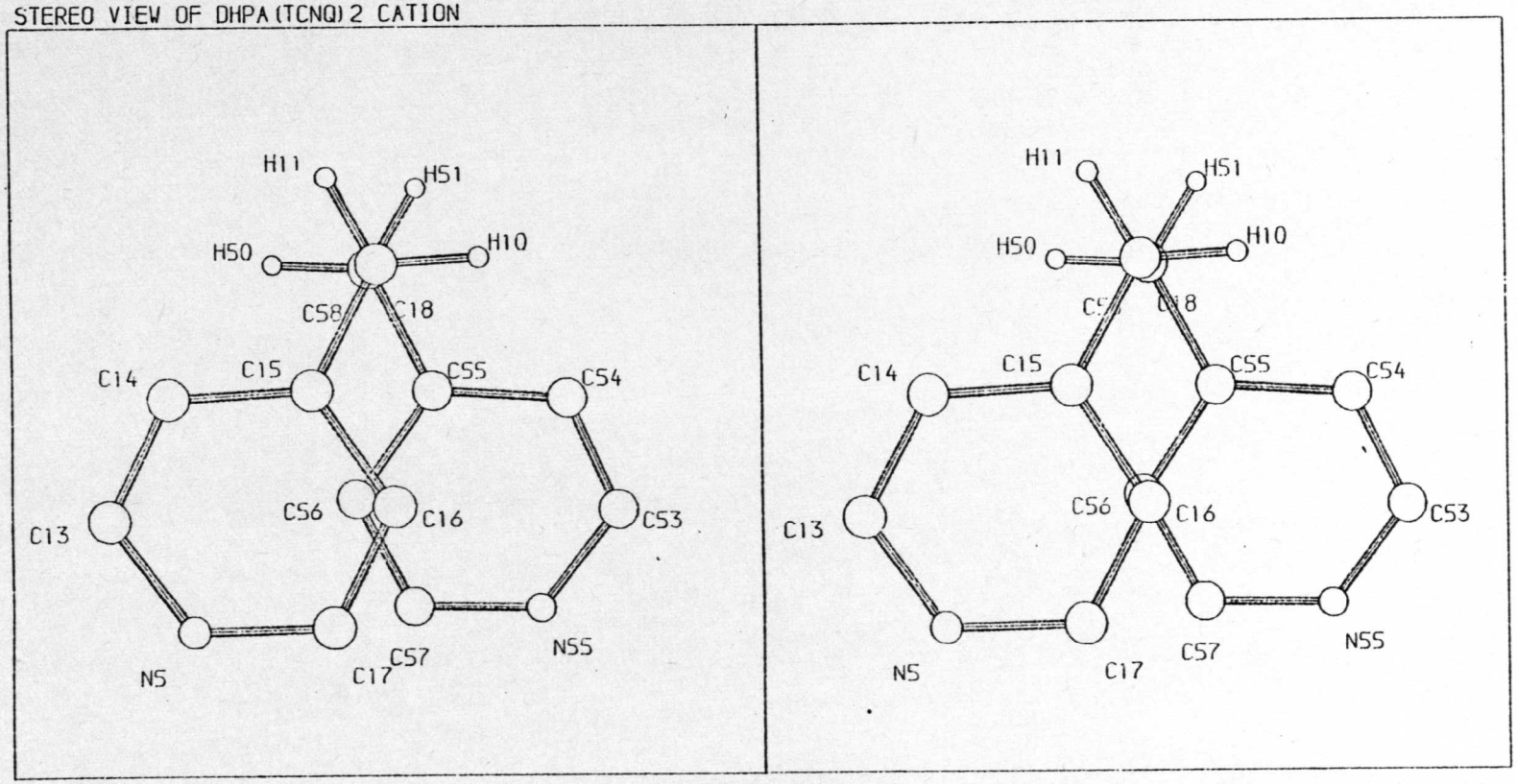

FIGURE 4.5

Fig. 4.6

Molecular geometry about H-bonded atoms.

Distances in Å; bond angles in degrees.

(H position refined).

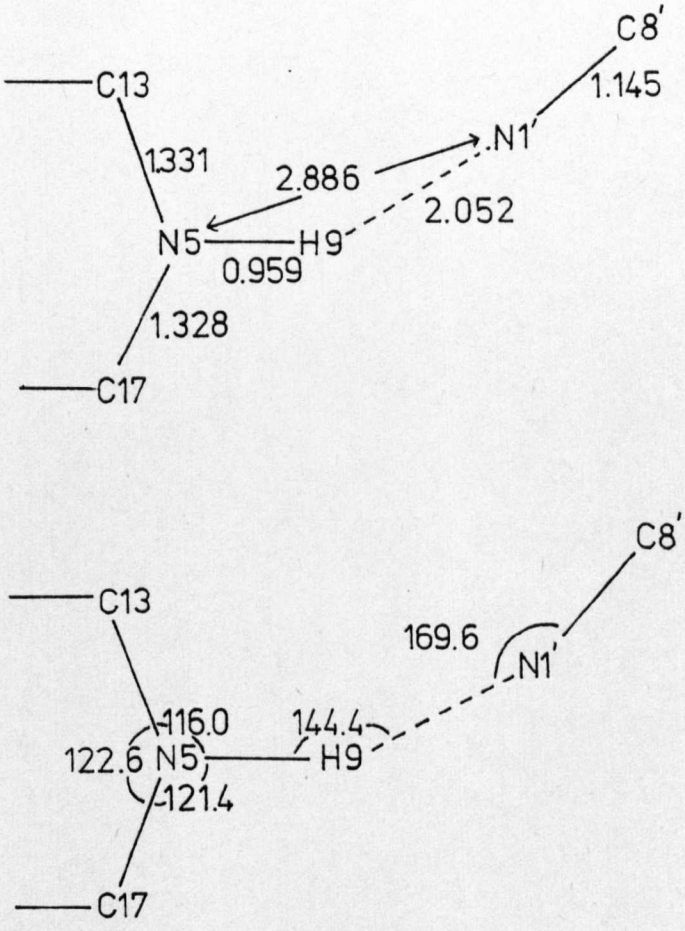

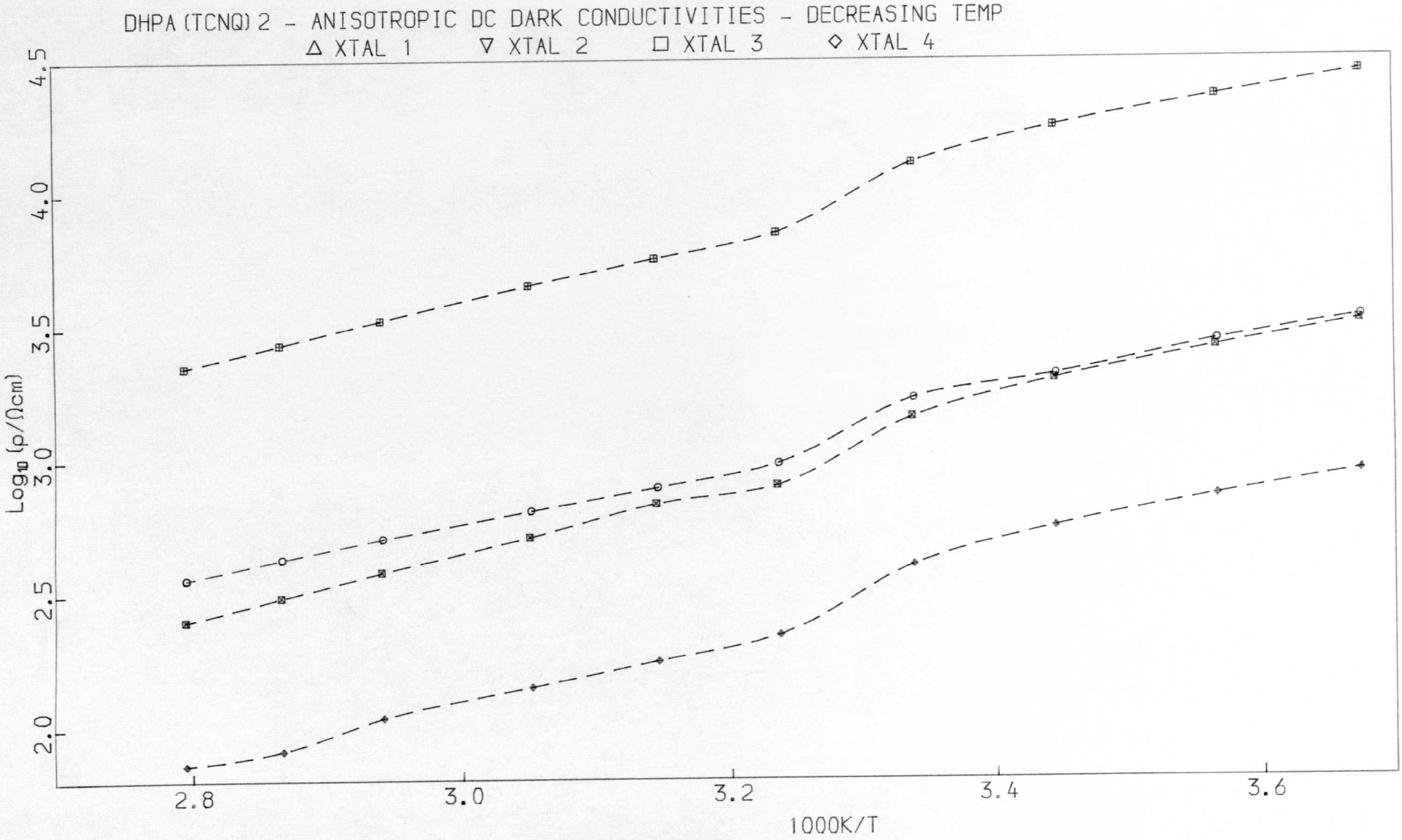
DHPA (TCNQ) 2 - ANISOTROPIC DC DARK CONDUCTIVITIES - DECREASING TEMP
△ XTAL 1
▽ XTAL 2
□ XTAL 3
◇ XTAL 4
Log10 (ρ/Ωcm)
4.5
4.0
3.5
3.0
2.5
2.0
2.8
3.0
3.2
3.4
3.6
1000K/T

FIGURE 4.7

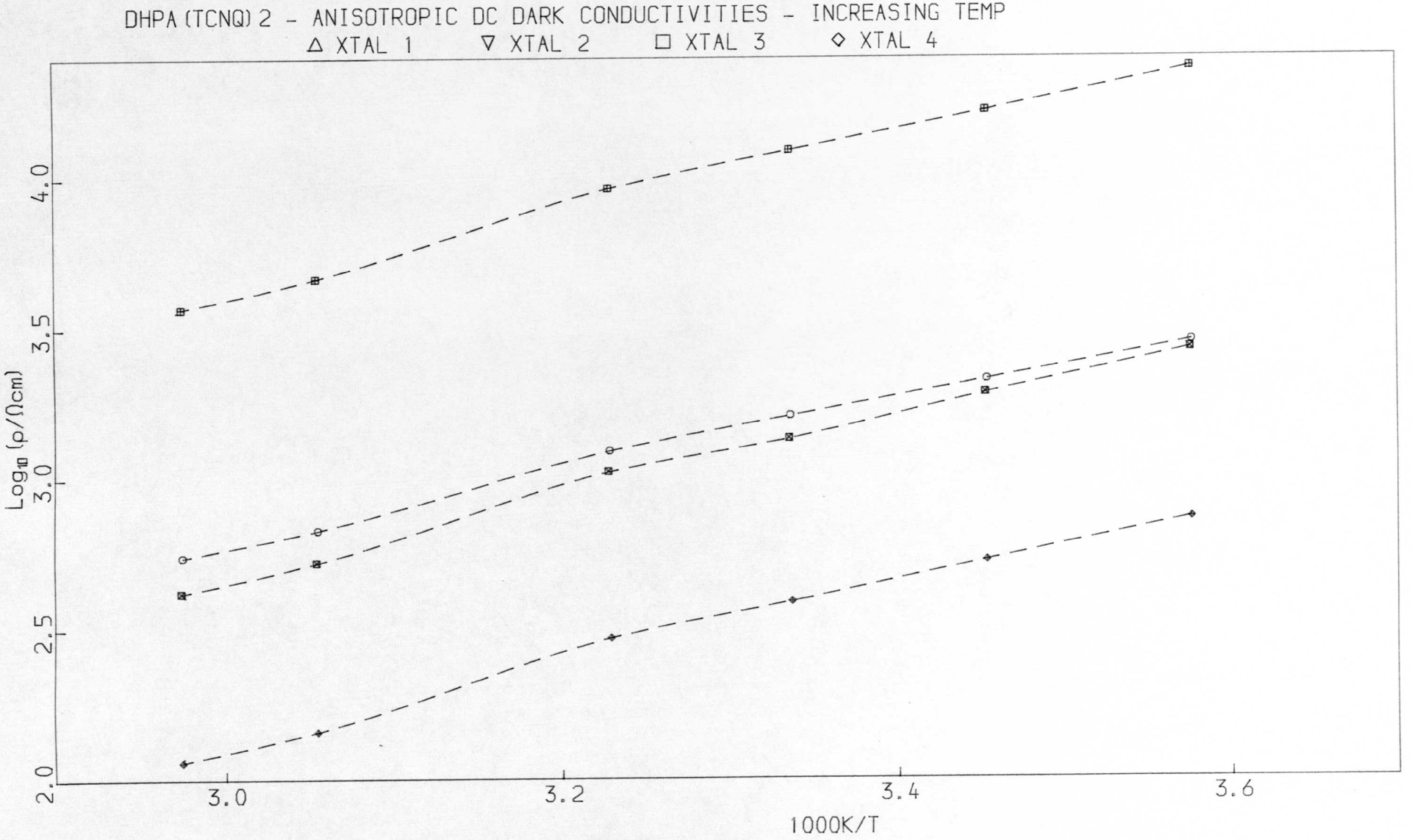
DHPA (TCNQ) 2 - ANISOTROPIC DC DARK CONDUCTIVITIES - INCREASING TEMP
△ XTAL 1
▽ XTAL 2
□ XTAL 3
◇ XTAL 4
Log10 (ρ/Ωcm)
4.0
3.5
3.0
2.5
2.0
3.0
3.2
3.4
3.6
1000K/T

FIGURE 4.8

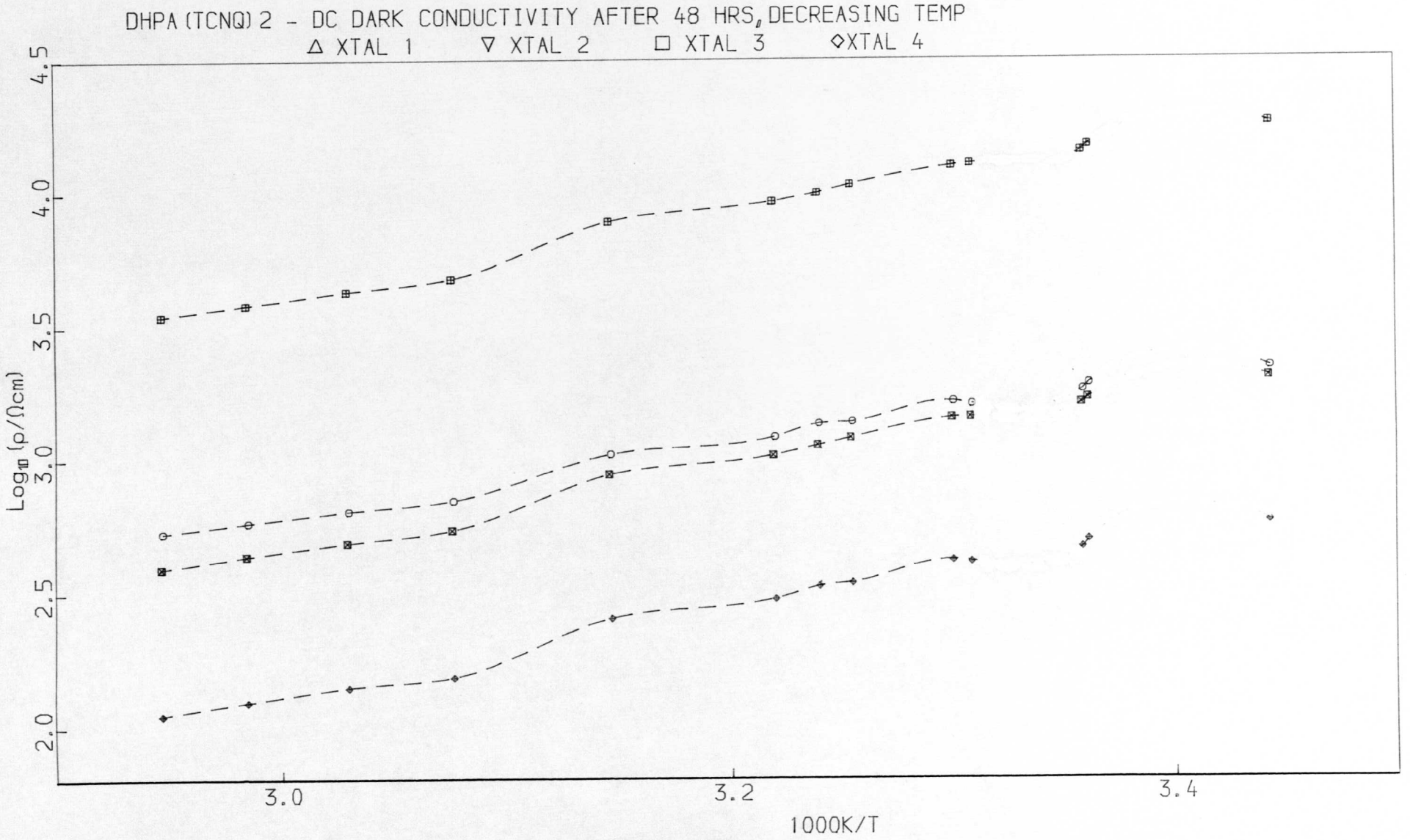
DHPA (TCNQ) 2 - DC DARK CONDUCTIVITY AFTER 48 HRS, DECREASING TEMP
△ XTAL 1
▽ XTAL 2
□ XTAL 3
◇XTAL 4
Log10 (ρ/Ωcm)
4.5
4.0
3.5
3.0
2.5
2.0
3.0
3.2
3.4
1000K/T

FIGURE 4.9

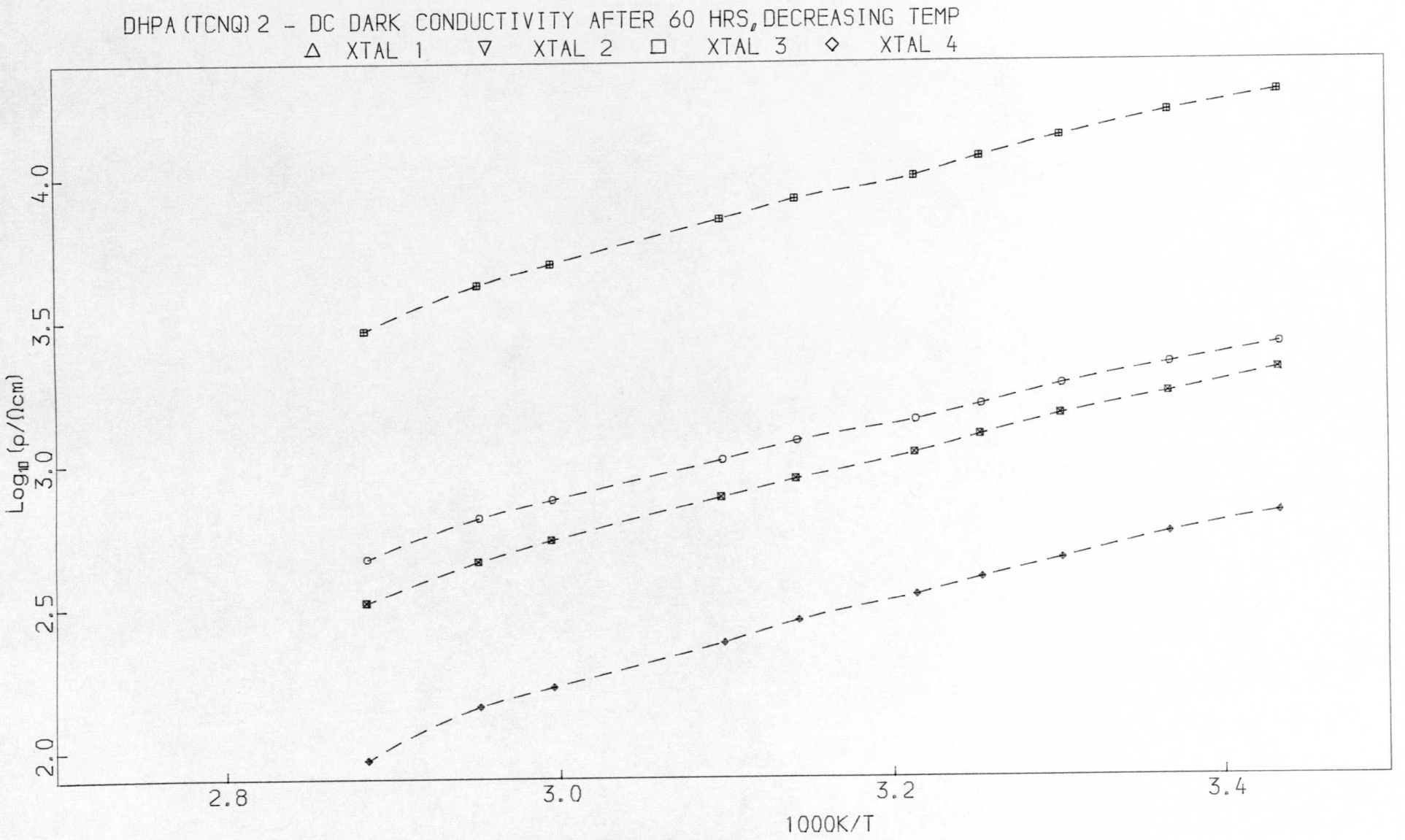
DHPA (TCNQ) 2 - DC DARK CONDUCTIVITY AFTER 60 HRS, DECREASING TEMP
△ XTAL 1 ▽ XTAL 2 □ XTAL 3 ◇ XTAL 4
Log10 (ρ/Ωcm)
4.0
3.5
3.0
2.5
2.0
2.8
3.0
3.2
3.4
1000K/T

FIGURE 4.10

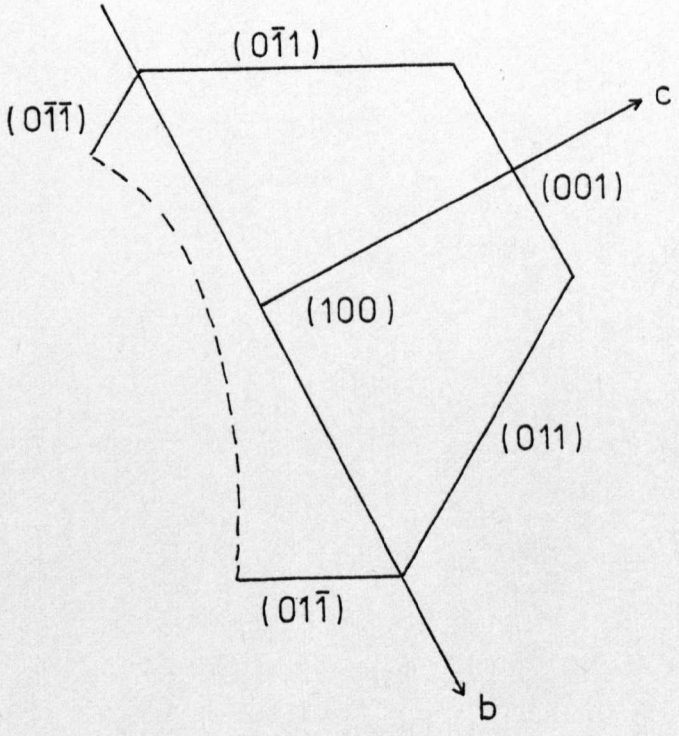

FIGURE 4.11

DHPA $(TCNQ)_2$- scale drawing of crystal used for diffractometry showing assigned faces

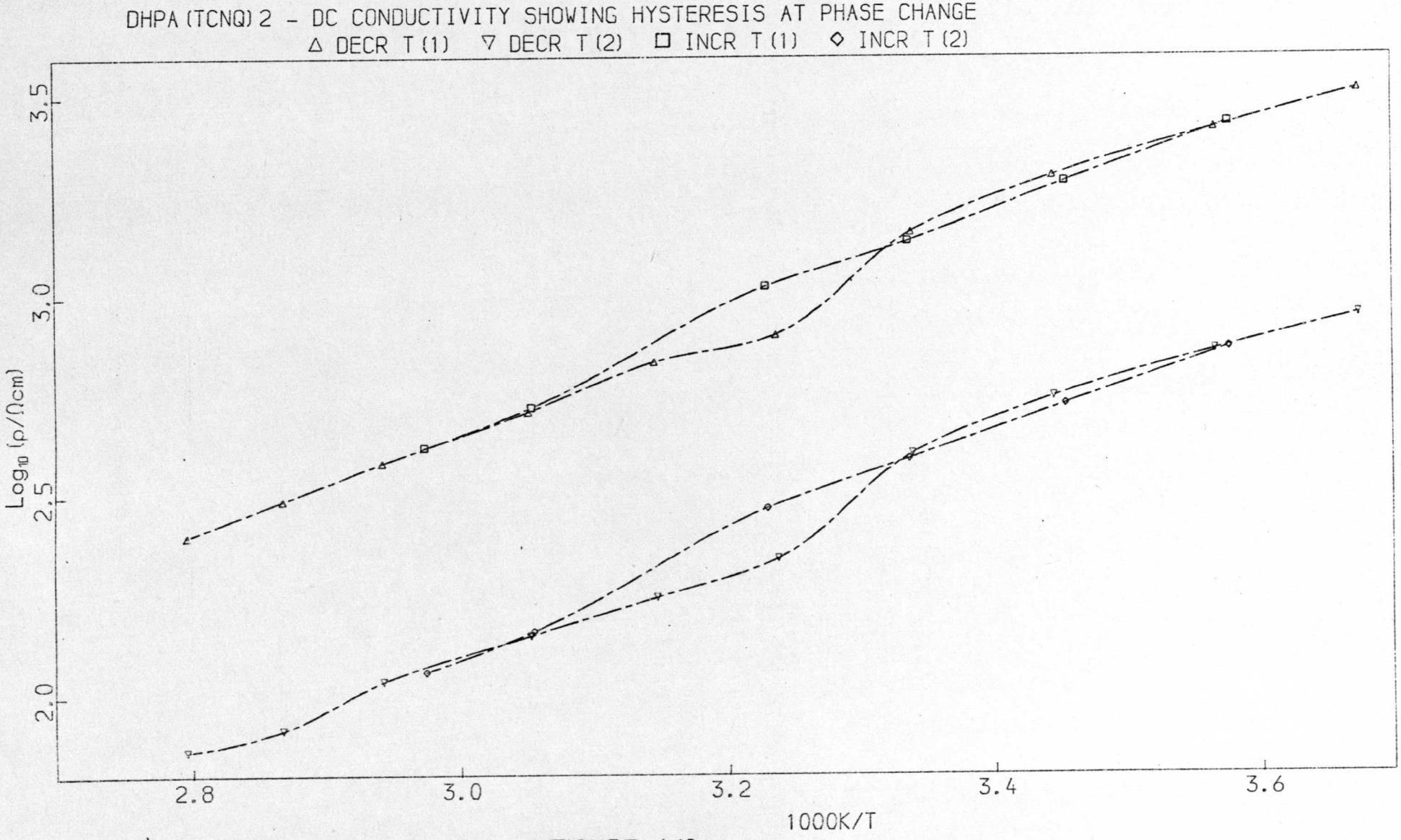
DHPA (TCNQ) 2 - DC CONDUCTIVITY SHOWING HYSTERESIS AT PHASE CHANGE
△ DECR T (1) ▽ DECR T (2) □ INCR T (1) ◇ INCR T (2)
Log10 (ρ/Ωcm)
3.5
3.0
2.5
2.0
2.8
3.0
3.2
3.4
3.6
1000K/T

FIGURE 4.12

Table 4.1

Bond lengths for DHPA $(TCNQ)_2$ in Å. E.s.d.'s in parentheses $\times 10^3$ Å

	Uncorrected	Corrected for libration
C(1) - C(2)	1.420 (3)	1.421
C(1) - C(6)	1.421 (3)	1.423
C(1) - C(7)	1.405 (3)	1.406
C(2) - C(3)	1.358 (3)	1.359
C(3) - C(4)	1.422 (3)	1.424
C(4) - C(5)	1.416 (3)	1.417
C(4) - C(10)	1.416 (3)	1.417
C(5) - C(6)	1.363 (3)	1.365
C(7) - C(8)	1.415 (3)	1.416
C(7) - C(9)	1.419 (3)	1.421
C(8) - N(1)	1.145 (3)	1.146
C(9) - N(2)	1.146 (3)	1.148
C(10) - C(11)	1.411 (3)	1.413
C(10) - C(12)	1.414 (3)	1.415
C(11) - N(3)	1.143 (3)	1.145
C(12) - N(4)	1.148 (3)	1.149

cont/..

Table 4.1 continued.

	Uncorrected	Corrected for libration
N(5) - C(13)	1.330 (3)	1.332
N(5) - C(17)	1.328 (3)	1.329
C(13) - C(14)	1.366 (4)	1.368
C(14) - C(15)	1.393 (3)	1.393
C(15) - C(16)	1.384 (3)	1.385
C(15) - C(18)	1.498 (3)	1.500
C(16) - C(17)	1.361 (3)	1.362
N(5) - H(9)	0.959 (31)	-
C(18) - C(18')	1.549 (5)	-

Table 4.2

Bond angles for DHPA $(TCNQ)_2$ in degrees. Estimated Standard deviations $\times 10^2$ in parentheses.

	Uncorrected	Corrected for libration.
C(2) - C(1) - C(6)	117.21 (18)	117.22
C(2) - C(1) - C(7)	120.65 (18)	120.62
C(6) - C(1) - C(7)	122.14 (18)	122.16
C(1) - C(2) - C(3)	121.83 (19)	121.79
C(2) - C(3) - C(4)	120.87 (18)	120.90
C(3) - C(4) - C(5)	117.48 (18)	117.50
C(3) - C(4) - C(10)	121.10 (18)	121.12
C(5) - C(4) - C(10)	121.33 (18)	121.29
C(4) - C(5) - C(6)	121.58 (18)	121.55
C(5) - C(6) - C(1)	120.99 (18)	121.02
C(1) - C(7) - C(8)	123.29 (18)	123.25
C(1) - C(7) - C(9)	121.47 (18)	121.50
C(9) - C(7) - C(8)	115.11 (18)	115.12
C(7) - C(8) - N(1)	177.21 (23)	177.21
C(7) - C(9) - N(2)	179.60 (25)	179.60
C(4) - C(10) - C(11)	121.36 (20)	121.38
C(4) - C(10) - C(12)	121.67 (19)	121.63
C(11) - C(10) - C(12)	116.81 (19)	116.83
C(10) - C(11) - N(3)	178.79 (27)	178.79

Cont./..

Table 4.2 continued

	Uncorrected	Corrected for libration
C(10) - C(12) - N(4)	179.35 (26)	179.35
C(13) - N(5) - C(17)	122.65 (22)	122.61
N(5) - C(13) - C(14)	119.75 (21)	119.79
C(13) - C(14) - C(15)	119.73 (21)	119.74
C(14) - C(15) - C(16)	117.82 (20)	117.78
C(14) - C(15) - C(18)	121.64 (20)	121.64
C(16) - C(15) - C(18)	120.52 (20)	120.56
C(15) - C(16) - C(17)	120.55 (20)	120.59
C(16) - C(17) - N(5)	119.49 (22)	119.49
C(15) - C(18) - C(18')	112.32 (16)	-
C(13) - N(5) - H(9)	116.00 (172)	-
C(17) - N(5) - H(9)	121.35 (173)	-

Table 4.3

Short Intermolecular contacts in Angstroms

TCNQ Intra-diad	< 3.6 Å	
Atoms		Distance
C(1) - C(1^{ii})		3.143
C(1) - C(2^{ii})		3.309
C(1) - C(3^{ii})		3.566
C(1) - C(5^{ii})		3.499
C(1) - C(6^{ii})		3.227
C(2) - C(6^{ii})		3.105
C(3) - C(7^{ii})		3.339
C(3) - C(8^{ii})		3.237
C(4) - C(7^{ii})		3.149
C(4) - C(8^{ii})		3.306
C(4) - C(9^{ii})		3.412
C(5) - C(7^{ii})		3.251
C(5) - C(9^{ii})		3.226
C(6) - C(7^{ii})		3.545

TCNQ Inter-diad	< 3.6 Å	
C(2) - N(1^{iii})		3.589
C(2) - N(2^{iv})		3.371
C(5) - N(1^{vi})		3.564
C(6) - C(9^{vi})		3.422

(vi is equivalent to A^{11} - A in figure 4.1b).

TCNQ - Cation heavy atoms	< 3.6 Å	
C(3) - N(5^{v})		3.444
C(4) - C(13^{v})		3.400
C(11) - C(15^{v})		3.502
C(12) - C(16^{v})		3.529
C(12) - C(17^{v})		3.485
N(1) - N(5^{vii})		2.885

Continued ....

Atoms	Distance
N(1) - $C(13^{vii})$	3.243
N(2) - $C(13^{viii})$	3.267
N(3) - $N(5^{ix})$	3.300
N(3) - $C(17^{ix})$	3.160
N(4) - $N(5^{xi})$	3.246
N(4) - $C(16^{ii})$	3.401
N(4) - $C(17^{ii})$	3.373
N(4) - $C(18^{x})$	3.386

Symmetry Operations

i	x	y	z	vii	1-x	y	$\frac{1}{2}$-z
ii	$1\frac{1}{2}$-x	$\frac{1}{2}$-y	1-z	viii	1-x	y-1	$\frac{1}{2}$-z
iii	$1\frac{1}{2}$-x	y-$\frac{1}{2}$	$\frac{1}{2}$-z	ix	$\frac{1}{2}$+x	$\frac{1}{2}$+y	z
iv	$1\frac{1}{2}$-x	y-$\frac{1}{2}$	1-z	x	$1\frac{1}{2}$-x	$1\frac{1}{2}$-y	1-z
v	$\frac{1}{2}$+x	y-$\frac{1}{2}$	z	xi	$\frac{1}{2}$+x	$\frac{1}{2}$-y	$\frac{1}{2}$+z
vi	$1\frac{1}{2}$-x	$\frac{1}{2}$+y	$\frac{1}{2}$-z	xii	$1\frac{1}{2}$-x	y-$\frac{1}{2}$	$\frac{1}{2}$-z

Table 4.4

Details of molecular planes (* denotes atoms not defining the plane).

1) TCNQ molecule

Equation of plane (all non-hydrogen atoms included):

$14.89857\,x - 2.13013\,y - 11.40980\,z - 6.54123 = 0$ (direct space)

or $0.50536\,x - 0.28766\,y - 0.81355\,z - 6.54123 = 0$ (orthogonal Å space)

Equation of plane (defined by the ring atoms):

$15.18717\,x - 1.95113\,y - 11.44655\,z - 6.69362 = 0$ (direct space)

or $0.51515\,x - 0.26349\,y - 0.81559\,z - 6.69362 = 0$ (orthogonal Å space)

Distances of atoms from planes:

Atom	Whole molecule (Å)	Ring atoms (Å)
C1	-0.07420	0.00970
C2	-0.07123	-0.00104
C3	-0.09979	-0.00847
C4	-0.11901	0.00934
C5	-0.14280	-0.00066
C6	-0.12975	-0.00886
C7	-0.02480	0.03663 *
C8	0.02256	0.09608 *
C9	0.07275	0.09735 *

continued

Table 4.4 continued

Atom	Whole molecule (Å)	Ring atoms (Å)
C10	-0.04147	0.16011 *
C11	0.08419	0.15471 *
C12	0.01342	0.10903 *
N1	0.07815	0.27123 *
N2	0.15989	0.15032 *
N3	0.20358	0.42014 *
N4	0.06850	0.19418 *

2) Cation

Equation of plane

12.29554 x - 2.68363 y - 11.59425 z + 0.13920 = 0 (direct)

or 0.41707 x - 0.36241 y - 0.83350 z + 0.13920 = 0 (orthogonal)

Distances of atoms from the plane:

Atom	Distance (Å)
N5	0.00133
C13	0.00606
C14	-0.00583
C15	-0.01188
C16	-0.00253
C17	0.00251
C18	0.01034
H9	0.33117 *
N1'	0.26823 *

continued

Table 4.4 continued

Distances of cation atoms from the plane of the TCNQ molecule:

Atom	Symmetry operation	Distance (Å)
N5	(2,1,1,0,0)	-0.8525
H9	(2,1,1,0,0)	-0.291

ATOM	X/A	Y/B	Z/C	U(ISO)
C(1)	0.76278(6)	0.1718(3)	0.3971(1)	
C(2)	0.79264(7)	0.0593(3)	0.4569(1)	
C(3)	0.83264(7)	0.1218(3)	0.4999(1)	
C(4)	0.84647(6)	0.3034(3)	0.4858(1)	
C(5)	0.81647(7)	0.4168(3)	0.4275(1)	
C(6)	0.77608(7)	0.3546(3)	0.3853(1)	
C(7)	0.72190(7)	0.1030(3)	0.3523(1)	
C(8)	0.69157(7)	0.2065(3)	0.2892(1)	
C(9)	0.70976(7)	-0.0812(3)	0.3623(2)	
C(10)	0.88070(7)	0.3653(3)	0.5239(2)	
C(11)	0.90558(8)	0.5392(3)	0.5011(2)	
C(12)	0.92026(8)	0.2516(3)	0.5802(2)	
N(1)	0.66620(7)	0.2838(3)	0.2368(1)	
N(2)	0.70006(9)	-0.2302(3)	0.3698(2)	
N(3)	0.91824(9)	0.6795(3)	0.4810(2)	
N(4)	0.94506(7)	0.1582(3)	0.6252(2)	
N(5)	0.40819(7)	0.5217(3)	0.3240(1)	
C(13)	0.39012(8)	0.6604(4)	0.2723(2)	
C(14)	0.41476(8)	0.8152(3)	0.2637(2)	
C(15)	0.45873(7)	0.8260(3)	0.3083(1)	
C(16)	0.47582(7)	0.6768(3)	0.3602(2)	
C(17)	0.45004(8)	0.5255(3)	0.3674(2)	
C(18)	0.48746(8)	0.9911(3)	0.2986(2)	
H(1)	0.7878	-0.0697	0.4680	0.0600
H(2)	0.8526	0.0388	0.5425	0.0600
H(3)	0.8251	0.5460	0.4171	0.0600
H(4)	0.7556	0.4394	0.3451	0.0600
H(5)	0.3571	0.6553	0.2403	0.0600
H(6)	0.4019	0.9212	0.2240	0.0600
H(7)	0.5073	0.6838	0.3923	0.0600
H(8)	0.4630	0.4161	0.4056	0.0600
H(9)	0.389(1)	0.418(4)	0.328(2)	0.037(8)
H(10)	0.5108	0.9980	0.3568	0.0600
H(11)	0.4676	1.1020	0.2999	0.0600

ATOM	U(11)	U(22)	U(33)	U(23)	U(13)	U(12)
C(1)	0.034(1)	0.034(1)	0.0255(9)	0.0009(8)	0.0045(7)	0.0009(8)
C(2)	0.034(1)	0.032(1)	0.034(1)	0.0015(9)	0.0034(8)	-0.0004(8)
C(3)	0.033(1)	0.034(1)	0.034(1)	0.0026(9)	0.0041(8)	0.0009(9)
C(4)	0.033(1)	0.038(1)	0.0282(9)	0.0009(8)	0.0070(8)	-0.0025(9)
C(5)	0.040(1)	0.032(1)	0.033(1)	0.0029(9)	0.0075(8)	-0.0039(9)
C(6)	0.038(1)	0.035(1)	0.0290(9)	0.0048(8)	0.0046(8)	0.0007(9)
C(7)	0.036(1)	0.035(1)	0.0295(9)	-0.0004(8)	-0.0006(8)	0.0003(9)
C(8)	0.038(1)	0.039(1)	0.034(1)	-0.0054(9)	-0.0009(9)	0.001(1)
C(9)	0.042(1)	0.042(1)	0.035(1)	-0.0001(9)	-0.0065(9)	-0.004(1)
C(10)	0.034(1)	0.040(1)	0.037(1)	0.0000(9)	0.0046(8)	-0.0070(9)
C(11)	0.040(1)	0.054(1)	0.046(1)	0.001(1)	0.004(1)	-0.010(1)
C(12)	0.035(1)	0.049(1)	0.046(1)	-0.001(1)	0.000(1)	-0.009(1)
H(1)	0.056(1)	0.057(1)	0.049(1)	-0.004(1)	-0.012(1)	0.013(1)
H(2)	0.079(2)	0.046(1)	0.062(1)	0.006(1)	-0.017(1)	-0.018(1)
H(3)	0.076(2)	0.058(1)	0.089(2)	0.012(1)	0.012(1)	-0.028(1)
H(4)	0.046(1)	0.068(2)	0.079(2)	0.011(1)	-0.012(1)	-0.003(1)
H(5)	0.046(1)	0.043(1)	0.055(1)	-0.0070(9)	0.0140(9)	-0.009(1)
C(13)	0.039(1)	0.064(2)	0.052(1)	-0.003(1)	0.002(1)	-0.002(1)
C(14)	0.041(1)	0.053(1)	0.047(1)	0.005(1)	0.005(1)	0.007(1)
C(15)	0.041(1)	0.034(1)	0.039(1)	-0.0038(9)	0.0114(9)	0.0012(9)
C(16)	0.040(1)	0.044(1)	0.045(1)	0.002(1)	0.0025(9)	-0.001(1)
C(17)	0.043(1)	0.042(1)	0.053(1)	0.005(1)	0.007(1)	-0.000(1)
C(18)	0.054(1)	0.033(1)	0.065(2)	-0.008(1)	0.023(1)	-0.004(1)

H	/FO/	/FC/	PHI
** K= 0 L= 0 **			
2	374	385	180
4	40	60	0
6	904	865	180
8	1514	1625	180
10	1234	1209	0
12	330	331	0
14	186	183	180
16	1074	1016	180
18	213	211	0
20	206	186	0
22	117	95	0
24	162	166	0
26	236	248	180
28	234	237	180
32	145	145	180
** K= 1 L= 0 **			
1	231	232	180
3	348	356	0
5	650	669	180
7	214	218	0
9	964	974	180
11	529	498	180
13	206	217	180
15	90	106	180
17	138	147	0
19	268	260	0
23	91	83	180
25	140	138	0
27	425	421	180
29	179	173	0
31	71	70	180
** K= 2 L= 0 **			
0	864	879	180
2	376	398	0
4	461	449	0
6	112	134	180
8	529	512	0
10	534	524	0
12	315	308	180
14	46	38	0
16	47	41	180
18	277	262	0
20	223	214	0
22	283	273	0
26	492	474	180
28	84	66	0
32	109	91	0
** K= 3 L= 0 **			
1	278	269	0
3	619	587	180
5	496	462	180
7	1139	1100	180
11	77	39	180
13	43	28	180
15	164	161	0
17	627	603	180
21	247	242	0
23	315	314	0
25	194	186	0
27	356	356	0
29	257	256	180
** K= 4 L= 0 **			
0	113	75	180
2	500	464	0
4	148	146	180
6	151	155	0
8	266	253	180
10	289	300	0
12	425	387	0
14	239	210	0
18	560	545	180
20	324	318	0
22	64	64	0
24	169	175	0
28	241	235	180
** K= 5 L= 0 **			
1	101	100	180
5	44	38	0
7	201	206	180
9	224	214	0
11	337	334	180
13	82	69	180
15	227	214	180
17	299	302	0
21	143	136	180
25	242	240	180
** K= 6 L= 0 **			
0	387	393	0
2	609	607	0
6	251	257	180
8	276	269	0
10	262	255	180
12	169	164	0
14	198	203	180
20	64	46	0
22	108	98	0
24	80	102	180
** K= 7 L= 0 **			
1	103	96	0
3	217	220	180
7	148	135	180
9	185	184	180
11	127	132	0
13	117	112	180
21	216	201	0
** K= 8 L= 0 **			
0	117	116	180
2	62	65	0
8	105	98	0
12	84	73	0
** K= 1 L= 1 **			
-33	138	133	180
-31	90	90	0
-27	76	77	0
-25	272	268	180
-23	107	97	0
-21	77	63	180
-19	355	350	0
-15	135	111	0
-13	401	388	0
-11	74	70	180
-9	328	335	180
-7	605	607	0
-5	258	259	0
-3	214	217	180
-1	811	834	0
1	1939	2176	180
3	553	595	180
5	234	233	180
9	1593	1672	180
11	576	590	0

H	/FO/	/FC/	PHI
13	39	94	0
15	323	309	0
17	606	609	0
19	205	198	180
21	119	113	180
25	127	131	0
27	123	114	180
29	137	146	180
31	174	191	0
** K= 2 L= 1 **			
-32	82	72	180
-28	438	437	180
-26	328	325	0
-24	262	268	0
-22	120	122	0
-20	80	85	0
-16	228	233	0
-14	277	266	0
-10	766	749	180
-8	778	758	180
-6	597	600	0
-4	577	564	0
-2	446	445	0
0	203	206	0
2	217	223	180
4	440	448	180
6	406	404	180
8	736	702	180
10	105	102	0
12	109	100	0
14	64	64	0
16	247	244	180
18	130	144	0
22	208	216	0
24	259	252	0
26	417	429	180
28	398	405	0
30	105	108	180
32	99	99	0
** K= 3 L= 1 **			
-31	67	65	0
-19	152	154	0
-17	152	156	180
-15	307	273	180
-13	80	87	180
-11	95	75	180
-7	379	391	0
-5	241	227	180
-3	46	45	180
-1	348	329	0
1	922	924	180
3	879	871	0
7	259	260	180
9	402	416	0
11	606	615	180
13	51	44	0
15	281	288	0
17	120	125	0
19	202	227	180
23	100	97	180
25	99	98	180
27	91	92	0
** K= 4 L= 1 **			
-26	105	114	0
-24	201	191	180
-22	251	246	180
-20	162	162	0
-18	740	717	180
-16	337	321	0
-14	145	130	180
-12	93	96	180
-10	421	424	0
-8	378	345	0
-6	79	78	0
-4	68	88	180
0	206	212	180
2	466	442	180
4	373	364	0
6	375	359	0
8	444	431	0
10	256	229	0
14	97	87	180
16	182	193	0
18	346	367	0
20	245	248	180
22	223	214	180
24	284	285	180
28	93	104	0
** K= 5 L= 1 **			
-27	192	179	0
-25	147	151	0
-23	136	130	180
-21	184	184	180
-19	318	298	180
-17	373	354	0
-15	161	169	180
-11	215	213	180
-9	196	193	180
-7	253	249	0
-5	102	99	180
-3	66	78	0
-1	229	218	180
1	340	326	0
3	96	83	180
5	47	52	180
9	267	279	0
11	62	62	0
13	228	230	0
15	377	377	180
17	253	256	180
19	71	87	180
27	106	100	0
** K= 6 L= 1 **			
-24	162	157	0
-20	108	100	180
-12	214	216	0
-10	181	193	0
-8	391	412	180
-6	229	230	0
-4	70	84	0
-2	124	125	0
2	188	183	180
4	184	197	180
8	527	533	0
10	238	239	180
14	61	73	0
16	67	82	180
18	160	161	0
22	88	87	180
** K= 7 L= 1 **			
-21	147	129	0
-19	79	76	180
-15	159	167	0
-13	259	228	180
-11	176	169	0
-9	128	121	0
-7	193	193	0
-5	205	204	0

H	/FO/	/FC/	PHI
-3	242	244	180
-1	283	274	180
1	325	325	180
7	58	35	180
9	304	306	180
15	226	230	0
19	138	136	0

** K= 3 L= 1 **

H	/FO/	/FC/	PHI
-14	144	130	0
-12	94	77	180
-10	130	113	180
-6	63	43	0
-4	191	171	0
-2	147	130	0
0	94	85	180
2	92	98	180

** K= 0 L= 2 **

H	/FO/	/FC/	PHI
-34	197	191	0
-26	56	51	0
-24	108	108	0
-22	85	96	180
-20	429	417	180
-18	218	186	0
-16	739	682	180
-14	1241	1240	0
-12	696	709	0
-10	359	361	0
-8	511	520	0
-6	234	222	180
-2	463	469	180
0	126	115	0
2	1245	1350	180
4	1413	1521	180
6	412	410	180
8	925	931	180
10	591	608	180
14	520	529	180
16	416	390	0
18	124	151	180
20	387	376	0
22	203	215	180
26	56	50	180
28	121	118	0

** K= 1 L= 2 **

H	/FO/	/FC/	PHI
-33	177	202	180
-27	196	198	180
-25	285	283	0
-21	121	122	180
-19	171	176	180
-17	336	348	180
-15	651	640	0
-9	435	431	180
-7	398	387	180
-5	2052	2197	0
-3	441	451	0
-1	438	456	0
1	1071	1178	180
3	452	469	0
5	1054	1133	0
7	504	519	0
9	182	170	0
11	1021	1032	180
13	337	301	0
15	93	84	0
17	270	247	0
19	211	204	0
21	302	299	180
23	229	246	0
27	70	60	180
29	131	141	0

** K= 2 L= 2 **

H	/FO/	/FC/	PHI
-30	117	108	0
-22	120	109	0
-26	127	110	0
-24	223	224	0
-22	196	193	0
-16	297	297	0
-14	861	854	180
-10	490	469	180
-8	913	877	180
-6	329	299	0
-4	72	95	0
-2	109	125	0
0	433	435	0
2	1413	1475	180
4	432	460	180
6	91	93	180
8	269	267	180
10	844	840	0
12	637	620	180
16	208	217	180
18	134	135	0

H	/FO/	/FC/	PHI
20	119	129	0
22	152	155	180
24	67	52	180
26	259	253	180
28	71	87	180
30	114	125	0

** K= 3 L= 2 **

H	/FO/	/FC/	PHI
-31	237	240	180
-29	96	94	0
-27	249	246	0
-25	229	216	0
-23	215	215	180
-21	472	478	180
-19	101	101	0
-17	307	300	180
-15	88	82	0
-13	411	390	180
-11	449	441	180
-7	731	689	0
-5	471	464	0
-3	587	570	0
-1	227	234	0
1	227	209	0
3	925	912	180
5	458	463	180
7	429	410	0
9	573	546	0
11	249	287	0
13	575	589	0
15	159	167	0
17	530	561	0
19	383	398	0
21	225	232	180
23	411	425	180
25	280	281	180
27	88	97	0
31	90	82	180

** K= 4 L= 2 **

H	/FO/	/FC/	PHI
-30	122	96	180
-26	113	116	0
-24	240	243	0
-22	179	175	0
-20	262	259	0
-18	375	372	180
-16	260	238	180
-14	149	145	0

H	/FO/	/FC/	PHI
-12	349	341	180
-10	43	13	180
-8	195	189	0
-6	508	494	180
-4	398	401	0
-2	159	139	0
0	466	471	180
2	89	89	0
4	310	323	180
6	324	330	180
10	138	120	180
12	127	128	180
14	196	205	0
20	134	148	180
24	252	255	180
28	90	85	0

** K= 5 L= 2 **

H	/FO/	/FC/	PHI
-27	161	160	0
-25	121	105	180
-21	136	123	0
-19	350	359	180
-17	371	341	0
-9	87	88	0
-7	75	70	0
-5	111	112	0
-3	377	383	0
1	169	179	180
3	265	266	0
5	181	187	0
7	162	173	180
9	271	280	0
11	72	76	0
13	551	582	180
15	452	462	0
17	71	55	180
21	213	221	0
23	164	168	180
27	82	72	0

** K= 6 L= 2 **

H	/FO/	/FC/	PHI
-24	67	70	180
-22	161	155	180
-16	58	57	0
-14	377	389	0
-12	57	46	180
-10	110	144	0
-8	157	186	180

H	/FO/	/FC/	PHI
-6	265	279	0
-2	62	21	0
0	254	250	180
2	411	421	180
4	141	127	180
6	341	369	180
8	339	329	0
10	448	469	180
12	143	137	0
14	182	177	180
16	153	134	180
18	112	120	0

** K= 7 L= 2 **

H	/FO/	/FC/	PHI
-19	82	71	180
-17	82	77	0
-15	261	253	180
-13	348	347	0
-11	113	113	180
-9	158	163	180
-7	147	153	0
-3	195	192	0
-1	127	133	180
1	139	186	0
3	159	157	180
5	197	214	0
7	339	332	0
9	287	288	180
11	135	178	0

** K= 8 L= 2 **

H	/FO/	/FC/	PHI
-14	163	170	180
-10	83	66	180
-6	114	103	180
-4	75	84	180
-2	64	48	180
2	111	125	0
4	82	80	180
8	60	66	180

** K= 1 L= 3 **

H	/FO/	/FC/	PHI
-33	89	105	180
-31	84	76	180
-29	58	33	180
-27	62	76	0
-25	106	100	0
-23	58	73	180

H	/FO/	/FC/	PHI
-21	397	396	0
-19	138	140	0
-17	276	268	180
-15	116	110	0
-11	89	82	0
-9	49	54	180
-7	89	80	180
-5	3628	3943	180
-3	461	457	0
-1	639	645	0
1	522	545	0
3	1589	1756	0
5	483	501	180
7	501	485	180
9	111	103	0
11	206	198	0
13	96	125	0
15	55	63	0
21	409	411	180
23	495	514	0
27	215	225	0
29	87	92	180
31	284	278	180

** K= 2 L= 3 **

H	/FO/	/FC/	PHI
-32	376	375	0
-30	114	105	180
-28	146	141	0
-26	118	106	0
-24	78	67	180
-22	323	331	180
-20	108	107	180
-18	192	201	0
-16	272	277	0
-14	349	345	0
-12	646	609	180
-10	209	181	180
-8	564	547	180
-6	696	679	0
-4	533	523	180
-2	300	303	180
2	354	365	180
4	223	233	0
8	68	54	180
10	413	418	0
12	137	150	180
14	352	367	180
16	213	224	0
18	135	142	0

H	/FO/	/FC/	PHI
20	281	271	0
22	400	428	0
24	416	428	180
26	82	61	180
32	128	122	180
** K=	3	L=	3 **
-21	246	251	0
-20	56	46	0
-19	131	127	180
-17	452	466	180
-16	56	55	0
-14	221	218	0
-13	276	260	0
-12	360	346	180
-10	106	107	0
-9	146	152	180
-7	761	697	0
-6	147	125	180
-4	192	191	180
-1	88	84	180
3	118	88	180
5	332	331	0
7	224	223	0
11	259	242	180
13	107	110	180
16	106	103	0
31	84	71	0
** K=	4	L=	3 **
-28	128	134	180
-26	111	116	180
-22	354	339	0
-18	212	207	180
-16	115	114	180
-14	45	41	180
-12	409	415	0
-10	196	205	0
-8	172	168	0
-6	249	219	180
-4	198	195	180
-2	116	101	0
0	213	212	0
2	55	59	0
4	220	194	0
6	121	105	0
8	92	96	180
10	352	357	180

H	/FO/	/FC/	PHI
12	455	468	0
14	325	335	180
16	130	131	180
18	197	186	180
20	420	437	180
22	75	73	180
24	213	212	0
28	90	94	0
30	75	67	0
** K=	5	L=	3 **
-25	98	85	180
-23	116	131	180
-21	60	54	180
-19	277	275	180
-17	144	134	0
-11	31	62	0
-9	174	176	0
-7	339	324	0
-5	284	279	0
-3	91	74	180
1	433	432	180
3	464	486	0
5	322	361	180
7	145	149	180
9	138	141	0
11	193	190	180
13	715	715	0
15	235	239	180
17	87	80	180
19	289	303	180
23	152	151	0
** K=	6	L=	3 **
-24	135	135	180
-18	84	85	180
-16	185	189	0
-14	186	174	180
-12	189	188	0
-10	99	112	0
-8	144	162	180
-6	71	47	180
-4	84	84	0
-2	81	91	180
0	183	175	180
4	221	233	180
6	161	157	0
8	188	180	0

H	/FO/	/FC/	PHI
10	80	95	0
12	293	287	180
14	114	107	0
18	133	122	180
20	118	103	0
22	89	103	180
24	97	90	180
** K=	7	L=	3 **
-19	151	145	0
-15	79	80	0
-13	278	272	180
-11	79	64	0
-7	59	30	180
-5	266	266	180
-3	322	325	180
-1	160	161	180
1	215	220	0
3	283	288	0
5	137	125	0
7	97	109	0
9	122	117	180
11	158	176	0
13	89	89	0
** K=	8	L=	3 **
-8	114	113	0
-4	146	142	180
0	136	118	180
6	79	81	180
8	99	82	0
10	65	30	180
12	71	45	0
** K=	0	L=	4 **
-34	109	100	0
-32	115	107	180
-24	172	174	0
-22	226	216	180
-20	112	96	0
-18	116	107	0
-16	227	218	180
-14	946	949	180
-12	822	858	0
-10	388	408	0
-8	211	200	180
-6	1421	1423	0

H	/FO/	/FC/	PHI
-4	4302	4024	180
0	42	39	0
2	754	767	0
4	551	523	180
6	265	249	180
8	670	647	0
10	477	449	0
12	1609	1638	0
16	451	448	180
18	148	140	180
20	138	146	0
22	341	345	180
24	239	244	0
26	272	282	0
28	116	119	0
30	185	187	0
** K=	1	L=	4 **
-33	133	134	180
-31	261	264	0
-29	220	214	0
-27	188	191	0
-25	57	50	0
-23	50	50	180
-21	214	214	180
-19	190	192	0
-17	152	156	0
-15	170	166	0
-13	120	121	180
-9	969	960	0
-7	145	141	0
-5	1587	1577	0
-3	1391	1373	180
-1	1447	1455	180
1	511	504	180
3	847	862	180
5	867	896	0
7	123	127	180
9	172	180	180
11	401	377	180
13	227	236	0
15	110	85	0
17	54	42	180
19	62	73	0
21	655	658	180
23	316	314	0
25	97	109	180
27	85	100	0
29	117	118	0

H	/FO/	/FC/	PHI
31	135	117	180
** K=	2	L=	4 **
-32	66	71	180
-30	308	305	0
-26	220	227	180
-24	219	228	180
-22	417	422	180
-18	271	256	180
-16	40	42	0
-14	142	148	180
-12	368	366	180
-10	285	284	0
-8	317	306	0
-6	73	61	0
-4	582	576	0
-2	56	49	0
0	330	340	180
2	53	48	180
4	730	738	0
6	430	424	180
8	209	201	0
10	360	368	0
12	154	156	180
14	244	225	0
16	186	185	0
18	148	152	180
20	113	120	180
22	297	279	0
24	67	46	180
** K=	3	L=	4 **
-31	185	173	180
-25	113	102	0
-23	303	302	180
-21	270	266	0
-17	62	64	0
-15	430	423	0
-13	94	81	0
-11	168	153	0
-9	161	153	180
-7	236	213	0
-5	446	438	180
-1	330	323	0
1	173	159	0
3	683	691	0
5	83	71	0
7	320	350	180

H	/FO/	/FC/	PHI
9	77	85	180
11	257	251	180
13	147	133	0
17	350	357	180
19	469	473	180
21	94	87	180
23	251	265	180
25	198	207	0
29	60	37	180
31	101	98	180
** K=	4	L=	4 **
-28	140	134	180
-26	159	145	180
-24	350	350	180
-22	253	244	0
-18	102	112	180
-16	363	360	180
-14	151	146	180
-12	80	82	0
-10	48	40	0
-8	333	318	0
-6	174	169	180
-4	362	337	0
-2	469	453	180
2	49	55	180
4	501	502	0
6	171	172	0
8	68	55	180
10	249	255	180
12	96	108	180
14	536	541	0
18	166	168	0
20	148	170	180
22	84	87	0
** K=	5	L=	4 **
-23	82	9	0
-21	144	139	180
-19	168	177	0
-17	195	199	0
-15	79	100	0
-13	325	319	180
-11	94	90	0
-9	114	135	0
-7	375	386	0
-3	55	80	180
-1	463	462	180

H	/FO/	/FC/	PHI
1	414	429	180
3	210	232	0
5	330	347	180
7	227	218	0
9	173	187	180
13	251	242	180
15	108	123	0
17	174	183	0
19	77	88	180
23	164	171	180

** K= 6 L= 4 **

H	/FO/	/FC/	PHI
-20	57	40	180
-16	54	35	180
-14	206	198	0
-12	222	228	180
-10	170	172	0
-8	196	196	180
-6	255	256	180
-4	176	170	180
-2	250	252	180
0	109	113	0
2	128	126	0
4	234	238	180
6	176	176	0
10	412	433	0
12	233	245	0
18	168	170	180
22	66	50	180

** K= 7 L= 4 **

H	/FO/	/FC/	PHI
-17	91	82	0
-15	193	198	180
-13	212	225	0
-7	243	250	0
-5	168	161	180
1	176	180	180
17	80	83	180

** K= 8 L= 4 **

H	/FO/	/FC/	PHI
-8	196	194	0
-6	95	86	0
-4	106	125	0
-2	92	99	180
0	72	67	180
2	176	155	0
6	154	146	0
10	117	105	180

** K= 1 L= 5 **

H	/FO/	/FC/	PHI
-33	62	7	180
-31	85	73	0
-29	158	153	0
-23	187	197	180
-21	132	176	0
-19	416	394	180
-17	376	368	180
-15	344	331	180
-13	118	107	180
-11	701	712	0
-7	476	465	0
-5	371	362	180
-1	493	484	0
1	176	177	0
3	192	180	180
5	1321	1312	0
7	524	516	180
11	326	315	180
13	76	52	180
15	147	147	0
19	115	118	0
21	498	489	180
23	76	79	0
25	218	221	0
27	123	119	180

** K= 2 L= 5 **

H	/FO/	/FC/	PHI
-32	247	247	0
-30	124	136	180
-28	164	169	180
-26	144	144	180
-24	140	139	0
-22	56	39	180
-20	188	191	180
-18	119	106	180
-16	119	116	180
-14	272	255	0
-12	648	629	0
-10	545	557	180
-8	363	361	180
-6	97	89	0
-4	95	80	180
-2	66	70	0
0	178	178	180
2	70	70	0
4	337	337	0
6	599	620	0
8	316	336	0
12	289	311	0
14	373	388	180
16	200	200	180
18	216	225	180
20	336	345	180
22	436	468	0
24	258	263	180
26	110	111	0
28	63	63	180

** K= 3 L= 5 **

H	/FO/	/FC/	PHI
-31	107	103	0
-27	77	78	180
-25	169	153	0
-23	315	305	180
-21	67	66	0
-19	317	314	0
-15	124	134	0
-13	215	202	0
-11	331	318	180
-9	80	91	0
-5	528	522	180
-3	624	638	0
-1	252	262	180
1	56	62	180
3	195	209	0
5	442	445	180
7	400	425	0
13	124	133	180
15	185	199	180
17	90	72	0
19	68	88	180
21	82	93	0
23	225	235	0
25	141	147	180

** K= 4 L= 5 **

H	/FO/	/FC/	PHI
-26	197	184	0
-24	292	284	180
-22	504	496	0
-20	229	217	180
-16	78	87	0
-14	125	131	180
-12	50	57	0
-10	134	130	180
-8	64	55	0
-4	257	267	180
-2	591	580	0
2	360	365	180
6	463	465	180
8	226	235	180
10	87	88	0
12	194	200	180
14	229	250	180
16	340	360	0
18	220	214	0
20	287	282	0
22	88	78	0
24	137	128	180
26	78	71	0
28	66	34	0

** K= 5 L= 5 **

H	/FO/	/FC/	PHI
-27	67	68	180
-23	134	147	0
-21	91	96	0
-19	152	156	0
-17	139	150	0
-15	176	192	0
-13	131	133	180
-11	48	56	0
-9	86	94	180
-7	128	132	180
-5	81	80	0
-3	461	455	180
-1	197	186	0
1	62	77	0
3	360	376	0
5	345	347	180
7	75	74	180
9	192	199	180
13	241	252	0
15	91	65	180
17	116	128	180
19	71	82	0
25	93	77	0

** K= 6 L= 5 **

H	/FO/	/FC/	PHI
-20	60	54	180
-14	126	138	180
-12	253	266	0
-10	121	113	180
-8	221	219	180
-6	271	280	180
-4	152	150	0
-2	68	34	0
0	125	119	0
2	313	312	0
4	532	531	180
6	207	213	0
8	298	313	0
10	183	172	180
12	62	49	0
14	108	116	180
16	94	98	180
18	163	156	0

** K= 7 L= 5 **

H	/FO/	/FC/	PHI
-17	90	83	0
-15	97	87	180
-7	92	94	0
-3	221	213	0
1	102	90	0
5	128	130	0
7	62	55	180
11	107	107	180
15	168	163	180

** K= 8 L= 5 **

H	/FO/	/FC/	PHI
-8	176	167	180
-6	62	67	180
-2	133	129	0
0	60	57	180
4	109	118	0
8	90	99	0

** K= 0 L= 6 **

H	/FO/	/FC/	PHI
-32	72	72	0
-30	203	225	0
-24	222	225	0
-22	242	226	180
-20	620	593	0
-18	300	284	180
-16	177	173	180
-12	97	103	180
-10	103	104	180
-8	76	86	180
-6	470	445	0
-4	245	254	180
-2	1236	1227	0
0	576	593	0
2	383	372	180
4	94	80	0
6	580	568	180
8	376	352	0
10	346	356	0
12	256	246	180
14	157	165	0
16	865	830	180
18	521	533	0
20	82	66	180
22	99	108	0
24	123	121	180
26	375	365	180
30	117	108	180

** K= 1 L= 6 **

H	/FO/	/FC/	PHI
-29	149	149	180
-27	208	202	180
-25	157	156	180
-23	66	53	0
-21	127	118	0
-19	196	206	180
-17	135	137	180
-15	181	173	180
-13	156	155	180
-11	452	440	0
-9	851	824	180
-7	507	485	180
-5	310	308	180
-3	139	120	180
-1	54	67	180
1	57	55	180
3	66	74	180
5	374	364	0
7	519	491	0
9	113	108	180
11	260	242	0
15	160	163	0
17	159	156	0
19	202	204	180
21	85	87	180
23	140	138	0

** K= 2 L= 6 **

H	/FO/	/FC/	PHI
-28	221	207	180
-26	183	183	180
-24	188	185	0

H	/FO/	/FC/	PHI
-22	216	217	0
-20	51	32	0
-18	254	257	0
-16	111	93	0
-14	257	244	0
-12	774	758	0
-10	726	713	0
-8	287	283	180
-6	409	405	180
-4	631	617	180
-2	107	115	180
0	684	680	0
2	268	278	0
4	169	145	0
6	793	739	180
8	319	295	0
12	153	164	0
14	165	163	180
16	450	430	180
18	180	194	180
22	119	111	0
24	142	152	0

** K= 3 L= 6 **

H	/FO/	/FC/	PHI
-31	100	94	180
-27	88	97	0
-25	156	151	0
-23	305	306	180
-21	102	108	180
-19	228	235	180
-17	171	178	0
-15	135	136	0
-13	141	133	0
-11	339	326	180
-7	134	142	180
-5	103	117	180
-3	329	315	180
-1	230	234	0
1	282	279	0
3	107	116	180
5	287	286	180
13	160	158	180
15	443	473	180
19	324	305	0
21	287	291	0
23	113	110	0
25	77	93	0
27	139	129	0
29	114	93	0

** K= 4 L= 6 **

H	/FO/	/FC/	PHI
-28	101	102	180
-24	165	176	180
-22	268	268	0
-20	304	307	0
-18	56	66	180
-16	141	148	0
-14	248	236	0
-12	136	138	0
-10	331	329	0
-6	305	299	180
-4	140	141	180
-2	93	91	0
0	75	75	180
2	84	89	0
4	236	250	0
6	52	36	180
8	178	175	0
12	208	201	180
14	261	283	180
16	62	34	180
18	199	201	180
20	115	117	0
22	135	124	0
26	65	64	180

** K= 5 L= 6 **

H	/FO/	/FC/	PHI
-25	144	139	180
-23	83	86	0
-21	110	106	180
-17	159	169	180
-13	154	168	180
-11	99	90	180
-9	56	49	0
-7	257	263	180
-5	344	345	180
1	98	105	180
3	458	471	0
7	230	213	180
9	493	524	0
11	78	84	180
15	187	182	0
17	89	114	180
19	68	60	180

** K= 6 L= 6 **

H	/FO/	/FC/	PHI
-22	85	71	0
-18	111	123	180
-12	187	189	0
-10	189	187	180
-6	145	134	180
-4	259	258	0
-2	230	227	0
0	156	154	0
2	270	271	0
4	514	506	180
6	331	344	0
8	388	381	180
10	172	177	0
12	74	74	0
14	60	74	180
18	171	160	180

** K= 7 L= 6 **

H	/FO/	/FC/	PHI
-17	217	226	180
-15	76	74	180
-13	84	93	0
-9	98	103	180
-7	127	131	180
-3	65	74	180
-1	114	108	0
3	87	83	180
5	67	67	0
7	136	128	0
11	91	74	180
13	203	191	0

** K= 8 L= 6 **

H	/FO/	/FC/	PHI
-2	206	194	180
0	73	45	0

** K= 1 L= 7 **

H	/FO/	/FC/	PHI
-31	128	116	180
-29	181	184	180
-27	66	68	180
-23	75	83	180
-21	183	190	0
-19	145	152	0
-17	297	305	180
-13	132	118	0
-11	247	234	180
-9	1631	1635	0
-7	169	159	180
-5	381	376	180
-3	272	253	180
-1	181	184	180
1	257	254	0
3	58	65	180
5	96	89	0
7	612	621	180
9	79	80	180
11	402	409	0
15	96	117	180
17	485	481	0
19	591	592	180
23	150	165	180
27	106	100	0
29	122	119	0

** K= 2 L= 7 **

H	/FO/	/FC/	PHI
-28	147	142	180
-26	267	266	0
-24	103	93	0
-22	100	104	180
-20	81	76	180
-18	70	53	180
-16	230	236	0
-14	301	288	180
-12	350	351	0
-10	947	937	180
-8	683	662	0
-6	780	775	0
-4	184	178	0
-2	525	515	0
0	435	439	180
2	271	276	180
4	76	81	0
6	259	270	180
8	55	52	180
10	113	118	0
12	200	212	180
14	111	119	180
18	129	129	180
20	203	213	0
22	50	59	0
24	110	132	180
26	98	89	180
28	171	156	0

** K= 3 L= 7 **

H	/FO/	/FC/	PHI
-29	85	75	180
-27	302	316	0
-23	74	74	180
-21	219	228	180
-19	94	104	0
-17	158	168	0
-15	153	146	180
-11	244	228	180
-9	202	210	180
-7	100	101	0
-5	172	168	0
-1	176	165	0
1	57	60	180
3	137	140	180
5	287	289	180
7	225	221	0
11	54	58	180
13	174	183	0
15	141	169	180
17	112	117	0

** K= 4 L= 7 **

H	/FO/	/FC/	PHI
-26	79	73	180
-22	219	223	0
-14	62	69	0
-12	132	132	0
-10	67	77	0
-8	211	202	180
-6	277	272	180
-4	286	290	180
-2	142	151	0
0	74	85	180
2	117	128	0
6	233	246	0
8	114	106	180
10	77	29	0
12	209	214	0
16	197	211	0
18	111	115	0
20	211	204	180

** K= 5 L= 7 **

H	/FO/	/FC/	PHI
-25	65	46	180
-13	260	273	180
-11	256	246	180
-9	143	142	180
-7	64	80	0
-5	75	67	0
-3	283	286	0
-1	439	457	180
1	127	138	0
3	152	167	0
7	242	239	0
9	512	529	180
11	66	34	0
13	157	156	180
15	269	277	0
21	112	97	0

** K= 6 L= 7 **

H	/FO/	/FC/	PHI
-20	141	139	180
-18	141	145	0
-14	60	66	180
-12	72	76	0
-10	91	95	180
-8	77	86	180
-6	137	143	0
-4	175	171	0
-2	204	206	0
0	50	28	0
2	113	102	180
6	163	161	180
8	338	339	0
10	206	214	180
12	224	232	180
18	146	140	0

** K= 7 L= 7 **

H	/FO/	/FC/	PHI
-9	56	42	0
-7	88	90	0
-5	61	50	180
-1	85	90	180
5	93	81	180
7	159	162	180
13	170	166	0

** K= 0 L= 8 **

H	/FO/	/FC/	PHI
-30	101	110	180
-28	233	233	180
-24	88	99	180
-22	205	208	180
-20	198	201	180
-18	204	200	0
-16	175	167	0
-12	104	102	0
-10	763	752	180
-8	184	186	0

H	/FO/	/FC/	PHI
-6	151	143	180
-4	172	135	0
-2	433	420	180
0	1072	1063	0
2	196	221	180
4	357	360	180
6	154	139	180
8	330	329	180
10	230	233	0
14	256	246	0
16	837	830	180
18	543	523	0
20	234	235	0
22	166	168	180
24	73	79	0
26	232	220	180
28	177	154	180

** K= 1 L= 6 **

H	/FO/	/FC/	PHI
-31	137	147	180
-25	167	178	0
-17	347	350	0
-15	223	228	0
-13	371	360	180
-11	291	288	0
-9	847	819	180
-7	571	538	0
-5	643	625	0
-3	319	302	0
-1	504	484	0
1	241	240	180
3	338	344	0
5	93	94	0
7	313	319	0
9	453	450	180
11	462	454	180
13	113	101	180
15	229	219	180
17	550	531	0
19	167	159	180
23	91	87	180
25	88	86	180

** K= 2 L= 8 **

H	/FO/	/FC/	PHI
-30	87	96	0
-28	85	91	180
-26	115	125	0
-24	113	110	0
-22	117	107	0
-20	57	54	0
-18	96	98	180
-16	205	205	180
-14	125	124	180
-12	360	359	180
-10	108	127	180
-8	273	253	180
-6	337	329	180
-4	94	82	0
-2	198	203	0
0	534	504	180
2	216	197	0
6	172	166	180
8	145	122	0
10	193	197	180
12	123	119	180
16	307	312	0
18	135	124	0
20	65	46	180
22	124	141	0
26	87	82	180
28	238	214	0

** K= 3 L= 8 **

H	/FO/	/FC/	PHI
-29	184	203	180
-27	305	300	0
-21	90	89	0
-19	75	83	180
-17	123	114	0
-15	226	229	0
-13	352	353	0
-11	222	215	180
-9	53	62	0
-7	49	28	0
-1	64	72	0
1	489	466	180
5	75	86	0
9	239	243	0
13	97	100	0
15	249	251	0
17	84	82	180
21	143	144	180

** K= 4 L= 8 **

H	/FO/	/FC/	PHI
-20	120	115	0
-18	188	188	180
-16	64	61	180
-14	97	104	180
-12	169	163	180
-8	488	493	180
-6	182	184	0
-4	59	65	180
-2	317	319	0
0	262	255	180
2	275	278	180
8	231	226	0
10	152	154	180
12	63	75	180
14	107	124	180
16	188	199	0
18	100	107	180
20	212	198	0

** K= 5 L= 8 **

H	/FO/	/FC/	PHI
-21	67	54	180
-19	62	48	0
-17	204	197	0
-15	85	77	0
-11	280	288	180
-9	231	237	0
-5	315	317	0
-3	465	466	0
-1	331	330	180
1	399	415	0
5	90	103	0
11	266	263	180
13	190	189	180
19	133	138	0
21	74	52	180

** K= 6 L= 8 **

H	/FO/	/FC/	PHI
-18	94	87	180
-16	107	118	0
-12	106	103	0
-10	125	119	180
-4	119	131	180
0	134	126	0
6	163	168	180
8	109	112	180
12	90	95	0

** K= 7 L= 8 **

H	/FO/	/FC/	PHI
-13	100	99	0
-11	69	58	180
-9	53	46	0
-3	141	133	0
-1	122	109	0
3	73	68	180
5	66	77	0
9	71	51	180

** K= 1 L= 9 **

H	/FO/	/FC/	PHI
-27	164	212	0
-23	159	170	180
-21	54	44	0
-13	52	52	0
-9	215	219	0
-5	99	96	180
-3	63	61	180
-1	53	60	0
1	271	263	0
3	160	165	180
7	160	150	180
9	58	67	180
11	302	323	0
17	86	103	0
19	348	345	180
21	73	74	0

** K= 4 L= 9 **

H	/FO/	/FC/	PHI
-24	148	156	0
-20	89	85	180
-18	33	36	180
-16	116	119	180
-12	72	71	180
-10	121	125	180
-8	264	262	0
-6	140	136	180
-4	134	122	180
-2	441	443	0
0	195	200	180
2	151	165	0
4	132	140	0
6	98	91	180
8	66	55	0
10	190	201	0
12	135	155	180
14	151	162	180
16	121	121	180
22	68	46	180

** K= 5 L= 9 **

H	/FO/	/FC/	PHI
-19	134	130	180
-17	170	168	0
-15	155	149	180
-11	107	96	0
-9	115	107	0
-7	400	396	0
-1	547	528	180
1	227	231	0
5	82	68	0
7	161	153	0
9	123	128	180
11	131	131	0
13	143	151	0
17	102	105	180

** K= 6 L= 9 **

H	/FO/	/FC/	PHI
-16	61	68	180
-12	71	61	0
-10	203	200	0
-8	99	98	180
-2	283	274	180
0	151	155	0
4	303	301	180
8	120	108	0
12	90	91	0

** K= 7 L= 9 **

H	/FO/	/FC/	PHI
-7	75	81	180
-1	73	59	0
3	151	154	0
5	122	125	180

** K= 0 L= 10 **

H	/FO/	/FC/	PHI
-26	251	262	0
-24	174	160	180
-20	179	190	0
-16	146	151	0
-14	176	190	0
-10	170	173	180
-8	216	222	0
-6	94	104	180
-4	130	122	0
-2	163	153	0
0	173	175	0
2	91	84	0
4	285	287	180
6	128	130	0

H	/FO/	/FC/	PHI
10	186	176	180
12	634	627	0
14	683	671	180
16	56	47	0
18	72	84	180
22	350	326	0

** K= 1 L= 10 **

H	/FO/	/FC/	PHI
-17	137	136	0
-15	366	375	180
-13	73	61	0
-11	193	188	0
-9	180	171	0
-3	312	299	180
1	445	431	180
5	95	91	0
7	230	237	180
11	325	318	180
13	168	170	0
15	158	166	0
17	153	146	0
19	79	84	180
21	170	173	180
23	83	99	0

** K= 2 L= 10 **

H	/FO/	/FC/	PHI
-26	133	133	180
-22	108	116	0
-16	127	137	180
-14	522	536	180
-12	209	211	0
-10	325	328	0
-8	288	301	0
-6	312	311	0
-4	217	212	180
0	148	136	180
2	564	553	0
4	69	61	180
6	147	149	180
10	75	68	180
12	190	200	0
14	327	328	0
20	83	79	180
22	151	155	180

** K= 3 L= 10 **

H	/FO/	/FC/	PHI
-25	79	65	0
-21	121	110	180
-17	104	116	180
-15	184	196	0
-13	461	460	180
-11	387	400	180
-9	172	170	180
-7	176	173	0
-5	168	166	0
-3	63	47	180
3	60	52	0
5	73	82	180
9	109	145	180
11	193	205	0
15	122	121	180
23	117	113	180

** K= 4 L= 10 **

H	/FO/	/FC/	PHI
-20	74	74	0
-18	102	104	180
-16	112	93	180
-10	148	150	0
-8	244	236	0
-6	71	68	180
-4	131	133	0
-2	168	178	0
4	65	53	180
6	67	48	180
8	73	72	180
10	241	259	0
14	142	152	0
16	92	70	0
18	112	105	180
20	101	79	180

** K= 5 L= 10 **

H	/FO/	/FC/	PHI
-19	67	65	180
-15	93	90	180
-9	215	215	0
-7	108	91	0
-5	145	142	180
-1	351	341	180
1	137	142	180
3	155	164	0
5	224	254	180
7	142	143	180
15	176	185	0

** K= 6 L= 10 **

H	/FO/	/FC/	PHI
-14	86	79	0
-6	96	91	0
-2	115	110	180
0	245	246	0
2	275	272	180
4	324	325	0
6	116	109	180
8	80	62	0
10	84	50	180

** K= 1 L= 11 **

H	/FO/	/FC/	PHI
-23	147	149	180
-21	54	8	0
-19	105	107	180
-17	67	58	180
-15	149	160	0
-13	280	284	180
-7	162	167	0
-5	324	325	180
-3	82	85	180
-1	180	185	0
1	156	152	180
3	234	232	0
7	167	168	180
11	480	486	0
13	334	324	180
15	133	133	0
17	77	70	0
23	88	89	0

** K= 2 L= 11 **

H	/FO/	/FC/	PHI
-24	63	71	0
-20	102	127	180
-18	267	285	0
-16	368	366	180
-14	498	509	0
-12	251	255	180
-10	384	393	180
-8	73	70	180
-6	133	137	180
-4	80	80	0
0	58	52	180
4	246	255	0
6	169	169	0
8	119	120	0
14	84	78	180
16	73	68	180
20	61	77	0

H	/FO/	/FC/	PHI
22	123	116	0

** K= 3 L= 11 **

H	/FO/	/FC/	PHI
-23	69	48	180
-17	83	109	0
-15	65	76	180
-13	68	76	0
-11	106	111	0
-9	147	153	180
-7	152	149	0
-5	147	147	180
-3	103	118	180
1	212	199	0
3	68	72	180
7	61	56	0
9	169	164	180
11	94	105	0
13	101	106	180
15	67	47	0

** K= 4 L= 11 **

H	/FO/	/FC/	PHI
-18	139	141	180
-16	57	45	180
-14	87	93	0
-12	216	213	0
-10	170	161	0
-8	220	221	0
-6	315	304	180
-4	217	219	0
2	63	51	180
4	201	215	180
8	87	85	180
16	91	100	0

** K= 5 L= 11 **

H	/FO/	/FC/	PHI
-17	143	135	0
-9	54	20	180
-7	80	108	180
-5	165	161	0
-1	98	104	180
1	76	75	180
3	134	129	180
5	152	154	0
9	116	112	0
11	156	161	180

** K= 6 L= 11 **

H	/FO/	/FC/	PHI
-10	88	97	180
-6	75	82	180
-2	75	76	0
0	64	61	180
2	106	115	0
4	218	203	180
6	158	153	0

** K= 0 L= 12 **

H	/FO/	/FC/	PHI
-24	112	111	0
-22	93	104	0
-20	217	232	180
-18	170	179	180
-16	72	81	180
-14	77	81	0
-12	170	166	0
-10	124	123	0
-8	162	156	180
-6	232	235	0
-4	608	613	180
-2	59	65	0
0	75	80	180
2	60	75	0
4	270	267	180
6	358	353	180
8	250	253	0
10	310	305	180
12	942	911	0
14	240	228	180
16	248	239	180

** K= 1 L= 12 **

H	/FO/	/FC/	PHI
-21	96	110	180
-19	123	127	180
-17	164	180	0
-15	226	234	180
-13	298	297	0
-5	77	77	180
-3	58	65	0
-1	128	124	180
1	61	64	0
3	87	98	180
5	164	174	0
7	233	226	0
9	137	132	0
11	133	127	0
13	91	103	180
15	92	97	0

H	/FO/	/FC/	PHI
17	97	97	180

** K= 2 L= 12 **

H	/FO/	/FC/	PHI
-20	148	144	0
-16	98	109	0
-14	76	87	180
-12	115	125	0
-10	166	166	0
-8	108	116	180
-6	121	118	180
-2	76	77	180
2	66	66	180
6	62	66	0
10	97	116	0
12	173	171	180
14	237	245	180

** K= 3 L= 12 **

H	/FO/	/FC/	PHI
-21	106	87	180
-19	63	75	180
-17	208	221	180
-15	145	168	0
-13	121	98	0
-11	105	108	0
-7	288	291	0
-5	189	179	180
-3	285	271	0
-1	119	104	0
1	99	91	180
3	113	110	0
5	86	94	180
13	64	73	0
17	85	72	0

** K= 4 L= 12 **

H	/FO/	/FC/	PHI
-16	79	78	180
-14	62	25	0
-12	275	267	0
-10	80	66	180
-8	79	78	0
-6	451	435	180
-2	139	140	0
4	161	160	180
10	83	92	0
12	160	175	180
14	121	128	0

H	/FO/	/FC/	PHI
** K=	5	L= 12	**
-13	131	134	180
-11	91	94	0
-7	268	249	180
-5	263	252	0
-3	207	202	180
3	122	124	0
7	146	147	0
9	107	112	0
** K=	1	L= 13	**
-21	181	190	180
-19	75	73	0
-17	83	82	0
-15	112	119	0
-9	74	67	180
-5	161	169	180
-3	177	183	0
-1	65	64	0
3	59	62	180
5	83	81	0
9	107	106	0
11	96	93	0
13	203	207	180
15	77	64	180
17	171	167	180
** K=	2	L= 13	**
-20	75	80	0
-18	97	97	180
-16	208	223	180
-14	87	89	0
-12	63	61	0
-10	71	43	0
-6	86	76	0
-4	106	109	0
-2	90	70	0
4	79	84	180
6	217	217	0
8	94	90	180
10	132	127	180
12	65	65	180
** K=	3	L= 13	**
-15	73	82	180
-11	75	96	180
-9	67	64	0
-7	130	127	0
-3	203	196	180
-1	71	64	0
5	174	171	0
7	148	148	180
9	81	76	180
11	66	81	0
13	167	167	180
** K=	4	L= 13	**
-14	151	144	0
-12	82	79	180
-10	181	188	180
-8	79	81	0
-6	357	346	180
-4	113	129	0
0	100	89	180
8	59	41	0
** K=	5	L= 13	**
-5	233	233	0
-3	128	109	180
** K=	0	L= 14	**
-16	89	83	0
-10	126	123	180
-8	179	185	180
-6	99	106	0
-4	182	174	180
-2	86	99	0
0	215	220	0
2	122	115	180
4	115	107	0
6	306	306	0
8	260	241	180
10	301	303	0
** K=	1	L= 14	**
-17	65	57	0
-15	59	75	180
-13	65	63	0
-9	71	73	180
-7	91	90	0
-5	67	64	180
-3	190	182	0
3	113	110	0
5	139	131	180
7	267	264	0
9	220	215	180
11	78	85	180
13	95	82	180
** K=	2	L= 14	**
-14	95	97	180
-4	153	155	0
-2	161	162	180
2	102	109	0
8	112	90	0
10	132	113	180
** K=	3	L= 14	**
-13	106	116	0
-11	188	179	180
-9	136	142	180
-1	222	207	180
1	81	66	180
3	68	51	180
5	181	177	0
** K=	4	L= 14	**
-6	124	124	180
-2	104	88	0
** K=	1	L= 15	**
-11	97	92	180
-9	181	190	0
-5	62	58	180
1	85	84	0
3	78	79	180
5	111	114	0
7	482	475	180
9	80	79	0
** K=	2	L= 15	**
-10	103	89	180
-6	69	63	0
0	134	132	180
2	78	78	180
4	97	94	180
6	117	118	0
** K=	0	L= 16	**
-4	78	80	0
-2	84	65	180

Chapter 5

The Crystal Structure of 1,2-bis(1-hydro-4-pyridinio) ethane (7,7,8,8,tetracyanoquinodimethamide)$_4$, DHPA^{2+}(TCNQ)$_4^{2-}$

5.1 Experimental

This compound, which was grown from 5% aqueous acetonitrile solution by electrocrystallisation (see also Chapter 6), formed thin (ca. 0.1 mm) black plate-like crystals at the edges of a rectangular Pt electrode of approximately 1 cm^2 surface area. A suitable crystal was selected and mounted upon a glass fibre using a minimum of rapid setting epoxy resin adhesive, and after mounting on a goniometer head and subsequent alignment of the crystal, an oscillation photograph (Cu Kα λ = 1.5418 Å) was taken on a Unicam camera. This showed that the crystal was mounted along the b-axis, since calculation of the appropriate cell dimension gave a value of approximately 3.85 Å, in close agreement with those values obtained for the highly conducting forms of DEPE(TCNQ)$_4$ [47] and DMPP(TCNQ)$_4$ [48] which are b = 3.84 Å and 3.87 Å respectively. The oscillation photograph also showed weak layer lines between the zero and first layer lines which corresponded to a cell dimension of ca. 11.85 Å, i.e. approximately three times that of the major cell.

Zero and first layer Weissenberg photographs of the major lattice layer lines showed that the cell, assumed on the basis of the similar structures mentioned earlier, was substantially correct and that the cell was monoclinic, $P_{2_1/C}$ from systematic absences.

An accurate orientation matrix was then obtained based on an indexing of 11 strong reflections for the major cell having $8^{\circ} \leqslant \theta \leqslant 11^{\circ}$. Intensity data for this cell were collected on the Hilger and Watts instrument using graphite monochromated Mo Kα (λ = 0.71026 Å) radiation. The intensity data were collected using a θ / 2 θ scan for $\theta \leqslant 20^{\circ}$ but due to the poor quality of the data no standard reflections were measured apart from those measured on re-starting data collection. Of 617 reflections collected, 525 were regarded as observed ($I > 2\sigma(I)$). Intensity data were corrected for Lorentz and polarisation factors, but not for absorption.

Following this initial data collection, intensity data were collected for the weak layer lines after first ascertaining that the reciprocal lattice points represented did, in fact, correspond to a cell whose b dimension was three times that of the major cell. These intensity data were not included in the present structure determination. However, should later workers find that the ca. 11.8 Å b cell dimension is more appropriate, it will only be necessary to re-index the present data set, and not the added intermediate layer lines, since these were indexed on the basis of this larger cell.

Crystal Data

DHPA $(TCNQ)_4$ $(C_{12}H_{14}N_2)^{2+}$ $(C_{12}H_4N_4)_4^{2-}$ M_r = 1002.2

Monoclinic, a = 12.894 Å, b = 3.933 Å, c = 27.580 Å, β = 109.95°

U = 1314.8 Å^3, Z = 1, D_c = 1.27 g.cm^{-3}

MoKα (λ = 0.71069 Å), μ = 0.88 cm^{-1}

Space group P_{2_1}/C (number 14)

5.2 Structure Determination and Refinement

The partial solution of the structure as reported here was on the basis of the Sharpened Patterson function, in which a strong vector at 0.594, 0.200, 0.144 was assigned as the A-A' TCNQ - TCNQ intermolecular vector thus giving a molecular centre at 0.297, 0.100, 0.072. The orientation of the TCNQ moiety was determined from the vector pattern around the origin (see Figure 5.1). Because it was only possible to collect data up to the h21 layer (i.e. the second layer, rotation about b) the y-coordinates of these vectors which were almost all either 0 or 0.5 are almost certainly bogus and so the tilt of the molecule with respect to the (010) plane was calculated by trigonometry to give a 3.2 Å perpendicular separation of TCNQ moieties from a 3.93 Å cell dimension. The TCNQ moiety was accordingly placed in this position and a series of structure factor calculations performed with the molecule being shifted in the y direction by increments of 0.05 b (i.e. 0.195 Å intervals). This showed that the original y coordinate of the molecular centre appeared to be the most correct.

In an attempt to verify the orientation of the TCNQ moiety a weighted reciprocal lattice plot, based on the observed integrated intensities, was made and compared with the Fourier transform for a flat TCNQ moiety (see Figure 5.2). This indicated that the orientation chosen was not inconsistent with the predicted transform, although the sparse data available did not enable a more definite conclusion to be reached.

With the TCNQ moiety in this position and orientation within the cell it would be necessary to have a cation centred at $z = \frac{1}{4}$. The

cation would therefore consist of two halves related by a 2_1 axis. The addition of $c/_4$ to every atom would cause the cation to lie across a centre of symmetry, which appears more likely, but would require the z - component of the A-A' vector in the Patterson function to have been half that of it's 'real' value. Re-examination of the Patterson function revealed a vector related by symmetry to x, z + $\frac{1}{2}$ for the old intermolecular vector and so structure factors were calculated on the basis of this trial structure. In order to eliminate effects due to any incorrect scaling the structure factor calculation was followed by an F_{obs}, rather than $F_{obs} - F_{calc}$, Fourier synthesis. However, this failed to reveal any indications of either an alternative orientation or position for the TCNQ moiety, or any fragments of the cation molecule. An F_{obs} Fourier synthesis on the original trial structure was equally unsuccessful in revealing a possible cation fragment.

At this stage in the structure determination it was decided to calculate structure factors on the basis of the coordinates of the TCNQ moiety which had led to the lowest R- value in the earlier trials. Instead of calculating structure factors after refinement it was decided to calculate them on the basis of the atomic coordinates as input, since on previous occasions refinement had led to extremely poor geometries for the symmetrical TCNQ.

The trial TCNQ structure at this stage had a conventional R = 0.41 and so constraints were applied to the geometry of the TCNQ moiety to maintain bond lengths and angles within values commensurate with those of the $TCNQ^{\frac{1}{2}-}$ moiety[7]. The planarity of the moiety was constrained by the addition of a dummy atom, with an occupancy of zero, at a position

within the cell corresponding to the centre of the TCNQ ring, and maintaining angles of 180° between symmetrically related atoms and the dummy atom. Four cycles of constrained isotropic refinement, followed by a difference Fourier Synthesis, revealed a possible cation ring fragment, which, when 4 of the peaks identified as possible atoms of the cation were included in the structure factor calculations, led to R = 0.40. However, on refinement this was reduced to R = 0.34, with two fairly strong peaks in the difference Fourier synthesis.

Close examination of the supposed cation fragment showed it to consist of two unrelated fragments which were, however, in the same general part of the asymmetric unit. After deletion of those 'atoms' which appeared to be least likely to be correct on the basis of their z coordinates a further difference Fourier synthesis failed to reproduce the deleted atoms and so it was assumed that the remaining five atom ring fragment was the more correct of the two.

If the present cation fragment is correctly placed about the 2_1 axis of the cell then there remains a further ring fragment to be found within the asymmetric unit in order to satisfy the requirements of the space group. Each fragment would have to possess an occupation parameter of 0.25 in order to fulfill the requirements of the cell volume as well. Figures 5.3a and 5.3b show projections of the cell along the a and b axes respectively, and Figure 5.4 shows the geometry of the cation fragment. Some of the atoms within this fragment possess temperature factors which are somewhat smaller than might be expected and it is possible that future investigations may enable this to be explained in terms of additional, as yet unaccounted for, electron density within

this area of the cell.

The structure at present may be described on average by a continuous stack of equally spaced TCNQ moieties with cations in disordered positions in channels between these stacks (on the 2_1 axis). The present conventional R = 0.28 is possibly significantly better than that obtained for DEPE $(TCNQ)_4$ (I) by Wallwork[47,49], whose final trial included all the atoms of the DEPE cation in calculated (though formally impossible) positions, as well as the use of layer scaling during structure factor calculation and refinement.

During previous work in this department Drew[2] measured powder compaction d.c. conductivities for both this compound, DHPA $(TCNQ)_4$, and the 1,2-bis(4-methyl-1-pyridinio)propane analogue and found them both to be highly conducting ($\sigma_{300} \sim 0.1 - 10$ ohm^{-1} cm^{-1}) semiconductors with low activation energies (E_a ca. 0.06 eV). These figures are consistent with the structures proposed, which both possess infinite stacks of TCNQ moieties. At the present moment work is in progress within this department to attempt to elucidate more fully the structures of the DHPA, DEPE, and DMPP highly conducting complexes. All three show weak intermediate layer lines, poor diffraction patterns and extreme difficulty in determining cation positions within the TCNQ lattice. It is likely that the complete solution of any one of these structures would enable the other two to be completely solved and to this end it is hoped that this present structure, that of DHPA $(TCNQ)_4$ (I) from electrocrystallised growth, will eventually yield a sufficiently credible structure.

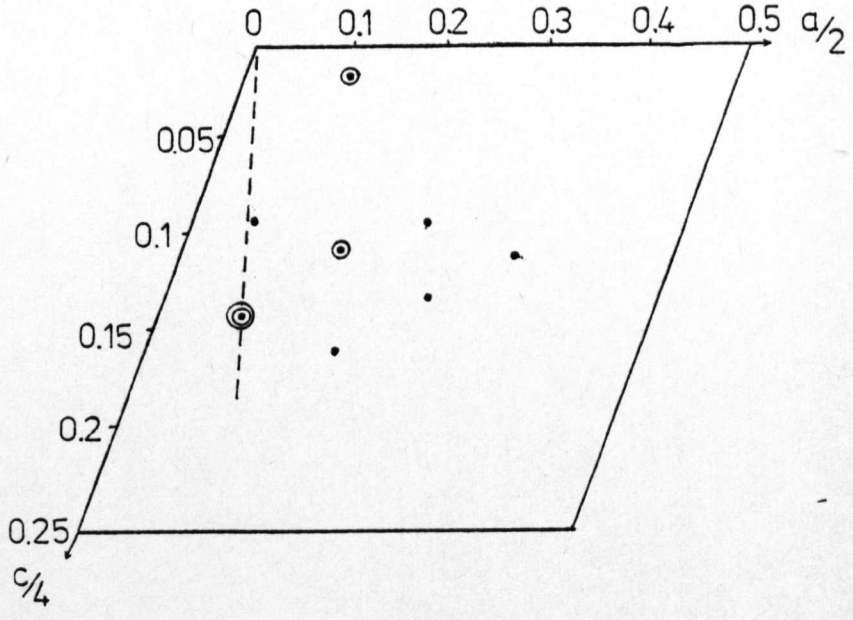

FIGURE 5.1

$\underline{DHPA(TCNQ)_2}$ Strong Sharpened Patterson vectors about the origin ($y = 0$ or $y = 0.5$)

TCNQ long axis shown -----

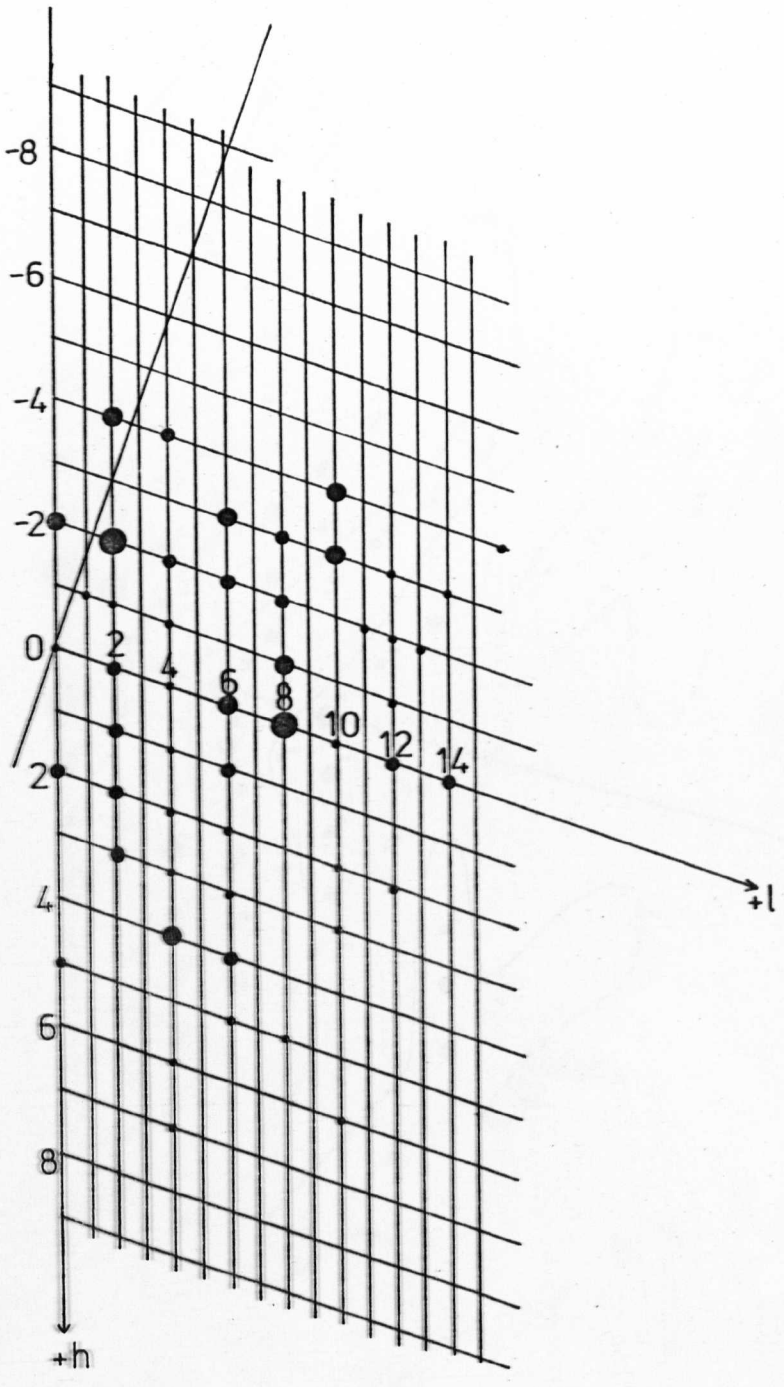
-8
-6
-4
-2
0
2
4
6
2
4
6
8
10
12
14
+l
+h

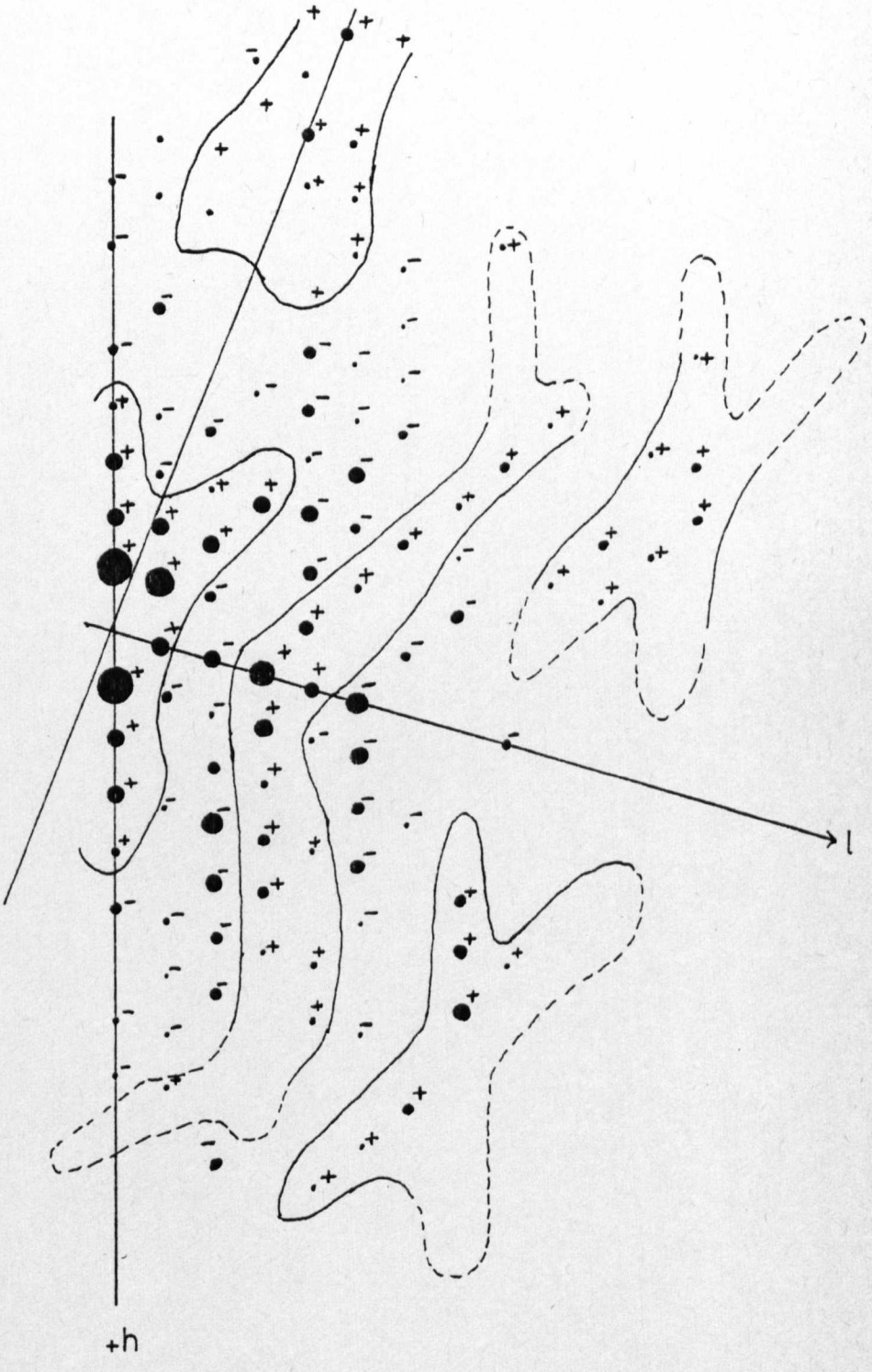

FIGURE 5.2

Fourier transform for flat TCNQ
(projected reciprocal lattice based on integrated intensity)

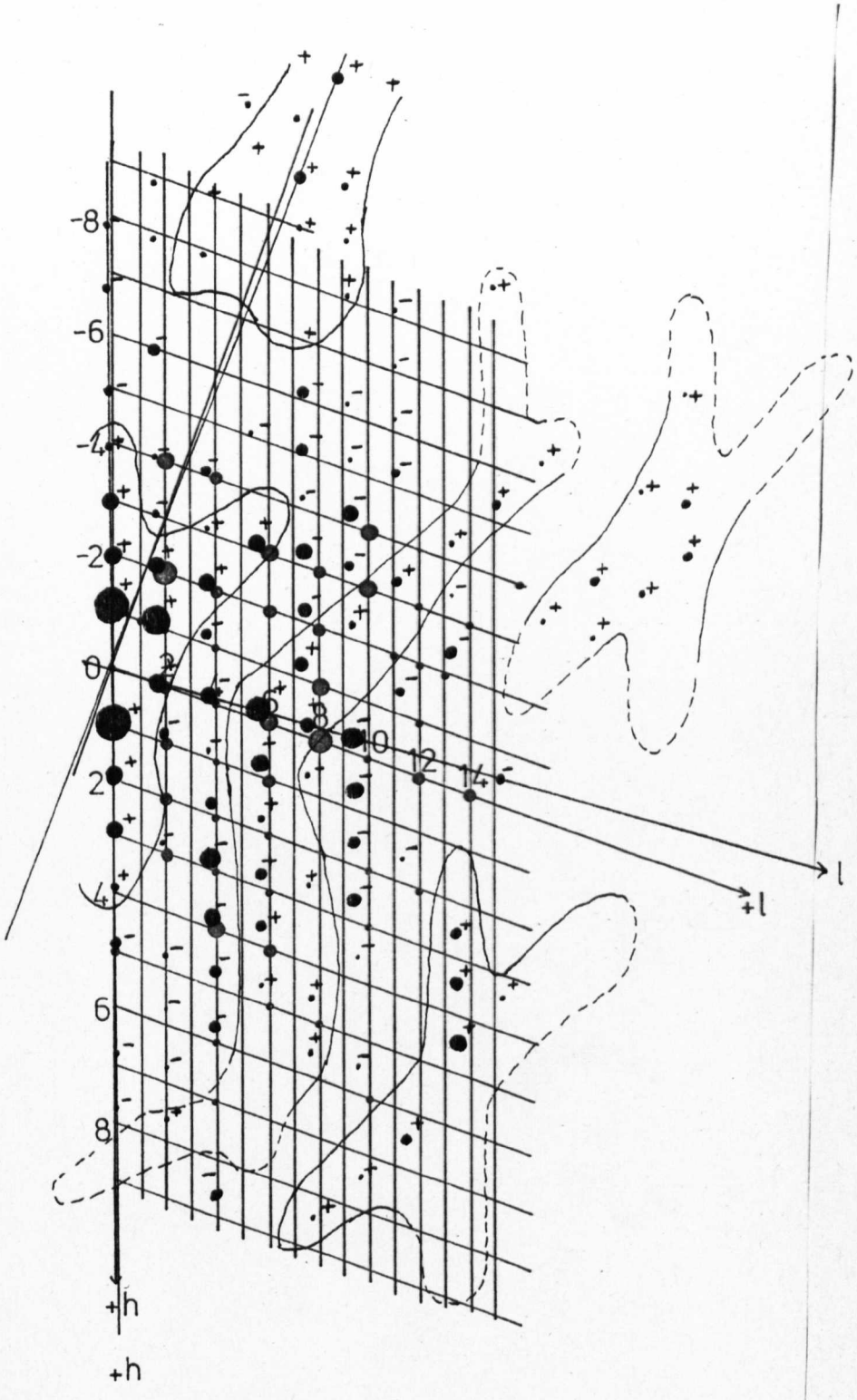

FIGURE 5.2

Fourier transform for flat TCNQ
(projected reciprocal lattice based on integrated intensity)

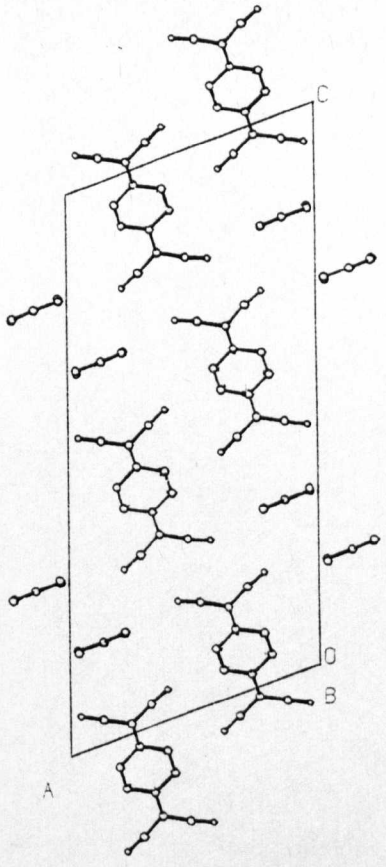

Projection along b

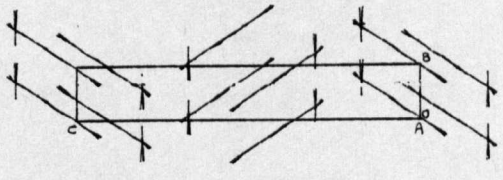

Projection along a

FIGURE 5.3a,b

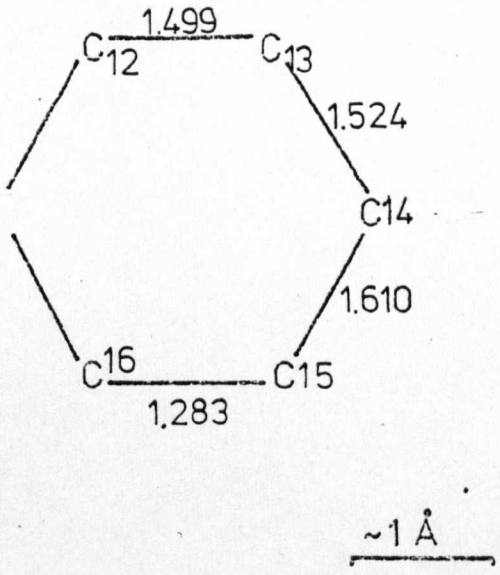

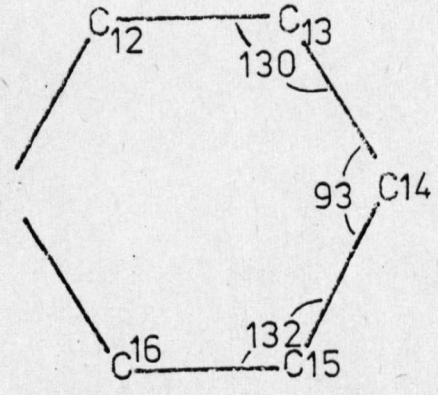

FIGURE 5.4

DHPA $(TCNQ)_4$ - cation geometry

ATOM	SERIAL	UISO	X	Y	Z
C	1	.036162	.333950	.313005	.117957
C	2	.031743	.415150	.201415	.096321
C	3	.040129	.386050	.005170	.053293
C	4	.015006	.273410	-.087215	.027071
C	5	.054240	.192902	.007503	.050123
C	6	.045398	.221136	.215018	.092427
C	7	.047461	.364272	.503729	.163139
C	8	.042022	.286078	.601338	.186831
C	9	.042992	.475413	.603699	.189790
C	10	.053081	.243370	-.287973	-.017435
C	11	.057028	.321912	-.409431	-.039789
C	12	.033166	.132170	-.390700	-.042914
N	1	.059799	.219714	.706562	.201473
N	2	.065398	.565037	.688412	.206531
N	3	.092308	.388406	-.501649	-.055680
N	4	.090132	.043463	-.482742	-.062784
C	15	.116660	.780417	.555632	.184332
C	12	.094394	.963016	-.057868	.178385
C	16	.076235	.776932	.937579	.185596
C	13	.146047	.965730	.515868	.182885
C	14	.111528	.866824	.294525	.182775

DHPA(TCNQ)4 - ATOMIC PARAMETERS

References to Chapters 2,3,4 and 5

1. S.C. Wallwork, Private Communication, (1976).
2. N.J. Drew, Ph.D. Thesis, University of Nottingham (1978).
3. International Tables for X-Ray Crystallography, Vol. IV, Kynoch Press, Birmingham (1974).
4. S.M. Rothstein, M.F. Richardson and W.D. Bell, Acta Cryst., (1978), A34, 969.
5. V. Shoemaker and K. Trueblood, Acta Cryst. (1968), B24, 63.
6. R. Long, R. Sparks and K. Trueblood, Acta Cryst. (1965), 18, 932.
7. G.J. Ashwell and S.C. Wallwork, Acta Cryst., (1979), B35, 1648.
8. D. Chasseau and S. Flandrois, Acta Cryst. (1977), B33, 2744.
9. R. Lalancette, W. Furey, J. Costanzo, P. Hemmes, and F. Jordan, Acta Cryst. (1978), B34, 2950.
10. G.J. Ashwell, D.D. Eley, N.J. Drew, S.C. Wallwork and M.R. Willis, Acta Cryst. (1977), B33, 2598.
11. J.H. Russell and S.C. Wallwork, Acta Cryst. (1972), B28, 1527.
12. C.K. Prout and P. Murray-Rust, J. Chem. Soc. (A), (1969), 1520.
13. M.M. Borel, A. Geffrouais, and M. Ledesert, Acta Cryst. (1977), B33, 571.
14. M. Meester and K. Olie, Cryst. Struct. Comm. (1975), 4, 725.
15. G.J. Ashwell, V. Bartlett, J.K. Davies, D.D. Eley, S.C. Wallwork, et al, Acta Cryst. (1977), B33, 2602.
16. J.H. Russell and S.C. Wallwork, Acta Cryst. (1971), B27, 2473.
17. L. Pauling, 'The Nature of the Chemical Bond, (3rd Ed. 1960).
18. A. Bosch and B. van Bodegom, Acta Cryst. (1977), B33, 3013.

19. H. Morssink and B. van Bodegom, Acta Cryst (1979), B35.

20. P. Kamminga and B. van Bodegom, Ph.D. Thesis, University of Groningen, (1979).

21. A. Hoekstras, T. Spoelder and A. Voss, Acta Cryst (1972), B28, 14.

22. G.J. Ashwell, D.D. Eley, R.J. Fleming, S.C. Wallwork and M.R. Willis, Acta Cryst. (1976), B32, 2948.

23. T. Sundaresan and S.C. Wallwork, Acta Cryst. (1972), B28, 2474.

24. G.J. Ashwell, D.D. Eley, S.C. Wallwork, M.R. Willis, G.D. Welch and J. Woodward, Acta Cryst. (1977), B33, 2252.

25. M. Laing and G. Carr, J. Chem. Soc. (A), (1971), 1141.

26. L.J. Admiral and G. Gafner, Chem. Comm. (1968), 1221.

27. M. Laing and E. Horsfield, Chem. Comm. (1968), 735.

28. M. Laing and G. Carr, Acta Cryst. (1975), B31, 2683.

29. L.R. Melby, R.J. Hardler, W.R. Hertler, W. Mahler, R.E. Benson and W.E. Mochel, J. Am. Chem. Soc. (1962), 84, 3374.

30. S.C. Wallwork, Acta Cryst. (1962), 15, 758.

31. Schroeder and Prince, Acta Cryst. (1976), B22, 3309.

32. G.C. Pimental and A.L. McClellan, 'The Hydrogen Bond', Reinhold, New York (1960).

33. B. Morosin, Acta Cryst. (1978), B34, 1905.

34. H. Kobayashi, F. Marumo and Y. Saito, Acta Cryst. (1971), B27, 373.

35. G.J. Ashwell, D.D. Eley, N.J. Drew, S.C. Wallwork and M.R. Willis, Acta Cryst. (1978), B34, 3608.

36. I. Blagborough, R. Blackshaw, T.J. Houghton and S.C. Wallwork To be published.

37. P. Goldstein, K. Seff and K.N. Trueblood, Acta Cryst. (1968), B24, 778.

38. 'Hydrogen Bonding in Solids', W.C. Hamilton and J.A. Ibers, Benjamin (New York), 1968 Review.

39. B. van Bodegom and Jan. L. de Boer; B. van Bodegom (Ph.D. Thesis) University of Groninger (1979).

40. T. Sundaresan and S.C. Wallwork, Acta Cryst. (1972), B28, 491.

41. G. Mihaly, K. Holczer and G. Grüner, Sol. Stat. Comm. (1976), 19, 1091.

42. Y. Iida, J. Phys. Chem. (1976), 80, 2944.

43. M. Murakami and S. Yoshimura, J. Phys. Soc. Jap. (1975), 38, 488.

44. D.R. Bates, Personal Communication.

45. M. Przyblski, A. Graja, A. Rajchel, M. Gawron and T. Borowaik, Acta Phys. Polonica (1979), A56, 67; M. Przyblski et al, Phys. Stat. Sol. (A) (1978), 50, K105.

46. M. Ahmed and L. Shields, J. Chem. Res. (1978), 12, 5523.

47. S.C. Wallwork, Private Communication.

48. G.J. Ashwell, Private Communication.

49. S.C. Wallwork, Organic and Biological Semiconductors Conf. (1980), Nottingham University.

50. P. Main, M.M. Woolfson and G. Germain (1978).

51. J.R. Carruthers and J.S. Rollett, Crystals suite of X-ray structure programs, Oxford University (1972).

Chapter 6 Experimental

6.1 Purification of Starting Materials and Preparation of Compounds Studied

6.11 Acetonitrile

The starting point in the purification of acetonitrile was from industrial grade material as supplied by Aldrich Chemicals (catalogue no. 11,008-6). This contains as main impurities water, aldehydes, and amines[1]. In particular high boiling organic impurities such as acetamide, butanedinitrile, dichlorobenzene, and others have been detected by gas chromatography and mass spectroscopy[2]. Originally in this work the drying techniques recommended by Riddick and Bunger[3] were used, where industrial grade acetonitrile was initially dried by repeated static drying over 'Drierite' (Anhydrous calcium sulphate, as supplied by W.A. Hammond and Co.), followed by repeated distillation over 'Drierite'. After this the solvent was repeatedly distilled off P_2O_5 until no further discolouration took place, when the solvent was finally distilled off anhydrous K_2CO_3 immediately prior to use. This latter stage was presumed to render the solvent neutral[4]. However, conductometric analysis and u.v./visible analysis showed that solvent prepared in this manner is only sufficiently pure and dry provided it is used immediately, and so a further method was sought.

The two essential features of pure acetonitrile in the context of this work are that it should be absolutely dry and neutral. Melby et al[5] have discussed the effects of water on TCNQ salts and have shown that in aqueous solutions $TCNQ^-$ dimerises to $(TCNQ^-)_2$, and also that these aqueous solutions undergo slow decomposition. Water is also thought to exchange with acetonitrile, viz:

$$CH_3CN + T_2O \underset{}{\overset{^-OH}{\rightleftharpoons}} CH_2TCN + HOT$$

in a base catalysed reaction[6], (where T is tritium, ^3H), and suitable acidic impurities can cause protonation viz:

$$2TCNQ^- + 2H^+ \longrightarrow TCNQ + TCNQ\,H_2$$

in almost quantitative yield[5,7,8]. Coleman et al[9] chose (as a final purification stage) to distil off gradient sublimed TCNQ, and showed by d.c. polarography that no impurity peaks existed up to 4.0V.

The purification technique finally chosen was that of Burfield et al[10]. Previous multistage drying and distillation over 'Drierite' was followed by repeated dynamic drying over 3A molecular sieve, a process which is claimed to yield super-dry (i.e. less than 1ppm H_2O content) solvent beyond the second drying stage (the water content being determined by Burfield et al by tritiated water activity measurements[6,10]).

The molecular sieve was activated by heating at 320°C for at least six hours, after which the activated desiccant was allowed to cool in a vacuum desiccator over P_2O_5 after purging with N_2 gas. This technique appeared to yield solvent of reproducible stability towards the salts studied. The final drying stages were normally performed by freeze distillation in a vacuum frame, and transfer of solvent to reaction or crystallisation vessel was by means of a nitrogen cover gas at a positive pressure (see figure 6.1).

As it appeared unlikely that Karl-Fischer titration[29,30] would be a sufficiently accurate measure of water content for the small quantities anticipated, a more suitable analytical technique was sought to determine this parameter of solvent purity. The technique finally chosen was a spectroscopic method based on the techniques of Barbetta and Edgell[11]. The absorbance of pure dry acetonitrile was obtained from transmittance information measured using a Perkin Elmer 157G infrared grating spectrometer at 3545 cm^{-1}, the position of the absorbance measurement being determined from a series of scanning spectra measured at differing added water contents. A typical series of spectra are shown in figure 6.2. A calibration graph of absorbance at 3545 cm^{-1} versus p.p.m. triply distilled water added (v/v) was obtained and is shown in figure 6.3. De-ionised water was distilled from leached pyrex glassware onto K_2CrO_3. From this it was distilled onto $KMnO_4$, and finally distilled into a silica vessel from which it was removed for use immediately.

The estimated baseline was obtained as the average of a number

of spectra measured for nominally 'dry' solvent batches, and may be taken to correspond to 'driest ever solvent' absorption. An independent check on the validity of the calibration was obtained by measurement of a series of spectra of CH_3CN + H_2O/D_2O mixture run against 'dry' acetonitrile as a solvent blank. By means of two variable path length infrared cells, one having windows of KBr and the other, reference cell, having windows of CsF, it was possible to obtain a baseline for identically dry CH_3CN in each cell which was reasonably linear. The spectra obtained for added amounts of HOD (see figure 6.4a) showed that the doublet in the CH_3CN/H_2O spectra at 3625 and 3660 cm^{-1} is due to solvent and/or non-aqueous impurities since the water peak in the blanked out spectra of CH_3CN/HOD is a singlet and has a maximum at approximately 3580 cm^{-1}. Thus the apparent increase in intensity of this doublet at 3625, 3660 cm^{-1} is in fact caused by the formation and increase in intensity of the nearby water peak and this supports the correctness of using the absorbance at 3545 cm^{-1} in the spectra of solvent samples run against air in the reference beam as a measure of water content.

The relationship between the absorption and added water content is confirmed by the close correlation between the increase in absorption due to water (ca. 3545 cm^{-1}) and that due to the deuterated form (ca. 2620 and 2700 cm^{-1}) as shown in figure 6.4b. The gradient obtained from the absorbance versus added H_2O/D_2O mixture at 3580 cm^{-1} (the observed maximum of this peak) is 0.017 up to 5 p.p.m. (v/v) added, in close agreement with the gradient measured (0.023) over the same range from a similar plot of absorbance at 3545 cm^{-1} versus added

pure H_2O. This also supports the assignment of this absorption to water present in the solvent. The wavelength (3545 cm^{-1}) determined by experiment in this work as the most appropriate at which to make absorption measurements was found to be in close agreement with that found by Barbetta and Edgell (w/cm^{-1} (CH_3CN) = 3547).

Solvent used for all re-crystallisation measurements was treated immediately prior to use with freshly activated 3A molecular sieve (8 hrs static drying) unless otherwise stated, and examined by i.r. spectroscopy to ensure consistency of drying from run to run within any particular solvent batch.

6.12 TCNQ

TCNQ as supplied commercially (Aldrich Chemicals, 99%) contains a number of impurities, of which the group I simple salts Na^+TCNQ^- and K^+ $TCNQ^-$, and the group VII halogens (notably bromine) are worthy of particular mention[12,13,14]. The TCNQ supplied was recrystallised once from triply dried and distilled (t.d.d.) acetonitrile with the addition of two to three drops of bromine to oxidise any $TCNQ^-$ impurities to TCNQ . This was followed by two further re-crystallisations from t.d.d. solvent under a N_2 cover gas, and gave well formed plates of orange crystalline material. All re-crystallisations were performed in pyrex glassware which had been previously leached with pure solvent and baked at 80°C before use. The material thus obtained was then placed in a gradient sublimator (see figure 6.5), flushed with N_2, and evacuated to typically ca.

5×10^{-6} torr. The tube was then heated to 130°C until sublimation was considered complete (typically, for a ca. 5g sample of TCNQ, this process took 48-68 hours), after which it was allowed to cool to ambient temperature whilst still under vacuum. Finally, the tube was flushed with nitrogen and removed from the apparatus and the orange/yellow material from the centre of the sublimed zone was removed for further sublimation. The process was usually repeated two further times and the resulting material was stored under nitrogen in a tightly closed vessel until immediately prior to use. Table 6.1 shows microanalysis figures for material after various stages in the treatment. Purity was also determined by visible/u.v. spectrometry (see also 6.4) and found to be as good as the technique will allow, with no detectable absorption at 842 nm, where $TCNQ^-$ would be the sole absorber if any were present[15]. Calculated values of ε^{o}_{395} were in excellent agreement with previously determined values obtained by other workers[e.g. 15, 22, 23].

6.13 Cations

The cations studied in this work were prepared as iodide salts from commercially available starting materials as supplied, and treated by multiple re-crystallisation before use in complex formation (see section 6.14).

6.14 Synthesis and analysis of the compounds studied

The two general methods used by the author of this work for

Table 6.1

Variation of composition of TCNQ with purification techniques as measured by microanalysis

	%C	%H	%N	
Calculated	70.59	1.96	27.45	△
Re-Crystallised twice	70.97	1.84	27.71	-0.52
Re-Crystallised twice + sublimed 1x	70.69	1.82	27.51	-0.02
Re-Crystallised 3x and sublimed 1x	70.66	1.72	27.07	0.55
As above + 1 extra gradient sublimation	70.62	1.84	27.46	0.08
As above, + 1 extra gradient sublimation	70.52	1.73	27.30	0.45

The last two sets of figures are probably a reflection of the accuracy of microanalysis. Typical errors in C, H, and N are approximately 0.3, 0.4, and 0.3% respectively.

$$\Delta = 100 - (\%C + \%H + \%N)\ \%$$

the preparation of the TCNQ salts studied were a) electrocrystallisation and b) standard solution chemistry organic synthesis. This section consists of the solution chemistry preparations; the electrochemical method is dealt with in detail in Section 6.5.

The general schematic route followed in the preparation of the salts studied was as follows: firstly, an appropriately quaternised cation salt was formed from suitable readily available precursors. The cation salt was then reacted in solution with a suitable source of $TCNQ^-$ and an appropriate concentration of $TCNQ^0$ for the stoichiometry of the salt required. The $TCNQ^-$ was usually either provided by the alkali metal simple salt $M^+ TCNQ^-$, or formed <u>in situ</u> by reduction of $TCNQ^0$ by I^- as the cation iodide[16]. This latter process is illustrated in the following example:

$$D^+ I^- + TCNQ^0 \longrightarrow D^+ + TCNQ^- + \tfrac{1}{2}I_2^0$$

$$2(\tfrac{1}{2}I_2^0) + D^+I^- \longrightarrow D^+I_3^-$$

Thus one advantage of the <u>in situ</u> formation of $TCNQ^-$ is that any free iodine is removed as I_3^-, thus decreasing the likelihood of free iodine being occluded in the crystal as an impurity. Another advantage of the method is that it is only possible to form a stoichiometric quantity of charged $TCNQ^-$ and so the stoichiometry of the product may be controlled by the amount of $TCNQ^0$ available in the reaction mixture. In the case of $DEPE^{2+} (TCNQ)_4^{2-}$, it has been reported by Ashwell[17,18] that the amount of water present in the reaction mixture can affect complex stoichiometry as well as

phase formation, yielding the so-called hemi-hydrated form, $DEPE^{2+}\ (TCNQ)_4{}^{2-}.H_2O_{0.88}$.

The general reaction scheme for the preparation of the quaternised pyridinium type cation salts studied in the work is based on

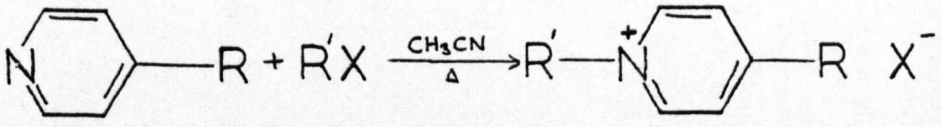

substituted pyridine

X = halogen, usually iodine

R-, R-' may be $-CH_3$, $-C_2H_5$, or another substituted pyridine, e.g. R = $-CH_2 - CH_2$ - py. The use of a polar solvent is normally preferred in order to step up the rate of reaction whilst retaining good dissolution of the starting materials.

6.15 Preparation of Cation Iodides

a) Preparation of 1,4-dimethylpyridiniumiodide, $DMPY^+I^-$

4-methylpyridine (ϒ-picoline, 9.0 cm^3) was thoroughly mixed with reagent grade ethanol (100 cm^3) and an excess of methyl iodide (14.0 cm^3) was added dropwise. After refluxing for 10 minutes the mixture was allowed to cool to ambient temperature, when large (ca. 4mm) plate-like yellow crystals were obtained. These were filtered from the mother liquor and re-crystallised twice from aqueous ethanol (80 : 20 v/v ethanol: water mixture).

	C	H	N	I
Calculated	35.71	4.26	5.96	54.03
Found	36.01	4.28	5.82	-

b) Preparation of 1,-methyl-4-ethylpyridinium iodide

4-ethyl pyridine (15 cm^3) was dissolved in reagent grade ethanol (100 cm^3) and an excess of methyl iodide (12 cm^3) was added dropwise. The colourless solution was refluxed for 20 minutes during which time it turned very pale yellow/green, and the solution was then cooled overnight in a dewar vessel from an initial temperature of 60°C. After six hours the solution was observed to have changed to an orange/brown colour, and after a further 162 hours at -1°C the solution was still orange/brown but no crystals were seen to have formed. Evaporation of solvent to 25 cm^3 using a rotary evaporator yielded pale yellow crystals which were filtered off and dissolved in triply distilled water. After three months pale cream plate-like crystals were obtained.

	C	H	N	I
Calculated	38.55	4.82	5.62	51.00
Found	38.59	4.57	5.65	-

(sample hygroscopic)

c) Preparation of 1,2-bis-(1-ethyl-4-pyridinio)ethene diiodide

1,2-bis-(4-pyridyl)ethene (3.1774g) was dissolved in triply

dried and distilled acetonitrile (200 cm^3) and ethyl iodide (32 cm^3, excess) was added dropwise. The mixture was refluxed for 2 hours, after which the solution was cooled from 60°C in a closed dewar vessel for 48 hours. Deep red, large (ca. 3mm) well-formed parallelepiped crystals were obtained which were filtered off and recrystallised twice further from triply dried and distilled acetonitrile

	C	H	N	I
Calculated	38.87	4.05	5.67	51.42
Found	38.46	4.38	5.54	51.07
(various batches)	38.90	4.32	5.58	51.36 *
	38.80	3.98	5.60	51.40 **

* well formed crystals after 1 recrystallisation from t.d.d. CH_3CN

** well formed crystals after 2 recrystallisations from t.d.d. CH_3CN

6.16 Preparation of TCNQ salts

The materials used were all purified in the manner discussed in the previous sections. Since only the cation iodides were used it was not necessary to use Li^+TCNQ^- as a source of $TCNQ^-$ [5,9,14] as discussed in 6.14; however, in those cases where both methods of preparation were undertaken, no significant differences were observed in crystal perfection or stoichiometry between the two methods.

The complex salts of DMPY, MEPY (which dimerised to form

DMPB), and DEPE were all prepared by dissolution of the appropriate quantity of pure $TCNQ^{o}$ in triply dried and distilled acetonitrile in the ratio required by the mechanism proposed by Coleman et al[16] of 3 cation iodide : 8 $TCNQ^{o}$. Dissolution was usually achieved by means of reflux, after which the yellow TCNQ solution was allowed to cool slightly before direct addition of solid cation salt. Reflux was then re-commenced and continued for a further 1-2 hours to ensure complete reaction, after which the solutions of the complex salts were allowed to cool in a Dewar vessel (initially at $60^{o}C$) for 48 hours. The crystals thus obtained were filtered and re-crystallised twice from t.d.d. acetonitrile before any subsequent usage.

The electro-crystallisation method of preparation of the simple salt of $DHPA^{2+}(TCNQ)_2^{2-}$ and of the highly conducting phase of the complex salt, $DHPA^{2+}(TCNQ)_4^{2-}$, is discussed fully in Section 6.5.

6.2 A/c Solution Conductivity measurements

6.21 Description of the temperature regulation apparatus

A schematic diagram of the apparatus used to control the bath temperature is shown in figure 6.6. The apparatus consists of an eighteen litre air-insulated rectangular water bath about which are sited one bath circulation pump, one fine temperature control cold sink pump, one combined 1KW heater and fluid dispersal pump unit, and one 8' x $\frac{1}{4}$" o.d. copper cooling coil, which is shaped in a 'multiple S' configuration see fig. 6.6 (insert) to provide an even cold sink for the entire bath. This coil is cooled by tap water

at between 5 and 7°C. The 1 kw heater is controlled by a synchronous motor driven mercury contact thermometer via the temperature programmer which is capable of giving up to six linear cooling rates varying from 6.8°C/hr to 0.8°/hr. Figure 6.7a shows the thermal stability and linearity of the various temperature programs. Simulation of Dewar cooling could also be performed using this apparatus by choice of a suitable cold sink temperature and figure 6.7b shows typical temperature versus time curves for simulated Dewar cooling. The linear temperature programmer is basically an electronically timed power relay with a variable-time-base duty cycle. Because of the nature of this device, the slow cooling rates (less than ca. 3°/hr) do show slight signs of the step nature of the mode of operation of the temperature program; however, at higher rates this effect is not observed, and in any case the deviation from true linearity was considered to be insignificant in terms of the experimental technique.

The crystallisation vessel was thermostated in the bath and the temperature of the solution determined by measurement of the bath temperature immediately adjacent to the vessel by means of a mercury thermometer. The stability of the bath temperature was found to be better than 0.1°C over the entire temperature range of the crystallisation process (typically 70°C - 20°C), although failure of any one bath circulation pump was capable of causing the stability of the bath to decrease to $\pm$ 0.1° and failure of two pumps to cause fluctuations of approximately $\pm$ 0.3°. The validity of the temperature measurement was confirmed by simultaneous measurement

during some of the crystallisation runs of the solution temperature directly by means of a 32 s.w.g. copper-constantan thermocouple enclosed in a one-piece Kel-F* protective sleeve and the bath temperature in the immediate vicinity of the cell by means of the Hg thermometer. The difference between the two measurements was found to be well within experimental error and in view of the experimental difficulties encountered in sealing the thermocouple in the cell in such a way as to form a vapour tight seal without the sealant perturbing the crystallising solution, it was considered that the measurement of the external temperature was sufficiently accurate for the purpose of these experiments.

6.22 Transfer of materials

Two methods were used for the transfer and dissolution of materials : during early work the apparatus shown in figure 6.8 was used. This consisted of a dissolution vessel into which a suitable weighed quantity of complex was previously introduced, a filtration link, and a crystallisation vessel from which the mother liquor could be removed without disturbing any crystalline material formed during the crystallisation process. All glassware was thoroughly cleaned using reagent grade acetone and baked at 85^{o}C for 2 hours prior to use. This apparatus proved unsuitable for determining conductance versus temperature curves for differing concentrations of complex in solution, and an alternative, simpler method was used in later work. In this second, later, technique, a round bottomed flask was

* 1,1,2-trifluoro-2-chloro-polyethylene

designed so as to minimise the amount of material required for each re-crystallisation. Weighed complex was added to this flask after purging with N_2 gas and a magnetic flea was placed in the flask. A reflux condenser, complete with drying tube, (self indicating silica gel was used as a drying agent) was connected to the flask and the flask was heated using a.water bath sited directly on a hot-plate magnetic stirrer. Dissolution was checked visually by means of a high intensity light source, as the solutions were strongly absorbing. All of the apparatus in contact with the solution or solvent vapours was thoroughly cleaned with 'analar' grade acetone and baked as before. This apparatus was also used to study crystallisation of product complex from a reaction directly. All of the glassware used in the two systems was manufactured from 'pyrex' glass.

6.23 Measurement of a/c conductance

The a.c. conductance of the solutions was measured across the platinum electrodes of the crystallisation vessel by means of a Wayne-Kerr B641 Autobalance Bridge, operating at 1592 Hz. A small degree of automatic range switching was made possible by the inclusion of a Leeds Northrop 'Speedomax' variable sensitivity chart recorder, to which was input a d.c. voltage corresponding directly to the moving coil meter reading on the conductance side of the Wayne-Kerr bridge. In this way, as the meter reading approached zero so the chart recorder pen carriage also approached the zero position, activating a reed switch which caused a mechanical

cam and push rod device, mounted upon an aluminium frame, to actuate the next range switch down. In this manner up to a maximum of three ranges could be measured directly on the chart recorder without operator intervention, although temperatures still had to be read manually. Temperature versus time graphs were plotted for all runs where it was not possible to make continuous temperature measurements and these enabled any intermediate temperatures to be determined. The apparatus is shown in plate 6.3.

6.24 Estimation of the phase ratio of the product

The ratio of the phases obtained under different crystallisation conditions was estimated visually and by means of powder sample X-ray diffractometry. Estimates of ratios obtained in this way are only semi-quantitative due to the effect of preferred orientation of crystallites on the intensity of the diffracted beam; however, the technique does show clearly those cases where mixed phases are present. The two diffractometer peaks most suitable for phase assignment were found to be the two intense ones at $2\theta = 27.2^{\circ}$ and $2\theta = 27.8^{\circ}$, where θ is the Bragg angle, these being due to DEPE $(TCNQ)_4$ phase I and phase II forms respectively.

6.3 D.C. Dark Conductivity Measurements

D.C. dark conductivity measurements were taken on a small number of selected crystals in order to determine whether a high or low conductivity phase had been obtained during crystallisation.

The cell used is shown in Fig. 6.9 and is based on the design of Drew[15]. Crystals were mounted on 33 s.w.g. insulated Copper wire by means of high conductivity silver paint (Acheson Electrodag 915) as shown in fig 6.10 , and the temperature of the crystal determined to within $\pm$ 0.8°C by means of a black-tipped copper-constantan thermocouple[19] mounted in close proximity to the crystal. Crystals were baked out within the cell at 85°C and ca. 5×10^{-6} torr for between 16 and 20 hours before conductivity measurements were commenced, the temperature being controlled by means of a 0.5 KW furnace into which the lower 15 cms of the cell fitted closely, and an Ether Digi thermostat set to 2% sensitivity. After bakeout, 4 cm Hg of helium gas (B.O.C. Research grade) was admitted to the cell in order to facilitate the attainment of thermal equilibrium. Helium gas was considered most appropriate for this as it is relatively inert and has a high thermal conductivity. The attainment of thermal equilibrium was monitored by a chart recorder in parallel with the thermocouple output. In order to avoid any errors due to possible non-ohmicity of the samples, all measurements were made at constant potential so that Ohm's Law could be applied to the circuit shown in Figure 6.10. Since $R_S \gg R_C$ (where R_S and R_C are the standard and crystal resistances respectively) then

$$i = \frac{V_S}{R_S} \qquad \text{(Ohm's Law)}$$

so that $R_C = V_C \cdot \frac{R_S}{V_S}$

where R_C is the crystal resistance (or, more, accurately, the sum of the crystal plus contact resistances) and V_C, V_S the potentials across crystal and standard resistances respectively. One further criterion applied to the experimental conditions was that the sample should not be appreciably heated, i.e. the current drawn by the circuit must be small. The empirical formula obtained by Drew[15] was used to determine suitable potentials for crystals of varying resistances:

$$\frac{V_C^2}{R_C} \ll 1 \text{ mW}$$

Temperatures throughout the conductivity measurements were made as follows: above 40°C an Ether Digi controlled air bath with 0.5 KW heater was used; between 10°C and 40°C a Dewar vesselled water bath was used, and below +10°C a 'methcol' slush bath in a large-necked 5 l Dewar vessel was used.

6.4 U.v./Visible Spectrometry

The stoichiometry of TCNQ salts was determined by u.v./visible spectrometry as microanalysis is relatively insensitive to large changes in stoichiometry for these complexes and certainly too inaccurate for determination of small, non-stoichiometric variations of salt stoichiometry[15]. The solution spectra of these salts, however, provide an accurate, fairly straightforward

measure of salt stoichiometry since two of the species present in acetonitrile solution, $TCNQ^{o}$ and $TCNQ^{-}$, show strong absorptions in different regions of the spectrum. Figure 6.11 shows the solution spectra of $TCNQ^{o}$ and Li^{+} $TCNQ^{-}$ in pure, dry acetonitrile. It can be seen that any absorption peak at 842 nm is solely due to $Li^{+}TCNQ^{-}$ (and in fact is due to the $TCNQ^{-}$ ion) whilst that at 395 nm may be due to either $TCNQ^{o}$ or $TCNQ^{-}$. Melby *et al*[5] used spectrophotometric determination of absorption at 420 nm and 842 nm to determine whether or not pure simple salts had been formed, and complex salt stoichiometry has been determined by measurement of absorption at 395 nm, and 842 nm by a number of workers[e.g. 5, 7, 22, 31, 33]. Figure 6.12 shows a typical complex spectrum. The complex stoichiometry may be determined as follows: if there is no significant absorption by the cation in the region of interest (which may be determined from the spectrum of the simple cation halide) and no back donation of charge from the $TCNQ^{-}$ to the charged heterocyclic ring of the cation occurs (which is probably true for the low concentrations used, ca. 10^{-6} M) then from Beer's Law:

$$A_{395} = (\varepsilon^{o}_{395} \cdot c_{o} + \varepsilon^{-}_{395} \cdot c_{-})\, l \qquad 6.1$$

and

$$A_{842} = \varepsilon^{-}_{842} \cdot c^{-}\, l \qquad 6.2$$

where A_n is the absorption at wavelength n nanometers

ε^{o}_{n}, ε^{-}_{n} are the extinction coefficients of $TCNQ^{o}$ and $TCNQ^{-}$ respectively at wavelength n nanometers

c_0 c^- are the molar concentrations of $TCNQ^0$ and $TCNQ^-$

and l is the path length in cm.

From equations 6.1 and 6.2

$$\frac{c_0}{c^-} = \left(\frac{\varepsilon^-_{842}}{\varepsilon^0_{395}}\right) \frac{A_{395}}{A_{842}} - \frac{\varepsilon^0_{395}}{\varepsilon^-_{395}} \qquad 6.3$$

and from this ratio the complex stoichiometry may be determined.

The extinction coefficients ε^0_{395}, ε^-_{395} and ε^-_{842} were determined from standard solutions of rigorously purified $TCNQ^0$ and Li^+TCNQ^- in t.d.d. acetonitrile and found to be in good agreement with those values obtained by other workers(e.g. 7,15,24). Absorption measurements at the appropriate fixed wavelengths were made using 0.1 cm matched glass cells and a Unicam SP500 u.v./visible spectrometer.

6.42 Determination of Complex Solubility

Because the absorption at 842 nm is solely due to $TCNQ^-$ ions in solution, and the number of $TCNQ^-$ ions present is wholly dependent upon the number of donor molecules (i.e. cations) present (in the absence of any donor impurities), determination of complex concentration is possible from measurement of the absorption at 842 nm in a solution of the complex. If this solution is saturated, then the resulting concentration may be converted into a solubility. A sufficient quantity of dry powdered complex was placed in a baked

glass flask after purging with N_2 gas and t.d.d. acetonitrile (ca. 25 ml) was added, after which the flask was tightly stoppered and sealed from atmospheric moisture by means of a 'Nescofilm' wrap around the stoppered joint. The solution was thermostated in a 50 l water bath controlled by a mercury contact thermometer for 24 hours at a temperature of 10° above that at which the solubility was required, after which the solution was thermostated at the required temperature for 36 - 48 hours. A 1 ml sample was then withdrawn by means of an 'Easifil' rapid flow 1 ml pipette and diluted 1 : 10 v/v with t.d.d. acetonitrile in order to obtain an absorption with the instrumental range (diluted 1 : 20 v/v for solutions above $35^{\circ}C$). A sample of the dilute solution was then measured in the spectrometer and the concentration and solubility determined from the relationship derived via equation 6.2:

$$S_T = \frac{A_{842} \quad MW \quad V_d}{\varepsilon_{842} \quad 1 \quad 1000}$$

where MW is the molecular weight of the complex

V_d is the total volume of the diluted saturated solution in mls,

and S_T is the solubility at temperature T in $g.ml^{-1}$

V_d is therefore 11 for temperatures below $35^{\circ}C$ and 21 for $T > 35^{\circ}C$.

In view of the uncertainities in determining the true equilibrium concentration a second method, using a water-jacketed magnetic-flea stirred sample was used for later solubility measurements, the equilibrium being determined as the point at

which no further change of absorption occurred with time. The samples were checked for decomposition by monitoring the A_{395}/A_{842} ratio and deducing the apparent stoichiometry.

6.5 Electrocrystallisation

Electrocrystallisation, the second general method of salt formation used by the author, relies on the fundamental property of $TCNQ^{o}$ to form the stable $TCNQ^{\cdot -}$ radical ion by reduction. In the previous method (see Section 6.14) the $TCNQ^{o}$ moiety was reduced *in situ* by I^{-}. The rate of growth of complex and the stoichiometry obtained is then determined by such factors as solubility, temperature, degree of super-saturation, presence or absence of complex nuclei or foreign nuclei, etc. If, however, the rate of formation of $TCNQ^{-}$ could be controlled by a cation- independent method, then the possibility of formation of different phases or stoichiometries of complex occurs. Rosseinsky *et al*[25] were the first workers to apply electrocrystallisation to the formation of conductive non-stoichiometric adducts of TTF with inorganic and organic anions. They found that the most highly conducting stoichiometry was preferentially formed at the anode. In view of this work it was decided to undertake a program of electrocrystallisation for some substituted bipyridinium type complexes which had been found to yield two conductivity phases in order to determine whether or not this technique could provide a means of forming suitable crystals of complexes hitherto only obtained in poor polycrystalline or powder form.

The basic circuit used is shown in Figure 6.13 and consists simply of a source of constant potential and an electrocrystallisation cell in the form of a roundbottomed flask into the base of which ca. 1.5 cm of Pt ribbon had been sealed and having also a removable Pt electrode which sealed the vessel tightly when in place. The constant potential was provided by one of two sources : below 2.0 V a potentiometer circuit was used to provide an accurate, known potential (Cropico type 3387 B potentiometer, 0 - 1.9 V, 0.05 A), and above 2.0 V a Farnell Instruments stabilised power supply (TSV 30/5EC) was used with a 12 ohm series resistor to provide appropriate sensitivity in the range 2.0 - 4.5 volts. As crystal growth was expected to occur on the cathode, it was arranged that this electrode was the removable one.

The general reaction scheme is as follows:
reduction of $TCNQ^{o}$ to $TCNQ^{-}$ occurs at the cathode surface:

$$TCNQ^{o} + e^{-} \xrightarrow[\text{electrode}]{\text{Pt}} TCNQ^{-\cdot}$$

Because of the increased concentration of negative charge in the vicinity of the cathode, cation material in solution will diffuse towards the charged region by electrostatic forces. When the chemical components of the system are sufficiently close, crystallisation can occur and act as a site for further growth provided that the surface layer of material formed on the electrode is sufficiently highly conducting to ensure that the reduction of further $TCNQ^{o}$ to

$TCNQ^-$ can occur. If a highly resistive layer is formed the process stops and no further reaction or growth occurs, so that the formation of the most highly conducting form of a material should be favoured if the reaction is to proceed[25]. Later work by Rosseinsky *et al*[26] showed that growth occured at the electrode surface rather than the external crystal surface and the formation of highly conducting stoichiometries has thus been attributed to the highly controlled growth conditions. A significant improvement in crystallinity is reported when a galvanostatic growth method is employed and this is thoughtto be due to the more precise control over the rate of crystal growth afforded by this technique.

A number of electrode geometries were investigated in order to determine the most appropriate configuration and electrode shape, of which the two most successful were found to be the plate cathode and the pseudo-spherical cathode (see Figure 6.14a and 6.14b). No success was obtained using point electrodes flush with a glass surface, or with thin plate surfaces (see Fig. 6.14c and 6.14d), two other configurations used by Rosseinsky *et al*[25].

Samples of materials grown under various conditions are shown in plate 6.1 and Table 6.2 shows a summary of materials prepared by the author and by undergraduate project students under the author's supervision during the course of this work. The photographs were taken using a Zeiss microscope and camera with Polaroid film back, illuminated by a variable intensity white light source via a pair of fibre optic light guides.

The practical method employed was as follows: the electro-

TABLE 6.2 Summary of Electrocrystallisation Results

Compound	Phase			
DHPA $(TCNQ)_4$	I	2.6 V	Rapid formation at plate electrode edges.	
DHPA $(TCNQ)_2$	Simple salt	0.8-2.2V	Well formed on pseudo-spherical electrode.	
DEPE $(TCNQ)_4$	I	2.0-2.8V	Diiodide used as cation No effect due to water.	(27)
DEPE $(TCNQ)_4$	I		Cation dichloride used Crystals still highly dendritic.	(28)
DBzBP $(TCNQ)_4$	I	Not observed at all.		
	II	0.8-1.9V	Low water content rectangular crystals. High water content needle crystals	(27)
BP $(TCNQ)_x$	No electrode growth.		Pi complex formation in the cold.	

crystallisation vessel was thoroughly cleaned with reagent grade acetone after which it was baked out at 85°C for at least two hours. An excess of TCNQ was then added, and an appropriate volume of t.d.d. acetonitrile added after purging with N_2 gas. The cathode was inserted and sealed with 'Nescofilm' and a potential applied by one of the two means previously discussed. Using this technique the author was able to obtain in a matter of hours crystals of DHPA $(TCNQ)_4$ phase I, the highly conducting phase hitherto only formed by slow diffusion growth under a constant temperature differential over a period of 3 months[15]. The crystals appeared to be better formed than those previously obtained, as evidenced by the external appearance and the greater number of significantly observable diffracted X-ray intensities (see Chapter 5). The author also prepared a large, well-formed crystal of DHPA $(TCNQ)_2$, the simple salt, by the electrocrystallisation method (see also Chapter 4). The electrode used, and the crystal obtained by this method, are shown in plate 6.2, and the cation salt used for the experiments, $DHPA^{2+}\ Cl_2^{--}$, was prepared by Drew[15] during previous work in the Department.

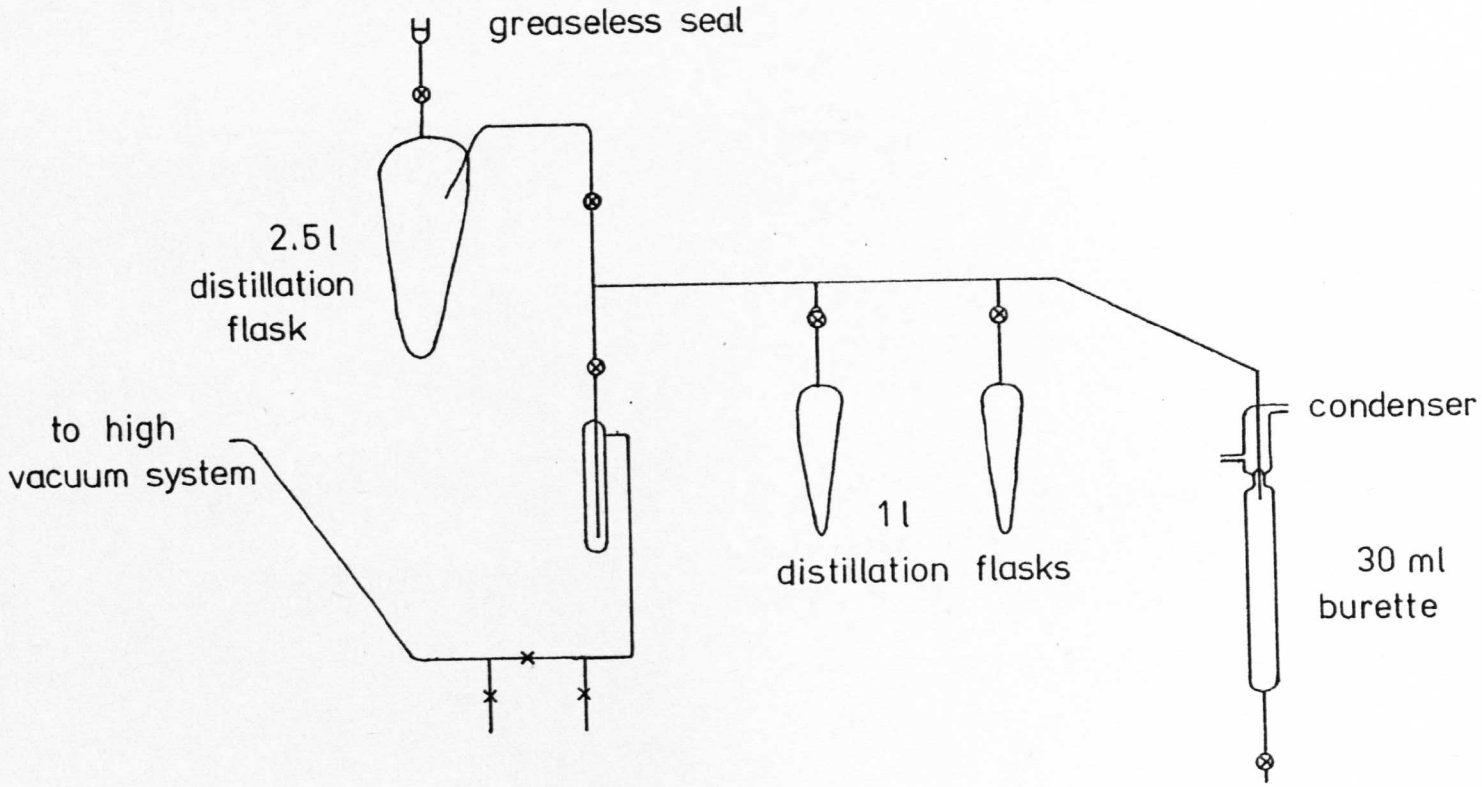

Figure 6.1 Schematic diagram of solvent frame

⊗ greaseless Teflon taps × greased taps

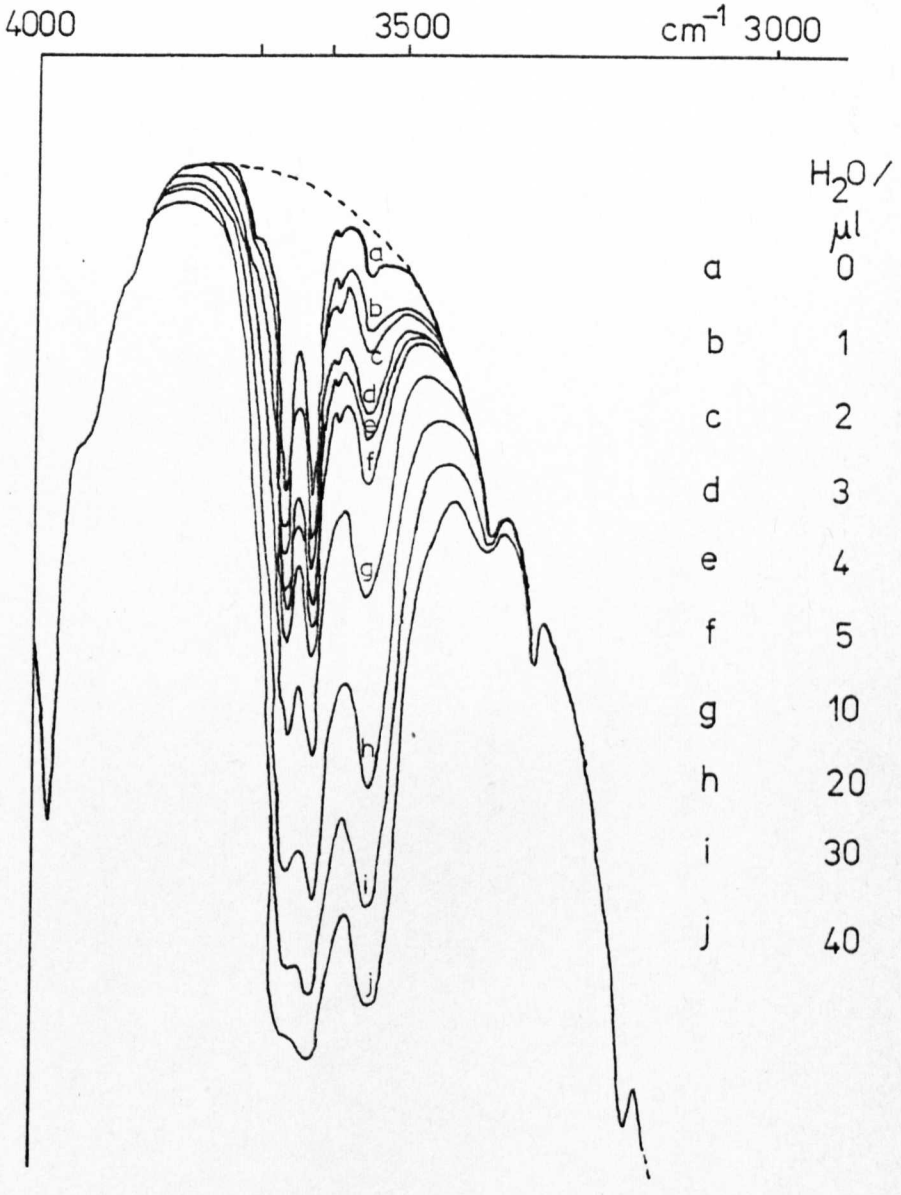

Absorption Spectra of CH_3CN / H_2O Mixtures.

FIGURE 6.2

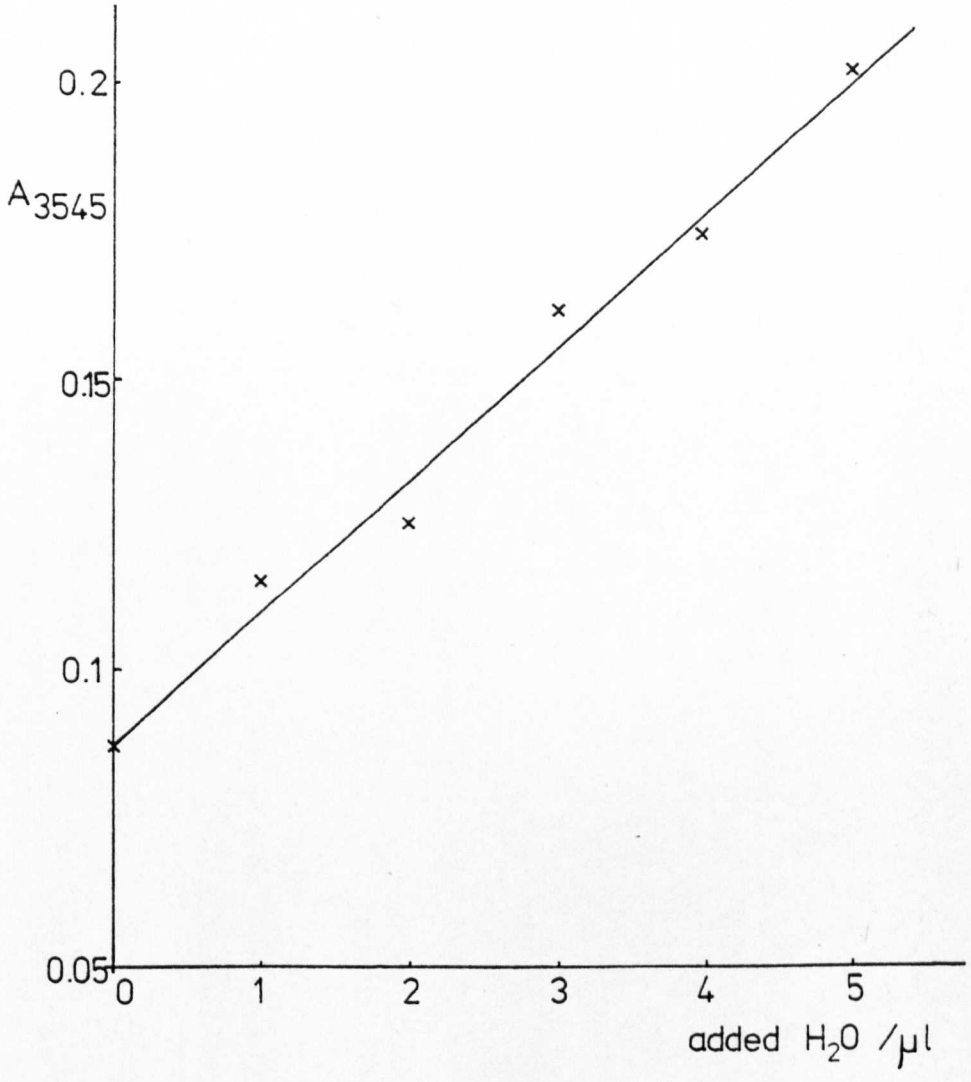

Figure 6.3

Calibration curve for CH_3CN / H_2O system.

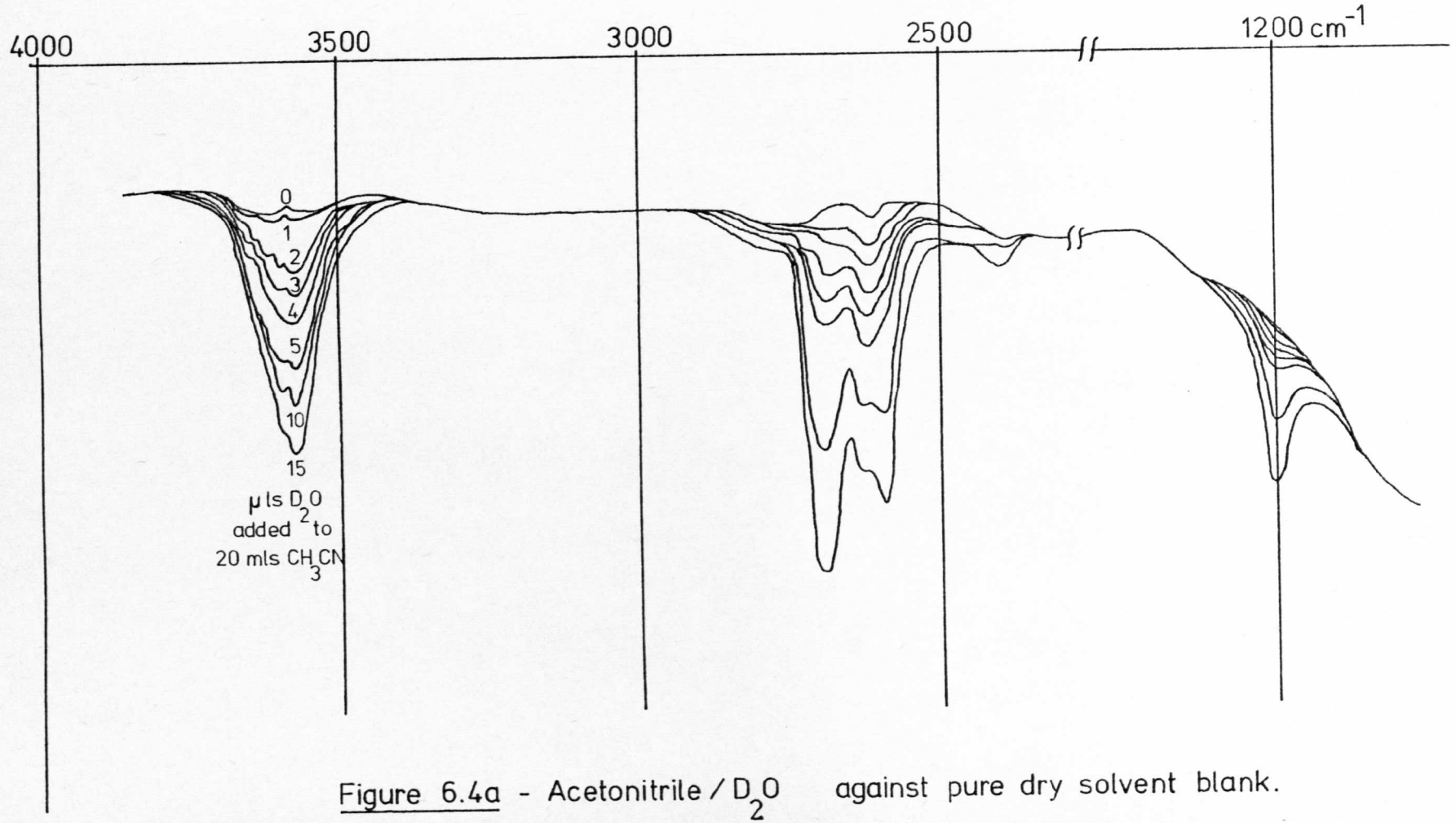

Figure 6.4a - Acetonitrile / D_2O against pure dry solvent blank.

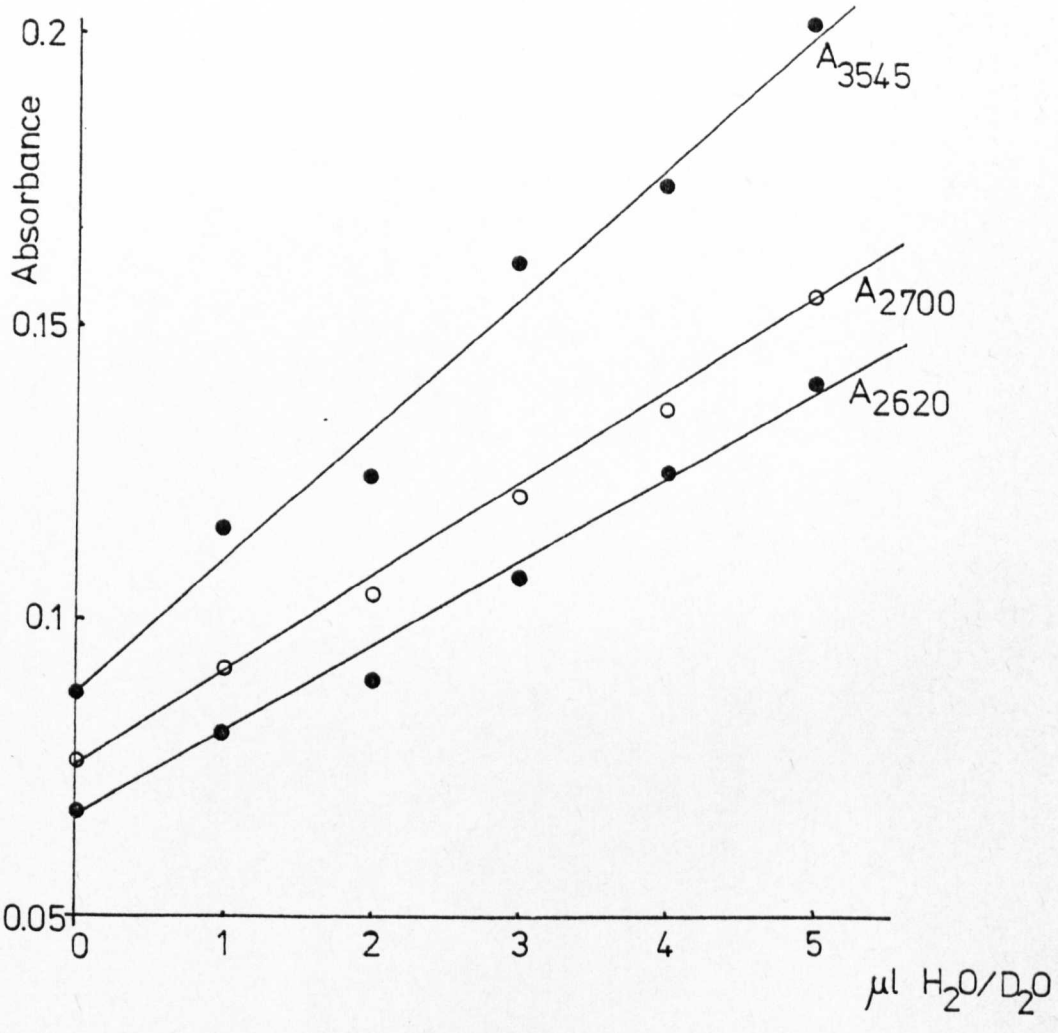

Figure 6.4b - Absorption versus added H_2O/D_2O mixture for CH_3CN.

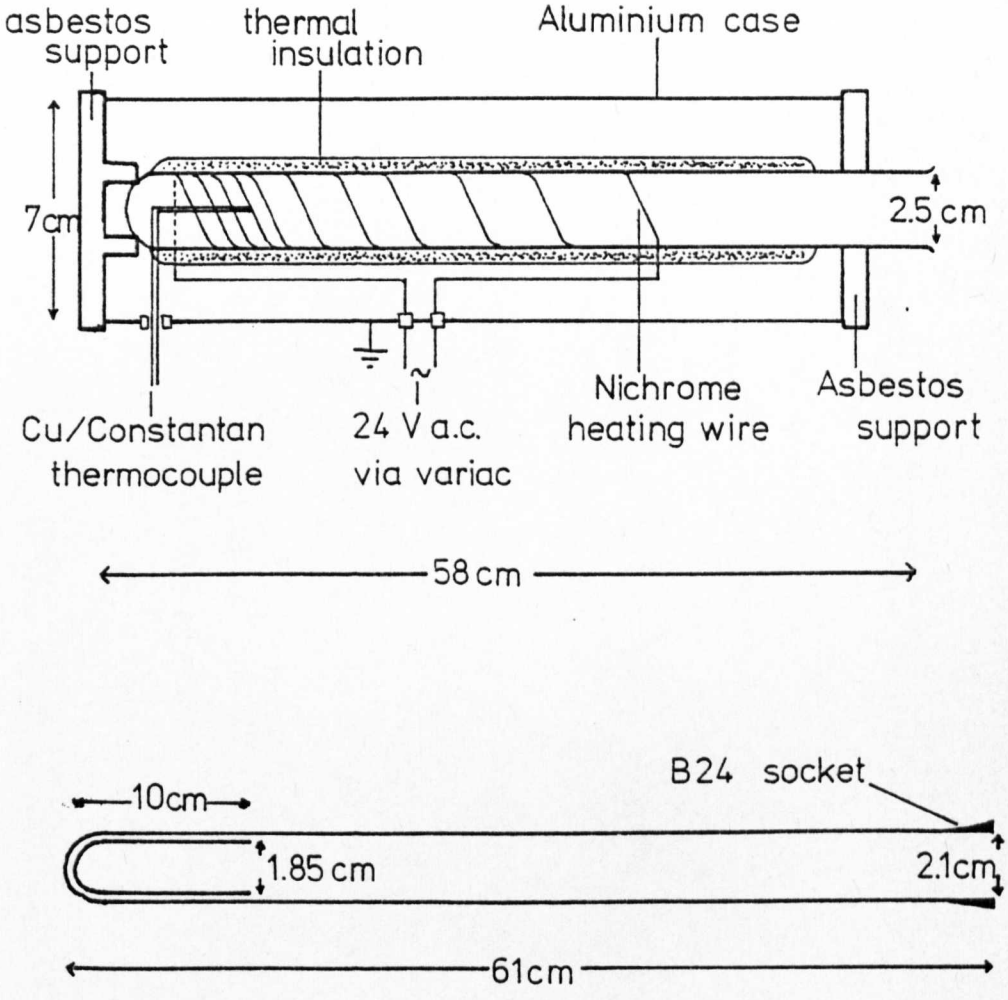

Figure 6.5 Gradient sublimation apparatus.

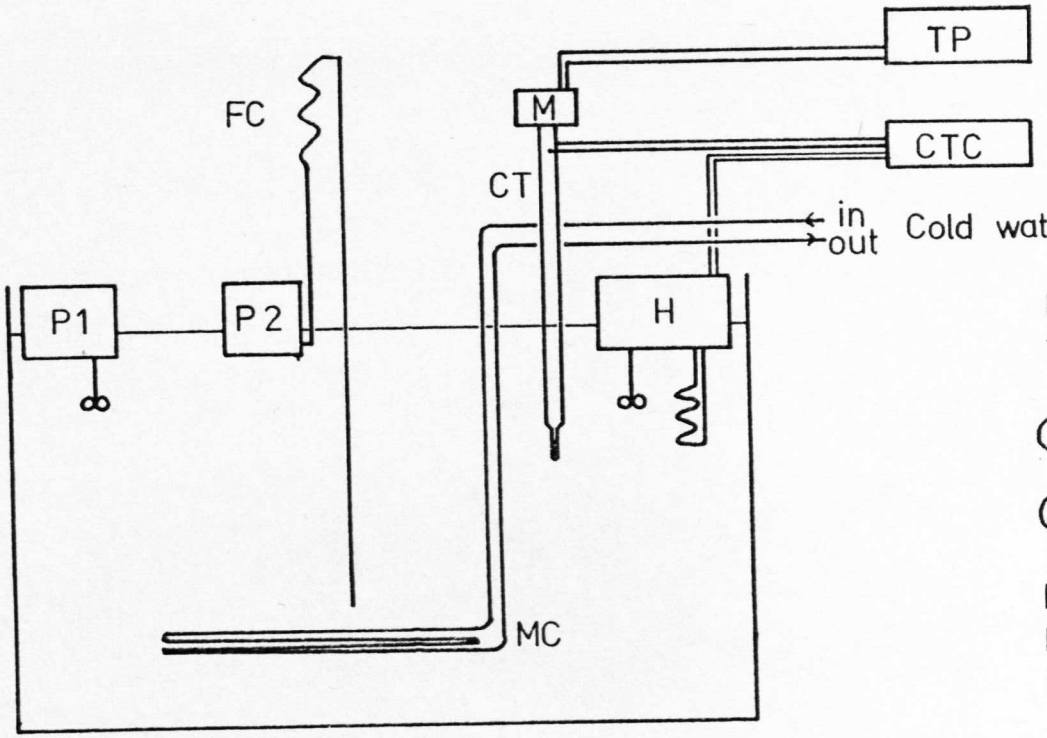

TP temperature programmer
CTC contact thermometer / heater controller
M 50 Hz synchronous motor

Main cooling coil
1/4" Cu tube:

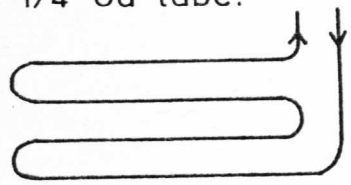

P1 circulatory pump
P2 fine control cooling pump
H 1 KW CT controlled heater, with constant circulation pump
CT contact thermometer
FC fine cooling coil
MC main cooling coil

Figure 6.6

FIGURE 6.7a

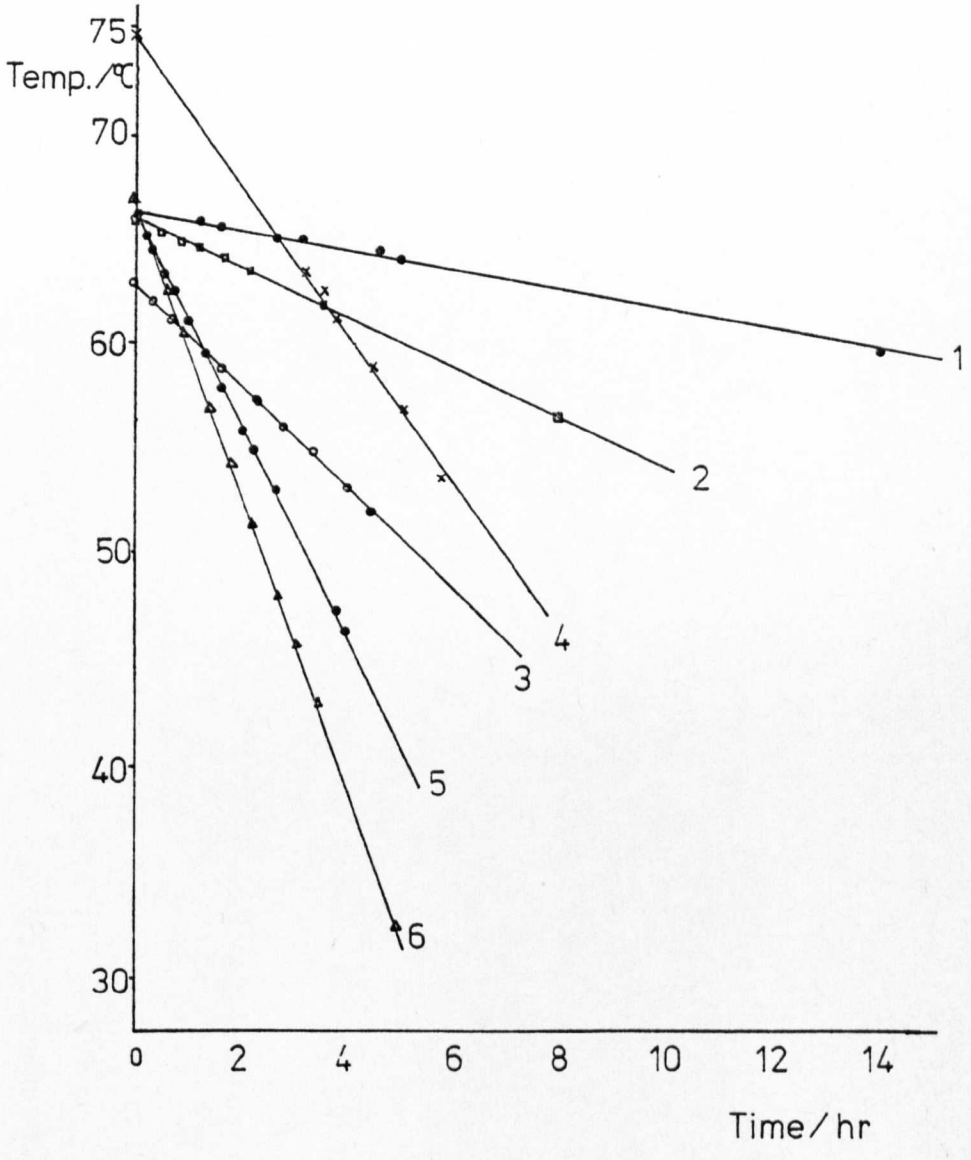

Linear Temperature Programs:

Rate	1	0.6 °hr^{-1}
	2	1.2 "
	3	2.4 "
	4	3.5 "
	5	4.9 "
	6	6.9 "

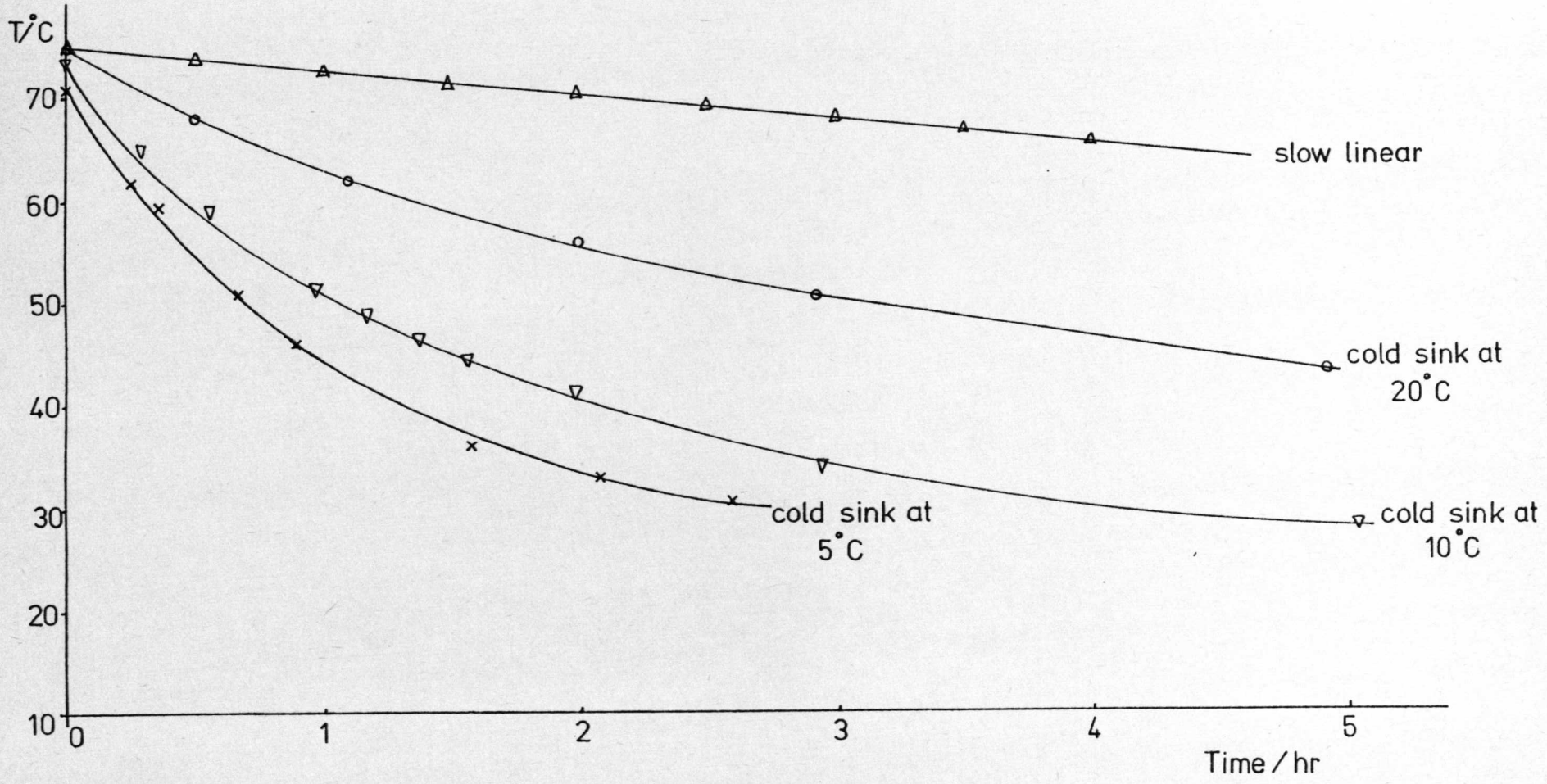

Figure 6.7b - Simulated Dewar cooling.

Fig. 6.8 CRYSTALLISATION STUDY APPARATUS

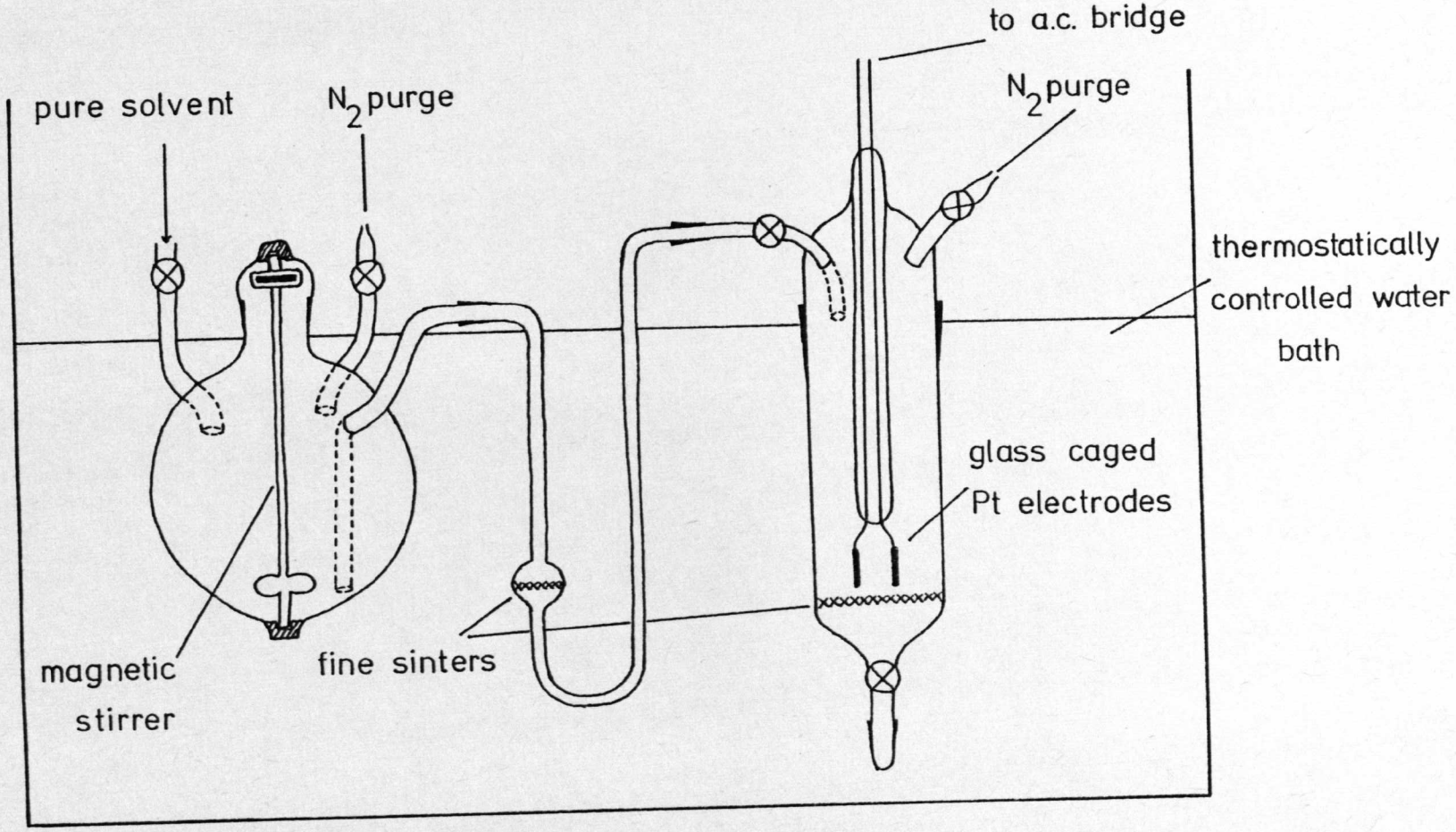

FIGURE 6.9

APPARATUS USED FOR RESISTANCE MEASUREMENTS

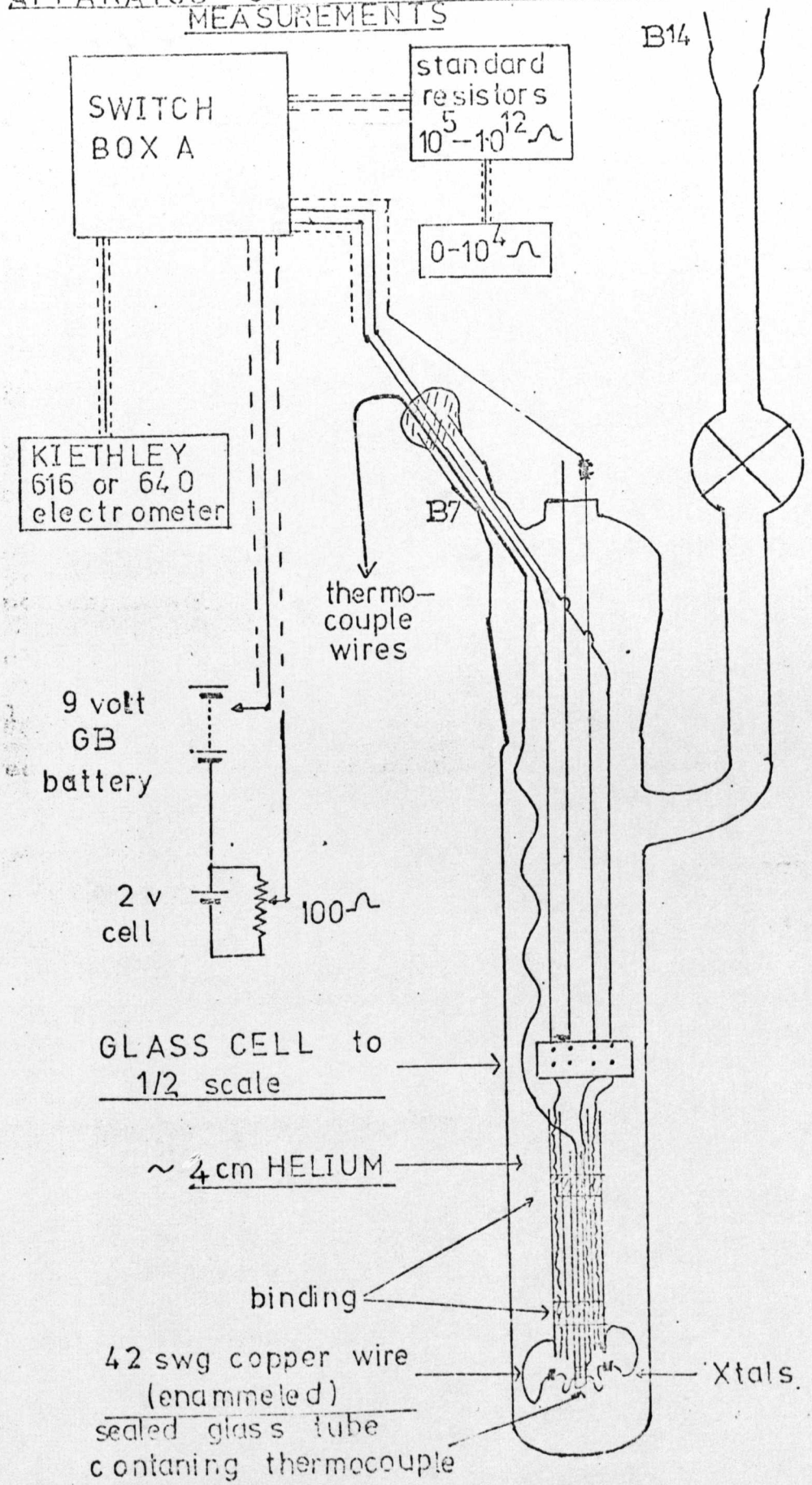

FIGURE 6.10

BASIC CIRCUITS USED AND SWITCHING

2 wire ($R_x > 200\,\Omega$)

a/

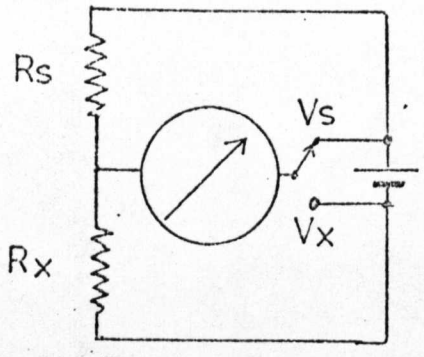

$$R_x = R_s \times \frac{V_x}{V_s}$$

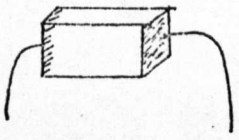

b/ 4 wire ($R_x \sim 0.01\,\Omega$ upwards)

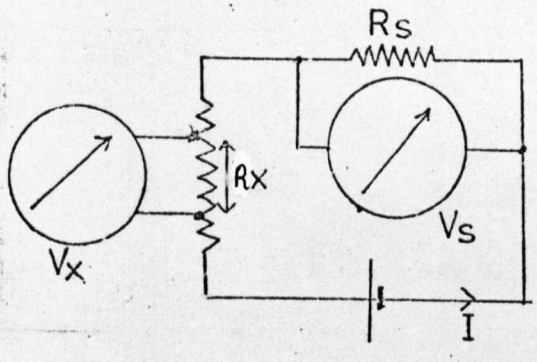

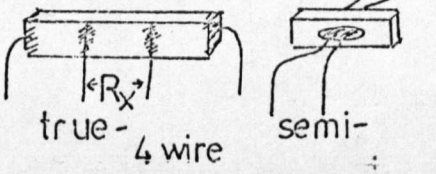

$$R_x = \frac{V_x}{I}$$

Switching Circuit

Switch box A

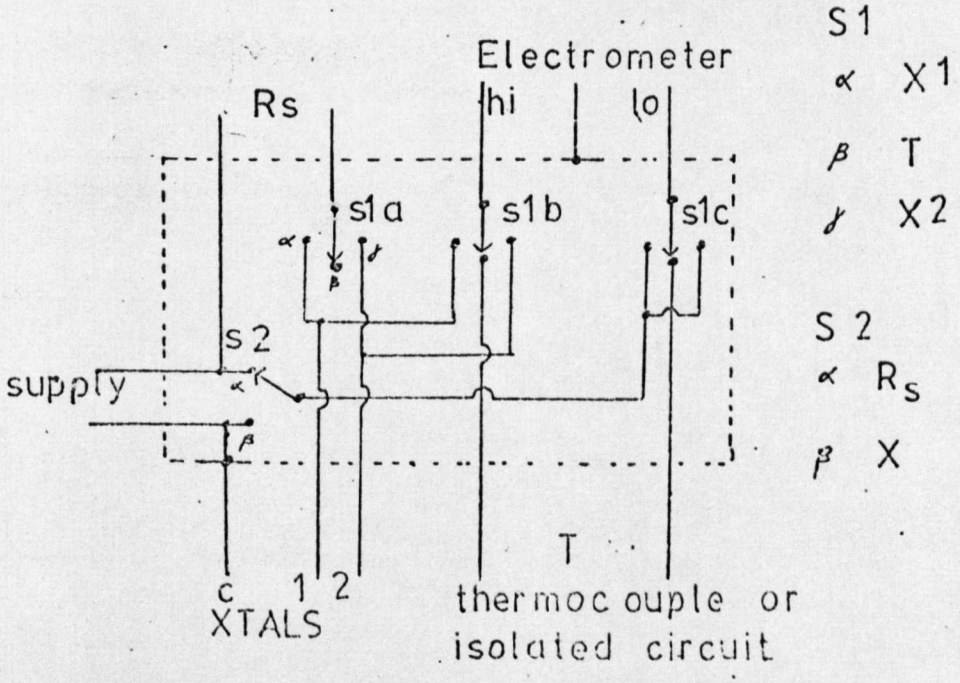

Fig. 6.11 Solution spectra of $TCNQ^{\bullet}$ and $TCNQ^{-}$.

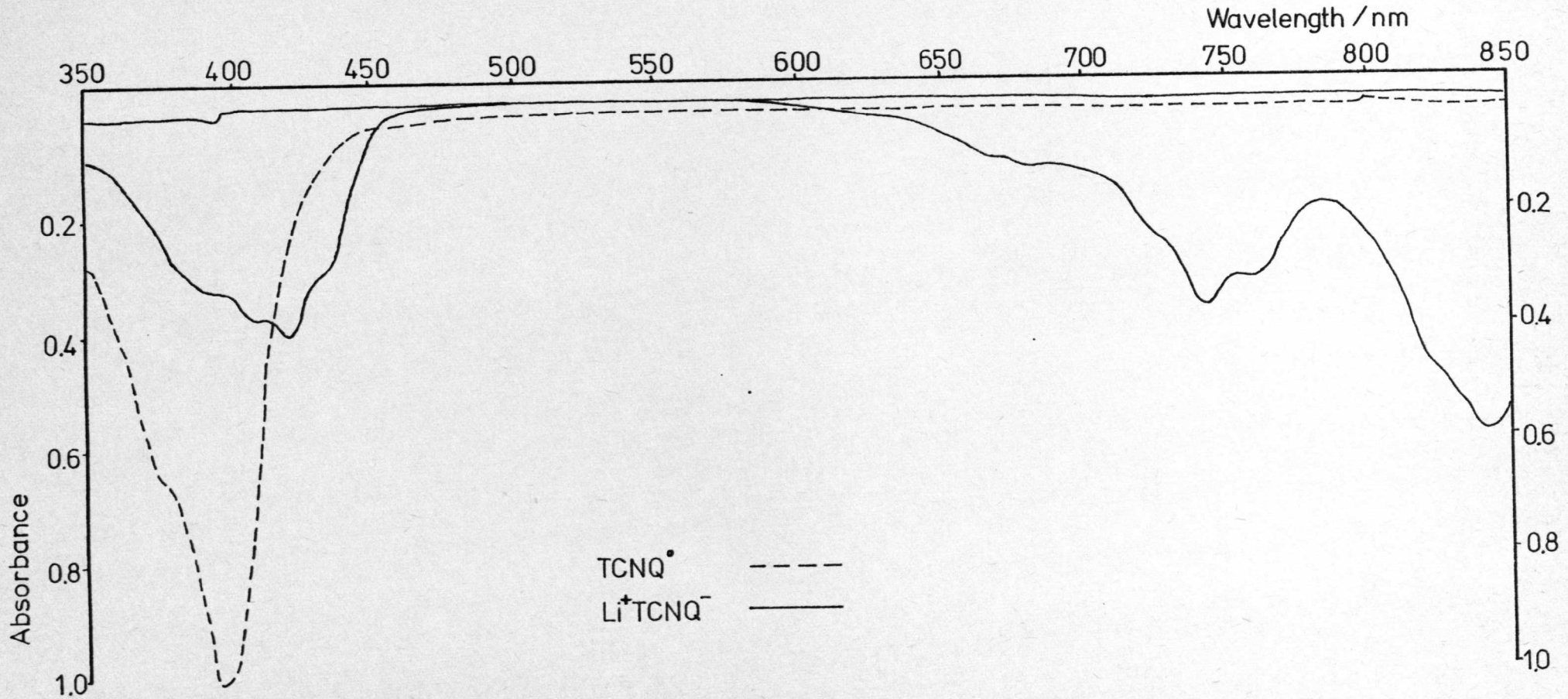

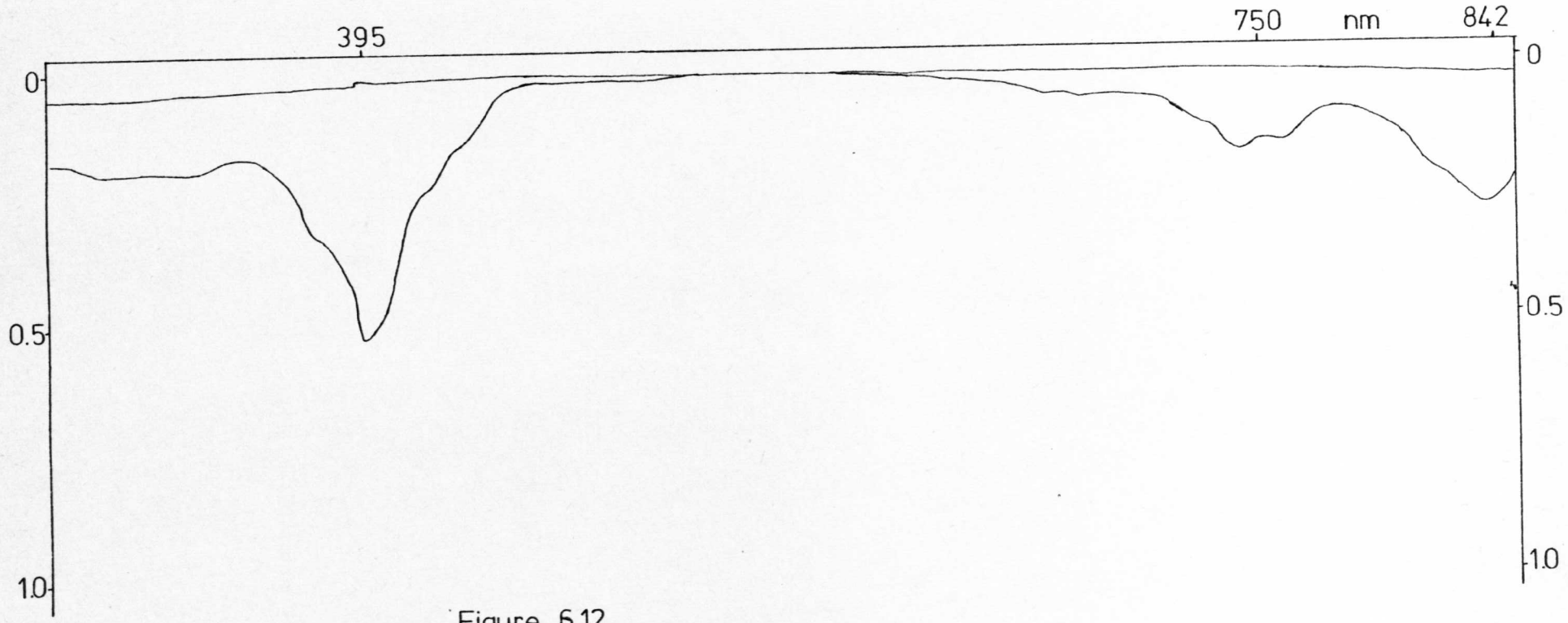

Figure 6.12

Solution spectrum of $DEPE(TCNQ)_4$ complex salt.

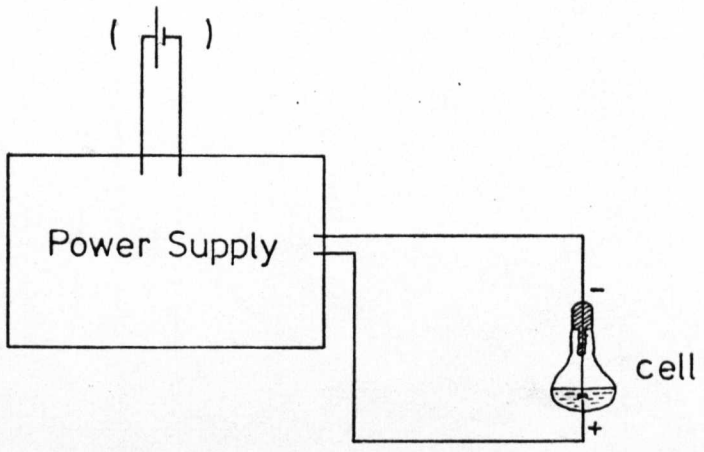

FIGURE 6.13

Basic circuit for electrocrystallisation

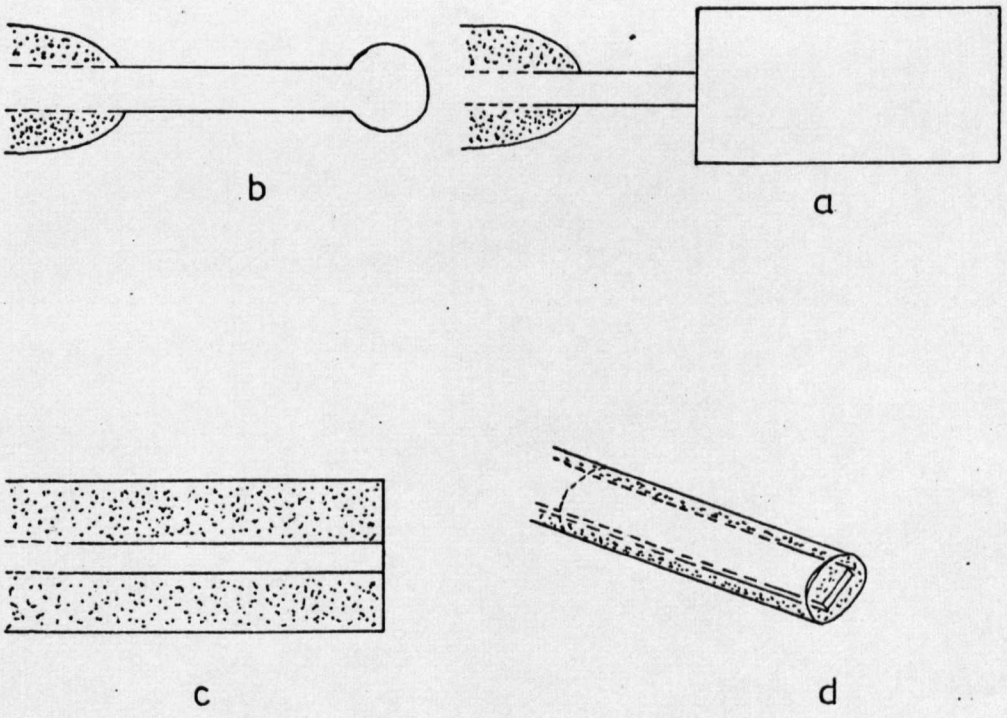

FIGURE 6.14

Electrode geometries used in electrocrystallisation studies

(a)

x30

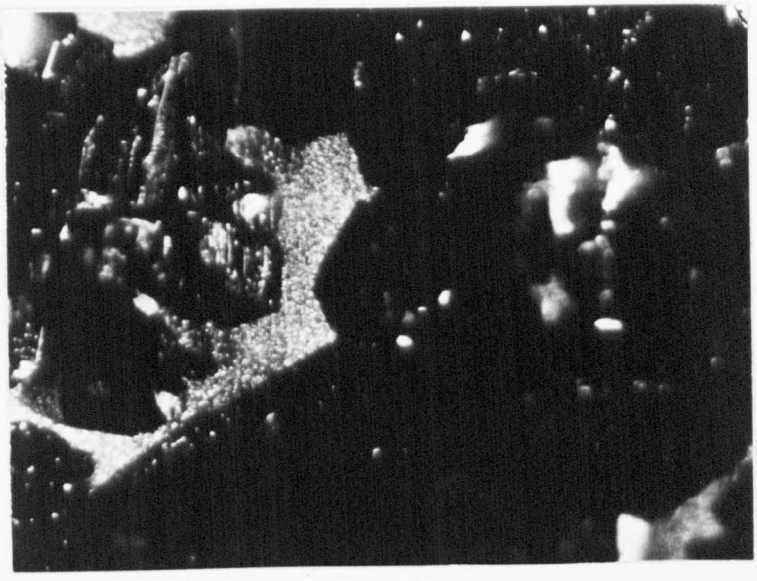

(b)

x50

(c)

x50

DHPA – on plate electrode - centre (a), (b)
- edge (c)

PLATE 6.1

x30

Electro-crystallised DHPA* (15 V, 48 hours, 3 mls H_2O added)

Pseudo-spherical electrode.

* simple salt

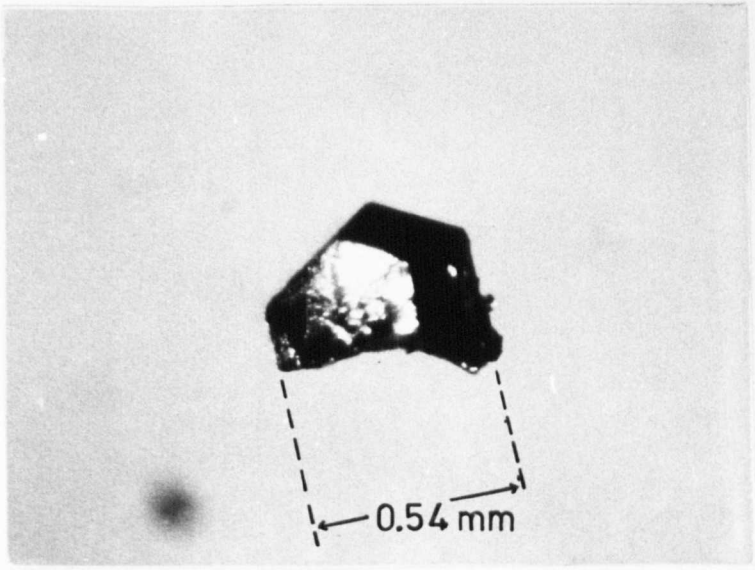

Single crystal used for diffractometry

PLATE 6.2

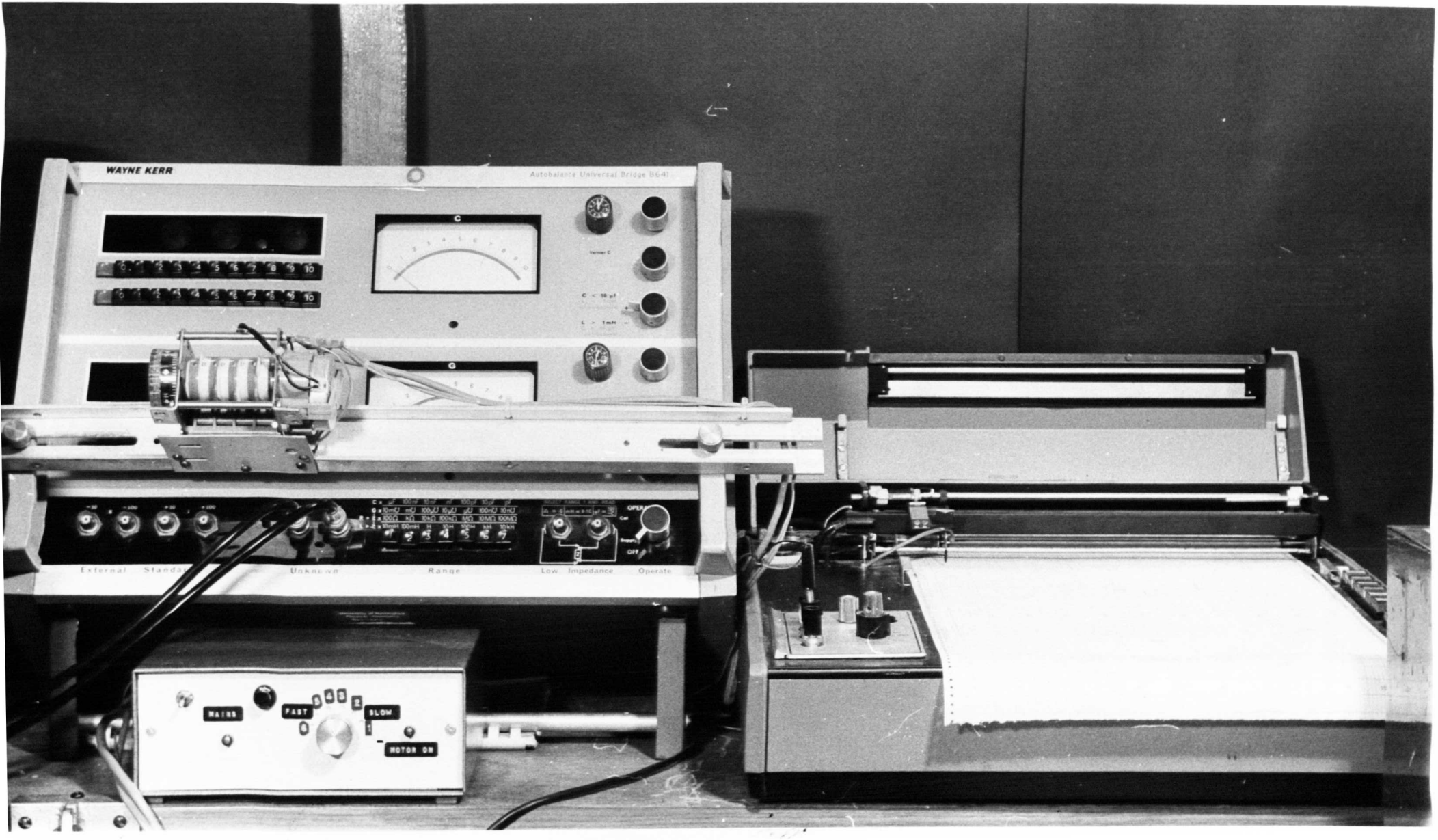
WAYNE KERR
Autobalance Universal Bridge B641
C
G
Range
Low Impedance
Operate
MAINS
FAST
SLOW
MOTOR ON

CHAPTER 7

CRYSTALLISATION STUDIES

Many of the complex salts of TCNQ involving bipyridyl- and bipyridinium-type cations have been found to crystallise in two electrically distinct forms, characterised by their electrical properties. In particular, Drew[15] observed two electrically distinct phases of DMPA$(TCNQ)_4$, of which the highly conducting phase ($\sigma_{300} \sim 1\,\Omega^{-1}\ cm^{-1}$) consisted of ill-formed platelets of typical thickness 0.1 - 0.05mm, and the low-conductivity phase ($\sigma_{300} \sim 2 \times 10^{-3}\,\Omega^{-1}\ cm^{-1}$) which consisted of somewhat thicker, ca. 3-5 mm, well-formed plates. The compound DMPP $(TCNQ)_4$ was also found by Drew[15] to exist in two forms, in which the high conductivity phase was found to consist of micro-crystalline hairs ($\sigma_{300} \sim 0.3\,\Omega^{-1}\ cm^{-1}$) amd the low conductivity phase ($\sigma_{300} \sim 5 \times 10^{-4}\Omega^{-1}\ cm^{-1}$) formed large black parallelepipeds. High and low conductivity phases of DEPA $(TCNQ)_4$ have been found by Welch[20] and Drew[15]. Ashwell et al[33,17] reported three phases of DEPE $(TCNQ)_4$, one of which comprised well-formed rectangular or hexagonal plates and the other two were comprised of highly dendritic 'fern-like' crystals. Of these two high conductivity phases, one was reported as being metallic in electrical conduction behaviour down to 30 mK and the other as a high-conductivity semi-conductor over the whole of the range studied. The high and low conductivity semi-conducting phases resulted unpredictably from the same method of preparation (whilst the so-called metallic phase was found on rare occasions amongst highly semi-conducting material).

Because of the inability of various research groups to reproduce the metallic phase it was considered essential that the factors affecting the growth of the two main phases of DEPE $(TCNQ)_4$ were investigated with the aim of determining the growth conditions necessary for the formation of crystals of phase I, the highly conducting semi-conductor phase, and phase II, the low conductivity phase, so that phase I crystals of a suitable size for 4- probe d.c. conductivity measurements could be reproducibly obtained.

The empirical observation that phase I grew from solutions of the complex salt which were cooled from 65°C to ambient over a period of some 6-8 hours, whilst (II) was formed by cooling over the same temperature range but over a period of some 40 hours suggested a research program in which various cooling rates were applied to solutions of differing concentration, in order to determine whether or not phase formation was dependent primarily on rate of cooling or on the temperature at which crystallisation occurred (and hence the concentration of species in solution). A technique was sought whereby the process could be followed dynamically, thus preventing problems due to 'dead-time' during measurements, and reasonably simply. For these reasons u.v./ visible spectrometry and interferometry were ruled out, on the one hand because of the real time required for the measurements and the perturbation of the solution upon sampling, and on the other because, although it would be very sensitive to changes in optical density of the solution, such as might be observed during crystallisation (due to either the removal of material from solution and subsequent deposition as solid matter or nucleation of the species), the solutions might have

proved too optically dense for the passage of the beam. For the same reasons the technique of light scattering was considered unsuitable because, although in theory it could provide information about the onset of nucleation and nucleus growth due to the formation of a pseudo- colloidal suspension of nuclei within the solution, the practical difficulties involved in observing any beam of panchromatic light through the intensely absorbing solution seemed to present a major obstacle.

The technique finally selected for use in studying the crystallisation of these complexes was that of a.c. conductance measurement. In acetonitrile solution these complexes behave as strong electrolytes[37] and form ionic solutions. They will therefore conduct an alternating current without undergoing chemical transformation provided that the a.c. frequency is sufficiently high. Upon crystallisation the number of ions in solution will decrease and consequently the resistivity of the solution must increase, so that following the conductance of the solution throughout this process should indicate not only the point of initial nucleation/growth but should also reveal any secondary processes such as nucleation and growth of a separate phase at lower concentrations, if such a process occurs.

In terms of electrolyte theory the system is sufficiently explained by the basic equations for strong electrolytes[e.g. 34]

$$R = \rho . \frac{l}{A} \qquad (7.1)$$

where R is resistance of the solution between the electrodes, ρ is the resistivity, and l and A are the length and cross-sectional

area of the portion of solution studied in m and m^3 respectively. Because of the possibility of further conduction outside this portion of the solution, the term l/A is usually replaced by a cell constant found by electrolysing a solution of known conductivity. This constant was determined for all the cells used by means of a standard aqueous solution of KCl of approximately the same resistance as the acetonitrile solutions of complex under investigation, the conductance of the triply distilled water being determined and allowed for in the calculation of the cell constants, which were determined from the equations of Barthel, Feurlein, Neuder and Wachter[36] at 25°C. The conductance of the electrolyte is thus described by:

$$K = \frac{1}{\rho} = \frac{c}{R} \qquad (7.2)$$

where c is the cell constant.

The inherent capacitance of the cell was balanced out in the usual manner using the capacitance arm of the Wayne-Kerr bridge. The problem of capacitance effects across the cell walls caused by using an aqueous thermostating medium[e.g. 35] was considered to be included and accounted for by this technique.

As a qualitative check on the phases of complex crystallising in the various runs X-ray powder diffraction traces were obtained for a number of the crystallisation products from the linear cooling experiments - the details are summarised in Table 7.1. X-ray powder traces were not obtained for all the high cooling rates of ca. $6.9^{\circ}C.hr^{-1}$ since visual inspection of the product showed it to be entirely dendritic in nature and identical in appearance to other phase I samples of DEPE $(TCNQ)_4$.

A random check on the phase of material from these runs by means of an X-ray powder diffraction trace showed it to consist entirely of phase I material and so no further sampling was undertaken. Unfortunately the results of these studies are only qualitative due to the small sample size involved causing practical differences and the possibility of preferred orientation.

7.1 Simulated Dewar Cooling

Figure 7.1 shows plots of a.c. conductance versus temperature for DEPE $(TCNQ)_4$ run under similar conditions to those obtained by slow Dewar cooling, yielding large, well-formed black parallelepipeds ca. 5mm x 5mm x 3mm. The solutions were initially all at the same nominal concentration, equivalent to that of a saturated solution at 68°C, since dissolution was performed using excess solid material in the apparatus shown in Figure 6.8; the variations observed in the conductivities of the three samples are thus a reflection of both the sensitivity of electrolyte conductance to the concentration of electrolyte and the effect of stirring time on the degree of dissolution achieved. The curves do show, however, a reasonably linear initial regime, from 68°C down to ca. 55°C, during which the decrease in conductance on cooling may be explained solely on the grounds of increased solvent viscosity and increased solvent-solute interactions and hence decreased ion mobility. The decrease in conductance over this temperature range is ca. 10%, of the same order as the increase in solvent viscosity, ca. 13%[40], and so there is no appreciable change in the number of ions present in solution. By ca. 55°C a degree of supersaturation has been

reached which is too great to be supported by the solvent system and so nucleation and crystal growth occur. It does not appear to be possible to separate these two phenomena by this technique - it might be expected that the process of nucleation would lead to a sharp decrease in conductivity, followed by a slower decrease due to the crystallisation process removing further electrolyte from solution as nuclei above the required critical size undergo growth to form true crystals. Careful study of the conductance of these solutions in this critical region, even at very slow linear cooling rates (ca. $4^{o}C.\ day^{-1}$), has failed to reveal this type of behaviour.

Figure 7.2 shows a series of cooling curves for a number of known concentrations of DEPE complex in solution. The cooling program was again a slow simulated Dewar scheme, and a steady increase in Tc (the critical temperature at which crystallisation occurs) with concentration may be seen. Tc is determined in all the figures from the point of intercept of extrapolations of the two linear regions, a method which also provides an estimate of the possible maximum error in the determination of the actual point of turn-over. Figure 7.3 shows a plot of critical temperature versus concentration, taken from the previous graph, in which it can be seen that there is a possible linear relationship between Tc and concentration. However, when these points are converted into solubilities (since the concentration at Tc should be that of a saturated sol^{n} at that temp.) these are seen to lie on a smooth curve (Figure 7.4) with a similar shape to those solubilities for phase II determined by equilibrium techniques, see figure 7.4a. In view of this it is most probable that figure 7.3 is best represented by the solid

curve shown. The apparently enhanced solubility, S_T, at temperature T^oC, of DEPE phase II complex determined from the T_c plot ($S_{35} = 1.22g.l^{-1}$ from figure 7.4) may only be thought of as a qualitative measure of the degree of supersaturation at the point at which crystallisation occurs under that particular cooling scheme, since a 100% degree of supersaturation is unlikely.

Figure 7.5 shows that the change in conductance associated with the crystallisation of material from solution is not an experimental artefact of the DEPE $(TCNQ)_4$ system, as the corresponding simulated Dewar cooling curves for DMPB $(TCNQ)_4$ show a similar change in conductance at 23^oC ($c = 1.437 \times 10^{-4}M$) and 32^oC ($c = 18.63 \times 10^{-4}M$), respectively. No solubility data are available for this salt in acetonitrile; however, the higher apparent solubility in this solvent of the DMPB complex may be a feature of the less polarised nature of the cation with respect to the DEPE cation due to the positive inductive effect of the two methyl groups present in DMPB.

7.2 Linear Cooling

At high linear cooling rates (see figure 7.6) the shift of T_c to lower temperatures (figure 7.7) results in an increase in the apparent solubility of the complex (figure 7.8), so that $S_{35} \approx 1.6g.l^{-1}$ at these cooling rates. Again this figure is greatly in excess of that value obtained by conventional techniques for phase II, and also in excess of those approximate values obtained for phase I by static dissolution (see figure 7.4a). The products from all of the crystallisable fast (ca. $6.9^o.hr^{-1}$) linear cooling runs were found to be highly dendritic

polycrystalline specimens of phase I material and no evidence of multiple phase formation was found.

The effect of various added impurities was investigated in order to attempt to determine a suitable sealant with which to support a thermocouple within the cell and immersed in the electrolyte solution (see also page 6.14). It was found that none of the protective sleeve materials used to isolate and support the thermocouple caused any change in the conductance of the solution; however, the addition of a small amount of Araldite (used previously to seal the thermocouple sleeve in the cell wall) caused a very significant change.

At slower linear cooling rates (ca. 2.40 hr^{-1}) the formation of a two-phased crystalline product was observed across practically the whole range of concentrations studied. Figure 7.9 shows a series of four concentrations of complex crystallised in the absence of any deliberately introduced impurity species. The effect of Araldite as an impurity can be seen in figure 7.10, in which the conductance of a solution of concentration 1.400×10^{-3} M was followed through sequential crystallisation runs, the product being re-dissolved between each run. The conductance decreases with increasing time (i.e. run number) and this may be rationalised in terms of the ability of $TCNQ^-$ to abstract hydrogen ions (38,39, and Ch.6) from any acid harderer present in the epoxy adhesive since the formation of the uncharged $TCNQH_2$ species from $TCNQ^-$ would decrease the concentration of ions and hence the conductance of the solution.

As a result of these (and other) investigations it was concluded that measuring external bath temperature was a sufficiently accurate

method for the determination of solution temperature, since direct solution temperature measurements by means of a Kel-F encapsulated copper-constantan thermocouple revealed a maximum discrepancy of $1^{o}C$ at the highest rates of cooling between the adjacent bath temperature and the internal solution temperature. Thus the Araldite to Kel-F vapour tight seal could be excluded from the cell top so preventing errors due to enhanced solvent aging by impurities. Figure 7.11 shows conductance versus time graphs for two different solutions of complex with the same concentration as that used before (figure 7.10) and the enhanced conductivity, together with an increase in T_c from ca. $28^{o}C$ to ca. $38^{o}C$ is immediately apparent. It is instructive to note also that X-ray powder diffraction traces of complex material crystallised in the presence of the acidic Araldite impurity showed two intense reflections with 2θ values of ca. 26.9^{o} and 27.8^{o} respectively whereas all other complex powder diffraction traces show two intense reflections at $2\theta = 27.2$ and 27.8^{o}. This tends to support the supposition that a chemical change occurs in the presence of Araldite impurity and may also explain the linear rather than convex solubility curve (see Figure 7.13) obtained from values of T_c for solutions with Araldite impurity (Figure 7.12). It is not known whether it would be possible to produce a pi-complex of DEPE with $TCNQH_2$ so that a direct comparison of the impurity product and this compound could be made.

Figure 7.14 shows crystallisation curves obtained from slow (ca. $1.2^{o}\ hr^{-1}$) linear cooling of the complex solutions. The plot of critical temperature versus concentration (Figure 7.15) is of the usual form and gives a solubility curve (Figure 7.16) with $S_{35} \sim 1.25 g.l^{-1}$.

The solubility curve determined from this slow linear cooling program is the lowest of all those obtained from critical temperatures taken from dynamic crystallisation measurements (2.4O/hr $S_{35} \simeq 1.3$g/l extrapolated; 6.9^{o}/hr $S_{35} = 1.6$ g/l) as is expected since this slower rate should represent a closer approximation to the static equilibrium condition which exists during conventional solubility measurements.

Extremely slow linear cooling curves (ca. 4^{o} day^{-1}) from nominally saturated solutions at 70^{o}C of DEPE $(TCNQ)_4$ in which phase II was used to provide initial powdered material for dissolution are shown in Figure 7.17. The initial conductance is of the same order as that of the simulated Dewar cooling runs from nominally saturated solutions (Figure 7.1) and the curves again show a distinct sigmoid form, with the low temperature pseudo-linear regime commencing at ca. 35^{o}C as before. Critical temperatures denoting the start of a deviation from the high temperature linear regime lie between 42^{o} and 54^{o}C, a somewhat lower range than that found for simulated slow Dewar cooling, which ranged from 48^{o} to 60^{o}. This may be explained by the more rapid rate of cooling obtained in the early stages of Dewar cooling, a rate which approaches ca. 7^{o}/hr, comparable with the fast linear cooling rates used in this work. Under these circumstances a greater degree of supersaturation could result from the more rapid cooling of the solution. However, direct comparison of the simulated slow Dewar Cooling and the 4^{o}/day linear cooling results is not possible since simulated Dewar cooling produced well formed, large crystals of phase II material (see plate 7.1) whereas the slow linear product was poorly formed and may have contained multiple phases and/or decomposition products.

Figure 7.18 shows a summary of the critical temperatures obtained from a number of cooling rates and concentrations together with details of the range of phases obtained. As a generalisation, higher critcal temperatures and concentrations, combined with high rates of cooling, yield phase I material whilst low cooling rates and low concentrations tend to favour production of phase II material. The change-over cannot be defined solely in terms of the cooling rate employed: for example, a mixture of phase I and phase II material was obtained at a slow linear rate (ca. 1.2^{o}/hr) from solutions whose initial concentrations were in excess of 10^{-3}M (see also Table 7.1) whilst cooling at the rate of 2.4^{o}/hr invariably yielded a mixture of the two phases at all crystallisable concentrations. The evidence from the X-ray powder data on the products obtained from crystallisations at this rate tend to indicate that higher concentrations (and hence a higher T_c) yield more of the phase I component in the mixture. The product obtained from the high linear cooling rate (6.7^{o}/hr) was inevitably phase I. Whilst the indications are that high concentrations and/or high crystallisation temperatures are necessary for phase I growth it has not been possible to separate the two effects - further work using a variety of similar solvents, such as benzyl cyanide, should enable these two related phenomena to be distinguished separately. It would also be extremely valuable to perform experiments using two linear rates of cooling, thus mimicing the Dewar cooling but at known, pre-defined rates - for example, rapid cooling to just above T_c for a particular concentration, followed by slow linear cooling through the crystallisation temperature may provide the conditions necessary

to encourage the growth of high quality crystals from nuclei of the desired phase as determined by the initial cooling rate and concentration limits.

TABLE 7.1

X-Ray Powder Data for DEPE $(TCNQ)_4$. CuKα Radiation

Rate deg C/hr	Run No.	Concentration $\times 10^{-4}$ M	Tc °C	$\frac{I_{27.8}}{I_{27.2}}$	Phase
6.7	6/14	10.55	29.9	0.06	I
2.4	3/4	9.96	27.4	1.14*	-
2.4	3/5	11.97	28.6.	0.56*	-
2.4	3/6	14.00	35.5	0.50*	-
2.4	3/7	15.95	38.1	5.56*	-
2.4	3/3-(i)	8.77	-	2.24	II, I
2.4	3/3,4-(i)	10.45	-	0.38	I, II
2.4	3/6 -(i)	13.98	37.8	0.40	I, II
2.4	3/6 -(ii)	13.98	37.9	0.56	I, II
2.4	3/7 -(i)	15.93	40.8	0.68	I, II
1.2	2/1	8.77	22.8	0.20	II
1.2	2/2	10.49	30.2	1.83	I, II
1.2	2/4	12.03	39.7	6.8	I
1.2	2/3	13.81	40.5	50	I

* denotes added Araldite impurity. Ratio refers to

$$\frac{I_{27.8}}{I_{26.9}}$$

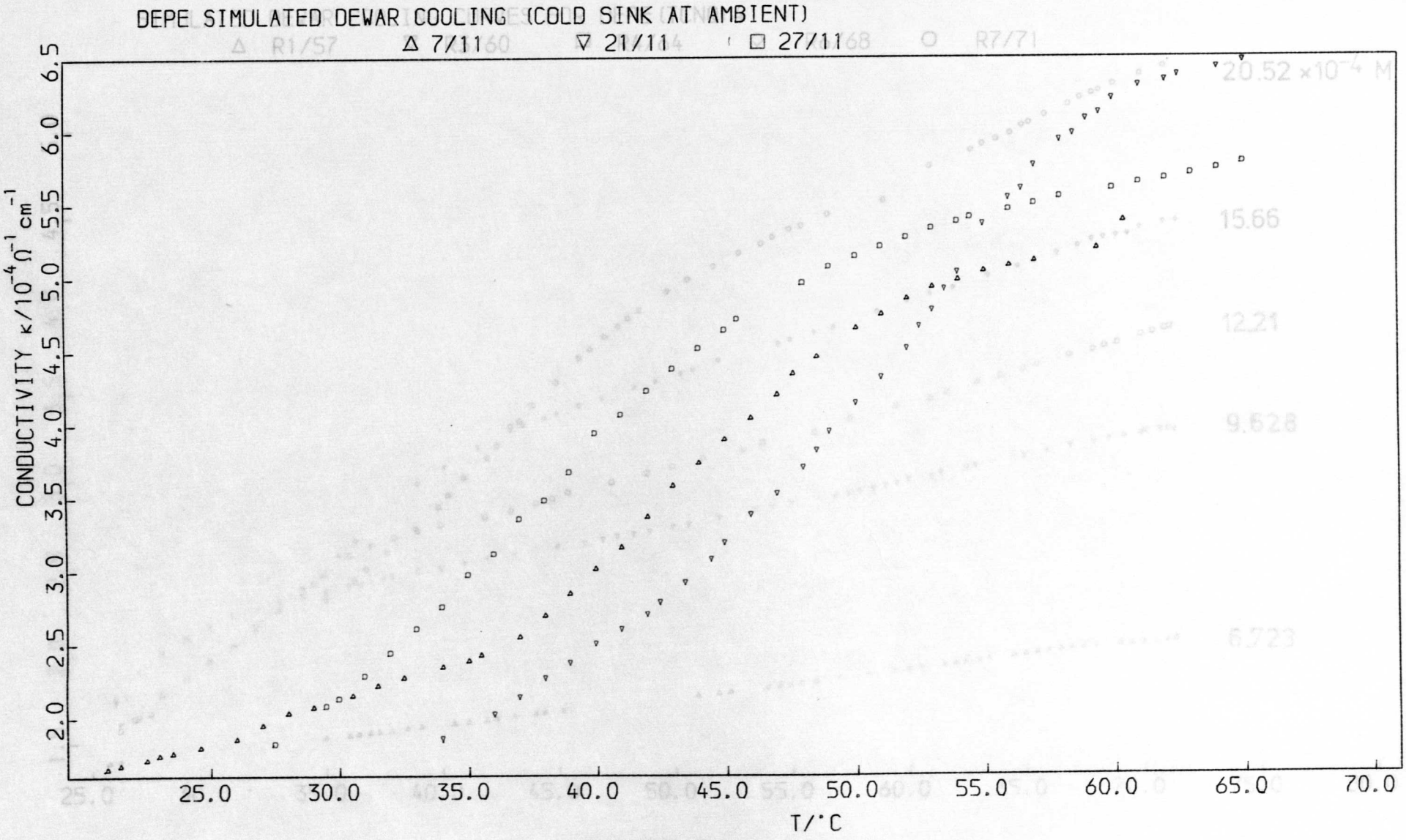
DEPE SIMULATED DEWAR COOLING (COLD SINK AT AMBIENT)
Δ 7/11
▽ 21/11
□ 27/11
CONDUCTIVITY κ/10⁻⁴Ω⁻¹cm⁻¹
2.0
2.5
3.0
3.5
4.0
4.5
5.0
5.5
6.0
6.5
25.0
30.0
35.0
40.0
45.0
50.0
55.0
60.0
65.0
70.0
T/°C

FIGURE 7.1

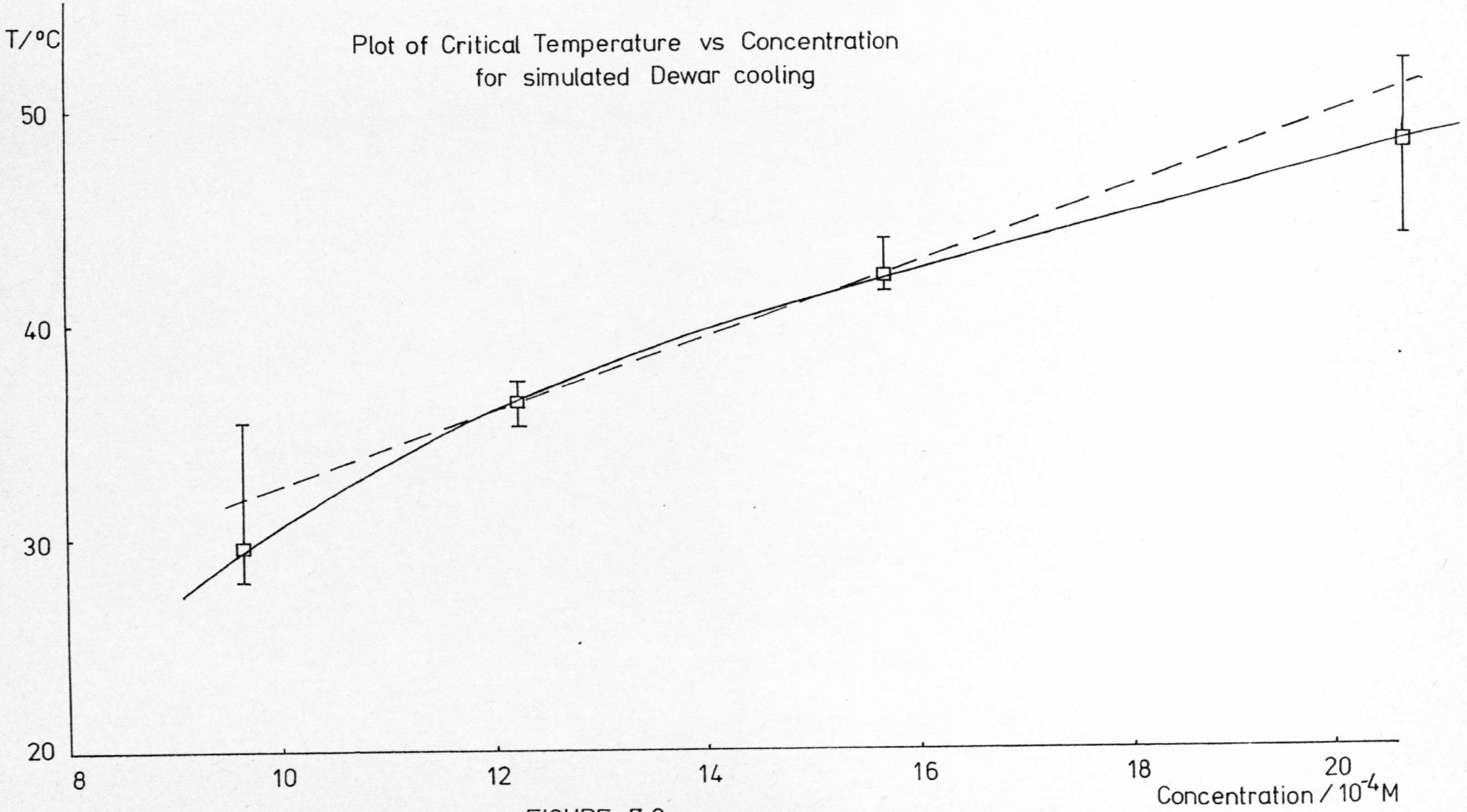
Plot of Critical Temperature vs Concentration
for simulated Dewar cooling
T/°C
50
40
30
20
8
10
12
14
16
18
20
Concentration / 10^{-4}M

FIGURE 7.3

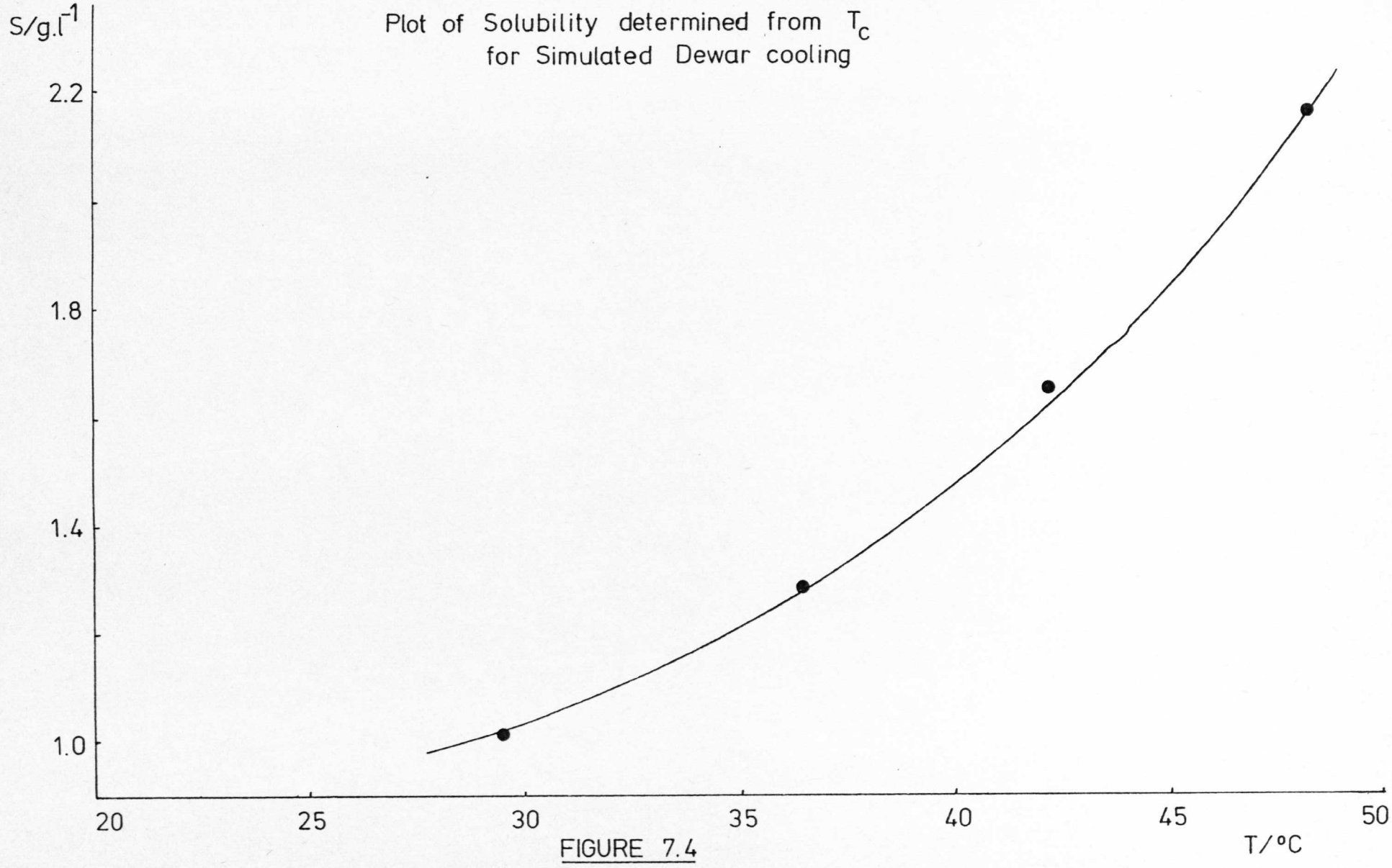
Plot of Solubility determined from T_c
for Simulated Dewar cooling
S/g.l^{-1}
2.2
1.8
1.4
1.0
20
25
30
35
40
45
50
T/°C

FIGURE 7.4

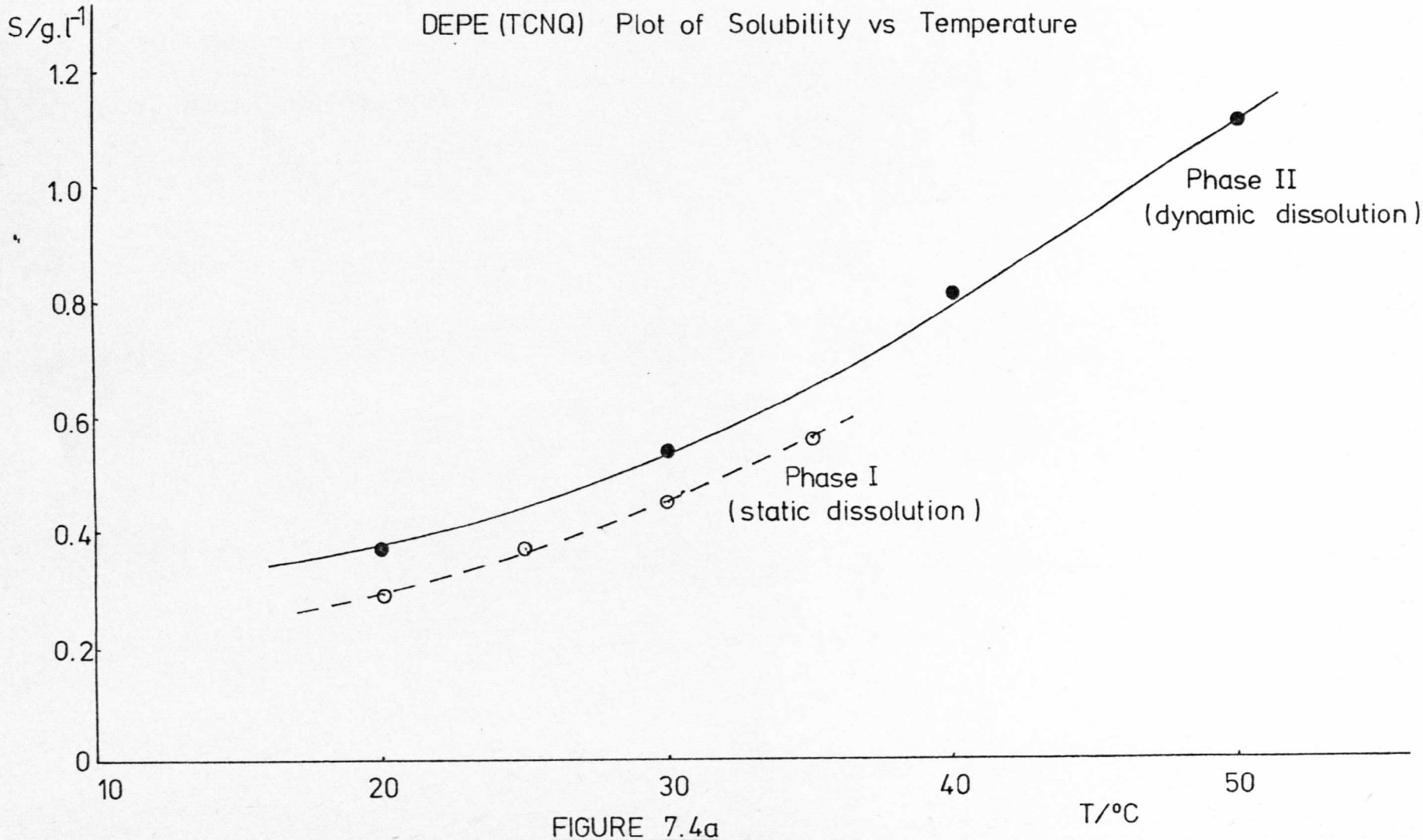
DEPE (TCNQ) Plot of Solubility vs Temperature
S/g.l⁻¹
1.2
1.0
0.8
0.6
0.4
0.2
0
10
20
30
40
50
T/°C
Phase II
(dynamic dissolution)
Phase I
(static dissolution)

FIGURE 7.4a

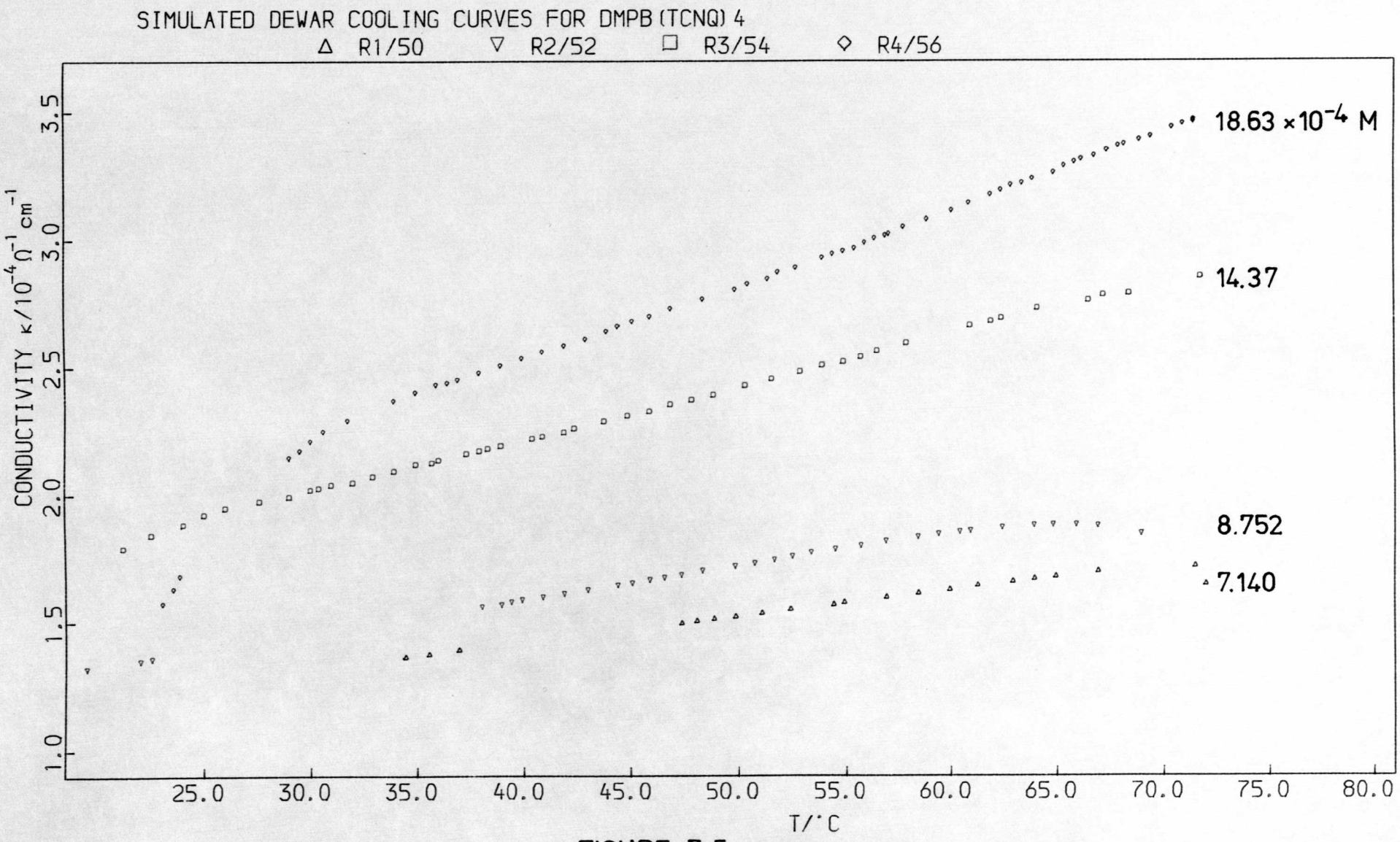
SIMULATED DEWAR COOLING CURVES FOR DMPB(TCNQ)4
Δ R1/50
▽ R2/52
□ R3/54
◇ R4/56
CONDUCTIVITY κ/10⁻⁴Ω⁻¹cm⁻¹
1.0
1.5
2.0
2.5
3.0
3.5
25.0
30.0
35.0
40.0
45.0
50.0
55.0
60.0
65.0
70.0
75.0
80.0
T/°C
18.63 ×10⁻⁴ M
14.37
8.752
7.140

FIGURE 7.5

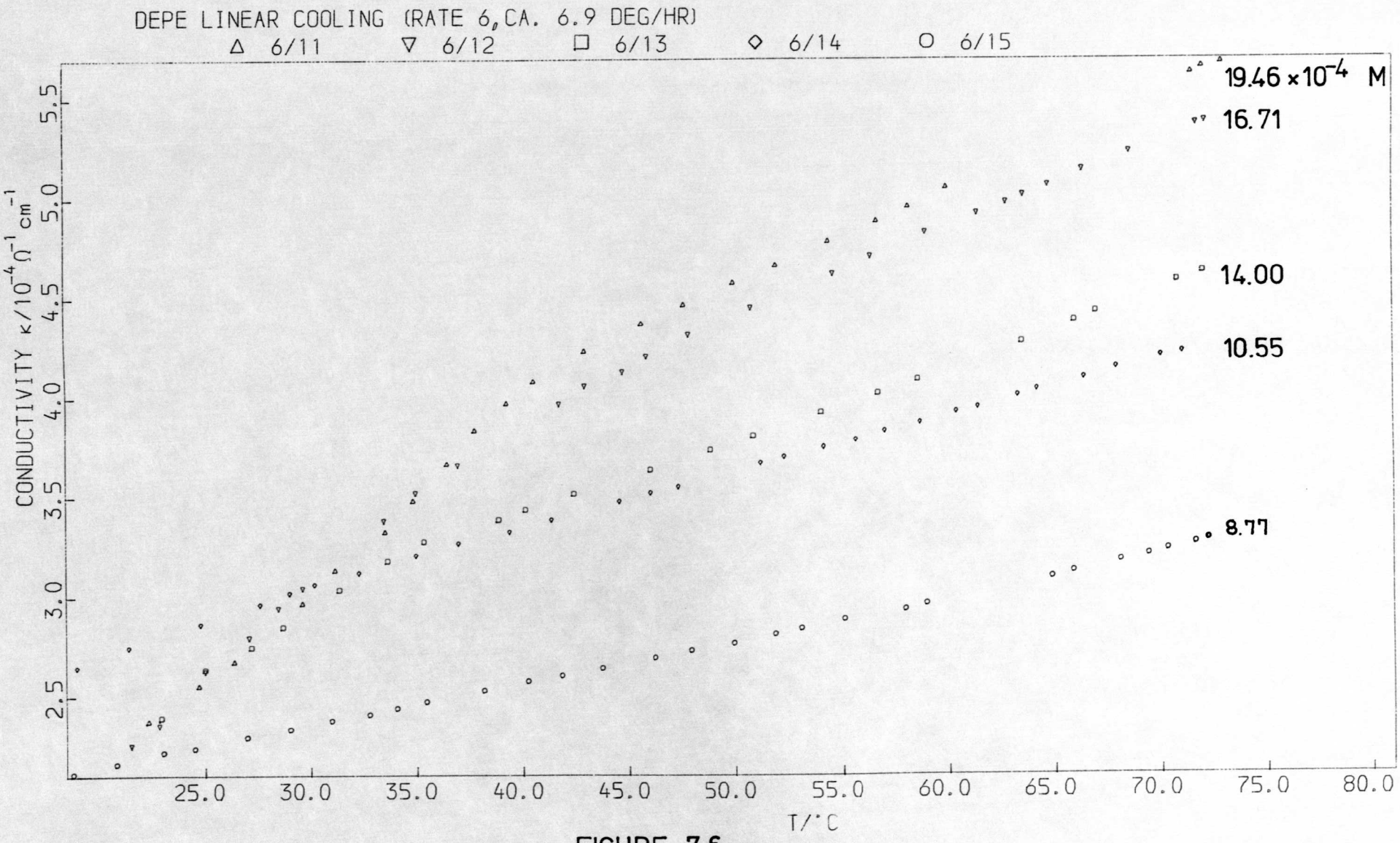
DEPE LINEAR COOLING (RATE 6, CA. 6.9 DEG/HR)
△ 6/11
▽ 6/12
□ 6/13
◇ 6/14
○ 6/15
19.46 × 10⁻⁴ M
16.71
14.00
10.55
8.77
CONDUCTIVITY κ/10⁻⁴Ω⁻¹ cm⁻¹
2.5
3.0
3.5
4.0
4.5
5.0
5.5
25.0
30.0
35.0
40.0
45.0
50.0
55.0
60.0
65.0
70.0
75.0
80.0
T/°C

FIGURE 7.6

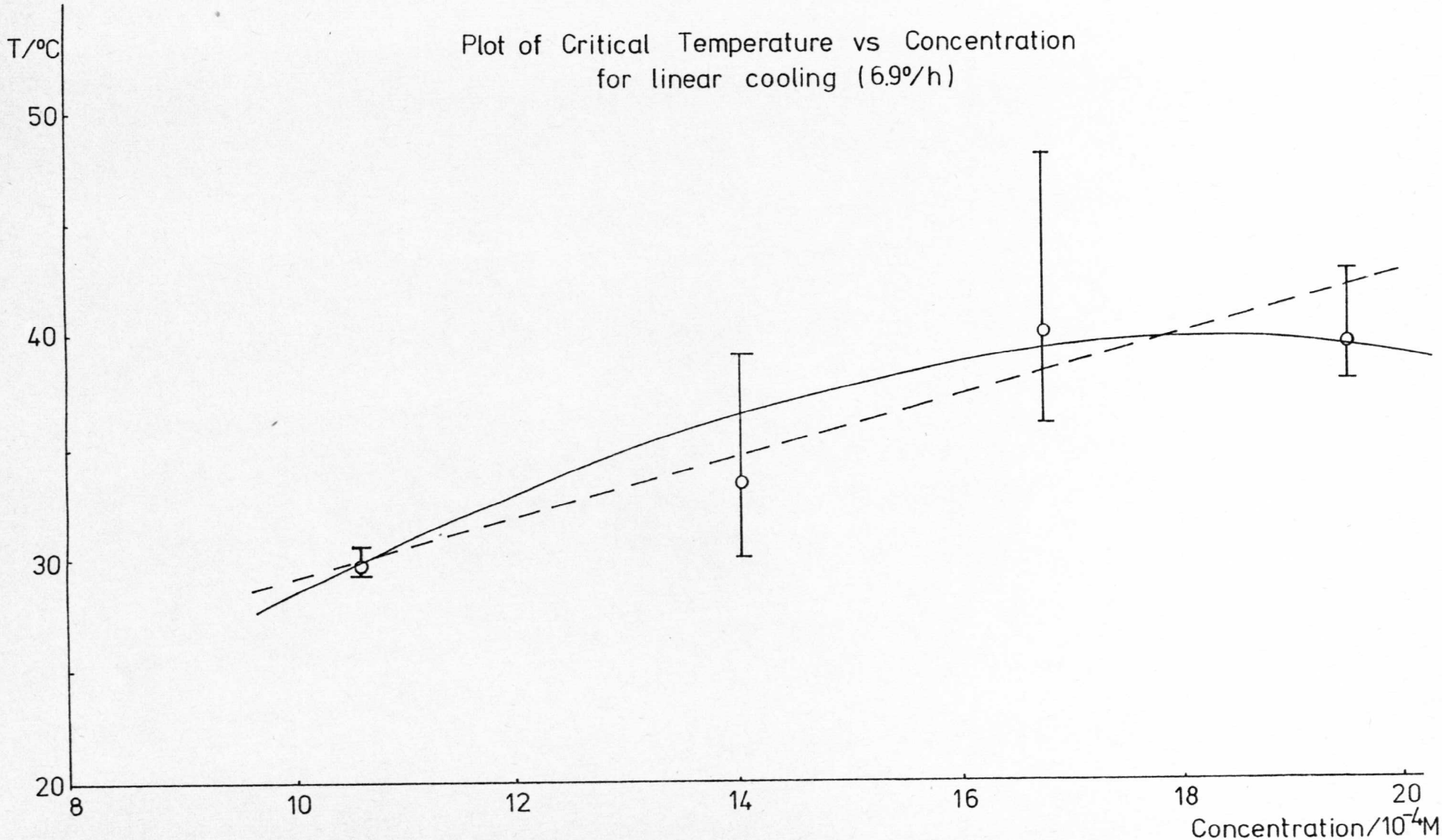
Plot of Critical Temperature vs Concentration
for linear cooling (6.9°/h)
T/°C
50
40
30
20
8
10
12
14
16
18
20
Concentration/10^{-4}M

FIGURE 7.7

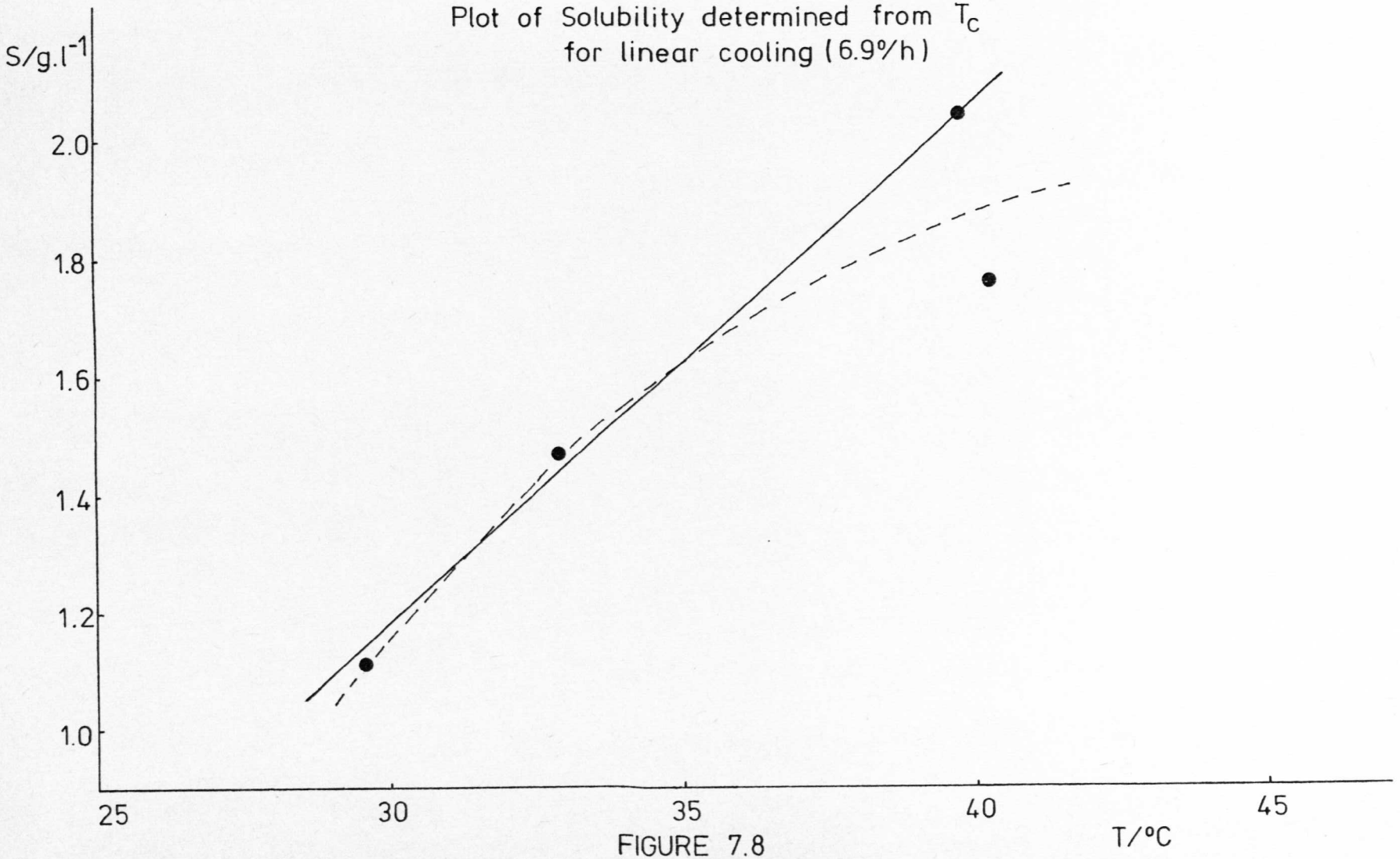
Plot of Solubility determined from T_c
for linear cooling (6.9%/h)
S/g.l^{-1}
2.0
1.8
1.6
1.4
1.2
1.0
25
30
35
40
45
T/°C

FIGURE 7.8

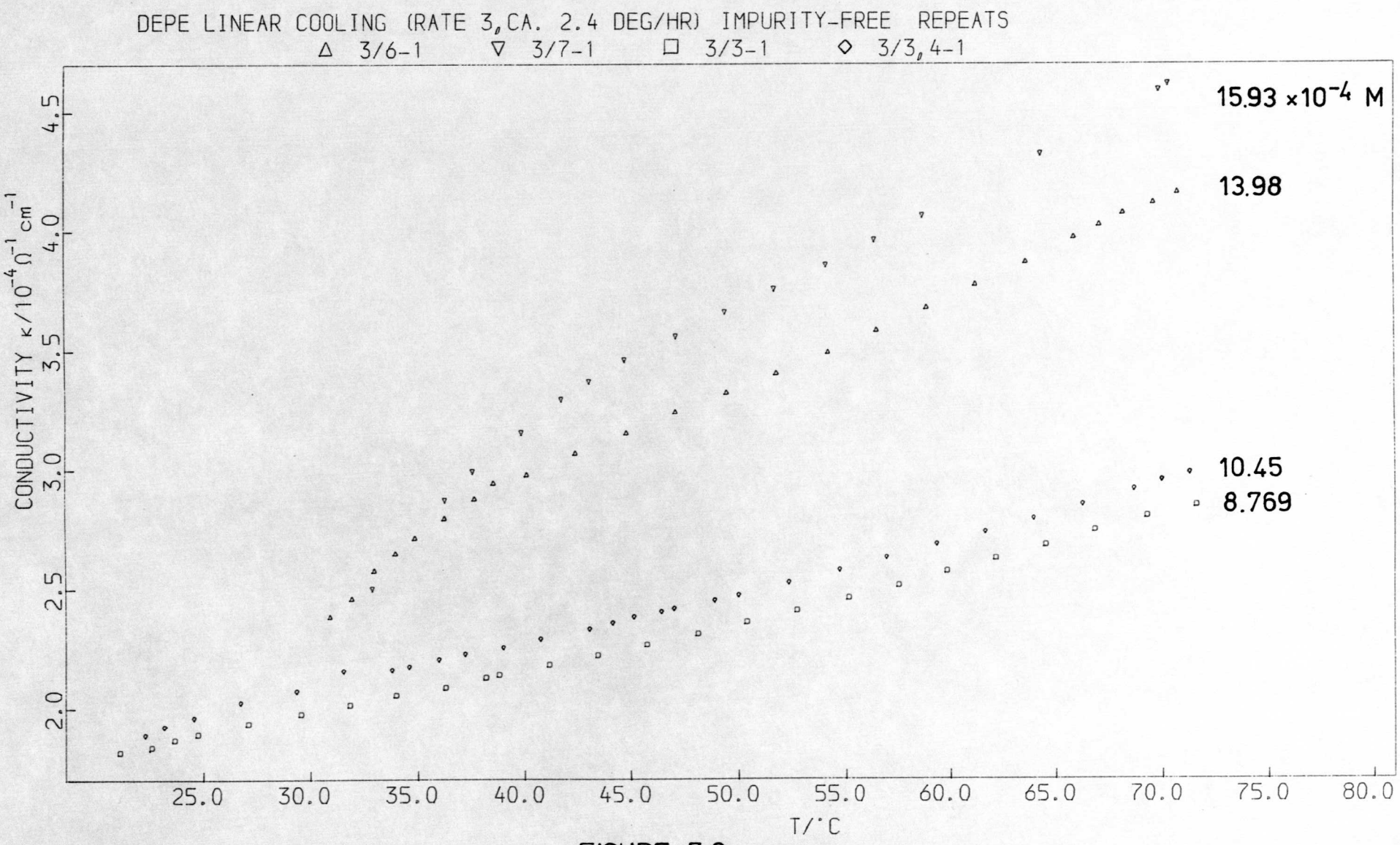
DEPE LINEAR COOLING (RATE 3, CA. 2.4 DEG/HR) IMPURITY-FREE REPEATS
△ 3/6-1
▽ 3/7-1
□ 3/3-1
◇ 3/3, 4-1
15.93 ×10⁻⁴ M
13.98
10.45
8.769
CONDUCTIVITY κ/10⁻⁴Ω⁻¹cm⁻¹
2.0
2.5
3.0
3.5
4.0
4.5
25.0
30.0
35.0
40.0
45.0
50.0
55.0
60.0
65.0
70.0
75.0
80.0
T/°C

FIGURE 7.9

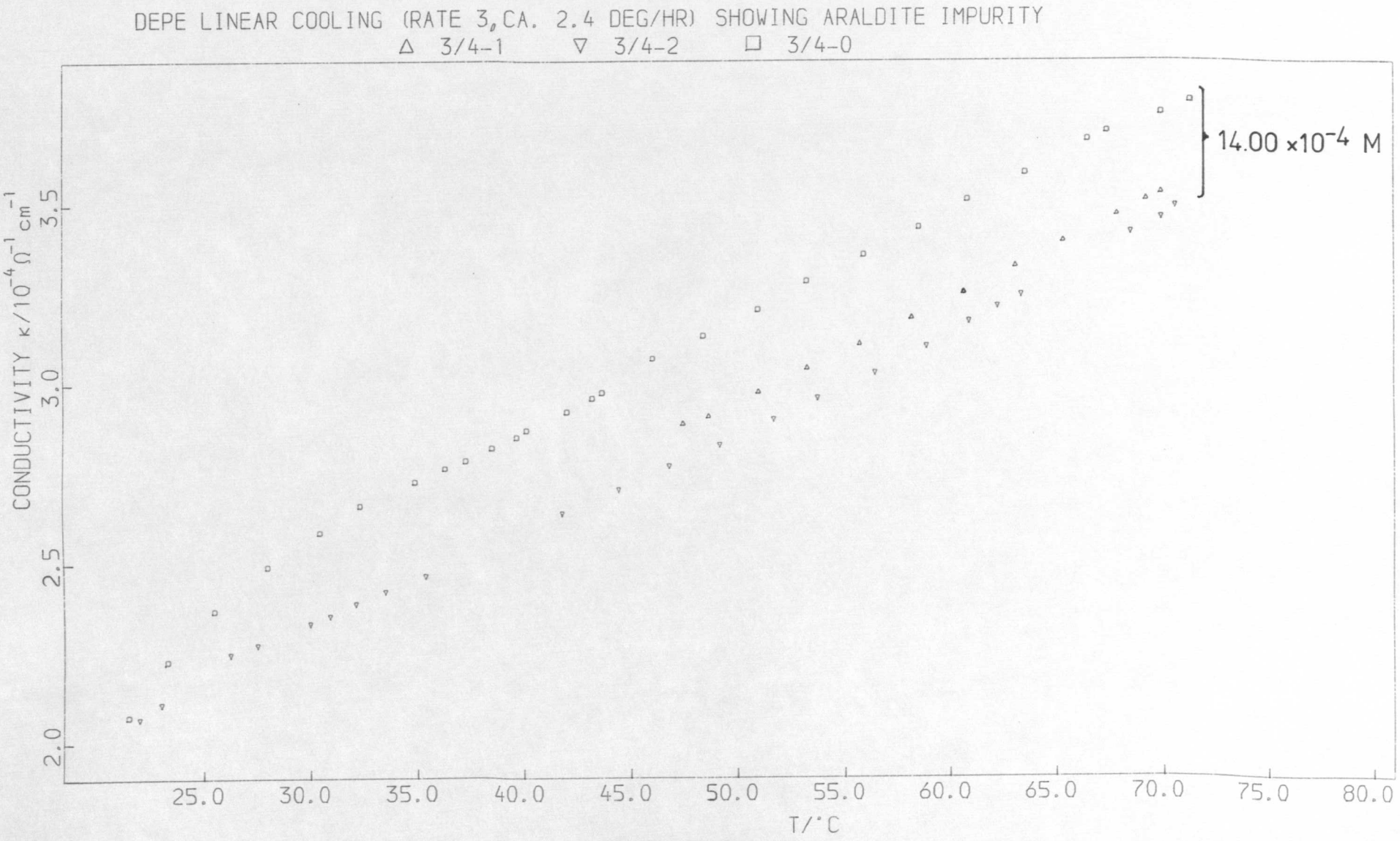
DEPE LINEAR COOLING (RATE 3, CA. 2.4 DEG/HR) SHOWING ARALDITE IMPURITY
△ 3/4-1 ▽ 3/4-2 □ 3/4-0
14.00 ×10⁻⁴ M
CONDUCTIVITY κ/10⁻⁴Ω⁻¹cm⁻¹
2.0
2.5
3.0
3.5
25.0
30.0
35.0
40.0
45.0
50.0
55.0
60.0
65.0
70.0
75.0
80.0
T/°C

FIGURE 7.10

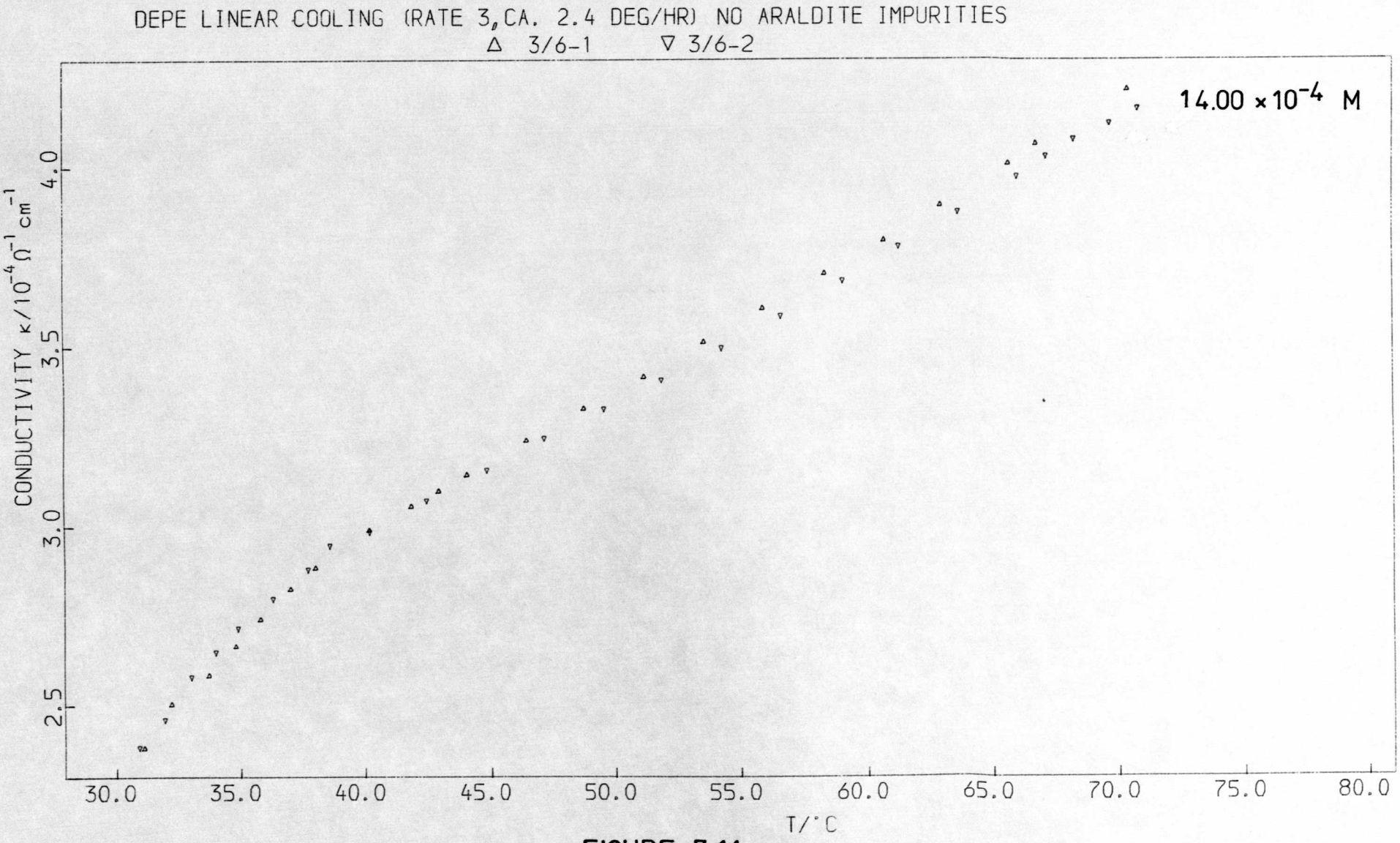
DEPE LINEAR COOLING (RATE 3, CA. 2.4 DEG/HR) NO ARALDITE IMPURITIES
△ 3/6-1 ▽ 3/6-2
14.00 × 10⁻⁴ M
CONDUCTIVITY κ/10⁻⁴ Ω⁻¹ cm⁻¹
2.5
3.0
3.5
4.0
30.0
35.0
40.0
45.0
50.0
55.0
60.0
65.0
70.0
75.0
80.0
T/°C

FIGURE 7.11

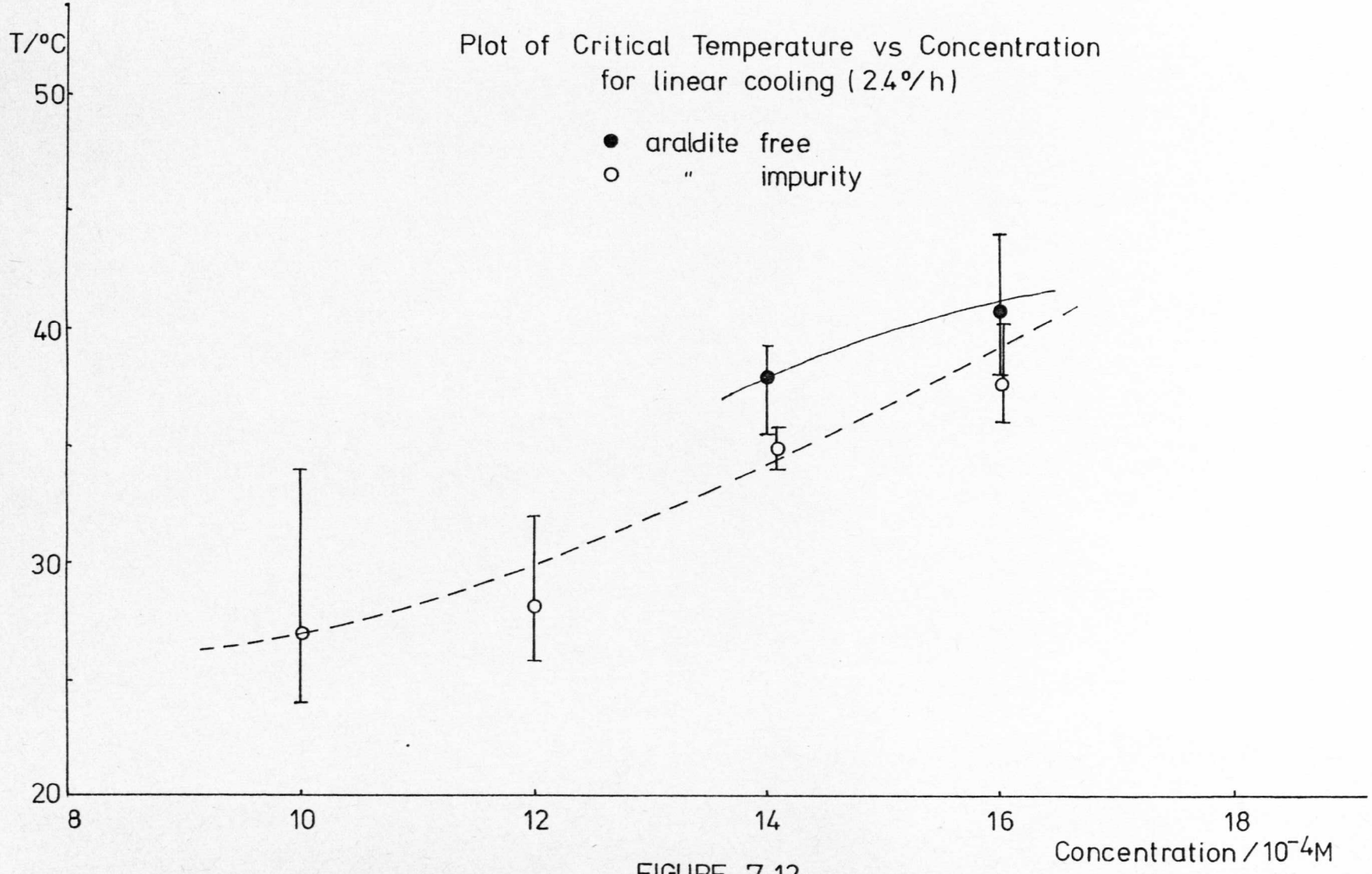
Plot of Critical Temperature vs Concentration
for linear cooling (2.4°/h)
● araldite free
○ " impurity
T/°C
50
40
30
20
8
10
12
14
16
18
Concentration / 10^{-4}M

FIGURE 7.12

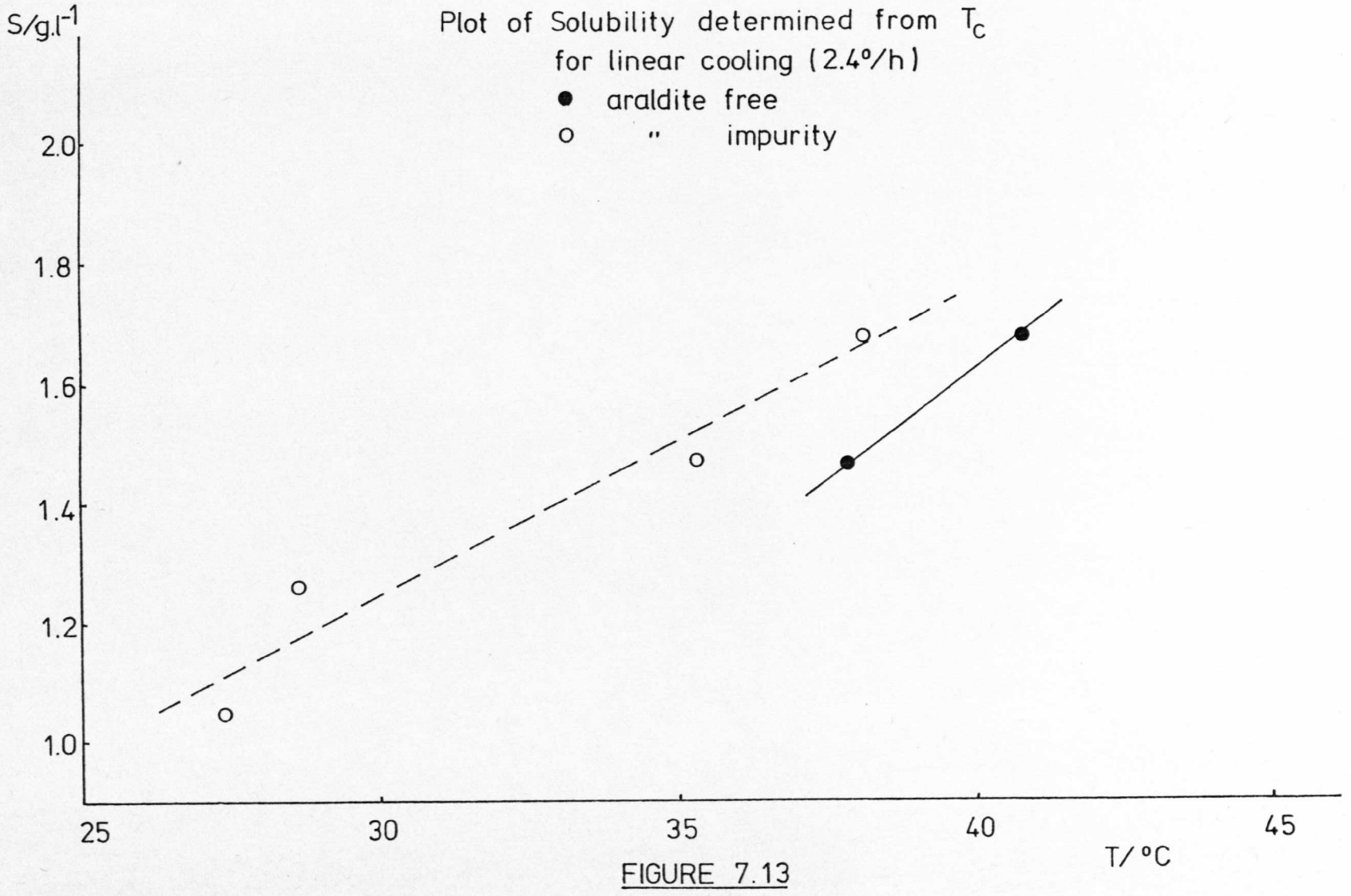
Plot of Solubility determined from T_c
for linear cooling (2.4°/h)
● araldite free
o " impurity
S/g.l^{-1}
2.0
1.8
1.6
1.4
1.2
1.0
25
30
35
40
45
T/ °C

FIGURE 7.13

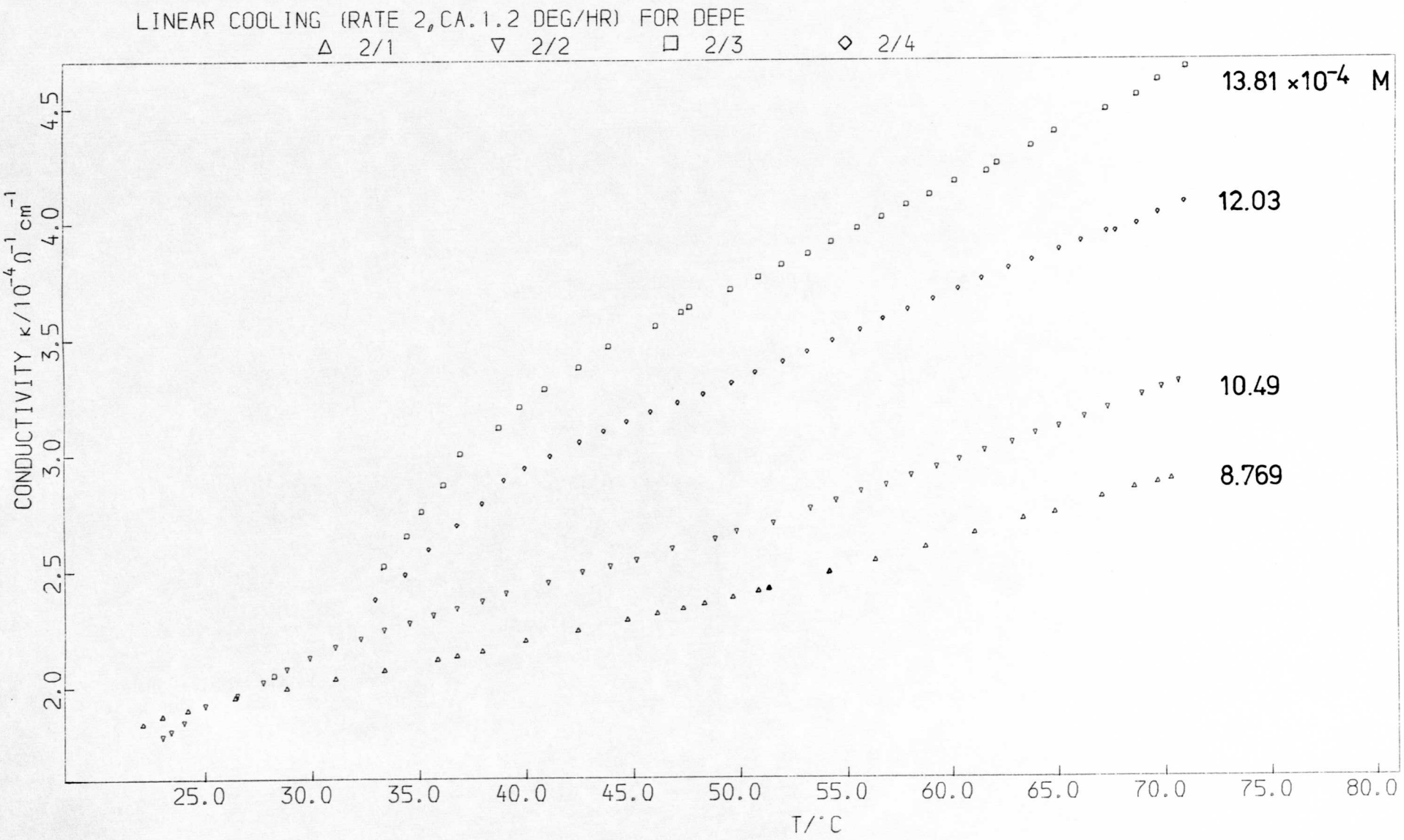
LINEAR COOLING (RATE 2, CA. 1.2 DEG/HR) FOR DEPE
△ 2/1
▽ 2/2
□ 2/3
◇ 2/4
13.81 ×10⁻⁴ M
12.03
10.49
8.769
CONDUCTIVITY κ/10⁻⁴Ω⁻¹cm⁻¹
2.0
2.5
3.0
3.5
4.0
4.5
25.0
30.0
35.0
40.0
45.0
50.0
55.0
60.0
65.0
70.0
75.0
80.0
T/°C

FIGURE 7.14

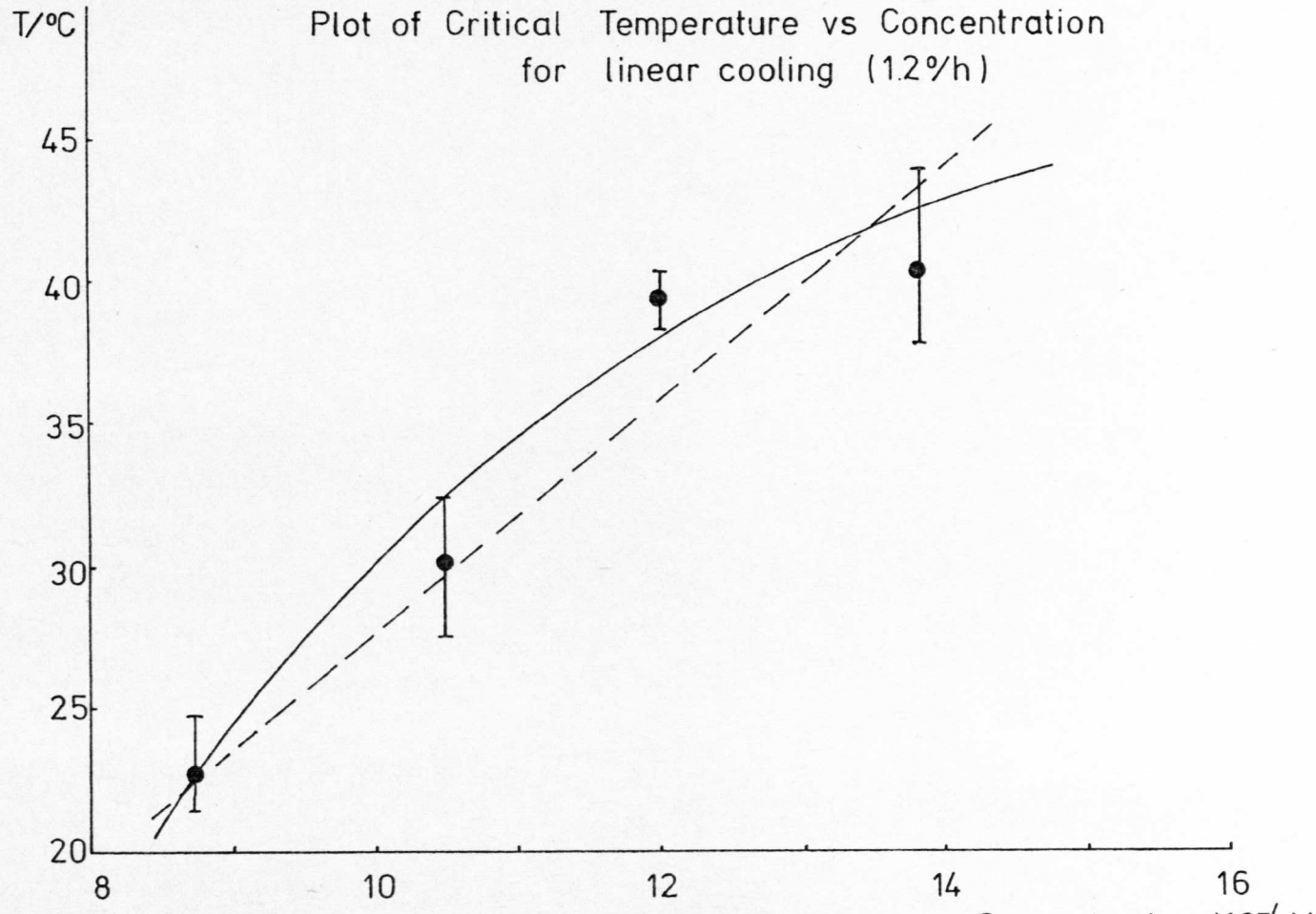
Plot of Critical Temperature vs Concentration
for linear cooling (1.2%/h)
T/°C
45
40
35
30
25
20
8
10
12
14
16
Concentration / 10^{-4} M

FIGURE 7.15

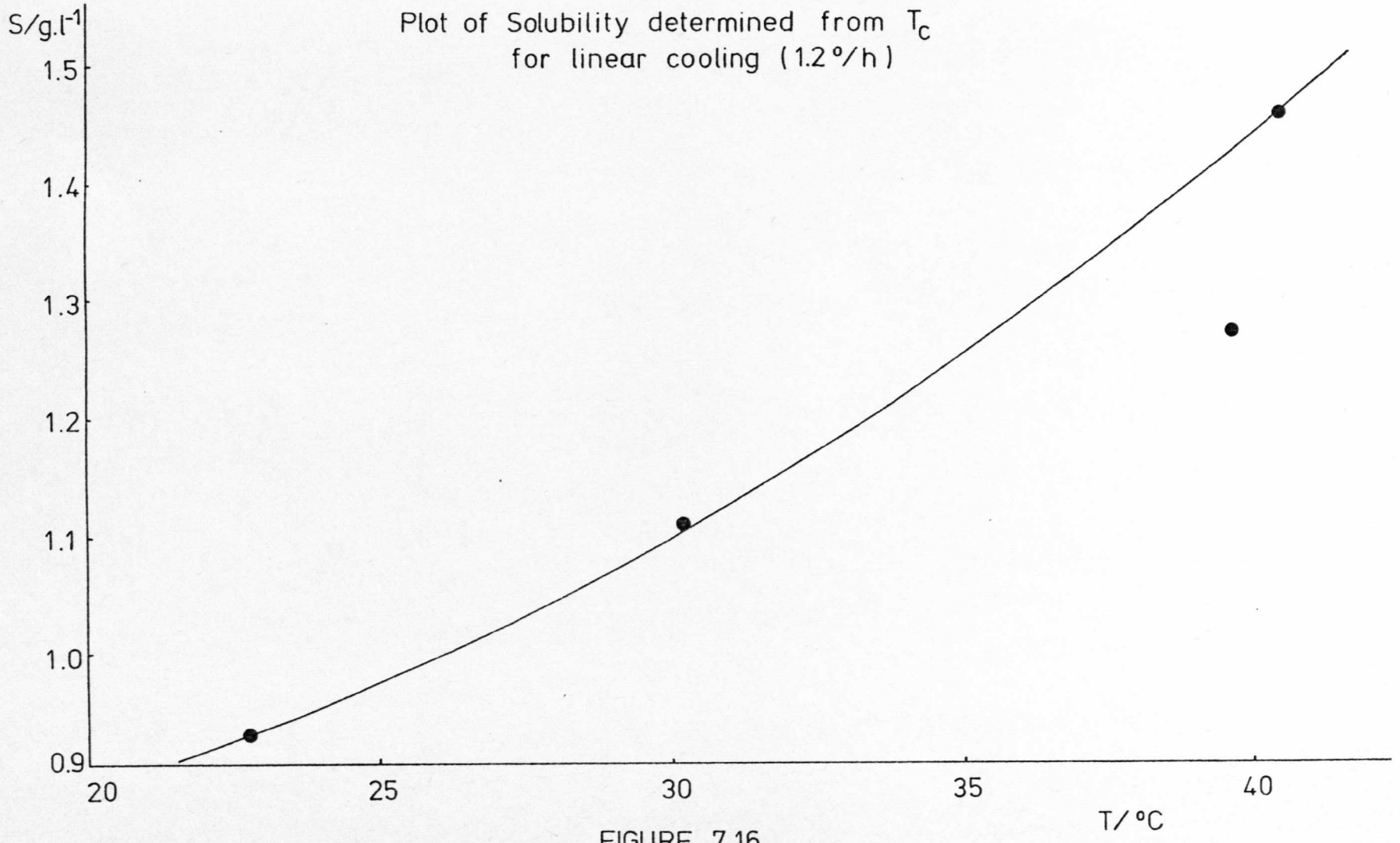
Plot of Solubility determined from T_c
for linear cooling (1.2°/h)
S/g.l^{-1}
1.5
1.4
1.3
1.2
1.1
1.0
0.9
20
25
30
35
40
T/°C

FIGURE 7.16

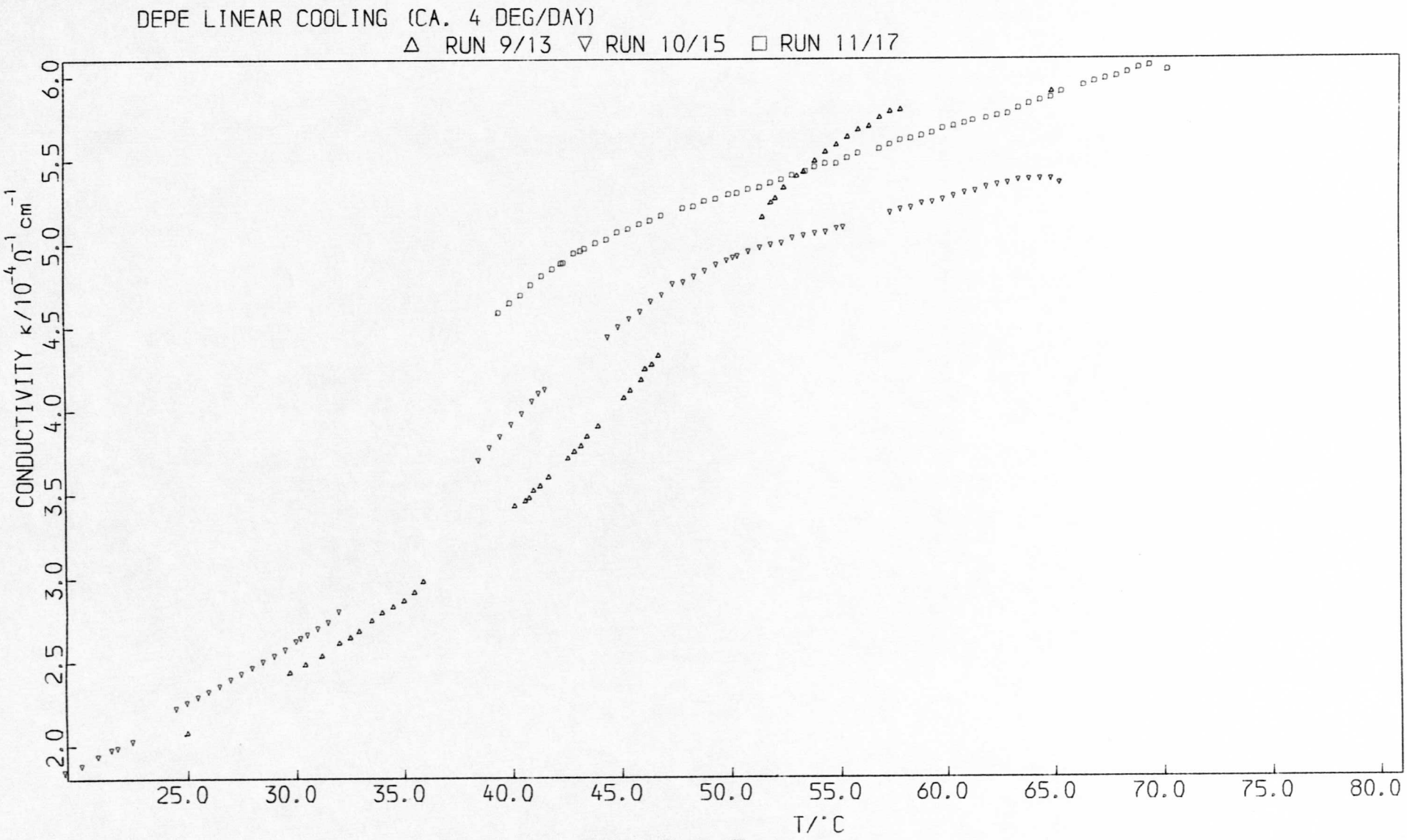
DEPE LINEAR COOLING (CA. 4 DEG/DAY)
△ RUN 9/13 ▽ RUN 10/15 □ RUN 11/17
CONDUCTIVITY κ/10⁻⁴Ω⁻¹cm⁻¹
2.0
2.5
3.0
3.5
4.0
4.5
5.0
5.5
6.0
25.0
30.0
35.0
40.0
45.0
50.0
55.0
60.0
65.0
70.0
75.0
80.0
T/°C

FIGURE 7.17

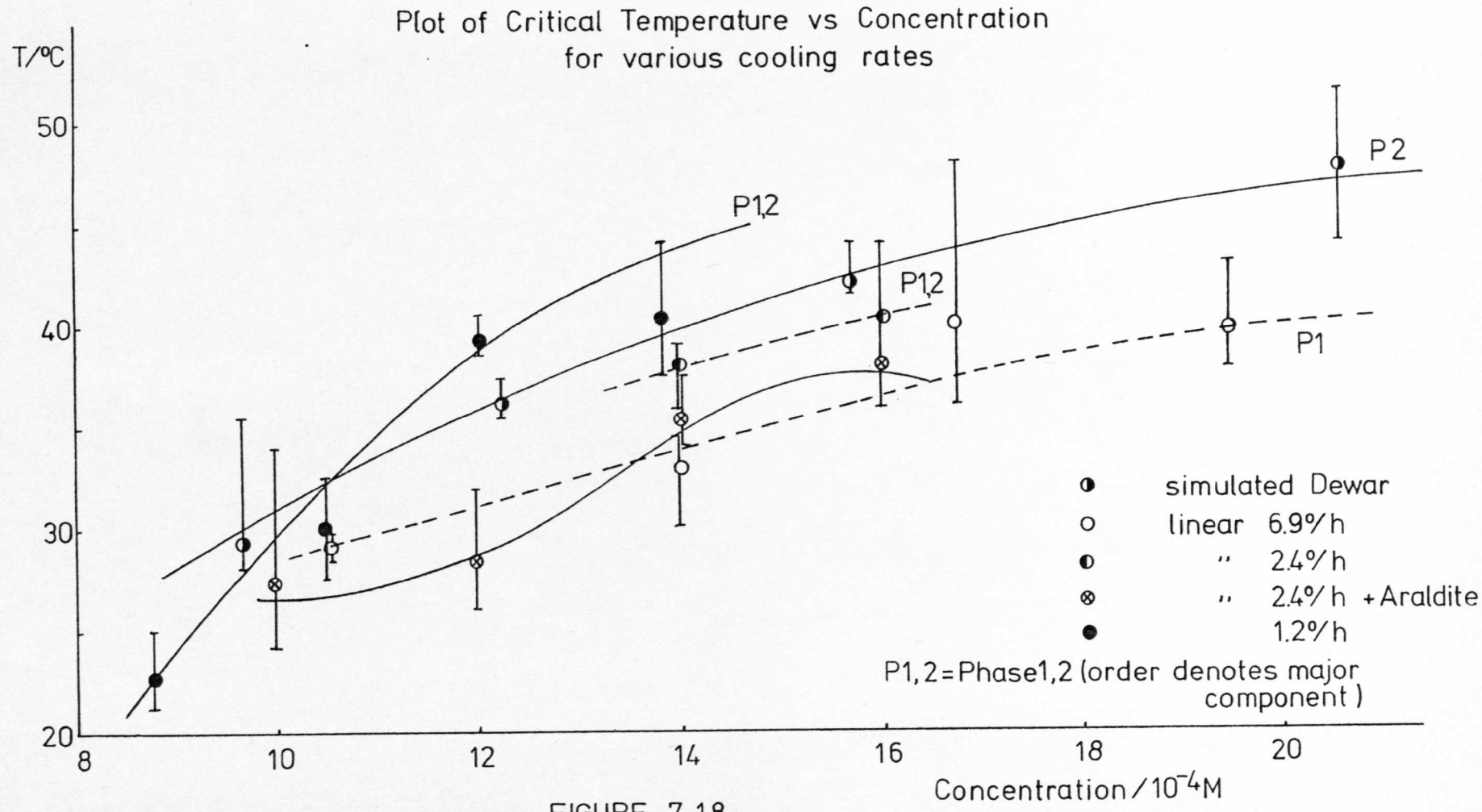
Plot of Critical Temperature vs Concentration
for various cooling rates
T/°C
50
40
30
20
8
10
12
14
16
18
20
Concentration / 10^{-4}M
P1,2
P1,2
P2
P1
simulated Dewar
linear 6.9%/h
" 2.4%/h
" 2.4%/h + Araldite
1.2%/h
P1,2=Phase1,2 (order denotes major component)

FIGURE 7.18

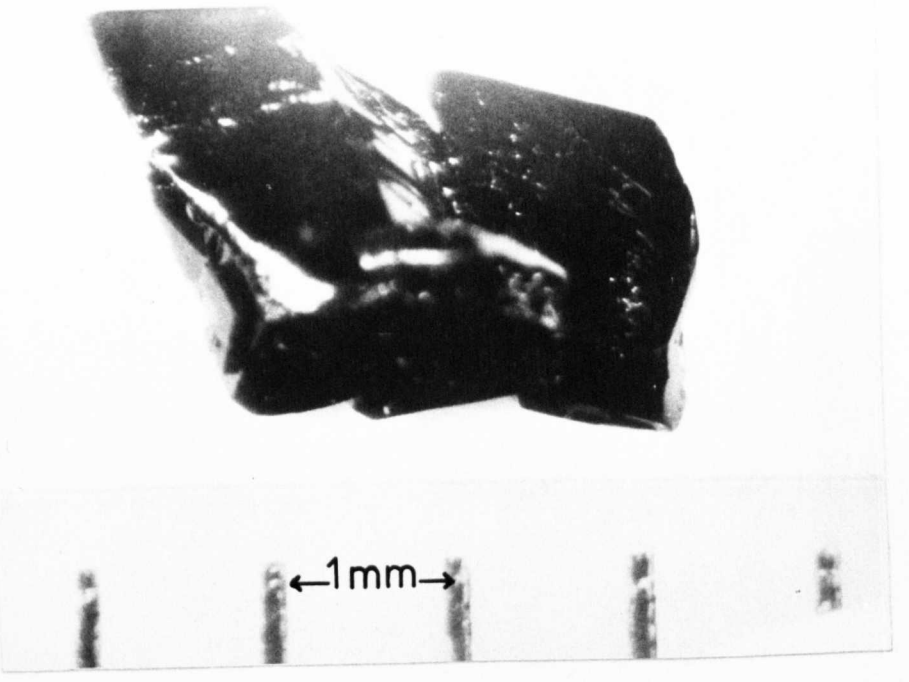

DEPE S10

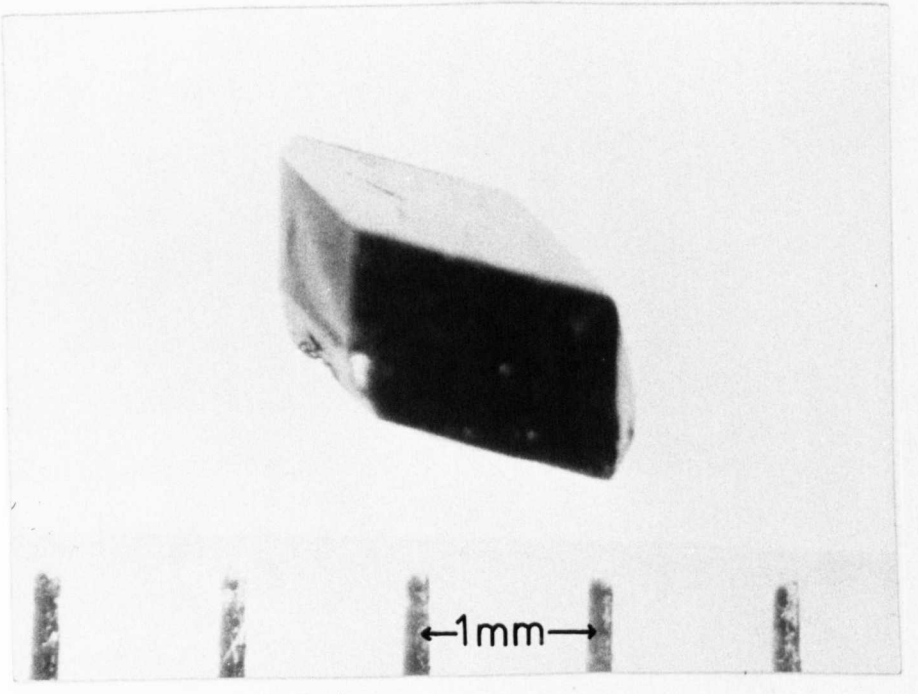

DEPE S4

PLATE 7.1

DEPE $(TCNQ)_4$ - well formed crystals from Ph II simulated Dewar cooling.

References for Chapters 6, 7.

1. J. O'Donnell, J. Agres and C. Mann; Anal. Chem (1965), 37, 1161.
2. M. Maruyama, Nippon Kagaku Kaishi (1978), 8, 1106.
3. J.A. Riddick and W.B. Bunger, 'Organic Solvents', Wiley, N.Y. (3rd ed.) 1970.
4. Walden and Burr, Z. Phys. Chem. (Leipzeig) (1929), 144A, 269.
5. L.W. Melby et al., J. Am. Chem. Soc. (1962) 84, 3374.
6. D.R. Burfield, Kin Her Lee and R.H. Smithers, J. Org. Chem. (1977), 42, 3060.
7. J. Neel and P. Dupuis, J. Etat. Solide (1970), 5, 91.
8. Y. Akihiko and S. Masahiro, Bull. Chem. Soc. Japan (1974), 47, 2152.
9. L.B. Coleman, Ph.D. Thesis, University of Pennsylvania (1975).
10. D.R. Burfield, Guat-Hong Gan and R.H. Smithers, J. Appl. Chem. Biotech., (1978) 28, 23.
11. A. Barbetta and W. Edgell, Appl. Spec. (1978), 32, 93.
12. L.B. Coleman, Phys. Rev. Lett. (1972), 29, 269.
13. J.N. Sherwood, Personal Communication.
14. P.S. Acker et al., J. Am. Chem. Soc. (1960) 82, 6408.
15. N.J. Drew, Ph.D. Thesis, University of Nottingham (1978).
16. R.B. Somoano et al, J. Chem. Phys. (1975), 62, 1061.
17. G.J. Ashwell, Phys. Stat. Sol. (b) (1978), 85,K7.
18. G.J. Ashwell, Personal Communication.
19. P.A. Kinzie, 'Thermocouple Temperature Measurements', Wiley Interscience (1973)
20. G.D. Welch, Ph.D. Thesis, University of Nottingham (1976)

21. G.J. Ashwell, Ph.D. Thesis, University of Nottingham (1972)

22. M. Murakami and S. Yoshimura, Bull. Chem. Soc. Japan (1978) 48, 157.

23. A. Rembaum, A. Herman, F. Stuart and F. Gutman, J. Phys. Chem. (1969), 73, 513.

24. A. Blyth, Boon, and P, Wright, Disc. Farad. Soc. (1971) 51, 110.

25. D.R. Rosseinsky, P. Kathigamanathan, and S.A. Mucklejohn, J.C.S. Chem. Com. (1979), 86.

26. D.R. Rosseinsky, Patent, April 1980.

27. M. Scarlett and P. Stallwood, Project Report, University of Nottingham (1979).

28. A. Hobbs, Project Report, University of Nottingham (1980).

29. G. Wernimont and F.J. Hopkins, Ind. and Eng. Chem. Anal. Ed. (1943), 15, 272.

30. P. Jackson, Ph.D. Thesis, University of Nottingham (1969)

31. T. K emény, Z. Pokó, G. Mihály, K. Holczer and G. Grű ner, Cent. Res. Inst. Phys. KFKI-1978-4.

32. E. Simonyi, J.F. Graczyk and J.B. Torrance, IBM J. Res. Dev. (1978) 22, 315.

33. G.J. Ashwell, D.D. Eley, S.C. Wallwork, M.R. Willis and J. Woodward Anals. N.Y. Acad. Sci (1978), 313, 417.

34. R.A. Robinson and R.H. Stokes, 'Electrolyte Solutions', Butterworth (1970).

35. G. Jones and R.C. Josephs, J. Am. Chem. Soc. (1928), 50, 1049.

36. J. Barthel, F. Freuerlein, R. Neuder and R. Wachter, J. Sol. Chem. (1980), 9, 206.

37. L.R. Melby et al., J. Am. Chem. Soc. (1960), 82, 6408.

38. A. Yamagishi and M. Sakamoto, Bull. Chem. Soc. Jap. (1974), 49, 2152.

39. A. Ohki, T. Nishiguchi and K. Fukuzumi, J. Org. Chem. (1979) 44, 766.

40. A. Ohki, T. Mishiguchi, K. Fukuzumi, Tet. (1979), 35(14), 1737-43

CONCLUSIONS

The structural studies reported in this work, whilst all being connected with the present research effort within the department into high/low conductivity organic salts based on the radical ion $TCNQ^{\cdot-}$, fall into two categories. The first group are those structures analysed in an attempt to clarify the three-phase system reported for DEPE $(TCNQ)_4$ and the second group are those structures investigated in connection with the studies of controlled phase formation by electrocrystallisation techniques.

The structural and d.c. conductivity analyses of the DMPY and DMPB complex salts show no evidence of multiple phase formation and possess structures which are typical of low conductivity (σ ca. 10^{-4} ohm^{-1} cm^{-1}) TCNQ complex salts. They show no unusual features in terms of the stacking of the TCNQ moieties, with only 'ring-exocyclic bond' and 'displaced molecule' overlaps being observed and involving molecular separations which are quite typical of these materials and show no unexpected interactions. It is therefore concluded that the DEPE $(TCNQ)_4$ highly conducting form (phase 1) does not consist of half-cation fragments from some (perhaps) radical-induced degradation of the DEPE cation species, as has been postulated to account for the presence of the formally impossible 'whole' cation within the $P2_{1/c}$ cell proposed. It therefore seems most probable that the DEPE structure is disordered and possesseseither a non-commensurate cation lattice or, as has been

alternatively postulated, a non-commensurate occluded water lattice, thus explaining the diffuse intermediate layer lines observed in the diffraction pattern and the overall poor quality of the data.

The radical-ion-induced dimerisation postulated for the DMPB structure (Chapter 3) may provide a new route for the synthesis of novel bipyridyl-type cations where the in-situ formation of such cations may be required (for example in those cases where the reactant cation salts used in the synthesis are unstable or possess undesirable properties such as being air sensitive or highly hygroscopic).

The structural analyses of the materials prepared by electrocrystallisation indicate the value of this technique in the controlled production of different conductivity phases of these compounds. The relative ease of production of the crystals of the high-conductivity phase of DHPA $(TCNQ)_4$ and the simple salt DHPA $(TCNQ)_2$, coupled with the development potential of this technique in terms of the crystalline perfection obtainable, indicate that consideration should be given to a more intensive research program in this area.

The results of the crystallisation studies show that phase formation is most easily controlled, under the present single rate linear cooling regimes, at cooling rates of *ca.* 1.2°C/hr. At this rate, phase formation may be controlled by variation of the concentration of the solution with phase 2 material crystallising as the major or sole component at concentrations below approximately 10^{-3}M and phase 1 material at concentrations above this. Further studies in this area would be most desirable and some consideration should be given to the use of alternative related solvents such as benzyl cyanide and

ethyl cyanide, multiple linear cooling programs, growth in electrical and magnetic fields and the design of a circulatory thermostated cell with facilities for simultaneous a.c. conductance and sample withdrawal, together with a short path length section with which to make visual and spectrophotometric observations in situ. This would also enable measurements of anisotropic growth rates to be made directly and related to the removal of material from the solution to the solid phase as determined conductometrically and spectrophotometrically.

APPENDIX

Other Related Structures with which the author has been significantly involved during the period of this work

1) 1,2-bis(1-(4-cyanobenzyl)-4-pyridinio)ethene $(TCNQ)_3$, $DCBP^{2+}\ (TCNQ)_3^{2-}$

In conjunction with Mr. J. Winfield and Ms. A. Shaw.

Data for this compound were collected on the Hilger and Watts instrument at ambient temperature (19°C) using graphite monochromated Mo Kα radiation and corrected for Lorentz and polarisation effects but not for absorption. The structure was solved using the Patterson method on the basis of 4938 significant reflections ($I > 3\sigma(I)$) and refined by least squares block-diagonal matrix techniques to a conventional R = 0.107.

Crystal Data

DCBP $(TCNQ)_3$ $(C_{28}H_{22}N_4)^{2+}(C_{12}H_4N_4)_3^{2-}$ $M_r = 1026.3$

Triclinic, a = 8.02(3), b = 11.65(1), c = 13.771(4) Å

$\alpha = 95.8(3)$, $\beta = 93.1(4)$, $\gamma = 97.5(4)$

U = 1276.0 Å^3, Z = 1, $D_c = 1.335$ g.cm^{-3}, $D_m = 1.32(2)$ g.cm^{-3}

Mo Kα ($\lambda = 0.71069$ Å), $\mu = 0.91$ cm^{-1}

Space group $P\bar{1}$ (number 2) assumed.

Figure 1 shows the structure projected along the a,b, and c axes of the unit cell, together with the molecular overlap diagram.

One TCNQ moiety is centred about the centre of symmetry at 0,0,0 and the other is in a general position. The cation lies centrosymmetrically about $\frac{1}{2},\frac{1}{2},0$ and separates the TCNQ triads in both the y and z directions. Examination of the bond lengths of the TCNQ moieties showed that the majority of the charge is carried by the TCNQ moiety in the general position, however, due to the high standard deviations of the bond lengths it was not possible to say with any greater accuracy what degree of charge each moiety possessed. The bond lengths and angles for the TCNQ moieties and the cation are shown in figure 2.

The angle between the planes of the TCNQ moiety centred about 0,0,0 and that in a general position is 0.65^{o} (based on the mean planes of the two moieties, including centrosymmetrically related atoms as required). This changes to 1.39^{o} when the angle between the planes defined by the ring atoms of each moiety alone are considered. The separation between TCNQ(A) and TCNQ(B) calculated on the basis of the best planes is 3.223 $\mathring{A}$. The benzyl ring of the cation is almost parallel to the TCNQ planes, forming dihedral angles of 13.22 and 12.60^{o} with TCNQ(A) and TCNQ(B) respectively.

Figure 2 shows the bond angles and distances of the cation and TCNQ moieties. The distortion of the benzyl ring and -CN substituent is evident, however, the geometry of the pyridinium ring is similar to that present in the non-cyano substituted analogous complex, 1,2-bis(1-benzyl-4-pyridinio)ethene $(TCNQ)_3$ [1]. Comparison of the molecular arrangements within the cell of both the present structure and that of Ashwell et al shows a greater degree of interaction between the cyano-benzyl-group and the TCNQ moieties than that found

in the benzyl substituted complex, as evidenced by the almost parallel orientation of the cyanobenzyl group with the TCNQ plane.

2) 1,2-bis(1-ethyl-4-pyridinio)ethene (7,7,8,8-tetracyanoquinodimethanide)$_2$, DEPE^{2+}(TCNQ)$_2^{2-}$

In conjunction with Mr. R. Blackmore and Mr. I. Blagborough.

Data for this compound were collected on the Hilger and Watts instrument using graphite monochromated Mo Kα radiation at ambient temperature and corrected for Lorentz and polarisation effects but not for absorption. The structure was eventually solved by a combination of direct methods (MULTAN 78) and Patterson techniques and refined to a conventional R = 0.040 for 2758 independent reflections ($I > 3\sigma(I)$).

Crystal Data

DEPE $(TCNQ)_2$ $(C_{16}H_{20}N_2)^{2+}(C_{12}H_4N_4)_2^{2-}$ $M_r = 648.2$

Triclinic, a = 11.400, b = 13.213, c = 13.315 Å

$\alpha = 95.77$, $\beta = 99.58$, $\gamma = 113.34^{\circ}$

U = 1753.8 Å^3, Z = 2, Dc = 1.227 g.cm^{-3}, Dm = 1.28 g.cm^{-3}

Mo Kα (λ = 0.71069 Å), μ = 0.83 cm^{-1}

Space group $P\bar{1}$ (Number 2), assumed.

Figure 3 shows projections of the cell down the a, b and c axes respectively, together with the molecular overlap diagrams showing overlap of the TCNQ moieties with each other and with the cation (TCNQ(C) only). The structure consists of triads of TCNQ moieties

stacked approximately along [1 0 1] , although the overlap between the ends of the triads is of the displaced molecule type and therefore does not form an infinite stack.

The triads are separated by an interrupted stack of cation and TCNQ moieties which lie approximately parallel to [1 0 0] . The separations of the mean planes of the various moieties are as follows: TCNQ(A) - TCNQ(B) = 3.21Å and TCNQ(C) - CATION = 3.72 Å. The dihedral angle between TCNQ(A) and TCNQ(B) is 1.1° whilst that between TCNQ(A) and TCNQ(C) is 58.8°, with the dihedral angle between the cation and TCNQ(C) being 5.7°. Thus, as is also apparent in the cell diagrams, the cation and the TCNQ moiety (sited across the centre at (0, $\frac{1}{2}$, 0) are almost parallel, with cation and TCNQ(C) moieties making angles of approximately 81° with (0 1 0), 87° with (0 0 1) and 20° with (1 0 0).

Figures 4 and 5 show the molecular geometry of the TCNQ and cation moieties respectively. Calculation of the degree of charge carried by each TCNQ moiety by the method of Chasseau and Flandrois[2] showed TCNQ(A) to carry -0.7e, TCNQ(B) to carry -1.0e and TCNQ(C) to carry -1.0e also. The sum of the charges (-2.7e) is in excess of the predicted -2.0e total (on the basis of charge neutrality). This could be explained either by the presence of positively charged, unaccounted for scattering matter, or by errors in the bond lengths of the moieties. Since a final difference Fourier synthesis failed to reveal the presence of any significant, unaccounted for scattering matter, it must be assumed that the difference in charge is due to

errors of geometry. The geometry of the cation is similar to that of the same cation present in the complex salt DEPE $(TCNQ)_4$ [3].

References

1. G.J. Ashwell, D.D. Eley, A. Harper, A. Torrance, S.C. Wallwork and M.R. Willis, Acta Cryst. (1977), B33, 2258.

2. D. Chasseau and S. Flandrois, Acta Cryst. (1977), B33, 2744.

3. G. Ashwell, D.D. Eley, R. Fleming, S. Wallwork and M. Willis, Acta Cryst. (1976), B32, 2948.

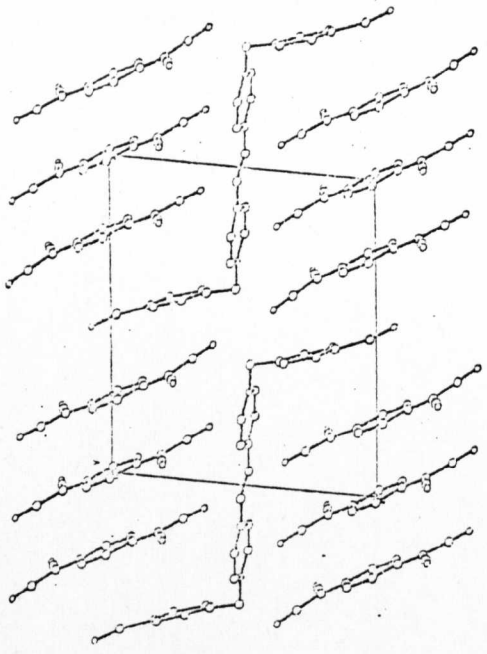

Projection along a

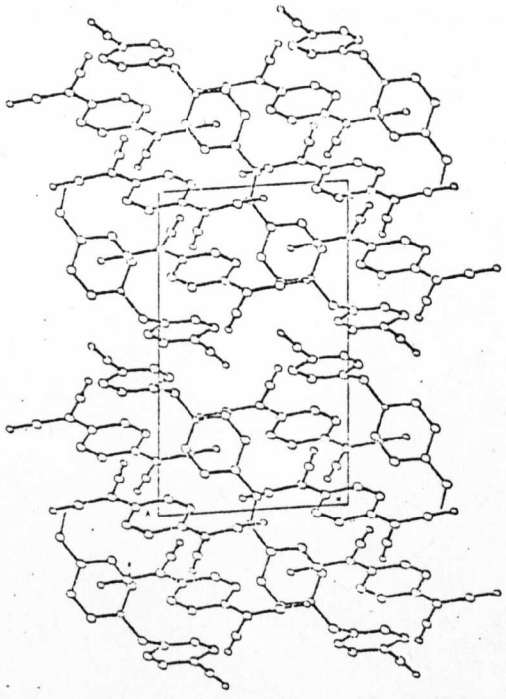

Projection along b

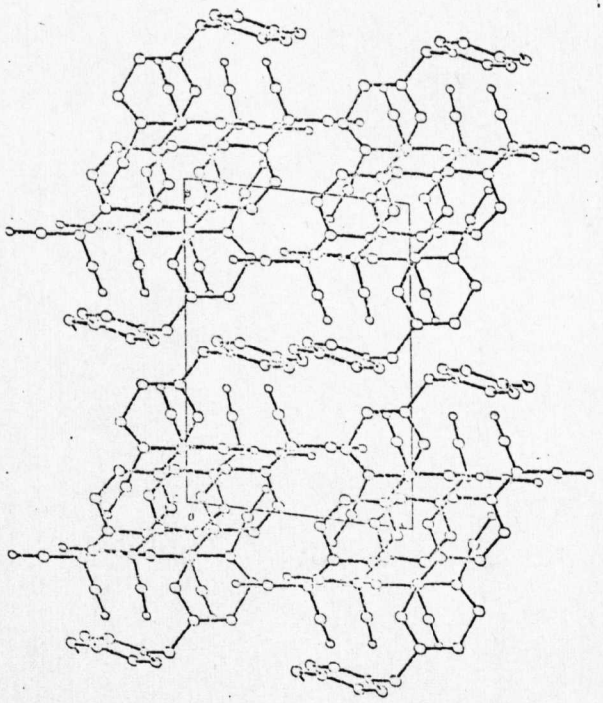

Projection along c

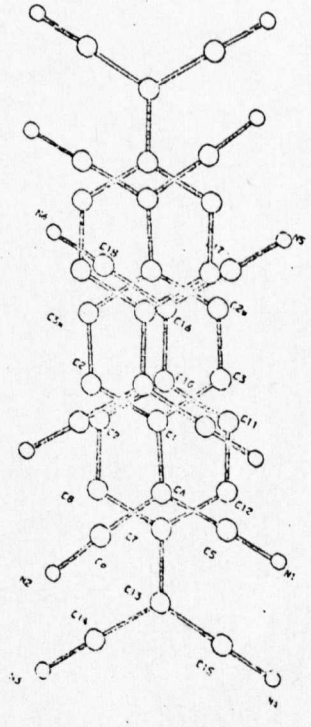

Molecular overlap

FIGURE 1

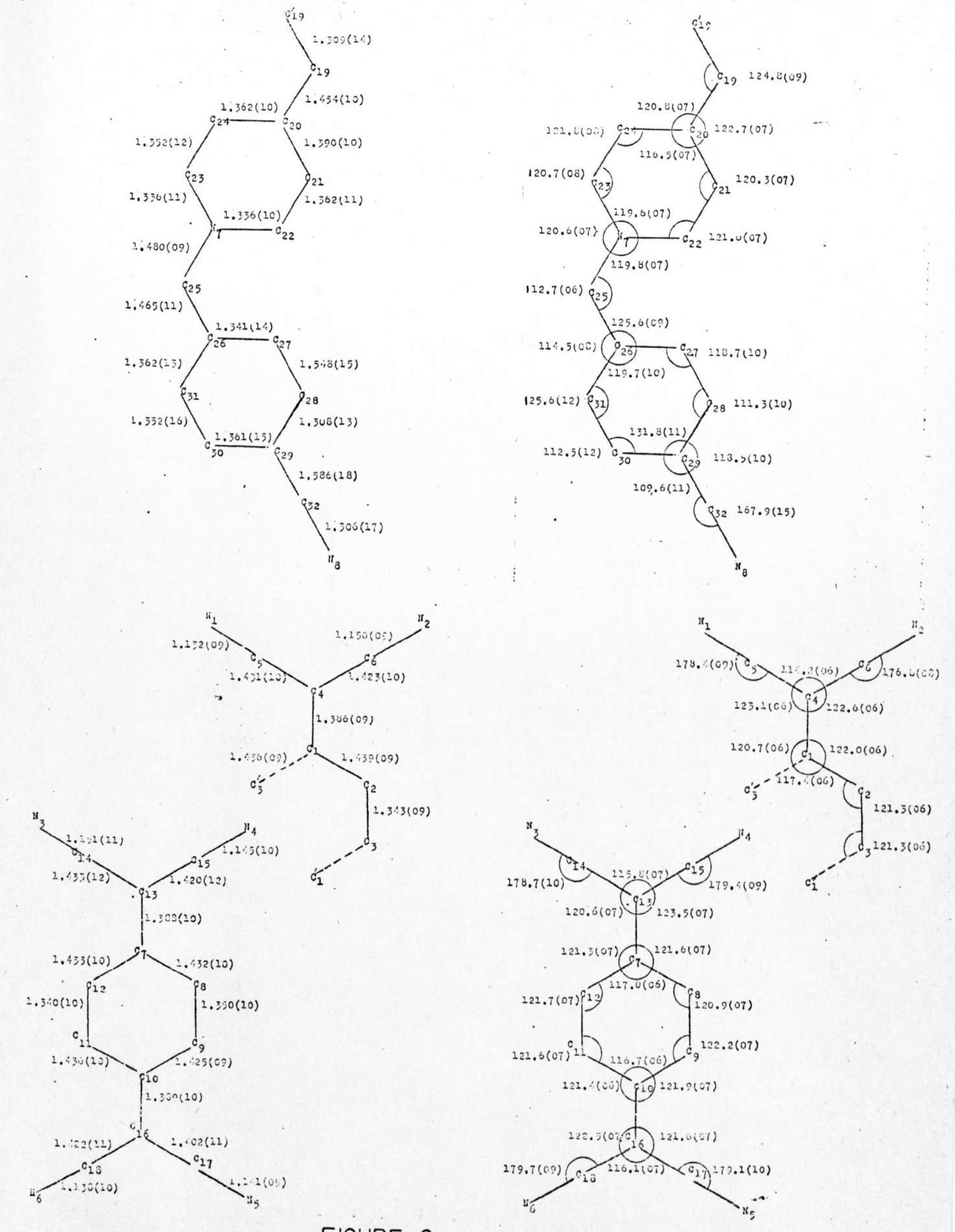

FIGURE 2

Bond lengths and angles for $DCBP(TCNQ)_3$

ATOM	U(11)	U(22)	U(33)	U(23)	U(13)	U(12)
C(1)	0.040(4)	0.042(4)	0.045(4)	0.008(3)	0.008(3)	0.009(3)
C(2)	0.041(4)	0.043(4)	0.056(5)	0.006(4)	0.008(3)	0.013(3)
C(3)	0.036(4)	0.045(4)	0.053(4)	0.009(3)	0.007(3)	0.009(3)
C(4)	0.044(4)	0.037(4)	0.056(5)	0.006(3)	0.008(3)	0.014(3)
C(5)	0.042(5)	0.042(4)	0.065(5)	0.003(4)	0.004(4)	0.010(3)
C(6)	0.039(4)	0.045(5)	0.071(5)	0.003(4)	0.010(4)	0.007(3)
N(1)	0.043(4)	0.063(5)	0.113(6)	0.009(4)	0.017(4)	0.006(3)
N(2)	0.057(4)	0.052(4)	0.106(6)	-0.010(4)	0.013(4)	0.009(3)
C(7)	0.054(5)	0.051(5)	0.045(4)	0.006(4)	0.006(4)	0.011(4)
C(8)	0.050(4)	0.046(4)	0.049(5)	0.001(3)	0.007(4)	0.008(4)
C(9)	0.042(4)	0.050(5)	0.049(4)	0.002(4)	0.010(3)	0.006(4)
C(10)	0.052(4)	0.046(4)	0.049(4)	0.005(3)	0.008(4)	0.004(3)
C(11)	0.052(5)	0.044(4)	0.057(5)	0.003(4)	0.011(4)	0.011(4)
C(12)	0.045(4)	0.043(4)	0.063(5)	0.004(4)	0.010(4)	0.008(4)
C(13)	0.055(5)	0.044(4)	0.055(5)	-0.003(4)	0.006(4)	-0.000(4)
C(14)	0.080(6)	0.067(6)	0.053(5)	0.005(5)	0.009(5)	-0.015(5)
C(15)	0.067(6)	0.054(5)	0.063(6)	0.008(4)	-0.013(5)	-0.001(4)
C(16)	0.054(5)	0.040(4)	0.054(5)	0.008(3)	0.014(4)	0.005(3)
C(17)	0.065(5)	0.043(5)	0.067(5)	0.007(4)	0.023(4)	0.006(4)
C(18)	0.058(6)	0.050(5)	0.064(5)	0.004(4)	0.012(4)	0.002(4)
N(3)	0.099(6)	0.081(6)	0.080(6)	-0.027(5)	0.027(5)	-0.011(5)
N(4)	0.064(5)	0.072(5)	0.104(7)	0.004(4)	0.001(5)	-0.002(4)
N(5)	0.085(5)	0.051(4)	0.112(7)	-0.000(4)	0.039(5)	0.005(4)
N(6)	0.057(5)	0.083(6)	0.103(6)	0.008(5)	0.017(4)	-0.002(4)
C(19)	0.044(4)	0.060(5)	0.049(4)	-0.000(4)	0.002(4)	0.000(4)
C(20)	0.044(4)	0.051(4)	0.049(5)	0.002(3)	0.001(4)	-0.009(3)
C(21)	0.061(5)	0.057(5)	0.043(5)	-0.007(4)	-0.007(4)	0.010(4)
C(22)	0.066(5)	0.051(5)	0.065(6)	-0.006(4)	-0.001(5)	0.019(4)
C(23)	0.057(6)	0.15(1)	0.042(5)	0.003(5)	0.007(4)	-0.024(6)
C(24)	0.041(5)	0.17(1)	0.043(5)	-0.009(6)	0.004(4)	-0.007(5)
N(7)	0.058(4)	0.052(4)	0.051(4)	0.009(3)	-0.009(3)	-0.013(3)
C(25)	0.084(6)	0.069(6)	0.057(5)	0.026(4)	-0.023(5)	-0.011(5)

ATOM	X/A	Y/B	Z/C	U(ISO)
C(1)	0.1227(8)	0.0949(6)	0.3356(5)	
C(2)	-0.0516(9)	0.0959(6)	0.3525(5)	
C(3)	-0.1676(8)	0.0358(6)	0.4200(5)	
C(4)	0.2443(8)	0.1885(6)	0.4212(5)	
C(5)	0.413(1)	0.1589(6)	0.3524(6)	
C(6)	0.2959(9)	0.2371(7)	0.1275(6)	
H(1)	0.5561(8)	0.1915(6)	0.3397(6)	
N(2)	0.1821(8)	0.3691(6)	0.1752(6)	
C(7)	0.3521(9)	0.1228(6)	0.2862(5)	
C(8)	0.1761(9)	0.1176(6)	0.2995(5)	
C(9)	0.0679(9)	0.0233(6)	0.2632(5)	
C(10)	0.1223(9)	-0.0751(6)	0.2109(5)	
C(11)	0.298(9)	-0.0692(6)	0.1977(6)	
C(12)	0.4069(9)	0.0243(6)	0.2329(6)	
C(13)	0.466(1)	0.2170(6)	0.3263(6)	
C(14)	0.411(1)	0.3102(8)	0.3867(6)	
C(15)	0.640(1)	0.2272(7)	0.3131(6)	
C(16)	0.0109(9)	-0.1725(6)	0.1750(5)	
C(17)	0.066(1)	-0.2693(7)	0.1242(6)	
C(18)	-0.164(1)	-0.1812(7)	0.1891(6)	
N(3)	0.369(1)	0.3348(7)	0.4195(6)	
N(4)	0.781(1)	0.2345(7)	0.3027(6)	
N(5)	0.112(1)	-0.3432(6)	0.0839(6)	
N(6)	-0.304(1)	-0.1877(7)	0.2003(6)	
C(19)	0.5172(9)	0.4342(7)	0.0552(5)	
C(20)	0.4055(9)	0.4359(6)	0.0693(5)	
C(21)	0.243(1)	0.5143(7)	0.0748(5)	
C(22)	0.142(1)	0.5104(7)	0.0922(6)	
C(23)	0.353(1)	0.457(1)	0.0975(6)	
C(24)	0.456(1)	0.459(1)	0.0781(6)	
H(7)	0.1959(8)	0.4612(5)	0.0944(5)	
C(25)	0.051(1)	0.4743(8)	0.0582(6)	
C(26)	-0.0273(9)	0.3636(6)	0.5975(5)	0.049(2)
C(27)	-0.195(2)	0.348(1)	0.6023(9)	0.116(4)
C(28)	-0.292(1)	0.2254(9)	0.5736(8)	0.090(3)
C(29)	-0.192(1)	0.1523(8)	0.5413(7)	0.076(3)
C(30)	-0.022(2)	0.163(1)	0.533(1)	0.124(4)
C(31)	0.053(2)	0.272(1)	0.5675(9)	0.130(4)
C(32)	-0.271(2)	0.024(1)	0.503(1)	0.149(5)
N(8)	-0.354(2)	-0.072(1)	0.454(1)	0.163(5)
H(1)	-0.0856	0.1665	0.0929	0.0500
H(2)	-0.2900	0.0038	0.9342	0.0500
H(3)	0.1342	0.1660	0.3468	0.0500
H(4)	-0.0562	0.0256	0.2722	0.0500
H(5)	0.3414	-0.1381	0.1601	0.0500
H(6)	0.5118	0.0264	0.2207	0.0500
H(7)	0.6313	0.4551	0.0462	0.0500
H(8)	0.2001	0.5368	0.6409	0.0500
H(9)	0.0226	0.5306	0.7963	0.0500
H(10)	0.3956	0.4360	0.6299	0.0500
H(11)	0.5759	0.4385	0.7708	0.0500
H(12)	0.0022	0.5400	0.6274	0.0500
H(13)	0.1439	0.4942	0.5581	0.0500
H(14)	-0.2696	0.4119	0.6285	0.0500
H(15)	-0.4125	0.2108	0.5808	0.0500
H(16)	0.0442	0.0999	0.5185	0.0500
H(17)	0.1360	0.2854	0.5685	0.0500

DCBP $(TCNQ)_3$ fractional coordinates

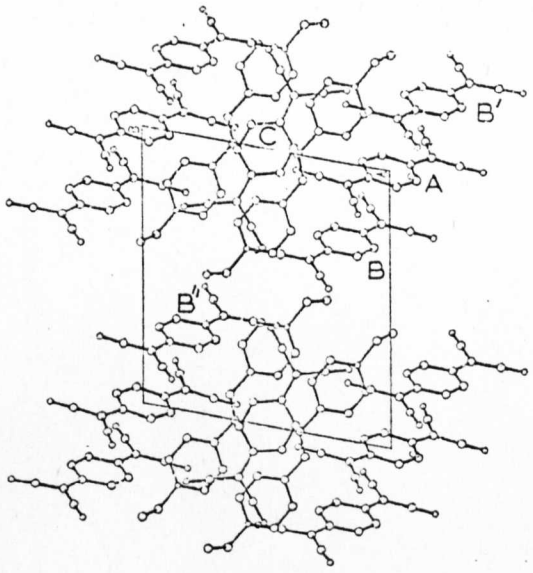

Projection along a

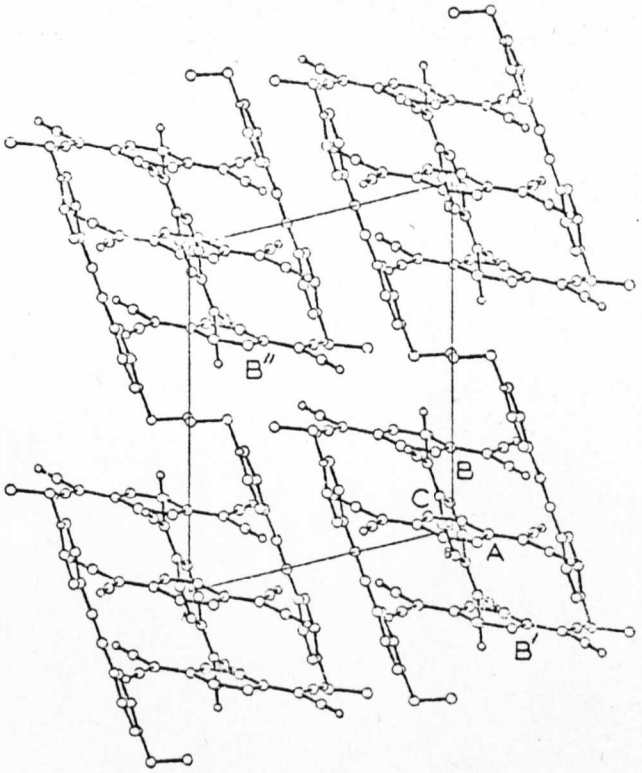

Projection along b

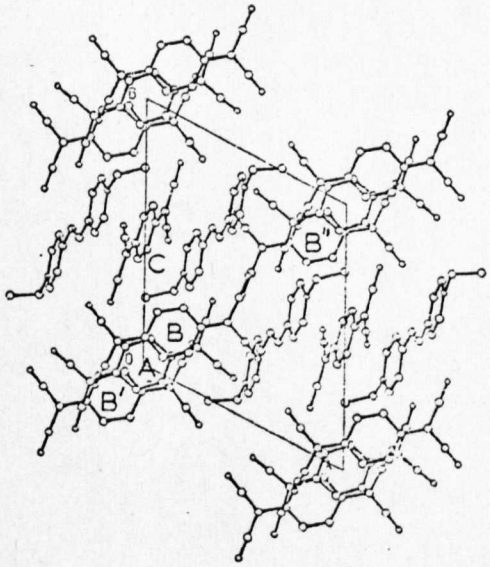

Projection along c

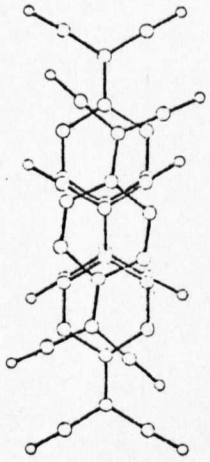

B'AB

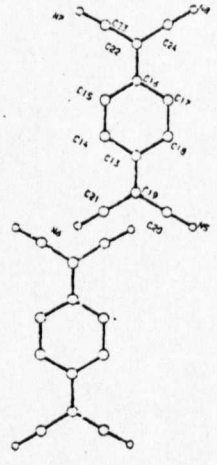

BB''

Molecular overlaps

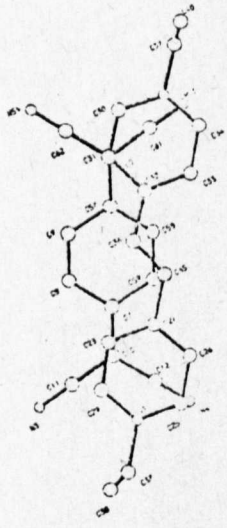

C & cation

FIGURE 3 - DEPE $(TCNQ)_2$

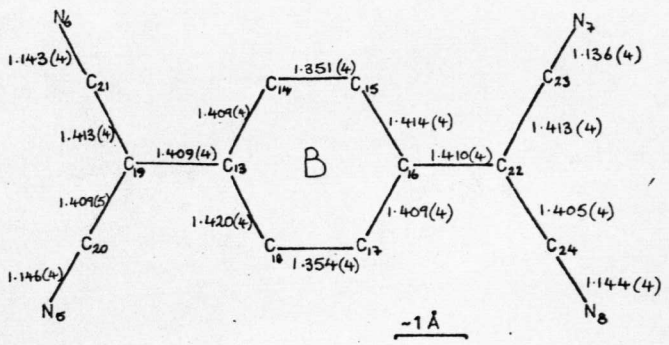

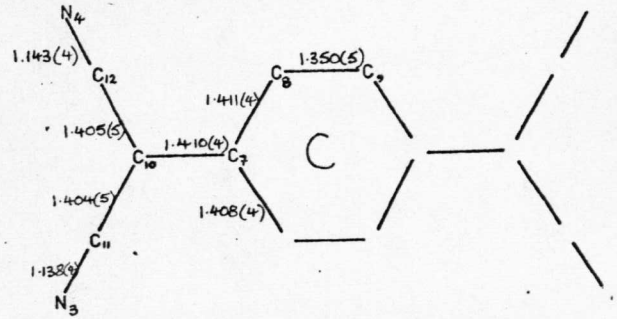

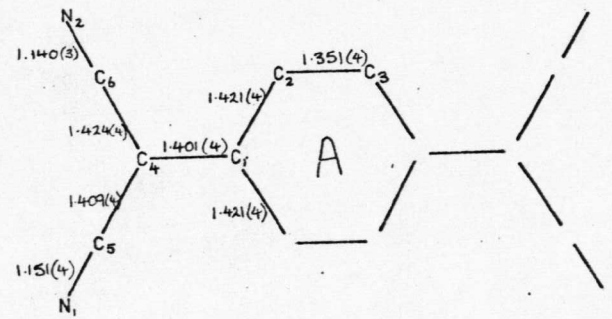

FIGURE 4 DEPE(TCNQ)$_2$

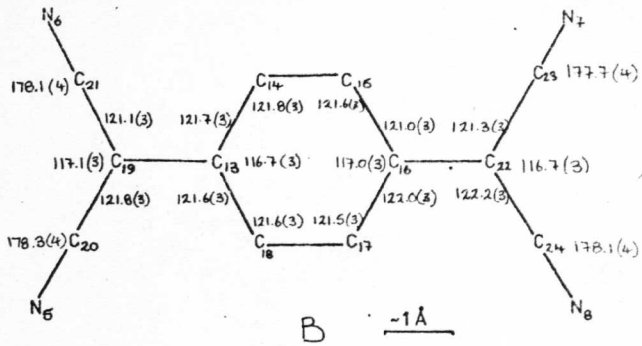

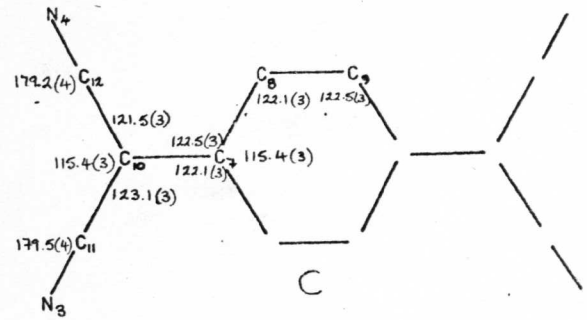

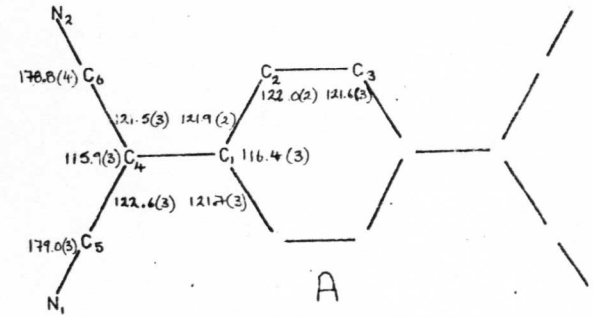

Bond lengths (Å) and angles (deg) with estimated standard deviations in parentheses

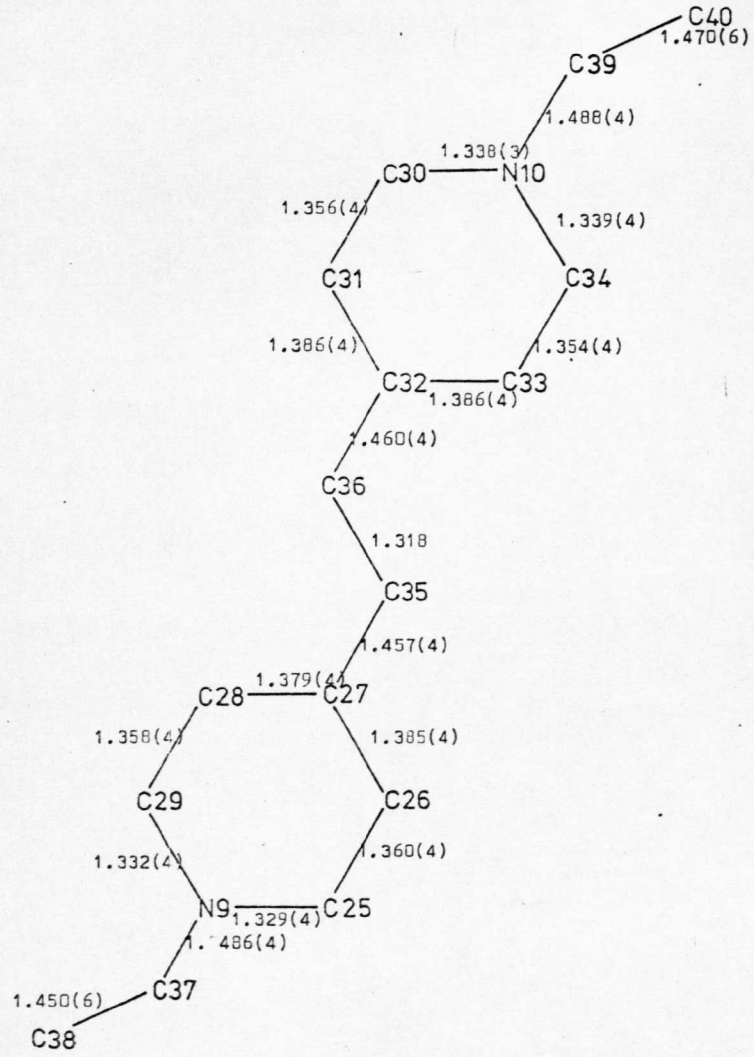

Figure 5 DEPE(TCNQ)$_2$

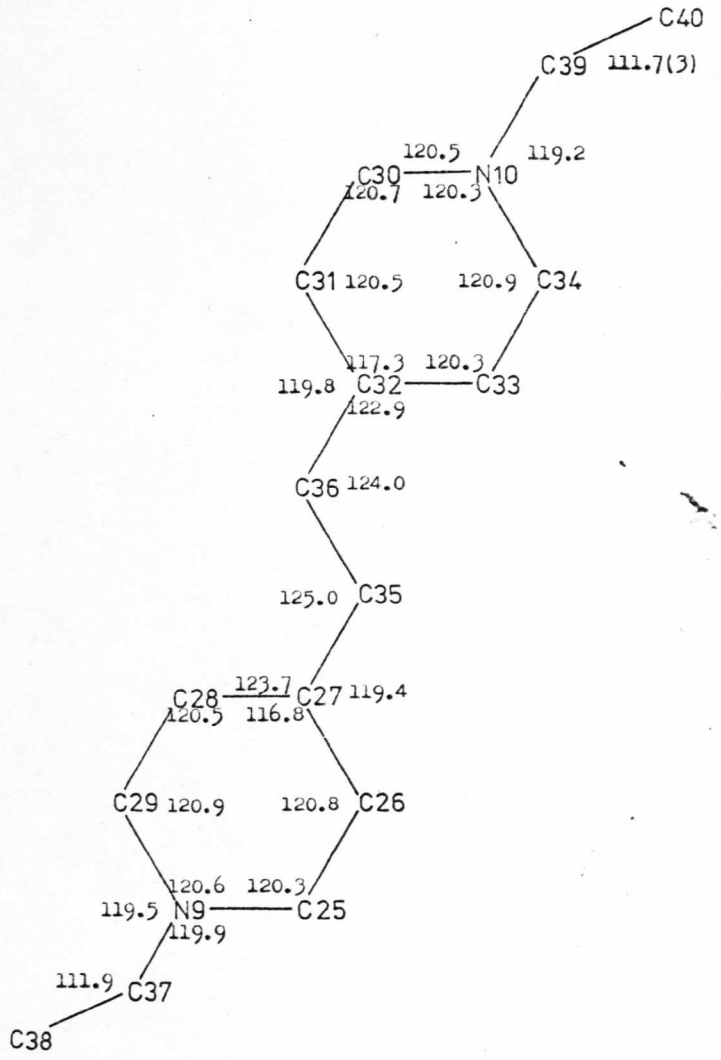

Bond Distances (Å) with estimated standard deviations in parentheses and Bond Angles (all estimated standard deviations 0.3 degrees).

ATOM	X/A	Y/B	Z/C	U(ISO)
C(1)	0.1346(3)	0.0852(2)	0.0379(2)	
C(2)	0.0343(3)	0.1094(2)	-0.0176(2)	
C(3)	-0.0629(3)	0.0236(2)	-0.0537(2)	
C(4)	0.2665(3)	0.1697(2)	0.0769(2)	
C(5)	0.3663(3)	0.1469(2)	0.1312(2)	
C(6)	0.3084(3)	0.2346(3)	0.0650(2)	
N(1)	0.4456(3)	0.1299(2)	0.1766(2)	
N(2)	0.3336(3)	0.3773(2)	0.0571(2)	
C(7)	-0.0475(3)	0.4405(3)	-0.1053(3)	
C(8)	-0.0339(4)	0.3855(3)	-0.0214(3)	
C(9)	0.0038(4)	0.4420(3)	0.0781(3)	
C(10)	-0.0047(3)	0.3822(3)	-0.2095(3)	
C(11)	-0.1354(4)	0.2649(3)	-0.2384(3)	
C(12)	-0.1071(4)	0.4391(3)	-0.2920(3)	
N(3)	-0.1038(4)	0.1698(3)	-0.2626(3)	
N(4)	-0.1111(4)	0.4844(3)	-0.3598(3)	
C(13)	0.2315(3)	0.2518(2)	0.3254(2)	
C(14)	0.1951(4)	0.2929(2)	0.2777(2)	
C(15)	0.0643(3)	0.2234(2)	0.2364(2)	
C(16)	0.0870(3)	0.1056(2)	0.2393(2)	
C(17)	0.0923(3)	0.0639(2)	0.2869(2)	
C(18)	0.2241(3)	0.1335(3)	0.3280(2)	
C(19)	0.4150(4)	0.3252(3)	0.3717(2)	
C(20)	0.5030(4)	0.2847(3)	0.4211(3)	
C(21)	0.4217(3)	0.4435(3)	0.3717(2)	
C(22)	-0.1330(3)	0.0341(2)	0.1969(2)	
C(23)	-0.2135(3)	0.0765(3)	0.1460(3)	
C(24)	-0.1910(3)	-0.0817(3)	0.2040(3)	
N(5)	0.5713(3)	0.2495(3)	0.4616(2)	
N(6)	0.5125(3)	0.5390(3)	0.3717(2)	
N(7)	-0.2272(3)	0.1142(3)	0.1062(3)	
N(8)	-0.2911(3)	-0.1752(3)	0.2127(3)	
C(25)	-0.2078(3)	0.5247(3)	-0.3717(2)	
C(26)	0.2542(3)	0.6001(2)	-0.2309(2)	
C(27)	0.2952(3)	0.5680(2)	-0.1873(2)	
C(28)	0.2635(3)	0.4576(3)	-0.1931(2)	
C(29)	0.2220(4)	0.3353(3)	-0.2862(2)	
C(30)	0.4140(3)	0.7141(2)	0.0986(2)	
C(31)	0.4336(3)	0.8266(2)	0.1019(2)	
C(32)	0.4287(3)	0.8990(2)	0.1929(3)	
C(33)	0.4064(3)	0.7559(2)	0.2833(2)	
C(34)	0.4332(3)	0.6808(2)	0.1930(2)	
C(35)	0.3320(3)	0.6501(2)	-0.0902(2)	
C(36)	0.3790(3)	0.6313(2)	0.0021(2)	
C(37)	0.1476(4)	0.3384(3)	-0.4745(2)	
C(38)	0.5256(4)	0.0451(3)	0.3821(2)	
N(9)	0.1928(3)	0.4190(2)	-0.3737(2)	
N(10)	0.4930(2)	0.8633(2)	0.2829(2)	
C(39)	0.0856(6)	0.2576(5)	-0.4930(4)	
C(40)	0.6755(5)	1.3080(4)	0.4195(3)	
O(1)	0.3692	0.1387	-0.0300	0.0500

ATOM	X/A	Y/B	Z/C	U(ISO)
H(2)	-0.1597	0.0490	-0.0935	0.0500
H(3)	-0.0671	0.3020	-0.0362	0.0500
H(4)	0.0169	0.3997	0.1345	0.0500
H(5)	0.2312	0.3760	0.2743	0.0500
H(6)	0.0063	0.2557	0.2022	0.0500
H(7)	0.0547	-0.0107	0.2904	0.0500
H(8)	0.2815	0.0098	0.3596	0.0500
H(9)	0.1840	0.5401	-0.4331	0.0500
H(10)	0.2645	0.6795	-0.2792	0.0500
H(11)	0.2886	0.4307	-0.1278	0.0500
H(12)	0.2133	0.3960	-0.2896	0.0500
H(13)	0.4326	0.7315	0.3513	0.0500
H(14)	0.4101	0.6008	0.1948	0.0500
H(15)	0.4303	0.3553	0.0744	0.0500
H(16)	0.4943	0.9804	0.1946	0.0500
H(17)	0.3359	0.7263	-0.0939	0.0500
H(18)	0.3608	0.5556	-0.0366	0.0500
H(19)	0.1734	0.3896	-0.5311	0.0500
H(20)	0.2148	0.3028	-0.4725	0.0500
H(21)	0.4805	0.9966	0.3672	0.0500
H(22)	0.4727	0.8980	0.4329	0.0500
H(23)	-0.0037	0.2118	-0.5623	0.0500
H(24)	-0.0371	0.3059	-0.4962	0.0500
H(25)	0.0023	0.2190	-0.4376	0.0500
H(26)	0.6855	1.0590	0.4845	0.0500
H(27)	0.7029	1.0481	0.3652	0.0500
H(28)	0.7011	0.9495	0.4309	0.0500

DEPE $(TCNQ)_2$ Fractional coordinates

ATOM	U(11)	U(22)	U(33)	U(23)	U(13)	U(12)
C(1)	0.065(2)	0.049(2)	0.064(2)	0.020(1)	0.023(2)	0.032(2)
C(2)	0.063(2)	0.047(2)	0.075(2)	0.024(1)	0.023(2)	0.033(2)
C(3)	0.067(2)	0.050(2)	0.071(2)	0.022(2)	0.021(2)	0.034(2)
C(4)	0.065(2)	0.046(2)	0.071(2)	0.019(1)	0.020(2)	0.031(2)
C(5)	0.066(2)	0.047(2)	0.080(2)	0.018(2)	0.026(2)	0.025(2)
C(6)	0.067(2)	0.055(2)	0.077(2)	0.021(2)	0.020(2)	0.030(2)
N(1)	0.074(2)	0.071(2)	0.112(2)	0.029(2)	0.022(2)	0.041(2)
N(2)	0.101(2)	0.055(2)	0.119(2)	0.037(2)	0.027(2)	0.034(2)
C(7)	0.070(2)	0.071(3)	0.089(3)	0.039(2)	0.030(2)	0.044(2)
C(8)	0.111(3)	0.069(2)	0.089(3)	0.039(2)	0.030(2)	0.056(2)
C(9)	0.109(3)	0.078(2)	0.092(3)	0.045(2)	0.031(2)	0.056(2)
C(10)	0.075(2)	0.077(2)	0.086(3)	0.035(2)	0.027(2)	0.046(2)
C(11)	0.099(3)	0.081(3)	0.095(3)	0.035(2)	0.036(2)	0.054(2)
C(12)	0.095(3)	0.081(2)	0.087(3)	0.030(2)	0.024(2)	0.048(2)
N(3)	0.166(4)	0.091(2)	0.122(3)	0.035(2)	0.040(2)	0.075(3)
N(4)	0.162(3)	0.104(3)	0.089(2)	0.038(2)	0.023(2)	0.068(2)
C(13)	0.074(2)	0.061(2)	0.050(2)	0.015(1)	0.022(2)	0.034(2)
C(14)	0.087(3)	0.055(2)	0.061(2)	0.013(2)	0.024(2)	0.041(2)
C(15)	0.081(2)	0.055(2)	0.069(2)	0.023(2)	0.026(2)	0.042(2)
C(16)	0.074(2)	0.056(2)	0.056(2)	0.021(1)	0.026(2)	0.039(2)
C(17)	0.073(2)	0.056(2)	0.066(2)	0.027(2)	0.024(2)	0.038(2)
C(18)	0.081(2)	0.064(2)	0.059(2)	0.024(2)	0.021(2)	0.044(2)
C(19)	0.085(3)	0.062(2)	0.052(2)	0.017(2)	0.017(2)	0.035(2)
C(20)	0.083(3)	0.072(2)	0.058(2)	0.020(2)	0.015(2)	0.025(2)
C(21)	0.081(2)	0.070(2)	0.059(2)	0.017(2)	0.015(2)	0.032(2)
C(22)	0.068(2)	0.059(2)	0.069(2)	0.030(2)	0.029(2)	0.039(2)
C(23)	0.076(2)	0.069(2)	0.088(2)	0.035(2)	0.036(2)	0.043(2)
C(24)	0.067(2)	0.074(2)	0.095(3)	0.040(2)	0.031(2)	0.040(2)
N(5)	0.097(2)	0.100(2)	0.086(2)	0.039(2)	0.012(2)	0.046(2)
N(6)	0.109(2)	0.069(2)	0.081(2)	0.017(2)	0.013(2)	0.029(2)
N(7)	0.100(2)	0.103(2)	0.129(3)	0.055(2)	0.036(2)	0.068(2)
N(8)	0.087(2)	0.082(2)	0.175(3)	0.070(2)	0.043(2)	0.041(2)
C(25)	0.091(2)	0.065(2)	0.057(2)	0.019(2)	0.011(2)	0.039(2)
C(26)	0.087(2)	0.057(2)	0.056(2)	0.015(2)	0.008(2)	0.036(2)
C(27)	0.067(2)	0.053(2)	0.051(2)	0.015(1)	0.013(1)	0.029(2)
C(28)	0.095(3)	0.059(2)	0.052(2)	0.018(2)	0.014(2)	0.039(2)
C(29)	0.110(3)	0.058(2)	0.056(2)	0.017(2)	0.018(2)	0.044(2)
C(30)	0.060(2)	0.049(2)	0.054(2)	0.012(1)	0.009(1)	0.025(1)
C(31)	0.085(2)	0.055(2)	0.053(2)	0.016(2)	0.009(2)	0.036(2)
C(32)	0.081(2)	0.056(2)	0.068(2)	0.015(2)	0.016(2)	0.038(2)
C(33)	0.081(2)	0.055(2)	0.054(2)	0.017(2)	0.017(2)	0.029(2)
C(34)	0.076(2)	0.048(2)	0.053(2)	0.014(2)	0.013(2)	0.028(2)
C(35)	0.067(2)	0.051(2)	0.055(2)	0.012(1)	0.012(2)	0.029(2)
C(36)	0.072(2)	0.050(2)	0.055(2)	0.014(1)	0.012(2)	0.030(2)
C(37)	0.103(3)	0.078(2)	0.056(2)	-0.000(2)	0.015(2)	0.034(2)
C(38)	0.095(3)	0.069(2)	0.061(2)	-0.006(2)	0.025(2)	0.028(2)
N(9)	0.086(2)	0.061(2)	0.045(1)	0.009(1)	0.013(1)	0.034(1)
N(10)	0.072(2)	0.055(2)	0.053(2)	0.007(1)	0.017(1)	0.028(1)
C(39)	0.180(6)	0.152(5)	0.094(4)	-0.045(3)	0.040(4)	-0.000(4)
C(40)	0.127(4)	0.131(4)	0.086(3)	-0.042(3)	0.023(3)	0.018(3)

DEPE $(TCNQ)_2$ Anisotropic thermal parameters